United States
Environmental Protection
Agency

Air and Energy Environmental
Research Laboratory
Research Triangle Park NC 27711

EPA/600/9-90/005c
January 1990

Research and Development

EPA

The 1990 International Symposium on Radon and Radon Reduction Technology: Volume III. Preprints

Session IV: Radon Surveys
Session V: Radon Entry Dynamics
Session VI: Radon in the Natural Environment
Session C-V: Radon Entry Dynamics—POSTERS
Session C-VI: Radon in the Natural Environment—POSTERS

February 19-23, 1990
Stouffer Waverly Hotel
Atlanta, Georgia

Session IV:

Radon Surveys

RADON EXPOSURE IN CONNECTICUT: ANALYSIS OF THREE STATEWIDE SURVEYS OF NEARLY ONE PERCENT OF SINGLE FAMILY HOMES

by: Alan J. Siniscalchi, M.S., M.P.H. (1), Lynne M. Rothney, M.P.H. (2), Brian F. Toal, M.S.P.H. (1), Margaret A. Thomas, M.S. (3), David R. Brown, Sc.D. (1), Maria C. van der Werff, B.S. (4), Carolyn J. Dupuy, M.S., S.M. (1)

(1) State of Connecticut Department of Health Services Hartford, Connecticut 06106-4474
(2) Yale University School of Medicine
(3) State of Connecticut Department of Environmental Protection
(4) U.S. Environmental Protection Agency Region I - work performed while employed with the State of Connecticut

ABSTRACT

Statewide radon measures are needed to establish comprehensive population estimates of risk. The Connecticut Department of Health Services has measured indoor radon concentrations in over 5,000 living units which represent nearly 1% of the homes statewide. Short-term exposure data were obtained from both lowest livable areas (i.e., basements) and lowest living areas in 3,378 houses. Long-term living area data were collected in over 500 homes. Analysis of these data has shown associations with home construction type including a strong positive correlation with house age. Analysis of over 1,000 homes with energy use data did not reveal an association between energy efficient homes and high radon levels. Differences in air and water levels have been identified among various geologic units. Consistent findings among the three surveys include geometric mean basement and living area radon levels and percent of homes exceeding 4 pCi/L.

INTRODUCTION

The State of Connecticut Department of Health Services (DHS) began receiving numerous telephone inquiries on radon following the discovery of elevated indoor air radon levels in Pennsylvania (1). Since the DHS lacked information on radon exposure in Connecticut, plans were made to investigate the distribution of radon in the state. In addition to providing information to residents concerned about radon, the Department wanted to determine the extent of the radon problem in Connecticut. The risk reduction priorities of the DHS needed to be refined by understanding the true hazard posed by this newly discovered residential risk. Moreover, if elevated radon levels were identified in certain areas of the state, then local health agencies could focus their risk reduction resources in these areas. Since risk determinations require exposure data, the DHS proceeded to assess Connecticut population exposure to radon.

A pilot project and three studies have been performed. The first study was the 1985-87 "Connecticut Radon Survey" (2). This study was followed by an expanded 1986-87 "EPA-Connecticut Radon Survey" of basement radon levels in 168 of Connecticut's 169 municipalities.

Results of the EPA-Connecticut Radon Survey were then utilized to plan the 1987-88 "Household Testing Program" where 3,400 homeowners were given radon testing kits in towns which were selected based on radon potential or in towns not previously sampled.

THE CONNECTICUT RADON SURVEY

The Connecticut Radon Survey was conducted between 1985 and 1987 to assess the predictive ability of geologic, hydrologic and household factors on well water and indoor air radon. In the first phase, homes were chosen in six areas thought to be potentially high in radon levels on the basis of the Bedrock Geological Map of Connecticut (3), and later, on the basis of an aeroradioactivity survey (4). The second phase expanded the survey to also include low and intermediate radon areas. Information from local health department well completion reports were also used. Private well water was sampled using the EPA scintillation method from 262 homes. The indoor air radon level was sampled with a single alpha track device placed in the living area for three winter months in 202 of the homes from which water samples were taken. These homes were located in 44 towns and represent sampling from 26 geologic formations.

The private well water radon levels ranged from 100 to 130,240 picocuries per liter (pCi/L) with a geometric mean level of 3,179 pCi/L. Twenty-six percent (26%) of the wells had water radon levels greater than 10,000 pCi/L. The long-term living area indoor air radon levels ranged

from 0.1 pCi/L to 25.6 pCi/L, with a geometric mean level of 1.25 pCi/L. Eleven percent (11%) of the homes with radon had levels greater than 4 pCi/L. Regression analysis estimated that 18% of the variation in indoor air radon can be attributed to radon in private well water, with a water to air ratio of 10,000 pCi/L to 1.6 pCi/L (C.I. = 0.80 to 3.40 pCi/L). Figure 1 shows this relationship.

Geologic, hydrologic and household parameters were analyzed for their ability to predict radon levels. Figures 2 and 3 show the mean water and air radon levels respectively, compared to the bedrock classifications as shown on the Connecticut portion (Figure 4) of a generalized bedrock mapping scheme of New England (5). Geology was a significant predictive factor of radon in both private well water and indoor air with granitic and sedimentary formations associated with higher and lower radon levels respectively. While the radon potential of bedrock may be generally characterized by such data, it is possible that water radon levels alone are sufficient to estimate the geologic radon potential. Indoor air radon measurements represent radon emissions not only from bedrock, but also from surficial materials and also appear to vary significantly with various household factors.

Hydrologic factors, foundation type and energy efficiency were examined. Only the depth of unconsolidated material overlaying the bedrock had a strong positive correlation with private well water radon levels. Homes with block wall foundations had higher indoor air radon levels than those with other types of foundations. Homes characterized by the homeowner as being more energy efficient did not have higher indoor air radon levels than homes characterized as being less energy efficient.

EPA-CONNECTICUT RADON SURVEY

During the summer of 1986 the DHS cooperated with the U.S. Environmental Protection Agency (EPA) to conduct a survey of basement radon levels in Connecticut using charcoal testing devices supplied and analyzed by the EPA Eastern Environmental Radiation Facility in Montgomery, Alabama. The survey design called for differing sampling densities based upon radon potential estimations conducted by a geologist from the Connecticut Department of Environmental Protection (DEP). The radon potential was estimated using geological mapping, the Connecticut Radon Survey results and aeroradioactivity mapping. A target sample number from 7 to 15 samples per town was established based on the radon potential estimation for each of Connecticut's 169 towns. The survey design called for distribution of charcoal testing devices to 1600 homes, and for placement in the lowest livable area (i.e. basement) of the house for two days. The devices were placed during the winter of 1986-87 by energy auditors from CONN SAVE, a non-profit energy conservation organization. Homeowners were offered a radon test when they requested

an energy audit. Testing was on a first-come first-served basis until the target sample number was reached in each town. At the time of kit placement, information on housing characteristics, air infiltration rate, and house location were recorded by the energy auditor. Air infiltration rates were later estimated with a computer model commonly used by energy conservation organizations.

A total of 1,572 homeowners agreed to participate in the survey, with a refusal rate of less than 1%. One hundred and forty seven or 9.4% of the tests, were dropped from the analyses due to improper testing or mail-in procedures. A total of 1,157 tests of detached home basements were included for the detailed analysis reported here. Nineteen percent (19%) of the basements tested exceeded the EPA guideline of 4 pCi/L. There were significant differences ($p \leq 0.05$) in the percentage of homes with radon levels greater than 4 pCi/L between major areas of the state. These regions were established by their estimated geological potential for radon. Furthermore, correlation analysis demonstrated strong associations between radon levels and geology. Detailed analysis with regard to specific bedrock units also showed strong associations, with homes above granitic rock units having higher radon values than homes overlaying sedimentary rock units. Of the many housing characteristics studied, the age of the house was the most predictive factor with older housing having higher levels (see Figure 5). Fieldstone and block foundations were also accompanied by higher radon levels compared to concrete and concrete mix foundations (see Figure 6). No association was found between radon levels and the estimated air infiltration rate. These findings are consistent with those of the previous survey.

Geographic Information System (GIS) analyses of indoor radon data with digitized aeroradioactivity mapping (4) showed a strong correspondence between the percentage of homes with basement levels that were greater than or equal to 4 pCi/L and the generalized aeroradioactivity mapping as measured in counts per second gamma radiation (see Figure 7).

Since a review of radon distribution revealed that some elevated radon occurs in all areas, the DHS issued an advisory in August 1987 stating that all Connecticut homeowners should have their houses tested for radon. The DHS then established a full-time Connecticut Radon Program.

HOUSEHOLD TESTING PROGRAM

In December of 1987 the Connecticut Radon Program began distribution of free radon testing devices under the Household Testing Program (HTP). The objectives of the HTP were: to provide free radon testing devices

and appropriate placement instructions to residents living in areas suspected of having high radon levels; to obtain additional data on radon concentrations in selected Connecticut municipalities; and to examine the ratio between basement and living area radon concentrations.

In planning the HTP, fifty-three cities and towns were identified by a geologist employed with the Connecticut Department of Environmental Protection (DEP) based on results of the previous two radon surveys and existing information on terrestrial radiation and bedrock geology. Thirty-eight of these municipalities were selected for the HTP based on the ability and interest of the local health departments or other local agencies to participate in the distribution of testing devices (see Figure 8).

Each municipality was given 200 charcoal testing devices and asked to recruit 100 volunteer households. One charcoal testing device was placed in the basement or other "lowest livable area" and the second device placed in the "lowest lived-in area." All testing device analyses were conducted by the same contract laboratory. Three hundred and forty households with living area radon concentrations over 4 pCi/L and/or basement radon concentrations over 20 pCi/L received alpha-track devices for long-term follow-up testing.

The results of the HTP were not different from those of the EPA-Connecticut Survey and the Connecticut Radon Survey (see Table 1). The data also revealed an apparently consistent 3:2 ratio between basement and living area radon concentrations (6). Analysis indicated that the basement radon level is strongly predictive of the upstairs or living area radon level (R^2=0.48, P$\swarrow$ 0.00001).

The program is now evaluating results of long-term (9-12 month) alpha track devices provided to the 340 participants (10%) whose living area radon levels exceeded 4 pCi/L or basement levels that exceeded 20 pCi/L. The program also examined the influence of waterborne radon on indoor air radon levels. Figure 1 showed the analysis of variation between radon in water and indoor air radon levels for the Connecticut Radon Survey. When HTP homes on private well water were compared to homes with public water the ratio of living area to basement air levels was 0.75 $\pm$ 0.46 versus 0.49 $\pm$ 0.29 respectively (mean $\pm$ SD, N = 50). This effect was non-linear which suggests that higher levels of water radon are more significant contributors to indoor living area radon exposure.

DISCUSSION

The Connecticut DHS and DEP have collected radon data on 5,036 households. Information on housing characteristics and detailed locations is available on nearly all of the units tested. Household locations have been mapped on U.S. Geological Survey topographic maps at

1:24,000 scale and digitized into the DEP computerized Geographic Information System (GIS). This information has proven to be extremely useful in evaluating the radon potential of specific areas of the state.

The GIS is being used to test correlations of radon occurance at various concentrations with geophysical data, specific geological materials and modifying environmental conditions. Statistical analyses of radon indoor air and water data with respect to Connecticut geological terranes and individual bedrock formations have produced geologically stratified sampling schemes for the EPA - Connecticut Radon Survey and the Household Testing Program. For the EPA - Connecticut Radon Survey, GIS analyses have shown a strong correspondence between aeroradioactivity mapping (4) and basement radon testing (see Figure 7). These analyses produced statewide radon potential mapping that is being used as a tool to increase our understanding of the locations of homes with radon levels above 4 pCi/L.

The aeroradioactivity data was also utilized by earlier researchers in conducting an epidemiological study of cancer rates in Connecticut (7). The weighted regression analysis by towns used by Walter, et al. did not reveal an increased cancer rate by radiation level. However, the authors cited the limited statistical power of the study which provided only a small probability of detecting a radiation effect if a two-fold excess cancer risk existed in the higher gamma areas. The present survey data suggests that towns are too large a unit to detect cancer increases from radon exposure.

The similarity in the results for both the percentage of homes above the guideline and geometric mean radon levels are especially notable when one considers the methodological differences in both device (short-term charcoal and long-term alpha track) and home selection among each of the three studies. For example, differences in bias of the selection among the three studies is shown in Table 1. The selection of households for the Connecticut Radon Survey and the Household Testing Program tended to be toward areas with higher radon levels (although to a lesser degree in the HTP). The homes tested in the EPA-Connecticut Survey were not selected in areas that were known for high or low levels. Thus, the selection bias of this study was neutral.

The results of these studies provided information to the Department that suggested radon exposure in Connecticut was higher than expected. Many local health departments then initiated their own surveys. This information was also used to plan a number of educational campaigns designed to encourage further testing among Connecticut residents.

The studies also provided information useful to the Department's evaluation of its risk reduction priorities. An analysis of the survey data has been used to generate estimates of the risk for developing lung cancer from radon exposure in Connecticut. Table 2 displays the

distribution of living area radon concentrations for the three studies. Analysis of the distribution of this data using the risk tables provided in the National Academy of Sciences BEIR IV report (8) and smoking information would predict 280 excess lung cancers could occur each year in Connecticut from exposure to radon in homes. Risk calculations using a U.S. EPA model (9) predict similar rates.

An extrapolation of this information yielded estimates of additional exposures to radon that occur in schools. Assuming a school population of 542,000 students with 10 years of exposure, an estimated 425 additional cases of lung cancer could result from radon exposure in schools alone (10). If, as chronic disease surveys (11) imply, that 19% of elementary and secondary school of students smoke, the excess cancer cases due to radon alone would be much higher.

This series of surveys illustrate the complexity of predicting radon exposures from limited measures of radon. Additional factors which are being investigated further are: the contribution of water radon in homes with private wells, the influence of differences in bedrock type within small geographic areas, and the radon contribution from unconsolidated materials, differences in housing characteristics and lifestyles of the population.

SUMMARY

The three Connecticut radon surveys show that a radon problem exists in the state. The studies also provided information on the differences in risk due to variability in exposure from housing type and location.

Information on the relationship between radon levels and geology will continue to be developed to refine our knowledge of the locations and conditions in Connecticut where radon may be of the highest risk. Local agencies can then focus educational and outreach efforts in these areas.

The studies have been the foundation for the establishment of a formal radon program within the DHS. Information from these studies will continue to guide the Program's efforts in public outreach and educational campaigns designed to encourage testing and appropriate mitigation within all Connecticut structures.

With the exception of the charcoal testing devices provided by the U.S. Environmental Protection Agency (EPA) for use in the EPA Connecticut Radon Survey, the work described in this paper was not funded by the EPA. Therefore, the contents do not necessarily reflect the views of the Agency and no official endorsement should be inferred.

ACKNOWLEDGEMENTS

The authors wish to thank Ms. Suzanne Lessard for her expert word processing assistance in the preparation of this paper, Ms. Laurie Gokey and Mr. Zygmunt Dembek for their review of the manuscript, and Mr. Marc T. Rothney for the preparation of Figures 1, 2, and 3. The authors also express their appreciation to the staff of CONN SAVE for their assistance in the EPA-Connecticut Radon Survey, the local health and other officials who participated in the Household Testing Program, and all the households who participated in these surveys.

REFERENCES

1. Logue, J. and Fox, J. Health hazards associated with elevated levels of indoor radon - Pennsylvania. Morbidity and Mortality Weekly Report (MMWR). 34:657, 1985.

2. Rothney, L.M. Connecticut radon survey of private well water and indoor air: assessing geologic, hydrologic and household parameters. Connecticut Department of Health Services, Toxic Hazards Section, Hartford, Connecticut, 1987. 45 pp.

3. Rogers, J. Bedrock geological map of Connecticut. Scale 1:125,000, Connecticut Geological and Natural History Survey. 1985.

4. Popenoe, P. Aeroradioactivity and generalized geologic maps of parts of New York, Connecticut, Rhode Island and Massachusetts. U.S. Geologic Survey Geophys, Inv. Map. GP-359, Scale 1:250,000, U.S.G.S. 1966.

5. Olszewski, W., Jr. and Boudette, E.L. Generalized bedrock map of New England, Scale 1:1,000,000, New Hampshire Water Supply and Pollution Control Commission and U.S. EPA Region I, 1986.

6. Toal, B.F., Dupuy, C.J., Rothney L.M., Siniscalchi, A.J., Brown, D.R., and Thomas, M.A. Radon exposure assessment - Connecticut. Morbidity and Mortality Weekly Report (MMWR). 38:713, 1989.

7. Walter, D.S., Meigs, J.W., and Heston, J.F. The relationship of cancer incidence to terrestrial radiation and population density in Connecticut 1935-1974. American Journal of Epidemiology 123:1, 1986.

8. National Research Council Committee on the Biological Effects of Ionizing Radiations. Health Risks of Radon and Other Internally Deposited Alpha-Emitters (BIER IV). National Academy Press, Washington, D.C., 1988. 602 pp.

9. Oge, M. Current ORP estimate of radon-induced lung cancer deaths in the general population. U.S. EPA memorandum, August 17, 1989.

10. Dupuy, C.J. and Rothney, L.M. Radon risk in schools. DHS memorandum, December 21, 1988.

11. Unpublished data. Center for Chronic Disease, Urban/Rural Health, Connecticut Department of Health Services. Connecticut Health Check data 1988.

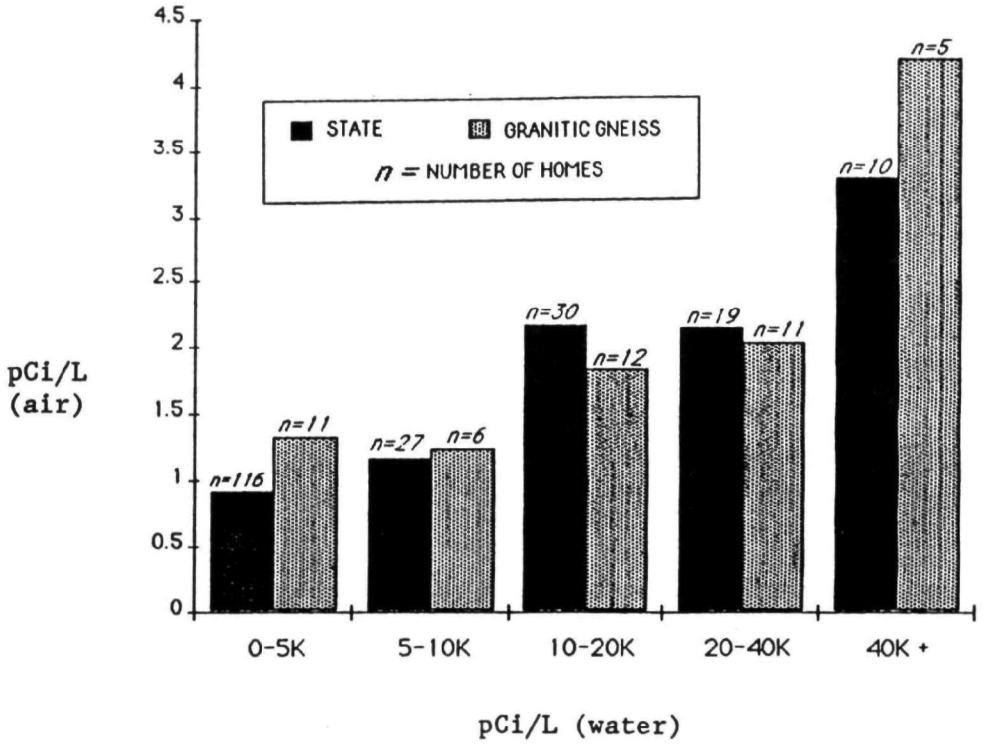

Figure 1. Connecticut Radon Survey: geometric mean indoor air radon levels by range of water radon levels.

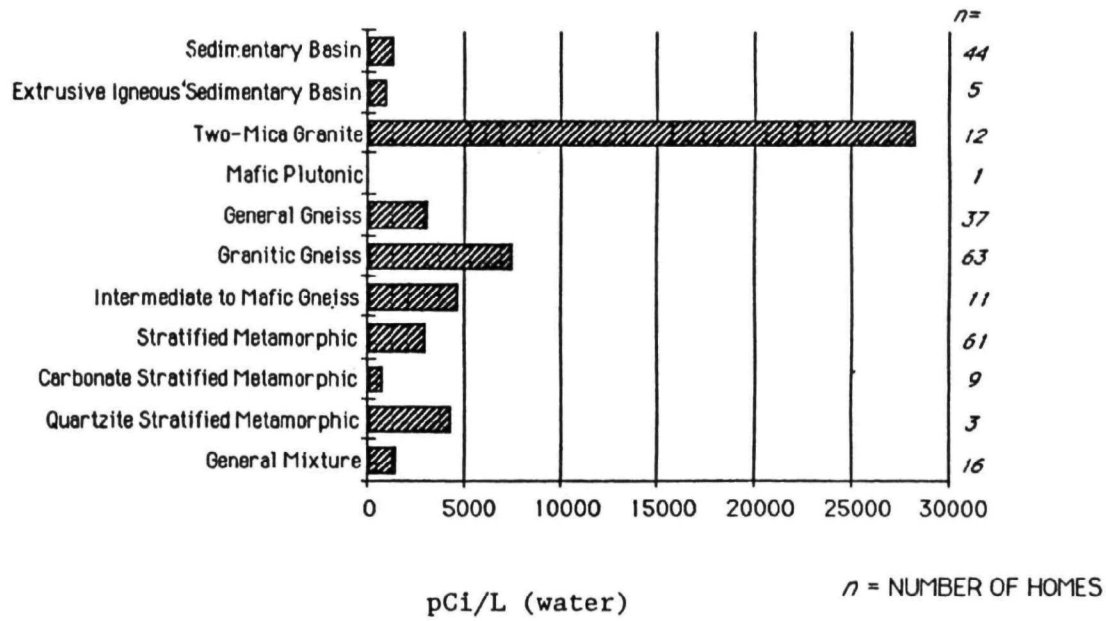

Figure 2. Connecticut Radon Survey: geometric mean water radon level by generalized bedrock type.

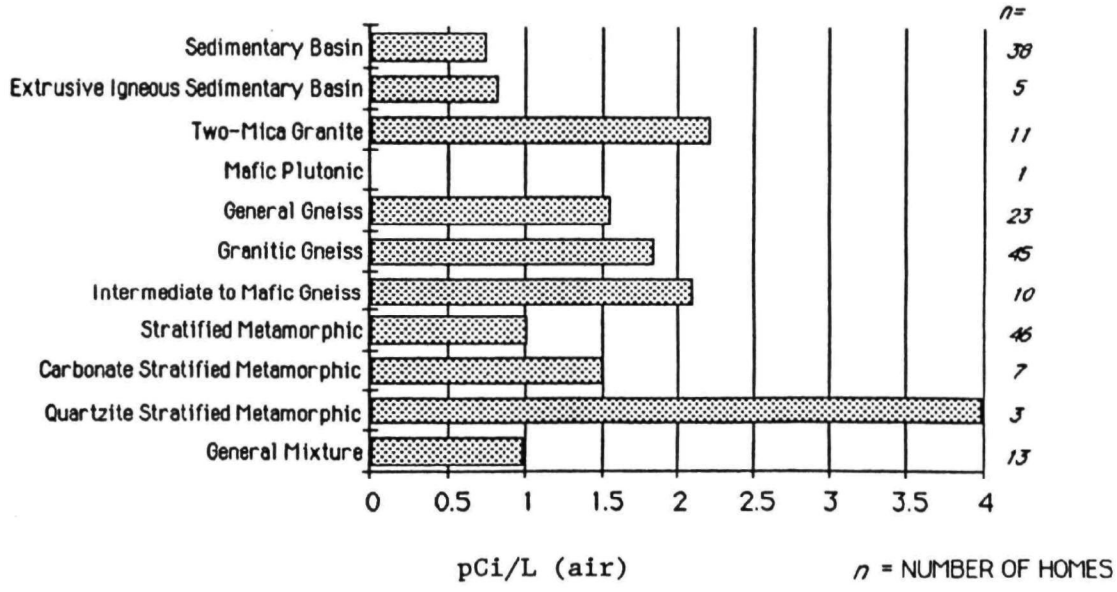

Figure 3. Connecticut Radon Survey: geometric mean air radon levels by generalized bedrock type.

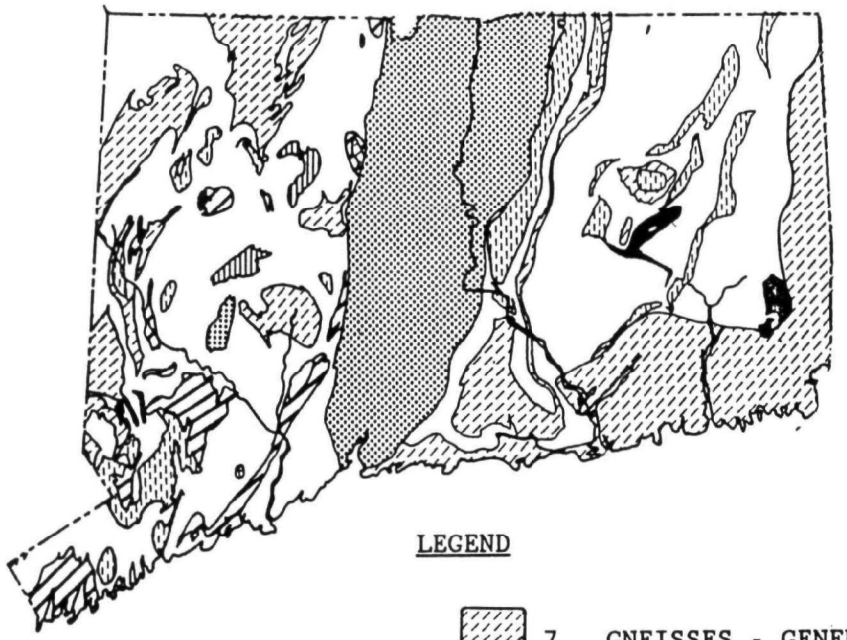

LEGEND

1. SEDIMENTARY BASIN

1a. EXTRUSIVE IGNEOUS SEDIMENTARY BASIN

2. TWO-MICA GRANITE

3. GRANITES OF CALC-ALKALINE COMPOSITION

4. ALKALIC PLUTONIC ROCKS

5. PLUTONIC ROCKS OF INTERMEDIATE COMPOSITION

6. MAFIC PLUTONIC ROCKS

7. GNEISSES - GENERAL

8. GNEISSES OF GRANITIC COMPOSITION

9. GNEISSES OF INTERMEDIATE TO MAFIC COMPOSITION

10. ULTRAMAFIC ROCKS

11. STRATIFIED METAMORPHIC ROCKS

11a. CARBONATE STRATIFIED METAMORPHIC ROCKS

11b. QUARTZITE STRATIFIED METAMORPHIC ROCKS

12. GENERAL MIXTURES OF ABOVE UNITS (AREAS NOT SHOWN)

Figure 4. Connecticut portion, generalized bedrock map of New England (modified from reference 5)

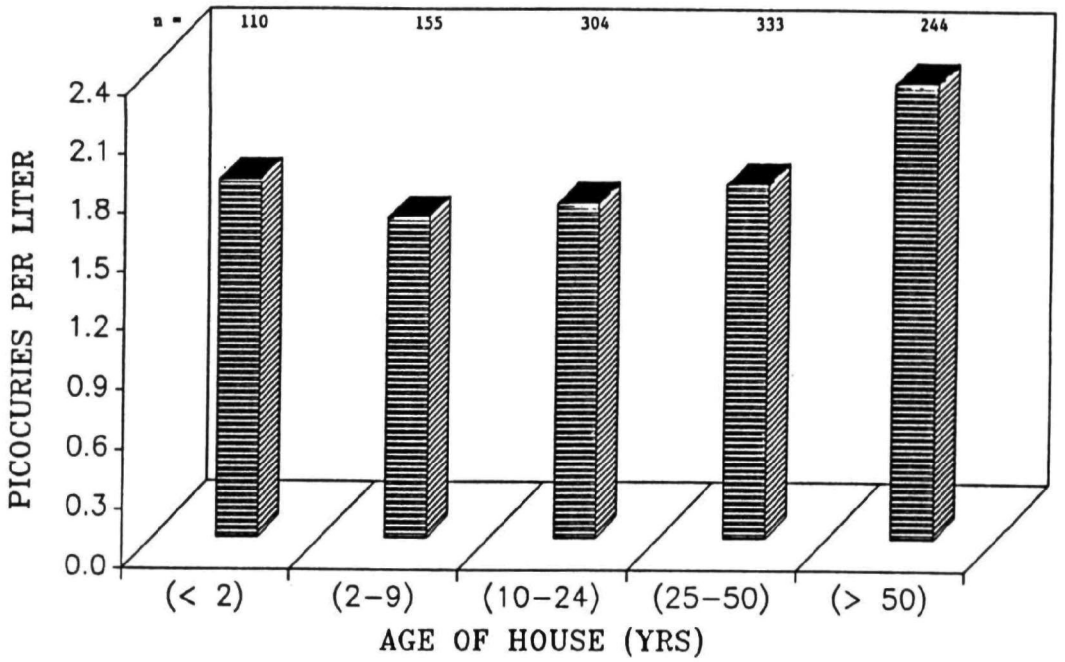

Figure 5. EPA - Connecticut Radon Survey: geometric mean radon levels by age of house.

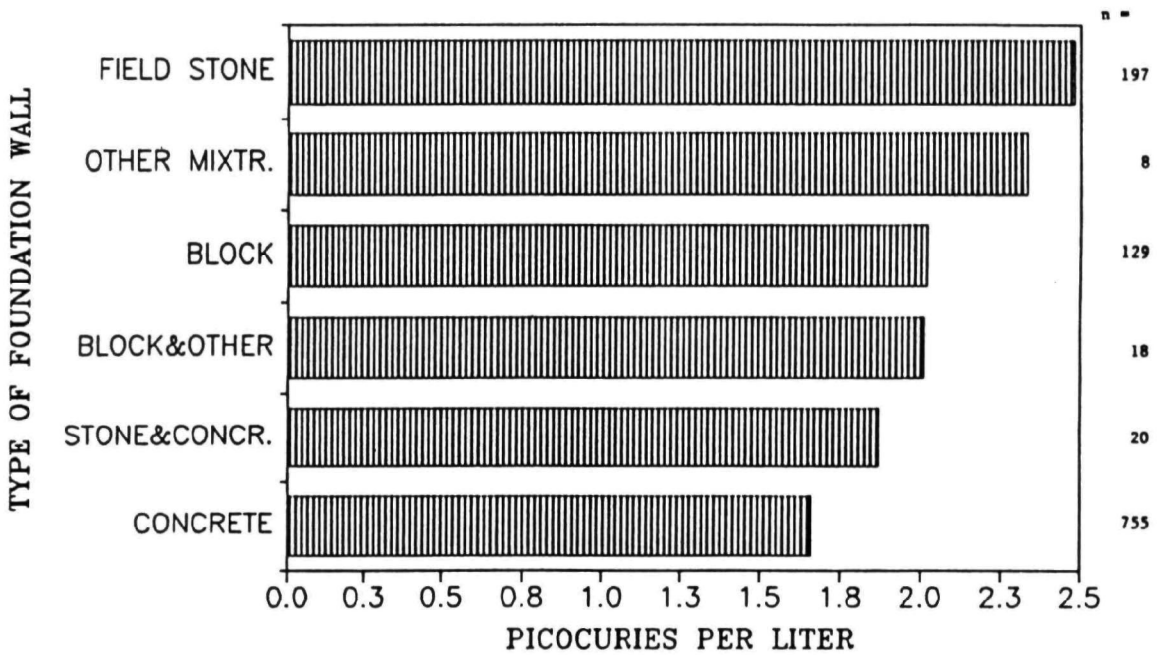

Figure 6. EPA - Connecticut Radon Survey: geometric mean radon levels by type of foundation wall.

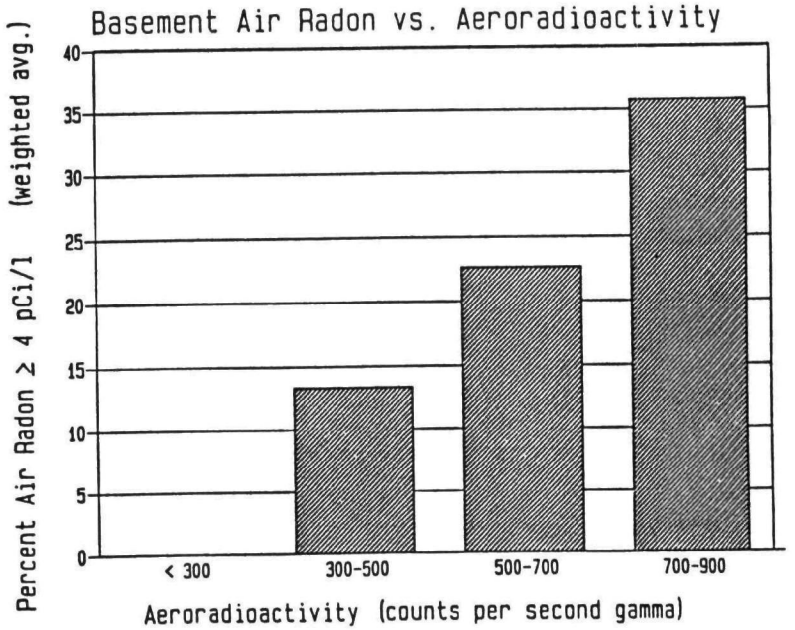

Figure 7. EPA - Connecticut Radon Survey: percent frequency of basements with 4 pCi/L radon levels by aeroradioactivity.

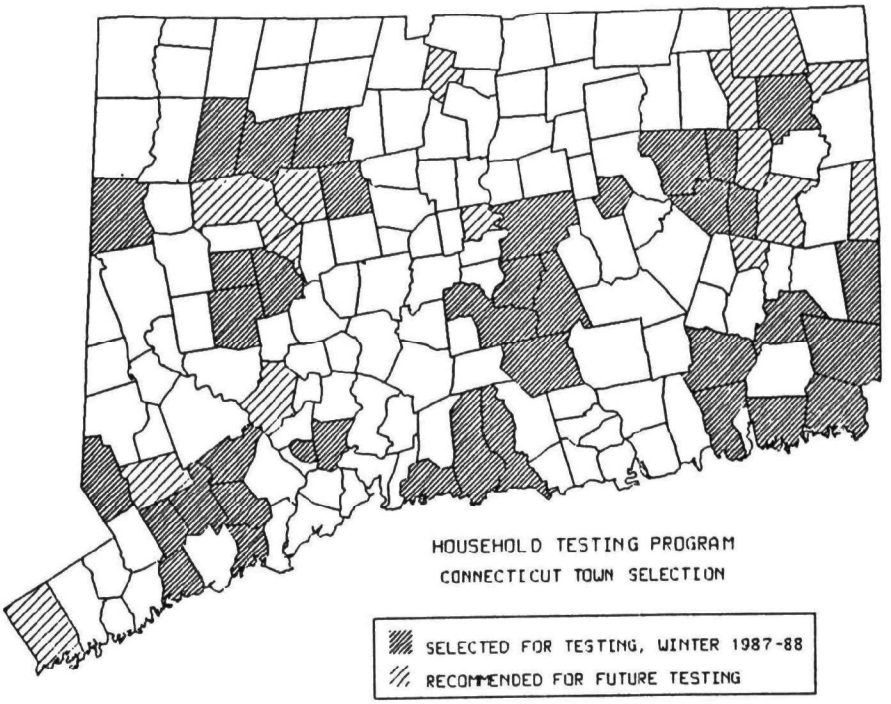

Figure 8. Household Testing Program: municipalities recommended and selected for testing.

TABLE 1. SUMMARY OF INDOOR AIR RADON SURVEYS CONDUCTED BY CONNECTICUT DEPARTMENT OF HEALTH SERVICES

Characteristic	Connecticut Radon Survey (n=202)		EPA-Connecticut Survey (n=1157*)		Household Testing Program (n=3409)	
Bias†	High		Neutral		High	
Survey device	Alpha-track		Charcoal		Charcoal	
	Results					
Location of measurement	% >4 pCi/L‡	Geometric mean (pCi/L)	% >4 pCi/L	Geometric mean (pCi/L)	% >4 pCi/L	Geometric mean (pCi/L)
Basement	NT§	NT	19%	2.1	21%	2.1
Lived-in area	11%	1.3	NT	NT	10%	1.3

*Number of detached houses out of 1425 total homes tested.
†Bias toward geologic locations with a higher probability of finding high radon homes.
‡Picocuries per liter.
§Not tested.

(from reference 6)

TABLE 2. DISTRIBUTION OF HOME LIVING AREA RADON CONCENTRATIONS (HOUSEHOLD TESTING PROGRAM DATA)

Percent	Radon Concentration (pCi/L)
90	$\angle$ 4 (geometric mean = 1.3 pCi/L)
6	4 - 9.9
3	10 - 19.9
0.5	20 - 49.9
0.4	50 - 99.9
0.1	$\geq$ 100

RESIDENTIAL RADON SURVEY OF TWENTY-THREE STATES

by: Jacolyn A. Dziuban[1]
Maureen Anderson Clifford[1]
S. B. White[2]
Jane W. Bergstein[2]
Barbara V. Alexander[2]

1. U. S. Environmental Protection Agency
2. Research Triangle Institute

ABSTRACT

This paper describes the cumulative results from 23 states that conducted surveys with the assistance of the Environmental Protection Agency (EPA) during the 1987, 1988 and 1989 heating seasons. It also describes the survey designs, provides population estimates of medians and means, and defines the proportion of households in each state exceeding specified exposure levels.

The goal of these surveys was twofold: to locate areas with elevated radon levels, and to characterize the statewide frequency distribution of radon screening measurements. Each survey was designed to provide a statistically valid comparison of radon levels in households in defined areas within each state and for each state as a whole. Overall, approximately 34,400 randomly-selected households provided screening measurements. Experience gained through these surveys will be highlighted and applied to the next series of state surveys scheduled for the winter of 1990.

This paper has been reviewed in accordance with the U. S. Environmental Protection Agency's peer and administrative review policies and approved for presentation and publication.

SURVEYS OF RADON LEVELS IN HOMES BY UNIVERSITY OF PITTSBURGH RADON PROJECT

Bernard L. Cohen
University of Pittsburgh
Pittsburgh, PA 15260

ABSTRACT

Data are analyzed on measurements of radon levels in numerous U.S. homes, accompanied by responses to questionnaires. Substantial bias reduction was accomplished by use of questionnaire responses, leaving 37,000 measurements in living areas and 33,000 in basements for the analysis. Variables studied include level with respect to ground where measurement was made, room type, age of house, recent weatherization actions, draftiness, location (urban-suburban- rural), air pollution, market value of house, annual household income, educational attainment of head of household, cigarette smoking, whether the house is rented or owner-occupied, and geographic section of U.S. Mean radon levels are determined for each response to questionnaire items (correlations), and for each pair of responses (cross correlations). Many interesting correlations and cross correlations are found, and their explanation and consequences are discussed.

From July, 1985 to January, 1988 the University of Pittsburgh Radon Project and its successor (starting in May, 1987), The Radon Project provided measurements of radon levels in homes almost exclusively in response to mail orders (cost - $12.00) stimulated by media publicity. This yielded a fairly broad national coverage. Each measurement was accompanied by a questionnaire which was filled out by the householder and returned before the result of the measurement was known. The purpose of this paper is to present results of the statistical analysis of these data. Preliminary reports on this work have been published in connection with presentations at conferences (Cohen and Gromicko 1988), but they were based on portions of the data and incomplete analysis.

The measurement and quality control procedures have been described previously (Cohen and Nason 1986, Cohen 1988, Cohen and Cohen 1989). Diffusion barrier charcoal adsorption collectors were exposed for seven days, after which the quantity of radon collected was measured by 40 minute counts of gamma rays under the 295 KeV, 352 KeV, and 609 KeV photoelectric peaks with NaI (Tℓ) scintillation detectors. Results are corrected for seasonal variations to best represent annual averages (Cohen 1989). Statistical uncertainties are about 45% at 18 Bq m^{-3}, 25% at 37 Bq m^{-3}, and less than 10% above 120 Bq m^{-3}.

Bias Reduction

Since our purpose is to obtain statistically meaningful data, it is important to reduce the biases in selection of houses measured as much as possible. Since these measurements are purchased by the householder, the potential for bias is very great. Bias reduction is done by use of the questionnaires.

One obvious source of bias is that poor people are less able to afford purchase of a measurement. To overcome this, the questionnaire includes questions about socioeconomic status, and data can be stratified on that basis. Another source of bias is that houses with high radon levels are much more likely to be remeasured. The questionnaire asks* "Has the radon level in this house been measured previously?" The ratio of mean radon levels for yes/no answers is 1.93 [1.61]; here and elsewhere in this paper, the first figure is for the main living areas of houses, and the figure in brackets is for basements. The expected effect is clearly evident, and it has been eliminated by requiring a "no" answer to the question. Our study is therefore restricted to first measurements on houses.

Another obvious source of bias is that a person is more likely to purchase a measurement if a nearby neighbor has a high radon level. The questionnaire therefore asks "How far away is the closest house you know to have a high radon level". The ratios of mean radon levels for distance D to distance 16 km or more (or don't know) are: D=0-1.6 km, 1.88 [2.11]; D=1.6-8 km, 1.20 [1.26]; D=8-16 km, 1.03 [1.15]. Based on these results, data were eliminated if D is less than 8 km.

The remainder of this paper deals with analysis of the 70,000 measurements described above. We will present mean radon levels for various situations. This raises the question of whether to use geometric or arithmetic means. A problem with the latter is that it is heavily influenced by very large measurements which, since they occur infrequently, introduces "random" fluctuations into the results. This is avoided by using geometric means. The latter would be heavily influenced by measurements close to zero which have large statistical uncertainty but this problem is avoided by setting a lower limit of 11 Bq m^{-3} (0.3 p Ci L^{-1}); any measurements below that were set equal to this lower limit. Mean radon levels will be presented, in units of the widely accepted world mean for houses, r_0, where r_0 = 37 Bq m^{-3} (1.0 p Ci L^{-1}).

---

*This question was suggested to the author by David Gur.

Questionnaire Items

The questionnaires were changed frequently, but the most persistently asked questions (names for later reference given in capital letters) were:

- LEVEL - "Is the room where test was made (a) mostly below ground level, (b) lowest floor above ground, (c) second floor above ground, (d) third or higher."

- ROOM - "Type of room where test was made (e.g., livingroom, bedroom) _____"

- AGE - "Age of house _____ (If not known, best guess)"

- WEATHERIZE - "How much has been done since 1975 to reduce heat loss from your house by weather-stripping, closing gaps under doors, sealing windows, etc.?
_____ much, _____ little, _____ nothing"

- DRAFTY - "How drafty is your house compared to other houses in your area?
_____ more than average, _____ about average, _____ less than average"

- LOCATION - "The location of the house is (check one):
_____ urban, _____ suburban, _____ rural"

- POLLUTION - "Is the air pollution in your area (check one):
_____ less than average, _____ about average, _____ worse than average?"

- VALUE - "What is the approximate market value of your house?" _____

- INCOME - "Annual household income?" _____

- EDUCATION - "Head of household's years of formal education beyond eighth grade (for example, high school graduate = 4)?" _____

- CIGARETTES - "How many cigarettes per day are smoked by all members of your household combined?" _____

- OWN - RENT - "Do you own or rent this house?" _____

Results

The analysis consists mainly of determining mean radon levels for each response to each questionnaire item for the total file and for each geographic area, and also for each pair of responses which we refer to as cross correlations. Since complete tables of cross correlations would be far too voluminous for this paper, these results will mostly be presented through discussion.

In Tables 1-3, for the total file the first entry (in parenthesis) is the number of responses in hundreds, the second entry is the mean radon level in units of r_0, and the third entry is the ratio of the mean radon level to the one designated 1.00. For the separate geographic areas, the second of these entries is omitted.

Level and Room

Table 1 gives the results for LEVEL and ROOM. It is evident that basements which are mostly below ground have about twice the radon level of first floor living areas. Levels on second floors are a few percent lower than on first floors. Only 4% of our measurements are from above the first floor, and only 0.2% are from above the second floor but, while statistics are poor, they are consistent in indicating substantially lower radon levels on third floors and above. High rise apartment dwellers are clearly grossly under-represented in our data.

The results on ROOM types in Table 1 can be better understood with the aid of the cross-correlation with level, shown in Table 4, with the last column giving the percent of cases where the room was mostly below ground. We see that the reason why family rooms, bedrooms, and halls in Table 1 have higher average radon levels than living rooms, dining rooms, and kitchens is because they are more frequently below ground. This represents another type of measurement bias: it seems probable that far less than 27% of U.S. bedrooms are below ground, but that below ground bedrooms are an incentive to purchase radon measurements. The residual room-to-room variations in Table 4 may be due to variations in the fraction of the room that is below ground; for example, "mostly below ground" rooms may average 60% below ground for living rooms vs. 90% for basements. Another factor is that below ground rooms that are used as living areas are less likely to have cracked walls and floors.

There have been claims that kitchens are not a suitable place for radon measurements. The fact that average levels are similar in living rooms, dining rooms, and kitchens in Tables 1 and 4 is strong evidence to the contrary.

Results for other questionnaire items are listed separately for living areas in Table 2 and for basements in Table 3. The first row of these gives mean radon levels for the entire data files - 1.68 for living areas and 3.34 for basements - and also shows the number of measurements in each geographic area.

Age

The results on AGE (of houses) indicate that radon levels increase during the first year. Houses 1 - 9 y old have the highest levels, and levels decrease monotonically with increasing age up to 80 y old where they are only about $\frac{2}{3}$ as high. For houses more than 80 y old, radon levels increase. The decrease out to 80 y and the increase beyond is observed for both living areas and basements; for all geographic areas; for all degrees of weatherization, draftiness, or pollution; for urban, suburban, or rural locations; for houses of all value above $40,000; for occupants of all EDUCATION, and of all incomes above $15,000 per year; and for both owner-occupied and rented houses. The only exceptions are houses valued at less than $40,000, or with occupant annual incomes below $15,000. For these, radon levels seem to increase slowly with AGE beyond 5 y.

Data on the former are shown in Table 5. The bottom row, which gives the ratio of radon levels for age 0-9/age 50-79, shows that this ratio increases monotonically from the lowest to the highest value houses. Also notable from Table 5 is the fact that expensive houses are predominantly new while low cost houses are predominantly old, with a steady progression between these extremes as the value changes.

Weatherize

The WEATHERIZE results in Tables 2 and 3 yield the surprising conclusion that tightening houses to conserve fuel has done essentially nothing to increase radon levels except perhaps in the SC-W area. With that exception, the most consistent finding is that houses where "little" has been done to weatherize have lower radon levels than those that have done "nothing" or "much". It is difficult to imagine an explanation for that behavior.

The ratio of mean radon levels for houses where "much"/"nothing" has been done is 1.06 for living rooms, 1.06 for dining rooms, 1.00 for kitchens, 0.97 for family rooms, 1.07 for bedrooms, 1.08 for halls and 0.99 for basements; there are no large differences among the various rooms. It is 1.02 [1.06] for houses less than 10 y old, increasing with age to 1.27 [1.21] for houses 50-79 y old, which seems reasonable since new houses would not have as many cracks, but it drops back to 1.12 [1.10] for ages over 80 y. It is 1.21 [1.09] for urban houses, 1.07 [0.98] for suburban, and 0.98 [0.95] for rural; perhaps weatherizing rural houses includes measures which prevent entry of radon from the ground(?). For houses that are more drafty than average, average, and less drafty than average, the "much"/"nothing" ratio is respectively 1.23 [1.67], 0.98 [0.96], and 0.93 [0.84]. This means that weatherizing increases radon levels only in exceptionally drafty houses, where the weatherization probably consisted mainly of sealing openings. In houses that are not drafty, this was presumably not done and perhaps insulation was added which might act to reduce radon entry. Of course, the judgement of how drafty the house is refers to the time of the measurement which is after the weatherizing has been completed.

The "much"/"nothing" ratio decreases monotonically with increasing values of the house: 1.26 [1.01] for less than $40,000; 1.14 [1.08] for $40-75,000; 1.01 [0.97] for $75-130,000; 0.93 [0.97] for $130-200,000; and 0.97 [0.88] for over $200,000; apparently weatherizing does most to reduce air exchange with outdoors in lower cost housing. A similar pattern for the ratio appears in the cross correlation with income: 1.15 [1.12] for incomes less than $15,000 per year; 1.04 [1.04] for $15-25,000; 1.07 [1.01] for $25-45,000; 0.99 [0.97] for $45-70,000; and 0.90 [0.92] for over $70,000. For owner-occupied houses, the ratio is 0.98 [0.94] vs. 1.19 [1.14] in rented houses. In summary weatherizing has increased radon levels by 15-20% in low cost houses, occupied by low income families, but has actually reduced radon levels in expensive houses owned and occupied by high income families. Perhaps wealthier people weatherize by improving insulation which does not affect air exchange, whereas poorer people seal cracks which inhibits air exchange and thereby increases radon levels.

It is interesting to note that the fraction of respondents who did much/little/ nothing to weatherize is about the same for all income levels, roughly 2/2/1. One might think that high income people would have done more because they are better able to afford the costs

of weatherizing, but on the other hand they are also better able to afford the cost of heating fuels.

Only 20% of our respondents said they have done nothing to weatherize their houses since 1975, whereas typical estimates are that about 50% of all houses have been weatherized. This can be explained by the fact that people who purchase radon measurements are untypically interested in home improvement.

Drafty

The correlations with how drafty a house is are large and consistent in Tables 2 and 3, as is expected from the fact that drafty houses have more air exchange with outdoors where radon levels are much lower than indoors. The ratio of mean radon levels in houses less drafty/more drafty than average is 1.56 [1.47] for our total files, and for geographic areas it is 1.58 [1.48] in NE (-NJ), 1.47 [1.38] in NJ, 1.48 [1.34] in SE, 1.59 [1.36] in MW, and 1.57 in SC-W. It is 1.39 in living rooms, 1.40 in kitchens, 1.76 in family rooms, 1.64 in bedrooms, and 1.46 in basements, with much of this variation explainable by statistics. There is no clear trend with age of the house, although there may be a peak at 10-19 y where the ratio is 1.80 [1.68], and the effect seems to be reduced for houses over 80 y old, ratio = 1.09 [1.22]. There does seem to be a dependence on weatherization activities; for houses where much, little, and nothing has been done to weatherize, the ratio is respectively 1.44 [1.12], 1.55 [1.40], and 1.91 [2.23]. As suggested above, perhaps weatherizing drafty houses consisted largely of sealing openings, which did increase radon levels.

For urban, suburban, and rural houses, the ratio is respectively 2.08 [1.55], 1.52 [1.41], and 1.49 [1.53], which seems to indicate that draftiness plays a more important role in urban homes. There is no consistent trend in the ratio with socioeconomic factors.

The ratio is substantially higher for owner-occupied than for rented houses, 1.58 [1.41] vs. 1.16 [1.25]. Perhaps rented houses have more very small openings which contribute in an important way to air exchange rates without affecting draftiness. Only 4.5% [4.0%] of owner-occupied houses, vs. 17% [17%] of rented houses were judged to be more drafty than average.

Location

The data in Tables 2 and 3 clearly indicate that rural houses have substantially higher radon levels than urban and suburban houses. One possible explanation is that rural areas are more windy, leading to stronger chimney effects which cause radon to be sucked in from the ground. Another suggestion[††] is that urban sewer drains go into storm sewers whereas rural drains go into the ground, leaving an open path for radon to come out of the ground, into the house. There may be other construction differences between urban and rural houses to explain this effect. The result is quite important since it means that urban people, who have more lung cancer, have lower radon exposure.

For most geographic areas, Tables 2 and 3 indicate that radon levels are substantially higher in suburban than in urban houses, but a major exception here is the Midwest (MW). This last is a "fluke" resulting from the fact that urban and suburban measurements came

from different areas; urban measurements came heavily from Columbus and Dayton, OH and Des Moines, IA, where radon levels are high, while one third of the suburban measurements are from the Chicago area where radon levels are comparatively low.

Since this case represents a potential serious weakness in this type of study, we consider it in more detail with reference to Table 6 where the geogrphic area is divided into its three principal components by zip codes. Note that the middle zip code range has much higher radon levels than the other two, and it includes far fewer suburban cases but more urban cases (note that what is perceived as "urban" in Iowa is not necessarily the same as in the Chicago area). It is easy to calculate averages from the data given, and in doing so one finds that, although the urban/suburban ratio (last column of Table 8) is less than unity for each of the three components, it is substantially greater than unity when all three are combined.

On the other hand, it should be recognized that when the whole nation is considered, with its multitude of variations in types of urban and suburban areas located in various geologic settings, the correct conclusion, that suburban areas have higher radon levels, does come through, and it also comes through in the majority of individual geographic areas.

While the question of urban vs. suburban radon levels involves some complications, there can be no question but that rural houses have appreciably higher radon levels than either. For our entire data file, the rural/suburban ratio is 1.31 in living rooms, 1.26 in dining rooms, 1.28 in kitchens, 1.29 in bedrooms, 1.34 in halls, but 1.47 in basements and 1.49 in family rooms. It is 1.45 for rooms mostly below ground vs. 1.28 on first floors and 1.24 on second floors. This may indicate that the reason for the difference is in the basement source.

The rural/suburban ratio vs. age of the house is 1.30 [1.26] for age 0-4, 1.23 [1.39] for age 5-9, 1.23 [1.44] for 10-19, 1.23 [1.43] for 20-29, 1.24 [1.47] for 30-39, 1.26 [1.38] for age 40-49, 1.53 [1.48] for age 50-79, and 1.50 [1.25] for ages over 80 y. It is 1.26 [1.46] for houses that have done much to weatherize, and 1.27 [1.48] for those that have done nothing. It is 1.29 [1.31] for drafty houses vs. 1.27 [1.42] in houses that are less drafty than average. We see in Table 7 that the ratio increases with increasing value of the house; expensive rural houses have much higher radon levels than expensive suburban houses, but there is far less difference for low cost houses. However, there is no indication of such a trend with income: progressing from the lowest to the highest income bracket gives rural/suburban ratios 1.24 [1.51], 1.35 [1.45], 1.30 [1.46], 1.28 [1.56], 1.28 [1.41]. The ratio is somewhat higher for rented than for owner-occupied houses, 1.51 [1.63] vs. 1.33 [1.44].

Pollution

The results in Tables 2 and 3 indicate that there is a clear negative correlation between air pollution and mean radon levels. High air pollution regions have lower levels than low pollution regions for each geographic section of the nation in both living areas and basements. It is difficult to concoct a direct cause-effect explanation; the most obvious one would be that in polluted areas people do not open their windows as much, but that would increase indoor radon levels, contrary to our finding. An obvious confounding relationship is that air pollution is highest in urban areas where we have found radon levels to be low.

The cross-correlation between LOCATION and POLLUTION is shown in Table 8. It is true that the great majority (71%) of rural houses are in regions of below average pollution,

while most suburban (62%) and urban (64%) houses are in areas of "average" pollution. Moreover 9% of urban houses, vs. only 4% of suburban and 1% of rural houses are in "above average" pollution areas. But still, among rural houses only, or among suburban houses only, or among urban houses only, low pollution areas have higher radon levels than high pollution areas by substantial factors both in living areas and in basements. One might assign part of the explanation to varying judgements on what is high or low pollution, or what is urban or suburban, or what is suburban or rural. But even suburban and rural highpollution areas have substantially lower radon levels than low pollution urban areas. This would seem to imply that the negative correlation between air pollution and radon is not due only to urban-rural effects.

The low/high pollution ratio of mean radon levels is 1.43 in basements, 1.31 in first floors, and 1.19 on second floors. This might be interpreted as indicating that the difference is due to basement entry. There is little variation in this ratio with room type (other than it is somewhat higher in basements and family rooms), with age of the house, with how much has been done to weatherize, or with how drafty the house is. There is also no systematic variation with any of our socioeconomic factors, value of the house, household income, or education of head of household. It is higher in rented than in owner-occupied houses, 1.83 [1.53] vs. 1.23 [1.37]. In summary, radon levels are substantially higher in low pollution than in high pollution areas, there is evidence that this is not simply due to urban-rural effects, but there is no clear hint from our studies of what these other causes might be.

Value

The results in Tables 2 and 3 seem to indicate that houses valued at less than $40,000 have about 15% lower radon levels than others, and there is a tendency for expensive houses to have lower levels than intermediate value houses. Mean radon levels in the cheapest houses are lower than in any other value category in 4 [3] of the 5 geographic areas and are second lowest in the remaining 1 [2] categories. They have the lowest mean radon level in kitchens, bedrooms, and basements, but the most expensive houses have the lowest in living rooms, dining rooms, family rooms and halls. Explanations for this are difficult to concoct.

The cross correlation between value and age is shown in Table 5. We see there that for living areas of houses less than 30 y old, the least expensive houses have substantially lower radon levels than the others, but for houses more than 30 y old, the least expensive houses have the highest radon levels. For basements, they have the lowest levels up to age 20, and the second highest levels above age 50. This switch-over can perhaps be explained by the fact that older low-value houses were often originally constructed as expensive houses but their value deteriorated by aging or by changes in the neighborhood.

[††] This suggestion was offered by David Gur.

About 10% of the "more drafty than average" houses, but only 3% of the "less drafty than average" houses are valued at less than $40,000. Among the more drafty houses, radon levels are nearly constant but declining with increasing value of the house, but for houses of average or lower draftiness, radon levels are lowest for the least and most expensive, and highest at intermediate value. About 13% of the urban houses, but only 2.5% of the suburban and 6% of the rural houses are valued below $40,000.

The cross correlation between LOCATION and VALUE is given in Table 7. We see there that lowest value houses have higher radon levels than expensive houses in urban areas, but the former have by far the lowest levels in rural houses. Intermediate value houses have the highest radon levels for all locations.

The cross correlation between VALUE and INCOME is given in Table 9. As expected we see that low income people live in low value houses and high income people live in high value houses with a steady progression between. But for each income level independently, intermediate value houses have the highest radon levels.

For owner-occupied houses, radon levels are lowest for the least and most expensive houses with a peak at about $75,000, but for rented houses low value houses have higher radon levels and these levels decline steadily with value.

Income

Table 2 indicates that houses of lowest income people have about 15% lower radon concentration than others, with no clear trend for incomes above $15,000 per year. According to Table 3, there is essentially no variation of radon level with income for basements.

The ratio of radon levels for annual incomes <$15,000/>$70,000 is 0.87 for living rooms, 0.70 for dining rooms, 0.92 for kitchens, 0.95 for family rooms, 0.69 for bedrooms, 0.87 for halls, and 0.94 for basements. The cross- correlation between INCOME and AGE is similar to that between VALUE and AGE (Table 5), with low income families having lower radon levels in new houses and higher levels in old houses, but the differences are less sharply defined here.

The ratio of radon levels for <$15,000/>$70,000 is 0.83 [1.04] for those who have done "much" to weatherize, 0.76 [0.93] for those who have done "little" and 0.65 [0.85] for those who have done "nothing". This monotonic trend confirms our previous conclusion that weatherizing increases radon exposure for poor people much more than for rich people. This ratio is 0.82 [0.84] for drafty houses, 0.78 [0.95] for houses of average draftiness, and 0.93 [1.02] in "less drafty than average" houses. Apparently the effect of income is largest in drafty houses, and almost disappears in houses that are not drafty.

This ratio is 0.84 [0.96] for urban, 0.76 [0.90] for suburban, and 0.73 [0.96] for rural houses, and it is 0.89 [0.96] for owner-occupied houses vs. 0.72 [0.82] for rented houses.

From Table 9 we note that for expensive houses radon levels increase monotonically with increasing income, but for houses valued at less than $40,000, averaging between living areas and basements there is a slow monotonic decrease with increasing income. Low income people living in expensive houses and high income people living in cheap houses have substantially lower radon levels than people living in houses matched to their income.

Education

The questionnaire item on head of household's years of formal education beyond eighth grade was apparently widely misunderstood because the majority of responses correspond to post-baccalaureate college education. Perhaps it was interpreted as total years of formal education. Nevertheless, the data do provide some information on trends of mean radon levels vs. education on a relative scale.

There is some indication in Tables 2 and 3 of a slight trend for more educated people to have higher radon levels. The ratio of mean radon levels for most/least educated is 1.03 in living rooms, 1.09 in dining rooms, 1.03 in kitchens, 1.15 in family rooms, 1.04 in bedrooms, 1.05 in halls, and 1.14 in basements.

The least educated have the lowest radon levels, averaging between living areas and basements, for houses of all ages, although the differences are by only a few percent for houses over 40 y old. They have the lowest radon levels for each response to the WEATHERIZE question, for each response to the DRAFTY question, for each response to the LOCATION question, for each response to the POLLUTION question, for each but the lowest VALUE of the house response, for all but one INCOME bracket, and for owner-occupied – but not for rented-houses. One reason for this unusually high degree of consistency is that there are reasonably good statistics for all responses to the EDUCATION question. The conclusion is that homes in which the head of household did not finish high school have about 10% lower radon levels than average.

Cigarettes

The results in Tables 2 and 3 clearly indicate that households with cigarette smokers have substantially lower radon levels than the others, but for some strange reason it seems like the difference decreases with increasing number of cigarettes smoked. It should also be noted from those tables that only 17% of all people who purchased radon measurements have smokers in their households, whereas 33% of American adults are smokers.

The ratio of mean radon levels between non-smokers and the average of the three categories of smokers (CIGARETTES=0/>0) is 1.13 in living rooms, 1.19 in dining rooms, 1.13 in kitchens, 1.06 in family rooms, 1.11 in bedrooms, 1.08 in halls, and 1.12 in basements. Our earlier indication that this ratio is much larger in living rooms and dining rooms (Cohen and Gromicko 1988) proved to be misleading.

The ratio is 1.06 [1.07] for houses of age 0-4, 1.12 [1.12] for age 5-9, 1.10 [1.10] for age 10-19, 1.06 [1.10] for age 20-29, 1.08 [1.11] for age 30-39, 1.08 [1.08] for age 40-49, 1.10 [1.07] for age 50-79, and 1.03 [1.12] for age over 80. Clearly there is little or no correlation with age of the house. There is similarly little correlation with how much has been done to weatherize and with whether the location is urban, suburban, or rural. For drafty houses, the ratio is 1.30 [1.15] whereas for average and less drafty houses it is respectively 1.03 [1.21] and 1.11 [1.07]. 7.7% [5.0%] of smokers vs 4.3% [3.8%] of non-smokers reported their houses to be excessively drafty.

There does seem to be a correlation with value of the house and income. The 0/>0 ratio is 1.32 [1.30] for house values below $40,000, 1.17 [1.18] for $40-75,000, 1.11 [1.01] for

$70-130,000, 1.10 [1.10] for $130-200,000, and 0.95 [1.03] for > $200,000, and it is 1.22 [1.22] for incomes below $15,000 per year vs. 1.10 [1.10] for annual incomes over $70,000. The ratio is about the same for owner-occupied as for rented houses — 1.14 [1.13] vs. 1.16 [1.10].

In summary, houses of cigarette smokers have about 15% lower radon levels than houses of non-smokers, with the effect almost twice as large for low income families living in low value houses, and almost disappearing for high income people living in high value houses.

Own-rent

The results listed in Tables 2 and 3 clearly indicate that owner-occupied houses have higher radon levels than rented houses; the own/rent ratio is 1.28 [1.14]. This is important because rented houses are grossly under-represented in our data base.

Cross correlations are hindered by the small numbers of rented houses, leading to relatively large statistical uncertainties. The own/rent ratio is 1.21 for living rooms, 1.23 for dining rooms, 1.31 for kitchens, 1.16 for family room, 1.23 for bedrooms, 1.50 for halls (with poor statistics), and 1.14 for basements. There is little systematic variation with age of the house except that for houses over 50 years old basement ratios fall below 1.00. The ratio is 1.24 [1.12] in houses where "much" has been done to weatherize, vs. 1.50 [1.36] where "nothing" has been done. Apparently weatherized rented houses are more like owner-occupied houses. The ratio is only 0.99 [1.07] in drafty vs. 1.35 [1.21] in "less drafty than average" houses. The ratio is 1.48 [1.20] in urban, 1.28 [1.17] in suburban, and 1.13 [1.04] in rural houses, a monotonic relationship. It is 1.08 [1.19] in areas where air pollution is below average vs. 1.60 [1.34] where pollution is above average, a rather large difference which is at least partly related to the urban- rural difference.

The own/rent ratio is below unity, 0.82 [1.06], for houses valued at less than $40,000, but increases with value to 1.16 [0.98] for $40-75,000, 1.38 [1.14] for $75-130,000, 1.21]1.52] for $130-200,000, and 1.48 [1.27] for >$200,000. The cross correlation with income seems to behave differently, 1.39 [1.38] for income <$15,000 per year, 1.08 [1.12] for $15-25,000, 1.36 [1.07] for $25-45,000, 1.56 [1.31] for $45-70,000, and 1.13 [1.19] for >$70,000. It is difficult to reconcile this difference except as statistical fluctuations. There is no systematic trend in the own/rent ratio vs. education of head of household.

In summary, the own-rent ratio seems to vary systematically with several factors but the reasons for these variations are obscure. Perhaps many of them are due to poor statistics as there are less than 100 rented homes in most categories.

References

Cohen, B.L.; Nason, R. A diffusion barrier charcoal adsorption detector for measuring radon concentrations in indoor air. Health Phys. 50: 457-463; 1986.

Cohen, B.L.; Gromicko, N. Variation of radon levels in U.S. homes with various factors. Jour. Air Polltuion Control Assn. 38: 129-134; 1988.

Cohen, B.L.; Performance characteristics of DBCA radon detectors. Rad. Protection magnet. 5:47-54; 1988.

Cohen, B.L.; Cohen, F.B. Error prevention at a radon measurement service lab. Rad. Protection Mngmt. 6:43-47; 1989.

Cohen, B.L.; Seasonal variations of radon levels in homes. Health Phys. - submitted; 1989.

The work described in this paper was not funded by the U. S. Environmental Protection Agency and therefore the contents do not necessarily reflect the views of the Agency and no official endorsement should be inferred.

Table 1: Mean radon concentration vs level with respect to ground and vs room type for various geographic areas of the United States "living" refers to the rooms listed other than "basement" Geographic areas refer to zip codes· NJ 07000-08999, NE 0-19999, SE - 20000-39999, MW - 4000-69999, SC + W 70000 99999 Under "U S total" column, the figure in parenthesis is number of measurements (in hundreds), the next number is the mean radon level in units of r_0 and the third number is the ratio of the mean radon level to the one marked 1.00 in the same column In other columns, the second of these numbers is not included

RESPONSE	U S TOTAL	NE (-NJ)·	NJ	SE	MW	SC+W
LEVEL						
below ground						
-basement	(251)-3 39-1 96	(92)-2 09	(47)-2 12	(31)-2.02	(69)-1 77	(8)-2 52
-living	(31)-2 86-1 65	(8)-1 68	(2)-1.62	(5)-1.56	(11)-1 45	(4)-2 07
1st above grd						
-basement	(8)-2 43-1 40	(3)-1 41	(1)-1.84	(1)-1 46	(1)-1 22	(5)-1 00
-living	(157)-1 73-1.00	(47)-1.00	(23)-1.00	(31)-1.00	(33)-1.00	(21)-1.00
2nd above grd	(20)-1 62- 94	(7)- 91	(4)- 94	(4)- 99	(3)- 88	(2)-1 16
3rd or higher	(1)-1 04- 60	(3)- 51	(2)- 70	(2)- .63	(2)- 54	(2)- 72
ROOM						
basement	(298)-3 32-2.27	(104)-2 44	(70)-2.46	(40)-2.38	(72)-1.92	(9)-2 30
living room	(106)-1 46-1.00	(33)-1.00	(28)-1.00	(16)-1.00	(17)-1.00	(12)-1.00
dining room	(26)-1 40- 96	(8)- .92	(8)- 98	(4)-1.03	(4)-1.01	(2)- 96
bedroom	(60)-1.83-1.25	(13)-1 14	(12)-1.21	(14)-1 28	(11)-1 33	(9)-1 17
family room	(80)-2 05-1 40	(20)-1 70	(22)-1 34	(15)-1.44	(17)-1 26	(6)-1 25
hall	(12)-1.77-1.21	(3)-1 17	(3)-1 24	(2)-1 22	(3)-1.29	(1)- 95
kitchen	(50)-1 46-1.00	(14)-1 02	(14)-1.07	(8)-1 08	(8)-1 04	(5)- 89

Table 2: Mean radon levels from measurements in living areas for various responses to questionnaire items See caption for Table 1

RESPONSE	U.S. TOTAL	NE (-NJ)	NJ	SE	NW	SC+W
		TOTAL LIVING AREAS				
	(374)-1.68	(105)-1.74	(94)-1.35	(73)-1.75	(67)-1.84	(41)-2.06
		AGE				
0-1	(4)-1.61-.84	(.7)-.95	(2)-.96	(.7)-.72	(.3)-.82	(.2)-.90
1-9	(103)-1.92-1.00	(25)-1.00	(23)-1.00	(27)-1.00	(13)-1.00	(14)-1.00
10-19	(84)-1.85-.96	(20)-.95	(21)-.96	(18)-1.05	(15)-.93	(10)-.94
20-29	(65)-1.65-.86	(16)-.81	(18)-.82	(12)-.96	(13)-.95	(6)-.83
30-39	(49)-1.57-.82	(14)-.87	(13)-.72	(7)-.82	(11)-.86	(4)-.91
40-49	(19)-1.47-.77	(6)-.73	(5)-.75	(3)-.69	(4)-.82	(2)-.86
50-79	(33)-1.22-.64	(11)-.58	(8)-.58	(4)-.63	(7)-.73	(3)-.81
80+	(24)-1.46-.76	(12)-.67	(5)-.88	(2)-.73	(4)-.81	(11)-.97
		WEATHERIZE				
much	(129)-1 76-1 02	(37)- 87	(24)-.99	(25)-1.06	(27)-1.07	(15)-1 21
little	(147)-1.60- 92	(42)-.84	(36)-.93	(27)-.98	(28)-.96	(14)-1.05
nothing	(63)-1.73-1.00	(17)-1.00	(14)-1.00	(16)-1.00	(9)-1.00	(7)-1.00
		DRAFTY				
more drafty	(11)-1 38- 85	(3)-.80	(2)-.92	(2)-.86	(2)-.82	(1)-.76
average	(173)-1.63-1.00	(48)-1 00	(40)-1.00	(35)-1.00	(32)-1.00	(17)-1.00
less drafty	(67)-2.17-1.33	(20)-1.26	(7)-1.35	(11)-1.27	(17)-1.30	(11)-1 19
		LOCATION				
urban	(26)-1.65-.98	(5)-.70	(1)-.69	(4)-.84	(9)-1.18	(6)-.89
suburban	(137)-1.69-1.00	(41)-1 00	(22)-1.00	(29)-1.00	(31)-1.00	(13)-1 00
rural	(67)-2.16-1.28	(23)-1.13	(12)-1.79	(10)-1.19	(12)-1.28	(10)-1.18
		POLLUTION				
<average	(89)-2.09-1.24	(27)-1.11	(13)-1.49	(14)-1.12	(19)-1.30	(14)-1 26
average	(105)-1.69-1.00	(32)-1.00	(15)-1.00	(23)-1.00	(25)-1.00	(9)-1.00
>average	(9)-1.64-.97	(2)-.75	(.6)-.92	(2)-.84	(2)-.78	(3)-1.12
		VALUE				
<$40,000	(13)-1.56-.86	(4)-.69	(.1)-.77	(2)-.73	(5)-.93	(2)-.81
$40K-$75K	(61)-1.82-1.10	(20)-.94	(2)-.94	(11)-.85	(20)-1.04	(9)-.96
$75K-$130K	(105)-1.81-1.00	(28)-1.00	(15)-1.00	(25)-1.00	(22)-1.00	(13)-1 00
$130K-$200K	(100)-1.56-.86	(24)-.76	(38)-1.02	(22)-1.05	(10)-.93	(7)-.96
>$200,000	(36)-1.61-.89	(12)-.75	(14)-1.23	(6)-1.03	(3)-.84	(2)-.88
		INCOME				
<$15,000	(9)-1.39-.85	(3)-.84	(1)-.74	(1)-.74	(3)-.74	(2)-.90
$15K-$25K	(28)-1.72-1.05	(9)-1.03	(3)-.89	(5)-.87	(6)-.95	(5)-1.25
$25K-$45K	(87)-1.75-1.07	(26)-1.07	(15)-.97	(16)-.95	(19)-1.06	(11)-1.15
$45K-$70K	(122)-1 64-1.00	(29)-1.00	(34)-1.00	(30)-1.00	(19)-1.00	(10)-1 00
>$70,000	(42)-1.79-1.09	(12)-1.10	(9)-1.15	(9)-1.08	(7)-.95	(4)-1.10
		EDUCATION				
<4	(85)-1.58-.96	(23)-1.08	(31)-1.01	(10)-.90	(10)-1.00	(10)-.91
4	(35)-1.63-.99	(11)-1.01	(8)-1.00	(5)-.97	(7)-.96	(3)-1.02
5-7	(68)-1.65-1.00	(21)-1.00	(15)-1.00	(12)-1.00	(14)-1.00	(7)-1.00
8	(58)-1.66-1.01	(15)-1.04	(15)-1.07	(12)-.99	(10)-.97	(5)- 99
>8	(172)-1.76-1.07	(46)-1.05	(33)-1.08	(40)-1.01	(33)-1 17	(19)- 94
		CIGARETTES				
0	(307)-1 72-1.00	(83)-1.00	(76)-1.00	(60)-1.00	(53)-1.00	(34)-1.00
1-5	(12)-1.50- 87	(4)- 82	(3)-.91	(2)-.85	(2)-.86	(1)-1 05
6-20	(34)-1.55-.90	(8)-.92	(6)-.89	(7)-.87	(3)-.90	
>20	(18)-1.62-.94	(5)-.96	(4)-.98	(4)- 90	(2)-.77	
		OWN - RENT				
own	(135)-1.91-1.28	(41)-1.35	(17)-1.92	(22)-1.24	(34)-1.23	(19)-1 11
rent	(6)-1.49-1.00	(2)-1.00	(.5)-1.00	(.9)-1.00	(2)-1.00	(1)-1.00

Table 3: Mean radon levels from measurements in basements for various responses to questionnaire items. See caption for Table 1.

RESPONSE	U S. TOTAL	NE (-NJ)	NJ	SE	MW	SC+W
		TOTAL BASEMENTS				
	(325)-3 34	(113)-3 69	(75)-2.97	(45)-3 47	(78)-3 07	(11)-4 45
		AGE				
0-1	(3)-3 23-.77	(9)- 64	(1)-.72	(.7)-.95	(.3)-1.06	(.1)-.84
1-9	(80)-4.18-1 00	(26)-1 00	(19)-1 00	(17)-1 00	(14)-1.00	(4)-1 00
10-19	(61)-3.74- 89	(19)-.92	(14)-.84	(10)-1.05	(15)-.87	(2)-.86
20-29	(55)-3 19-.76	(18)-.81	(13)-.64	(6)-.81	(14)- 85	(1)-.92
30-39	(46)-2 67- 64	(16)-.69	(10)-.54	(4)-.59	(14)-.72	(7)- 68
40-49	(20)-2 72- 65	(7)- 66	(4)-.54	(3)- 65	(5)-.77	(4)- 59
50-79	(37)-2 69- 64	(14)- 62	(8)- 48	(3)- 61	(11)-.89	(8)- 66
80+	(21)-3 40- 81	(11)- 72	(4)- 71	(1)- 85	(5)-1.09	(.3)-1 06
		WEATHERIZE				
much	(116)-3 49- 99	(41)- 94	(21)-.87	(15)-.97	(33)-1.16	(4)-1 50
little	(136)-3 14- 89	(48)- 88	(32)- 82	(17)- 90	(33)-1 00	(4)-1 17
nothing	(49)-3 53-1.00	(16)-1 00	(12)-1 00	(9)-1 00	(10)-1 00	(2)-1 00
		DRAFTY				
more drafty	(11)-2 71- 86	(5)- 82	(2)- 91	(1)-.94	(3)-.96	(.4)- 32
average	(178)-3 14-1 00	(62)-1 00	(40)-1 00	(24)-1.00	(44)-1 00	(6)-1 00
less drafty	(80)-3 96-1 26	(30)-1 21	(12)-1 26	(10)-1 26	(24)-1 31	(3)-1 26
		LOCATION				
urban	(31)-3 10-1.02	(9)-.82	(1)-.64	(3)-.76	(14)-1.34	(2)-.80
suburban	(166)-3 05-1 00	(61)-1 00	(35)-1 00	(22)-1 00	(42)-1.00	(5)-1 00
rural	(64)-4.43-1.45	(26)-1.17	(14)-1.84	(8)-1.63	(14)-1 61	(2)-1.11
		POLLUTION				
less than av	(100)-3 96-1.31	(36)-1 18	(20)-1.49	(11)-1.41	(28)-1 04	(3)-1.05
average	(142)-3.02-1.00	(53)-1 00	(26)-1 00	(20)-1 00	(38)-1.00	(4)-1 00
more than av	(9)-2 85- 94	(3)- 95	(1)-.77	(1)-.75	(3)- 55	(2)-1 24
		VALUE				
<$40,000	(11)-2.96- 83	(4)-.64	(.1)-1.06	(.4)-.84	(6)-.99	(.2)- 53
$40K-$75K	(51)-3 40- 95	(19)- 89	(9)-.82	(4)-1.01	(26)-1 01	(2)-.68
$75K-$130K	(81)-3 58-1.00	(28)-1.00	(8)-1 00	(15)-1 00	(25)-1.00	(5)-1 00
$130K-$200K	(75)-3 30- 92	(23)- 81	(25)-1.16	(15)-1.13	(9)- 92	(2)-1 17
>$200,000	(56)-3 28- 92	(19)- 76	(26)-1 33	(6)- 94	(4)- 87	(7)-1 12
		INCOME				
<$15,000	(6)-3.30- 96	(2)- 86	(.5)-1.07	(.3)-1.14	(2)-.99	(.2)-.94
$15K-$25K	(19)-3.34-.97	(8)-.86	(2)-.88	(2)-1.07	(7)-1.06	(.6)- 90
$25K-$45K	(71)-3.37- 98	(25)-.94	(10)- 90	(9)-.97	(23)-1.01	(3)-.99
$45K-$70K	(92)-3.44-1.00	(27)-1.00	(24)-1.00	(17)-1.00	(20)-1.00	(3)-1.00
>$70,000	(56)-3.45-1 00	(19)- 95	(17)-1.10	(8)-.94	(10)-.98	(2)-1.16
		EDUCATION				
<4	(65)-3 00.89	(25)- 83	(19)-.87	(6)-.86	(11)-1.10	(2)-.76
4	(10)-3 41-1.01	(4)-.96	(3)- 91	(2)-1.12	(2)-1.09	(.5)-1 14
5-7	(22)-3.38-1.00	(7)-1.00	(6)-1.00	(3)-1.00	(5)-1.00	(1)-1 00
8	(23)-3 54-1.05	(7)-1 07	(7)-1.05	(5)-.93	(4)-1 07	(9)-1 03
>8	(215)-3 42-1.01	(73)- 97	(44)-1.00	(32)-.87	(58)-1.21	(7)-1 14
		CIGARETTES				
0	(258)-3.42-1.00	(88)-1 00	(60)-1 00	(38)-1 00	(61)-1 00	(9)-1 00
1-5	(9)-2.92-.81	(3)- 85	(2)-.92	(1)-.93	(2)-.76	(.3)- 91
6-20	(34)-1.55-.90	(10)- 95	(6)-.89	(3)-.96	(8)-.87	(7)-1.05
>20	(16)-3 07-.85	(5)- 91	(3)-1.01	(2)-.98	(5)- 80	(3)-.89
		OWN - RENT				
own	(203)-3 37-1.14	(74)-1 24	(38)-1.23	(25)-1.32	(57)-.96	(6)-1 65
rent	(5)-2.95-1.00	(2)-1 00	(.7)-1.00	(.6)-1.00	(2)-1.00	(.2)-1.00

Table 4. Cross correlation between room type and level with respect to ground. Number in parenthesis is number of measurements (in hundreds), and other number is mean radon level in units of r_0. Last column is the percent of cases for each room type where level is below ground.

ROOM TYPE	BELOW GROUND	FIRST ABOVE	SECOND ABOVE	% BELOW GROUND
LIVING ROOM	(2)-2 41	(42)-1 58	(3)-1 54	4 0
DINING ROOM	(3)-1 40	(10)-1 55	(.8)-1 31	2.5
KITCHEN	(1)-1 92	(16)-1 60	(1)-1 36	5 1
FAMILY ROOM	(17)-2 84	(22)-1 92	(.8)-1 83	43
BEDROOM	(9)-3 17	(18)-1 82	(7)-1 69	27
HALL	(1)-2 94	(4)-1 73	(8)-1 57	21
BASEMENT	(251)-3 39	(8)-2 43	---	97

Table 5. Cross correlation between age of house and value of house. L and B refer to living areas and basements respectively. See caption for Table 4. Last column is ratio of radon levels for value <$10,000/>$200,000. Bottom row is ratio of radon levels for age 0-9/age 50-79.

	VALUE					
AGE	<$40,000	$40-75,000	$75-130,000	$130-200,000	>$200,000	<$ 40,000 / >$200,000
0-4	L(.6)-1.57	L(5)-2 02	L(14)-1 96	L(18)-1 79	L(8)-1.86	1 18
	B(.2)-3.75	B(2)-3.83	B(10)-4 32	B(15)-4 10	B(14)-4.39	1 17
5-9	L(.9)-1 20	L(7)-1 80	L(16)-2 14	L(15)-1 91	L(5)-1.88	1.57
	B(2)-2 81	B(3)-3 95	B(10)-4 48	B(10)-4 07	B(7)-4.05	1 44
10-19	L(1)-1.31	L(12)-1 98	L(25)-2 05	L(23)-1 78	L(7)-1 78	1 36
	B(6)-2 99	B(7)-3 48	B(18)-4 15	B(15)-3 84	B(11)-3 51	1 17
20-29	L(1)-1 42	L(11)-1 96	L(19)-1 77	L(17)-1 47	L(5)-1 48	1 04
	B(9)-3.15	B(9)-3.65	B(16)-3 58	B(12)-2 90	B(8)-2.62	0 83
30-39	L(2)-1 96	L(10)-1 95	L(13)-1 58	L(11)-1 27	L(4)-1 49	0 76
	B(2)-2 58	B(12)-3 06	B(11)-2 74	B(9)-2 27	B(6)-2 45	0 95
40-49	L(1)-1.84	L(5)-1.63	L(5)-1 37	L(4)-1 27	L(1)-1 36	0 74
	B(1)-2.47	B(5)-3.18	B(5)-2.82	B(4)-2 42	B(2)-2 68	1 09
50-79	L(3)-1.53	L(7)-1 46	L(7)-1 26	L(7)-0 91	L(3)-1 07	0 70
	B(3)-3.00	B(8)-3 14	B(8)-2 26	B(6)-2 44	B(5)-2 37	0 79
80+	L(2)-1 59	L(4)-1.55	L(5)-1 58	L(5)-1 29	L(2)-1 33	0 84
	B(2)-3.63	B(4)-3 87	B(4)-3.43	B(4)-3 61	B(3)-2 73	0 75
0-9 / 50-79	L - 90	L -1 31	L -1 63	L -2 03	L -2 05	
	B -1.09	B -1 24	B -1 68	B -1 67	B -1 78	

Table 6: Breakdown of geometric mean and arithmetic average radon levels for location = urban (U), suburban (S), and rural (R) Last column is ratio of U/S for previous column

ZIP CODES	STATES (NUMBER)	NUMBER	MEAN	AVERAGE	AV U/S
40000 -49999	OH (10), MI (15), IN (3), KY (2)	U- 309	1 75	2 75	0 95
		S-1436	1.68	2 91	
		R- 548	1.98	3.43	
50000 -59999	WI (2), MN (2), IA (9), ND (.8), SD (.5), MT (.5)	U- 366	3.28	4 87	0 99
		S- 409	3 41	4.91	
		R- 416	2.70	4 44	
60000 -69999	IL (20), MO (3), KS (1), NE (3)	U- 206	1.13	1.69	0 79
		S-1231	1.45	2.15	
		R- 186	2 02	3.09	
40000 -69999	ALL OF ABOVE	U- 881	2 05	3 38	1 18
		S-3076	1.74	2.87	
		R-1150	2 22	3.72	

Table 7: Cross correlation between location and value of house Last column is ratio of mean radon levels in previous two columns See caption for Table 5

VALUE	URBAN	SUBURBAN	RURAL	RURAL/SUBURBAN
<$40,000	L-(3)-1.66	(3)-1.53	(4)-1.68	1 10
	B-(4)-2.76	(3)-2.70	(3)-3.45	1.28
$40-75,000	L-(8)-1 85	(22)-1 89	(15)-2.11	1 12
	B-(10)-3 52	(23)-3 01	(12)-4 26	1.42
$75-130,000	L-(7)-1 82	(41)-1 86	(19)-2 42	1.30
	B-(7)-3 49	(43)-3.22	(16)-4.87	1.51
$130-200,000	L-(3)-1 31	(31)-1.63	(12)-2.25	1 38
	B-(3)-2.76	(38)-3.07	(12)-4.49	1 46
>$200,000	L-(2)-1 37	(24)-1 47	(9)-2 14	1.46
	B-(2)-2 04	(39)-3 02	(13)-4 52	1 50

RADON IN NORWEIGAN DWELLINGS

T.Strand [1], B.M.R. Green [2] and E.Stranden [3]

[1] National Institute of Radiation Hygiene, Østerås, Norway
[2] National Radiological Protection Board, Oxfordshire, United Kingdom
[3] Radforsk A/S, Fjellhamar, Norway

ABSTRACT

The results of a large scale survey of radon concentrations in Norwegian dwellings are reported. Measurements of radon have been made in 7500 dwellings representing all 450 municipalities. The dwellings were selected by a random sampling procedure based on data from the Central Bureau of Statistics. The number of measurements in each municipality is proportional to its population. The measurements were performed by nuclear track detectors from the National Radiological Protection Board in United Kingdom. The results will be used in an epidemiological study on radon and lung cancer.

INTRODUCTION

From 1983 to 1986 a pilot survey of radon in Norwegian dwellings was carried out (1). In the winter seasons measurements of radon were performed in a total of about 1500 detached houses from 79 out of the 450 municipalities of Norway. These municipalities included about 30% of the total population. Taking into account seasonal differences in radon concentration and that multifamily houses were not included in the survey, the year average of radon concentration in Norwegian dwellings was estimated to be between 80 and 100 Bq/m^3. Comparing these estimates with those from other surveys in other countries, it was concluded that the overall level of radon in Norwegian dwellings is about the same as in Sweden and Finland (2,3). Owing to weaknesses in the sampling procedure (no random selection of dwellings) and because the integration time in the measurements was only 5-7 days, it was recognised that it would be difficult to use this material in any kind of epidemiological study on radon and lung cancer.

In 1986, financial support for a large scale epidemiological study on radon and lung cancer in Norwegian dwellings were given from the Norwegian Cancer Society. The study was started in early 1987 and has been conducted as a collaboration between the National Institute of Radiation Hygiene, the Cancer Registry of Norway and the National Radiological Protection Board in United Kingdom. The objectives and strategy of the study have been presented in an earlier paper (4).

In this paper, some initial results of the radon survey are reported. These data are combined with earlier radon data and information on the building stock and indoor occupancy patterns to give a better estimate of the average radon concentration in Norwegian dwellings. The results from the epidemiological part of the study will be presented later.

MATERIAL AND METHODS

SELECTION OF DWELLINGS

The aim of the survey is to obtain a representative average value of the indoor radon concentration for each of the 450 municipalities in Norway for use in an epidemiological study of radon and lung cancer. The number of dwellings in each municipality is proportional to the population except for the two largest cities, Oslo and Bergen, where somewhat smaller samples were taken due to the higher population density.

Influx of radon from the subsoil and bedrock is the main source of indoor radon in Norwegian dwellings. For an average Norwegian detached or undetached house about 90% of the source term is due to the influx of radon from the ground. For blocks of flats and other multifamily houses the picture is somewhat different: The radon concentrations are generally much lower, and building materials, which are not usually correlated with geology, are usually the most important source of indoor radon. Less than 15% of the population live in flats or other multifamily houses (5). In Oslo, the largest city, about 65% of the population are living in flats. Due to the significant differences in radon levels between houses and flats, it was necessary to stratify the sampling procedure. A census data base with information on the building stock is available at the Central Bureau of Statistics. This data base was used for the selection of dwellings. The sampling procedure is similar to that used in a large scale survey of natural γ radiation in Norwegian dwellings (6).

Because the financial resources were limited, is was necessary to limit the number of measurements to about 10,000. From an epidemiological point of view it was found more appropriate to do one measurement in 10,000 dwellings instead of two measurements in 5,000 dwellings. From an earlier study (1), the radon concentration in bedrooms was found to be on the average about 10% lower than in living rooms. This difference can be explained by the fact that in a large proportion of single family houses the bedrooms are often better ventilated and are on a floor above the living room. However, the higher occupancy in the bedroom compared to other parts of the house means that the measurements in bedrooms would be a good indicator of the relative radon exposure of the population at the municipality level.

THE MEASUREMENTS

The measurements were performed by NRPB type nuclear track detectors (7,8). Preparation, calibration and analyses were performed at the NRPB in United Kingdom, while the distribution of dosemeters to the householders were organized from the National Institute of Radiation Hygiene in Norway. Each month, for a period of 18 months (from March 1987 to October 1988), about 550 detectors were issued to householders in different municipalities. The integration time for the measurements was 6 months. In order to avoid any difficulties from long-term variations in radon concentration in the estimates of annual average of radon concentration for each municipality, the detectors were spread evenly over all seasons of the year. After six months, the householder was asked to return the detector and a questionnaire to the National Institute of Radiation Hygiene. The detectors were stored in a very low radon atmosphere (<10 Bq/m^3) for a maximum of a week at the institute before it was sendt to the NRPB for analysis.

The detectors were sent to the householders without first asking for their agreement to take part in the study. It was anticipated that this procedure would increase the percentage of selected households taking part in the study. A variety of reasons, such as detectors returned without completed questionnaire, changes of address, an unwillingness to participate, lost detectors and so on, meant that the final number of valid measurements was about 7,500 out of the initial 10,000, a success rate of 75%. There was no geographical pattern in the missing fraction of measurements.

RESULTS AND DISCUSSION

In figure 1, a frequency distribution of the measurements for the whole country is shown. The distribution is found to be log-normal. The arithmetic mean of the measurements is calculated to be 53 Bq/m³. Owing to the fact that the sampling procedure was population based and that the measurements in each municipality were evenly distributed in time, this mean value is a good estimation of the annual average radon concentration in Norwegian bedrooms. On an individual level it may be necessary to correct for the seasonal variations in radon concentration. Owing to climatic conditions, concentrations in winter are usually somewhat higher than in summer.

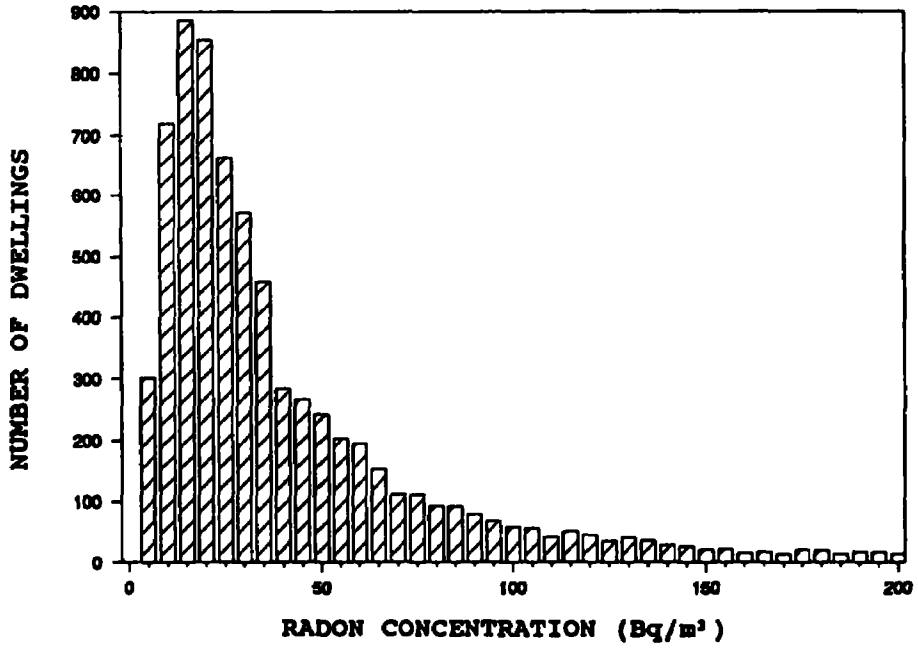

Figure 1. Frequency distribution for radon concentration in bedrooms in Norwegian dwellings.

The frequency distribution in figure 1 has been truncated at 200 Bq/m³. However, about 4% of the results were above 200 Bq/m³ and about 0.3% above 800 Bq/m³. The highest values were found in the eastern part of southern Norway. In this region of the country there are relatively large occurrences of precambrian to silurian rocks like alum shales and granites. Measurements on samples of alum shale from the upper cambrian or lower ordovician period have shown

concentrations of radium up to 4,500 Bq/kg, which is about 100 times higher than the normal level in rocks and soils. In an ealier survey of radon in dwellings on typical alum shale ground (9), more than 75% of the dwellings had an average radon concentration in the heating season above 200 Bq/m³. In our survey, the lowest concentrations were found in dwellings on caledonian ground with large occurrences of gneisses.

In most detached and undetached houses, living room and kitchen are located on the first floor (ie groundlevel). However, in a large proportion of the dwellings, the bedrooms are located one floor higher. In such houses the radon level is assumed to be somewhat lower in the bedroom(s) than in the rooms on the first floor. On the questionnairies, information on "what floor the main bedroom is located" were recorded. In figure 2, the average radon level is shown for bedrooms in the basement, on the first floor and on the second floor. On the average, the radon level was found to be about 20% higher if the main bedroom was on the first floor and 240% in the basement relative to a bedroom on the second floor. According to census data from the Central Bureau of Statistics (5) we may assume that the living room are located on the first floor in all detached and undetached houses in Norway. Assuming that the average radon concentration for the category "bedroom on the first floor" is a representative average for the radon concentration in living rooms for detached and undetached houses, it is possible to correct the annual average of radon concentration in bedrooms to become a more representative estimate for the average in the dwelling. In these estimates it is assumed that 50% of the time indoors is spent in the bedroom, 40% of the time in the living room and 10% of the time in the basement. If the bedroom in located on the basement floor, it is assumed in the calculations that 40% of the time is spent on the first floor. From these calculations the average radon concentration in Norwegian dwellings was estimated to 60 Bq/m³. This average is somewhat lower than the estimate from the pilot study. This may partly be explained by the unrandomized sampling in the pilot study and partly by the fact that the pilot measurements were performed during the heating season in detached houses only.

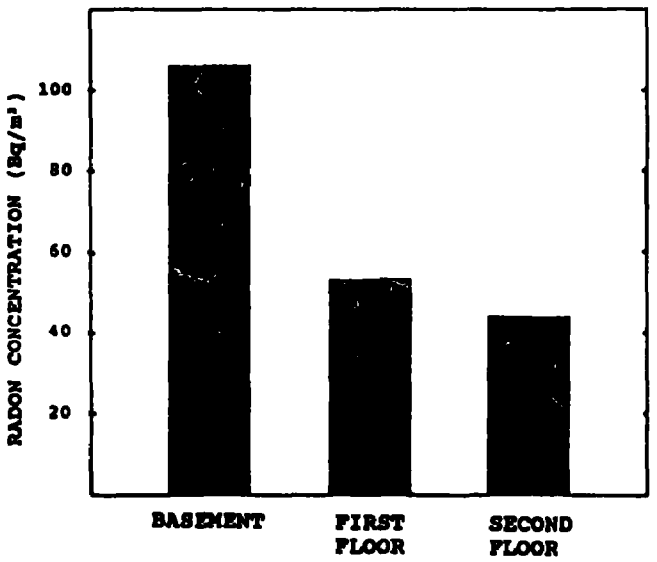

Figure 2. Average radon concentration in bedroom for different categories of dwelling according to on what floor the bedroom is.

In figure 3, the arithmetic averages are calculated for different categories of dwelling. As illustrated the average concentration in detached and undetached houses is 30-35% higher than in blocks of flats. The higher level of radon in detached/undetached houses was expected owing to the fact that the influx of radon from the ground has been found to be the most the most significant source of radon in Norwegian dwellings.

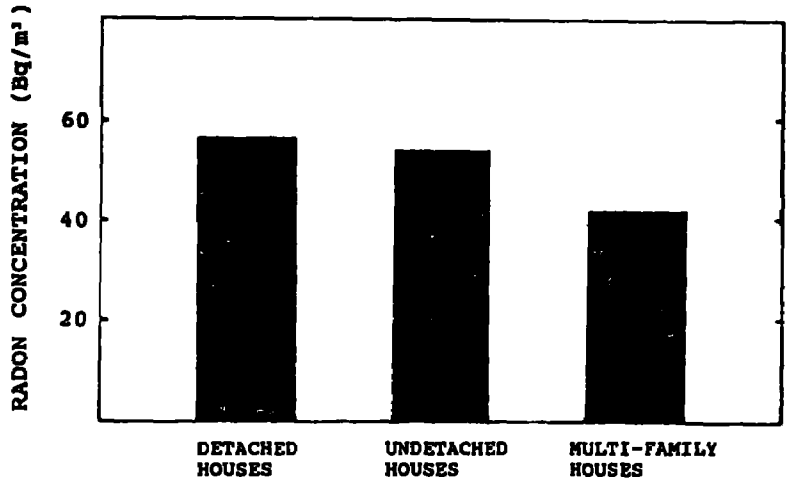

Figure 3. Average radon concentration in the bedrooms for different categories of dwellings in Norway.

In figure 4, average radon concentration in bedrooms are calculated for different categories of dwellings according to year it was built. All types of dwellings are included the estimates. The average radon level does appear to be higher in newer dwellings. This may be attributed in part to the "save energy campaign" in the seventies. It is to be expected that the air exchange rate in newer houses will be less than in older houses.

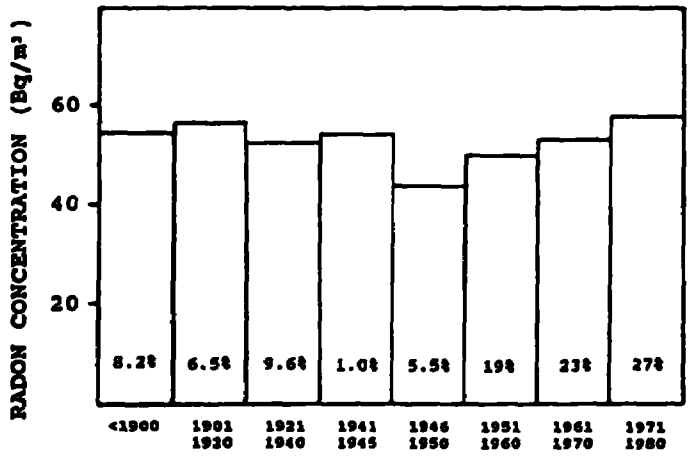

Figure 4. Average radon concentration in bedrooms according to the year the house was built. Percentage of the total sample are included in the histogram for each category.

CONCLUSIONS

The annual average of radon concentration in Norwegian bedrooms is calculated to be 53 Bq/m^3. The radon concentrations were found to be about 30-35 % higher for bedrooms in detached and undetached houses than in blocks of flats. There was no significant seasonal dependence in the results. The highest concentrations were found in the eastern part of southern Norway. However, it is assumed that the radon level in bedrooms on the average is somewhat lower than in the living room. In a large proportion of Norwegian houses, the bedrooms are located one floor higher than the living room and kitchen. By assuming that most living rooms are located on the first floor, by using an average factor for the ratio between bedrooms on the second and first floors to estimate the level in the living room and by assuming that that an average of the concentration in the bedroom and living room is representative for the dwelling, we estimate the average radon concentration in Norwegian dwellings to be 60 Bq/m^3. This is 30-40% lower than the earlier estimates (1).

ACKNOWLEDGEMENTS

This work was supported by the Norwegian Cancer Society - Landsforeningen mot kreft.

The work described in this paper was not funded by the U.S. Environmental Protection Agency and therefore the content do not necessarily reflect the views of the Agency and no official endosrement should be inferred.

REFERENCES

1. Stranden, E. Radon in Norwegian dwellings. In: Proceedings of the Symposium Radon and its Decay Products: Occurrence, Properties, and Health Effects, New York, April 13-18, 1986. American Chemical Society Symposium Series 331, p.70-83.
2. Swedjemark, G.A. and Mjønes, L. Radon and radon daughter concentrations in Swedish homes. Radiat.Prot.Dosim. 7 (1-4): 341-345, 1984.
3. Castren, O., Winquist, K., Makelainen, I. and Voutilainen, A. Radon measurements in Finnish houses. Radiat.Prot.Dosim. 7 (1-4): 333-336, 1984.
4. Stranden, E., Magnus, K., James, A.C., Green, B.M.R. and Strand, T. Radon and lung cancer: an epidemiological study in Norway. Radiat.Prot.Dosim. 24 (1-4): 471-474, 1988.
5. Central Bureau of Statistics. Census data. Personal Communications, 1986.
6. Strand, T., Magnus, K. and Stranden, E. Sampling strategy for a large scale indoor radiation survey - a pilot project. Radiat.Prot.Dosim. 14 (3): 251-255, 1986.
7. Bartlett, D.T., Gilvin, O.J., Still, R., Dixon, D.W. and Miles, J.C.H. The NRPB radon personal dosimetry service. Jour.Radiol.Prot. 8: 19-24, 1988.
8. Bartlett, D.T. and Bird, T.V., Technical specification of the NRPB radon personal dosemeter. Chilton, NRPB-r208 (London, HMSO).
9. Stranden, E. and Strand, T. Radon in an alum shale rich Norwegian area. Radiat.Prot.Dosim. 24(1-4): 367-370, 1988.

Session V:

Radon Entry Dynamics

A Simplified Modeling Approach and Field Verification of Airflow Dynamics in SSD Radon Mitigation Systems

Kenneth J. Gadsby, T. Agami Reddy, Rajiv de Silva, and David T.Harrje

Center for Energy and Environmental Studies
Princeton University
Princeton, NJ 08544, USA

Abstract

The airflow characteristics in the subslab area of a building must be known in order to provide engineering guidance for designing a subslab depressurization (SSD) radon mitigation system. An earlier study had described our research effort to model subslab flows as radial airflow through a porous media confined between two impermeable disks. A laboratory device was also built to experimentally determine the aerodynamic pressure drop versus flow model coefficients for a variety of subslab gravel materials and to test the validity of our modeling approach.

This paper will address the issue of how the simplified model approach along with the laboratory-determined pressure drop coefficients can be used as a rational means of assessing subslab connectivity in actual houses. Preliminary field verification results in a house with gravel under the basement slab are presented and discussed. The way in which the simplified modeling approach could be useful to professional mitigators is described. Illustrative figures of the pressure field extension map from closed-form solutions are presented. Experimental results of the subslab pressure field under single and dual suction penetrations (perimeter and central locations) are shown. Finally, certain practical aspects relating to proper engineering design of the SSD system are addressed and initial recommendations are made.

This paper has been reviewed in accordance with the U.S. Environmental Agency's peer and administrative review policies and approved for presentation and publication.

Introduction

An EPA sponsored workshop was held at Princeton University to summarize available knowledge on various radon mitigation diagnostic techniques (1). The emphasis of the workshop was on diagnostics since each house, housing subdivision, and region may have different characteristics which would require that special attention be paid to system design in order to maximize mitigation system performance and minimize installation cost. This issue was of particular importance since it was found that a large number of mitigated houses still had

radon levels above the recommended guideline of 4 pCi/L. In fact a recent study (2) found that 64% of the mitigated houses in New Jersey, where post-mitigation measurements have been made, remained above the recommended radon level. Diagnostics are therefore crucial for providing information relevant and necessary to the successful design and implementation of a radon mitigation system.

A survey of the workshop participants indicated that systems based on SSD account for more than 50% of all installed systems. (Another promising technique involves subslab pressurization. Since the two techniques are similar in terms of subslab dynamics of induced airflow, they can both be treated in the same scientific framework.) In the pre-mitigation diagnostics phase, the degree of "connectivity" under the slab as well as the permeability characteristics of the subslab medium must be determined before a suitable SSD system can be designed. Proper attention to these aspects will ensure that reasonable flows, and hence the desired degree of depressurization, will prevail at all points under the slab. Lowering the pressures at all points of the subslab to values below those of the basement/crawlspace/living area will then greatly reduce the flow of radon-rich soil-gas into the building.

Parallel with the above aspect is the concern that presently mitigators tend to over-design the SSD system in order to err on the safe side. In doing so, more radon (a 10-fold increase has been cited in Ref.3) from the soil is removed and vented to the ambient air than would have occurred naturally. There is the need to try to prevent these overly robust SSD mitigation systems and therefore decrease exhaust emissions of radon and conditioned indoor air, while simultaneously ensuring that the indoor radon levels do not exceed the recommended value.

We are currently involved in the formulation and verification of a rapid diagnostic protocol for subslab and wall depressurization systems designed to control indoor radon levels (4). It is hoped that the protocol will lead not only to the ability to distinguish between houses that are hard or easy to mitigate, but also to the articulation of a more rational and scientific approach which would be of special usefulness to the ever-increasing body of professional mitigators.

Our approach to the formulation of the diagnostics protocol consists of: (i) a practical component in that specific guidelines would be suggested so that the effectiveness of the engineering design of the radon mitigation system would be enhanced, and (ii) involvement of scientific studies at a more fundamental level which would both lend credence and enable defining the guidelines more rationally. This paper will briefly address the scientific component of the protocol and present preliminary validation of the previously suggested simplified modeling approach to predict the subslab pressure-induced flow by a single central suction hole (5). This paper will also show how the closed-form solutions thereby obtained could be conveniently used to generate figures useful to the professional mitigator. Aspects relating to the proper engineering design of the piping system will also be addressed.

Previous Work

Following an earlier study (6), we had forwarded arguments to support the suggestion that subslab airflow of a residence with either gravel or soil under the concrete slab be visualized as occurring in radial streamlines terminating at the central suction point (5). It was pointed out that the Reynolds number (Re) indicates the flow regime, where Re is defined as:

$$Re = (q/A)\ (1/\upsilon_a)\ (d_v/\phi) \qquad (1)$$

where q = total volumetric flow rate,
A = cross sectional area of the flow (in the case of radial flow through a circular bed of radius r and thickness h, the area $=2\pi rh$),
υ_a = kinematic viscosity of air,
d_v = equivalent diameter of pebbles, and
ϕ = void fraction or porosity of the gravel bed.

It was then shown that subslab airflow under actual operation of mitigation systems is likely to be turbulent if a gravel bed is present under the slab, and laminar when soil is present (6).

The core of any model is the formulation of the correlation structure between pressure drop and Re (or flow rate). For laminar flow, Darcy's law holds and we have (7):

$$(1/\rho_f\ g)\ (dp/dx) = a\ (q/A) \qquad (2)$$

where ρ_f = density of the flowing fluid, and
g = gravitational constant.

In the case of turbulent flows, a model such as the following is widely used:

$$(1/\rho_f\ g)\ (dp/dx) = a\ (q/A)^b \qquad (3)$$

The left side is the pressure drop in head per unit bed length, and the parameter "a" can be loosely interpreted as the resistivity of the porous bed to the flow of the particular fluid. The permeability k of the porous bed is given by:

$$k = (\upsilon_a/g)\ (1/a) \qquad (4)$$

It was then shown in Ref. 5 that the following closed-form solutions are obtained for the pressure drop (in units of head of water) in a homogeneous bed with a circular boundary and with a single suction hole at the center of the disk, see Fig. 1:

For laminar flow:

$$[p(r)-p_a]/(\rho_w\ g) = a\ (\rho_a/\rho_w)\ (q/2\pi h)\ \ln(r/r_o) \qquad (5)$$

where ρ_w and ρ_a are the densities of water and air respectively.

For turbulent flow:

$$[p(r)-p_a]/(\rho_w g) = a\,(\rho_a/\rho_w)\,[(q/2\pi h)^b]\,[1/(1-b)]\,(r^{1-b}-r_o^{1-b}) \qquad (6)$$

The practical implications of the parameters a and b are that, if they are really constant for a given bed material and can be determined by actual experiments in the field, they will serve as indices by which a mitigator will be able to assess how much of the area from the suction hole he can hope to access for a given suction pressure.

In order to evaluate the soundness of the mathematical derivation presented above and also to determine the numerical values of the empirical coefficients, a laboratory model consisting of a 2.4 m diameter circular section and 0.15 m deep was constructed as shown in Figs. 2 and 3. The top and bottom impermeable disks were made from 2 cm thick plywood, and a wire mesh at the outer periphery of the disks was used to contain the gravel between the disks. The apparatus allowed experiments to be conducted with a maximum disk spacing (depth of gravel bed) of 9.5 cm.

A 3.8 cm diameter hole was drilled at the center of the disk to serve as the suction hole. Nine holes, whose layout is shown in Fig. 3, were drilled on three separate rays of the top disk and fitted with a sleeve of 1.3 cm inner diameter PVC pipe with chamfered entrances at either end. Pressure measurements at these nine holes would then yield an accurate picture of the pressure field over the entire bed.

A number of different experimental runs were performed on the laboratory apparatus using two different sizes of river-run gravel (1.3 and 1.9 cm diameter). Least square regression for both the constant "a" and exponent "b" was performed on the observed experimental pressure drop data using eq.(6) (since the flow in the gravel bed was determined to be turbulent). Table 1 summarizes the different experiments performed using the laboratory apparatus and the values of the physical parameters obtained.

Field Verification

The irregular boundary conditions and the non-homogeneity in subslab beds that arise in practice are however not easily tractable with a simple expression such as eqs. (5) and (6), and resorting to a numerical computer code may be the only rigorous way to proceed in order to predict pressure fields under actual situations (8,9). We shall show in this section that our simplified approach nevertheless has practical relevance in that it could be used to determine which areas under the slab have poorer connectivity.

The house under investigation (H21) has a partial basement with a gravel bed under the basement slab. As shown in Fig.4, the basement though rectangular, is close to being square (6.45 x 7.60 m). It has two sides exposed to the ambient air above grade, while the other two sides are adjacent to slab-on-grade construction. Initially, one suction hole of 0.1 m diameter was

drilled at roughly the center of the basement slab to which a temporary mitigation system was installed. Though 19 holes were drilled across the slab (Fig. 4), two of them (holes 11 and 12) were found to be blocked beneath the slab. Consequently, data from only 17 holes have been used in this study. This blockage was later found to be due to the presence of an oversized footing for a support column.

Three sets of runs were carried out which, depending on the airflow rate through the single suction pipe, are termed:

i) 28 L/s - High flow,
ii) 23.4 L/s - Medium flow, and
iii) 18.1 L/s - Low flow,

Note that our analytical expression for the pressure field under turbulent flow given by eq. (6) is strictly valid for a circular disk with boundary conditions at $r = r_o$ and $p = p_a$. We approximate the rectangular basement by a circle of 3.5 m mean radius. We need to also include the extra path length of ambient air flowing down the outer basement wall, going under the footing, and then flowing through the subslab gravel into the suction hole. We estimate this to be about 2 m. Consequently, we find that $r_o = 5.5$ m. The thickness of the subslab gravel bed, h, has been found to be about 5 cm.

The gravel under the slab, though river-run, was found to be highly heterogeneous in size and shape. In general, its average size was slightly less than 1.3 cm. However, we decided to use the properties of the 1.3 cm gravel determined experimentally in the laboratory (see Table 1).

Fig. 5 shows the observed and calculated pressure drops for the high and low flow rates. Readings from holes 13 and 14 are lower and we suspect poorer connectivity to these holes; i.e., some sort of blockage in this general area. We note that the agreement between model and observation (Fig. 5) is indeed striking, given the simplification in our model and also the various assumptions outlined above.

Fig. 5 indicates which areas under the slab are non-uniform. A better way of illustrating how well the model fares against actual observations is shown in Fig. 6. The solid line represents the model predictions while observations are shown by discrete points. We note again the satisfactory predictive ability of this modeling approach and also the fact that certain holes have pressure drop values higher than those predicted by the model.

In order to illustrate the fact that our approach is sensitive to the selection of type of gravel bed, Fig. 7 presents the experimental observations plotted against model predictions with gravel bed coefficients taken to be those that correspond to the 1.9 cm gravel. We note the very large differences between model prediction and observed pressures over the entire basement, thereby suggesting that our approach has enough sensitivity to be of practical relevance.

An alternate approach, to the one adopted here and described above, would be not to assume specific gravel bed coefficients but to determine these from regression. This entails using eq.(6) along with the data set of actual observations and determining the parameters k and b by regression. Since b is not a parameter that varies greatly (5), we have chosen two different values of b (1.6 and 1.7) to see what difference this leads to in terms of the coefficient of determination (R^2) and in the values of k.

Regression results are summarized in Table 2. We have performed three trial runs. Trial 1 uses all data points while, in trial 2, pressure drop observations from holes 11 and 12 (holes that are blocked) have been removed. We note that the R^2 improves dramatically, from 0.80 to 0.96. For trial 3, holes 9 and 10 have been equally removed in order not to bias the regression since these holes have high pressure drop values. We note that the R^2 of trial 3 is 0.88, an improvement over that of trial 1.

Other than the very high R^2 values found, the <u>most</u> striking feature is that regression yields a value of k which is practically identical to that of the 1.3 cm gravel determined experimentally in our laboratory apparatus. This suggests that even a visual inspection of the porous material under the slab can be an indicator good enough for a mitigator to select a standard bed material before using the physical properties of the material get a sound <u>estimate</u> of what the suction pressure ought to be in order to generate a certain pressure field under the slab. The need to categorize commonly found subslab material, deduce their aerodynamic pressure drop coefficients in laboratory experiments, and then tabulate these in handbooks seems to be an avenue worth pursuing.

<u>Graphical Representation</u>

The approach developed here will show how closed-form solutions for the pressure drop in porous beds can be represented in graphical form suitable for professional radon mitigators. Let us illustrate our approach using the simplest case of a circular porous bed with radial inflow between two impermeable disks. From the discussion in the above section, it would seem that we could apply our model equally to square basements and to houses with a partial basement.

Eq. (5) is valid for laminar flow which would prevail where soil is the subslab material (5). It can be written as:

$$\Delta p_h(r)\, k = (\upsilon_a/g)\ (\rho_a/\rho_w)\ (1/2\pi)\ (q/h)\ \ln(r/r_o) \qquad (7)$$

where Δp_h is the pressure drop in head of water and is equal to $[p(r)-p_a]/(\rho_w\, g)$.

Four curves have been plotted in Fig. 8 for four values of (q/h): 1.0×10^{-3}, 5×10^{-3}, 1×10^{-2}, and 2×10^{-2} m^2/s. Thus, if the values of (r/r_o), (q/h), and k are known, $[\Delta p_h(r)]$ can be obtained from this figure.

For gravel under the slab, the flows will probably be turbulent and the pressure drop is given by eq. (6) which can be rewritten as:

$$\Delta p_h(r)\ F = (1/k)\ (\upsilon_a/g)\ (\rho_a/\rho_w)\ [(1/2\pi)^b)]\ [1/(1-b)]\ [(r/r_o)^{1-b}-1] \quad (8a)$$

$$\text{where } F = \{[r_o^{(1-b)}]\ (q/h)^b\}^{-1} \quad (8b)$$

Figure 9 shows plots for $[\Delta p_h(r)\ F]$ vs. (r/r_o). Two curves have been plotted for the two values of b and k. Figures 10a, 10b, and 10c show plots for the correction factor F for different values of r_o and (q/h) values of 0.05, 0.5, and 7.5 m^2/s, respectively. Each graph has two curves, each representing a different value of b (1.4 or 1.6). It is easily seen that these figures can be utilized to obtain values for $\Delta p_h(r)$ for given values of r, r_o, and q/h.

Figures 8, 9, and 10 show how, from a closed-form equation, figures can be generated which would be useful to practitioners. The figures are not meant to cover the entire gamut of conditions which may arise in actual practice.

Post-mitigation Measurements

The temporary mitigation system was removed and a permanent mitigation system was subsequently installed in house H21 which consisted of two suction holes, of 0.1 m diameter, one near the center of the basement slab and one close to (about 0.3 m from) the outside wall which we shall refer to as the perimeter suction hole. The locations of these holes are also shown in Fig. 4.

As part of the post-mitigation diagnostic measurements, we performed a series of measurements of the subslab pressure field under three suction pressures with:

i) both suction pipes open to the suction fan,
ii) the perimeter suction pipe blocked off and the central suction pipe open, and
iii) the central suction pipe blocked off and the perimeter suction pipe open.

Figure 11 depicts the pressure field obtained with the above layout under suction pressure of 150 Pa in the main exhaust pipe. The objective of a SSD mitigation system is to create a pressure field under the slab which is lower than the pressure above the slab (i.e., in the basement). We contend, moreover, that the pressure field should be as uniform as possible over the entire subslab area since this would avoid excess radon-rich soil gas being drawn into the mitigation system and vented to the ambient air. Fig. 11 shows that in case (iii), with only the perimeter pipe open to the exhaust, the pressure field distribution is the most uniform of the three cases. In this regard, this design is more advantageous than the other two. This conclusion is all the more striking since it seems, at first glance, to be contrary to expectations.

Pressure Drop Considerations

There are basically three different sources of pressure drops in the mitigation system:

$$\Delta p_{total} = \Delta p_{bed} + \Delta p_{ent} + \Delta p_{pipe} \quad (9)$$

where Δp_{bed} = pressure drop in porous bed,
Δp_{ent} = pressure drop due to change of direction and that associated with entrance effects into the mitigation pipe, and
Δp_{pipe} = pressure drop in the mitigation pipe.

The pressure drop in the subslab bed is given by equations akin to eq. (5) or (6). The pressure drop at the entrance to the suction pipe involves accounting for the following effects: (i) change in flow direction, (ii) change in cross-sectional area, and (iii) entrance effects at the throat of the suction pipe. From an engineering viewpoint, it is more convenient to treat these together. In accordance with actual practice (10), we propose the following simplified empirical equation for the head loss:

$$\Delta p_{ent}/\rho_w g = K_p [1-(A_p/A_b)]^2 (V_p^2/2g) \quad (10)$$

where K_p is the dimensionless pressure loss coefficient which should not depend on the velocity or the bed thickness, and is a constant for a specific type of bed material,
A_p is the cross-sectional area of the suction pipe,
A_b is the surface area of a cylinder of diameter equal to that of the suction pipe and height equal to the thickness of the porous bed, and
V_p is the velocity of air in the suction pipe.

If d_p is the diameter of the suction pipe, then:

$$A_p/A_b = (\pi d_p^2/4) (1/\pi d_p h) = d_p/4h \quad (11a)$$

and

$$V_p = q/A_p = 4q/\pi d_p^2 \quad (11b)$$

Table 3 assembles the results of determining the entry pressure loss coefficient for three flow rates. We note that K_p values are exactly the same, a gratifying result. This enables us to place a certain amount of confidence in our model for the entrance losses.

The pressure drop in the piping includes losses due to elbows, fittings, as well as straight pipe. Following Ref. 10, losses in the straight pipe are given by:

$$\Delta p_{pipe} = f (L/d_p) (q/A)^2/2g \quad (12)$$

Pressure losses in bends and fittings are normally expressed in terms of

an equivalent pipe diameter. For example, a 90° elbow has the same pressure drop as a straight pipe of length equal to about 25 times the pipe diameter (10).

Since the primary objective of the mitigation system is to create a suction pressure under the slab only, we can define a hydrodynamic effectiveness of the mitigation system based on these three pressure drops:

$$\text{Hydrodynamic effectiveness} = \Delta P_{bed} / \Delta P_{total} \quad (13)$$

We have computed these various pressure drop values for house H21 in order to get an idea of their relative magnitude. The mitigation system (with one suction hole only) in house H21 has about 7 m of straight pipe of 0.1 m diameter and three 90° elbows. This translates into a total length of $7 + (3 \times 2.5 \times 0.1) = 14.5$ m.

Table 4 assembles the various pressure drops in the three elements of the mitigation system. While ΔP_{bed} and ΔP_{ent} have been measured, ΔP_{pipe} has been calculated from eq. (12). The hydrodynamic effectiveness defined by eq. (13) is also given.

Table 4 shows that ΔP_{pipe} is negligible compared to ΔP_{bed}, while ΔP is about one third of ΔP_{bed}. The hydrodynamic effectiveness, close to being independent of the flow rate, is about 75%. Thus 75% of the energy used by the suction fan goes directly into creating the subslab depressurization while the rest can be regarded as being redundant expenditure of energy. Though present knowledge does not permit us to suggest a particular value for the optimal hydrodynamic effectiveness, we suggest that future engineering guidelines dealing with mitigation system design specify a working range for this index.

Concluding Remarks

This paper briefly presents a simple model for predicting the pressure field under the slab of a house when subjected to a single central suction hole. Though both laminar and turbulent flow regimes can be handled, the equations assume a circular geometry of the slab. Verification of these models in the field is presently limited to one house with a relatively uniform gravel bed. We propose to extend this modeling approach to slabs of rectangular configuration with any number of suction holes placed arbitrarily, and to perform more field testing.

This paper highlights the need of performing experiments in the laboratory in order to determine the aerodynamic pressure drop versus flow coefficients of commonly found subslab materials. We have also illustrated by means of sample figures how closed-form equations are eminently suited to the generation of design figures useful to the practical mitigator. We have equally documented the effect of relative suction hole placement (i.e. either at the center or the perimeter) on the subslab pressure maps in a square basement with river-run gravel under the slab. Finally, certain practical views regarding proper piping design of the mitigation system in view of pressure drop considerations are addressed.

Acknowledgements

The assistance of R. Gafgen during the experimental phase of this study is acknowledged.

Nomenclature

A	cross-sectional area of flow
a	parameter representative of the resistivity to flow of the porous bed
b	pressure drop exponent for turbulent flow in gravel beds
d	diameter
d_v	equivalent diameter of pebbles
F	correction factor given by eq. (8b)
f	friction factor
g	acceleration due to gravity
h	thickness of porous bed
K_p	pressure loss coefficient at entry to suction pipe
k	permeability of porous bed
L	length of pipe
Δp	pressure drop
p	pressure
p_a	atmospheric pressure
q	total volume flow rate
R^2	coefficient of determination of regression
Re	Reynolds number
r	radial distance from center of the suction hole
r_o	outer radius of the laboratory apparatus
SEM	standard error of the mean of the regression estimate
V	air velocity
x	distance along flow
ρ	density
υ	dynamic viscosity
ϕ	porosity of porous bed

Subscripts

a	air, ambient
b	porous bed
ent	entrance
f	fluid
p	pipe
w	water

References

1. D.T. Harrje & L.M. Hubbard, Proceedings of the Radon Diagnostics Workshop, April 13-14, 1987 (EPA-600/9-89-057) (NTIS PB89-207898), June 1989.

2. J. Wang & M. Cahill, Radon reduction efforts in New Jersey, paper presented at the Annual Meeting of the National Health Physics Society, Boston, MA, July 4-8, 1988.

3. D.C. Sanchez, Technical issues related to emission releases from subslab radon mitigation systems, presented at ASCE National Conference on Environmental Engineering, Austin, TX, July 9-12, 1989.

4. K.J. Gadsby, L.M. Hubbard, D.T. Harrje & D.C. Sanchez, Rapid Diagnostics: Subslab and Wall Depressurization Systems for Control of Indoor Radon, Proceedings: The 1988 Symposium on Radon and Radon Reduction Technology, Volume 2, EPA-600/9-89-006b (NTIS PB89-167498), March 1989.

5. T.A.Reddy, H.E.Black III, K.J.Gadsby, D.T.Harrje & R.G.Sextro, Modeling air flow dynamics through a homogeneous porous bed with relevance to proper design of radon mitigation systems using subslab depressurization, PU/CEES draft report, Center for Energy and Environmental Studies, Princetion University, Jan. 1990; also, "Airflow dynamics under subslab depressurization: Simplified model approach and preliminary validation" paper presented at the Third Annual AARST Conference, Baltimore, Oct. 16-17, 1989.

6. T.G. Matthews, D.L. Wilson, P.K. TerKonda, R.J. Saultz, G. Goolsby, S.E. Burns & J.W. Haas, Radon diagnostics: Subslab communication and permeability measurements, Proceedings: The 1988 Symposium on Radon and Radon Reduction Technology, Volume 1, EPA-600/9-89-006a (NTIS PB89-167480), March 1989.

7. M. Muskat, The Flow of Homogeneous Fluids through Porous Media, McGraw-Hill, 1937.

8. C. de O. Loureiro, "Simulation of the Steady-State Transport of Radon from Soil into Houses with Basement under Constant Negative Pressure", LBL-24378, Lawrence Berkeley Laboratory, Berkeley CA 1987.

9. J.M.Barbar & D.E.Hintenlang, Computer modeling of subslab ventilation systems in Florida, paper presented at the 34th Annual Meeting of Health Physics, Abstract No. TAM-E8, Albuquerque, NM, 1989.

10. ASHRAE, Handbook of Fundamentals, American Society of Heating, Refrigeration and Air-Conditioning Engineers, Atlanta, 1985.

Table 1. Summary of laboratory experiments using river run gravel and the physical parameters deduced in Ref. 5

Experiment	Diameter of particles nominal (m)	Diameter of particles measured (m)	Measured porosity	Pressure drop exponent	Permeability of bed (m^2)
A1+A2	0.013	0.011	0.374	1.60	9.4×10^{-9}
A3	0.019	0.022	0.424	1.40	34×10^{-9}

Table 2. Results of regressing experimental data using eq, (6)

Trial run	b	k (m^2)	SEM	R^2	Remarks
1	1.6	9.13×10^{-9}	6-7%	0.80	With all data points
	1.7	7.5×10^{-9}		0.80	
2	1.6	7.1×10^{-9}	3%	0.96	With data of holes 11 and 12 removed
	1.7	5.8×10^{-9}		0.97	
3	1.6	10.0×10^{-9}	5%	0.88	With data of holes 9, 10, 11 and 12 removed
	1.7	7.3×10^{-9}		0.87	

Table 3. Determination of the pressure loss coefficient at the throat of the mitigation suction pipe in house H21

Run	Total airflow (L/s)	Suction pressure before entry (cm water)	Suction pressure after entry (cm water)	K_p
1	18.3	1.300	1.664	0.053
2	23.4	1.938	2.540	0.053
3	28.4	2.700	3.589	0.053

Table 4. Relative pressure drops in the mitigation system of house H21

Run	Total airflow (L/s)	Δp_{bed} (cm water)	Δp_{ent} (cm water)	Δp_{pipe} (cm water)	Hydrodynamic effectiveness (%)
1	18.3	1.30	0.363	8.0×10^{-3}	77.8
2	23.4	1.94	0.602	13.0×10^{-3}	75.9
3	28.4	2.70	0.889	17.7×10^{-3}	74.9

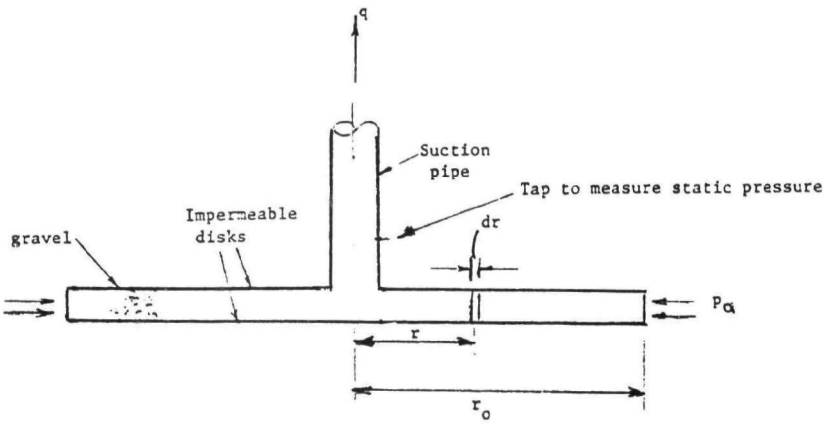

Fig. 1 Schematic of a model to duplicate flow conditions occurring beneath the concrete slab of a residence when induced by a single suction point. The airflow is assumed to be radial flow through a homogenous porous bed of circular boundary.

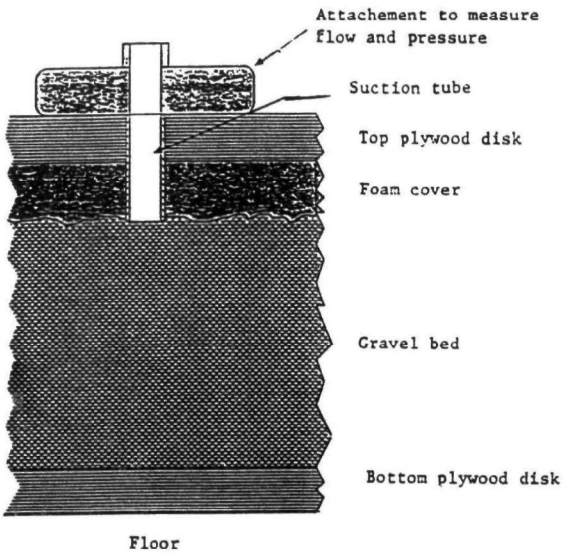

Fig. 2 Cross-section of the experimental laboratory apparatus.

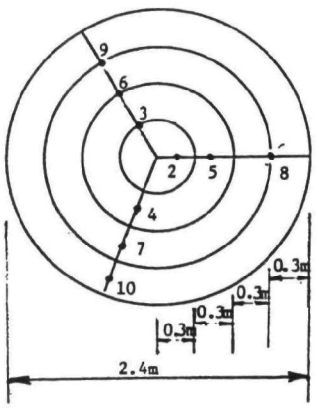

Fig. 3 Layout of the test holes to measure static pressures in the porous bed.

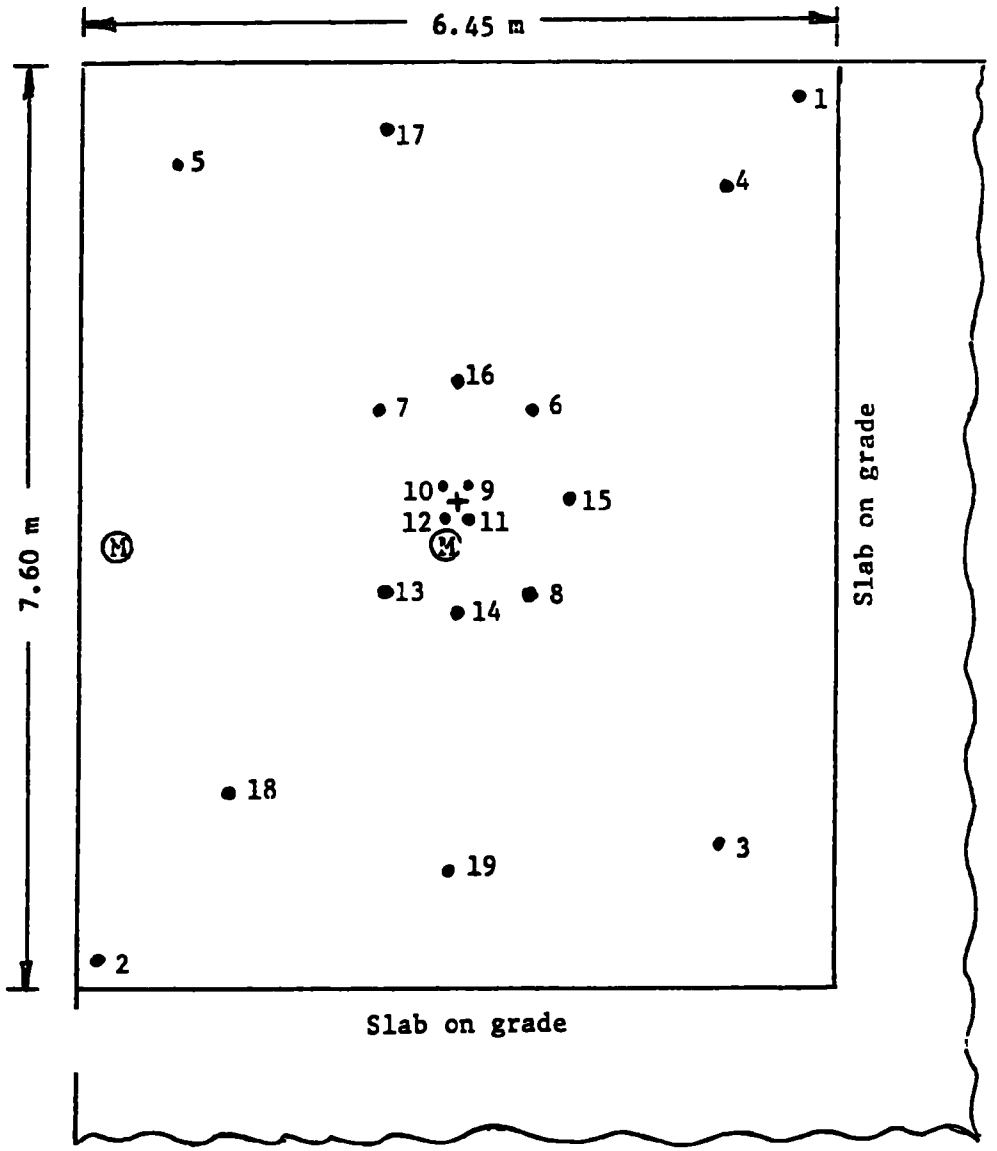

Fig. 4 Plan of the basement slab showing the relative positions of the various subslab penetrations. The suction hole of the temporary mitigation system is marked as +, while the location of the central and perimeter suction holes (M) of the final mitigation system are also shown.

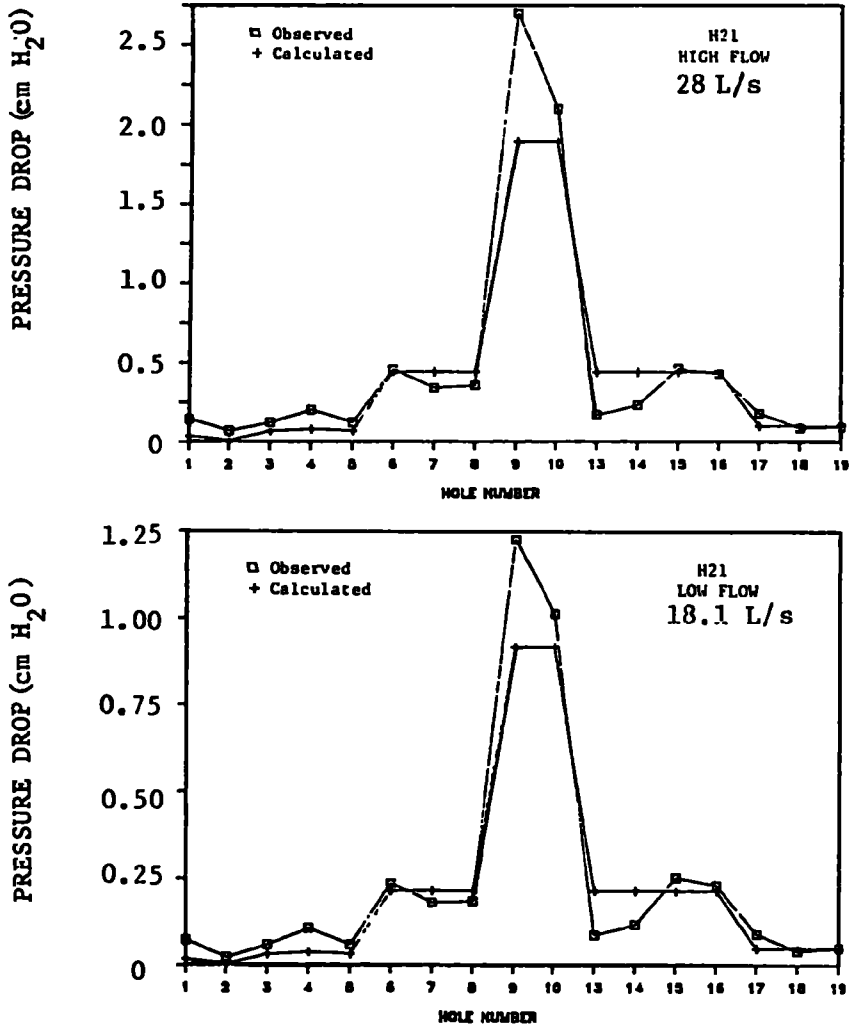

Fig. 5 Using coefficients for 1.3 cm gravel (b = 1.6 and k = 9.4 x $10^{-9}m^2$). Data of holes 11 and 12 not included.

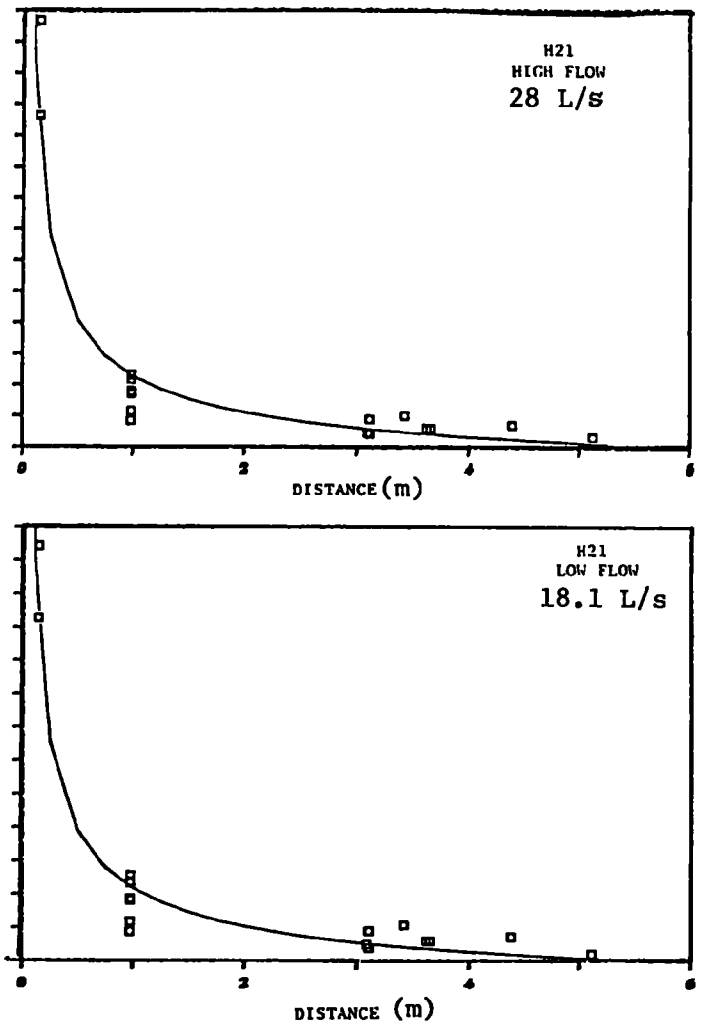

Fig. 6 Comparison of observed and computed pressure drops using coefficients of 1.3 cm gravel. Data of holes 11 and 12 not included.

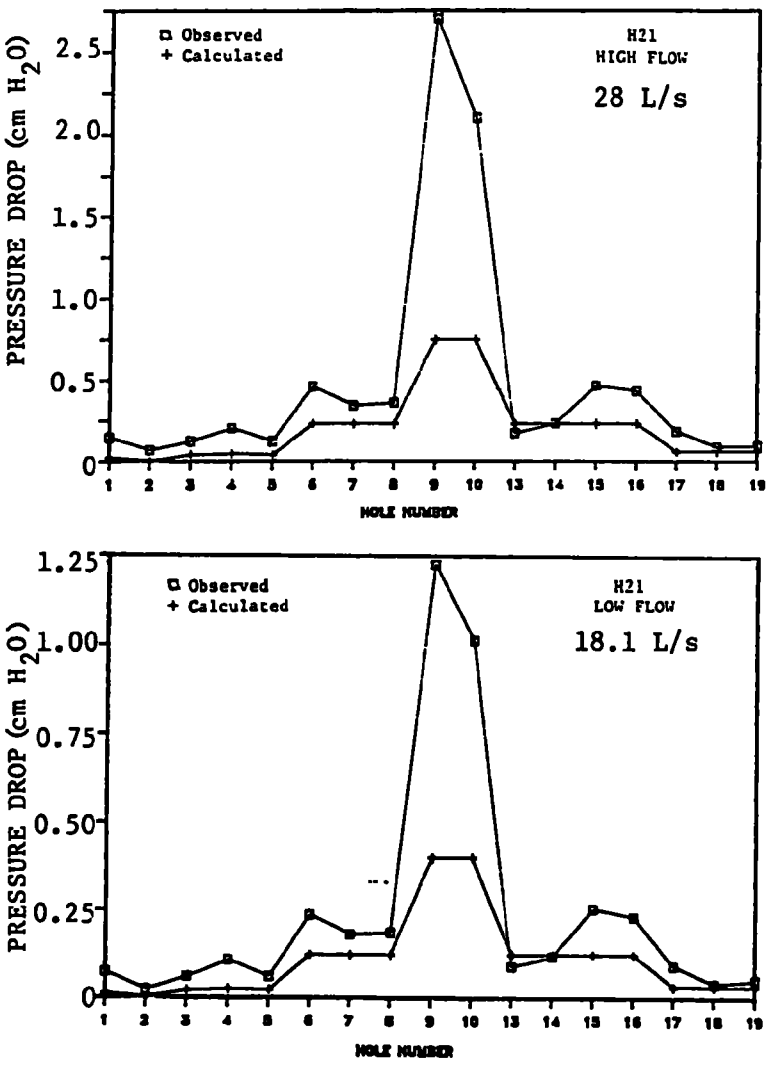

Fig. 7 Using coefficients of 1.9 cm gravel (b = 1.4 and k = 3.4 x 10^{-9} m^2).

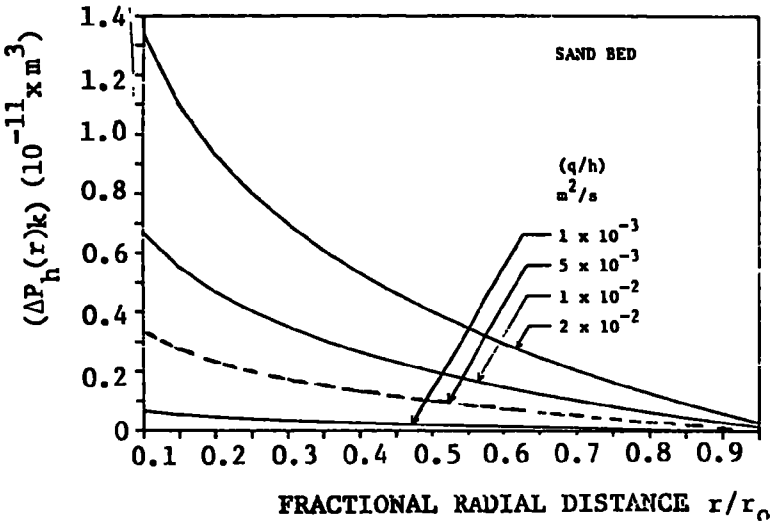

Fig. 8 Pressure drop in a sand bed with radial airflow between two impermeable disks.

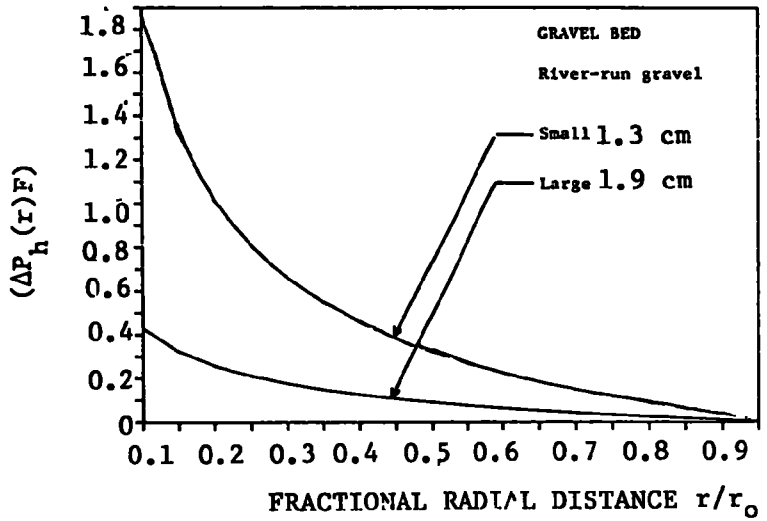

Fig. 9 Pressure drop in a gravel bed with radial airflow between two impermeable disks. The correction factor F can be determined from Fig. 10.

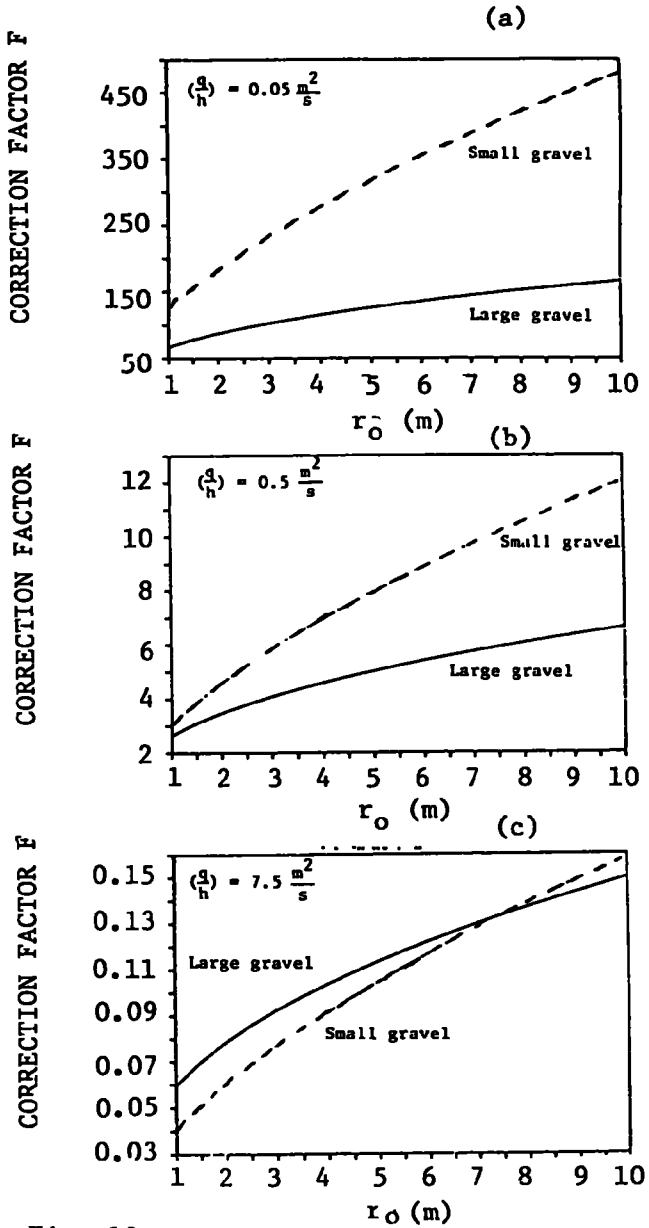

Fig. 10 Correction factor F for gravel beds to be used in Fig. 9.

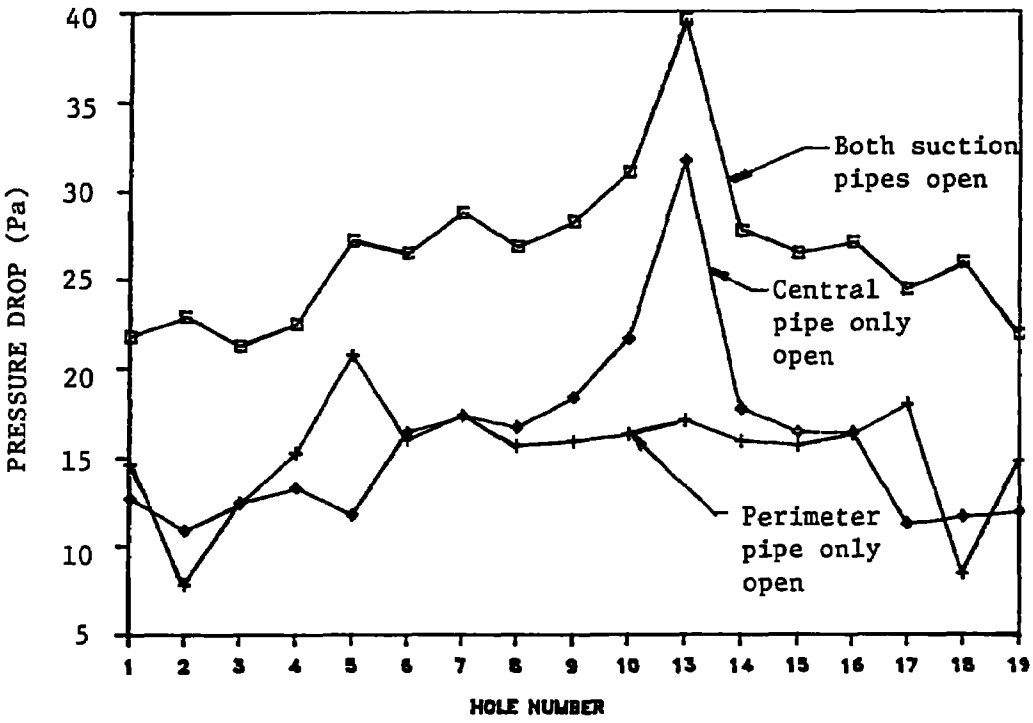

Fig. 11 Subslab suction pressure fields generated by the mitigation system when different suction pipes are used.

THE ROLE OF DIFFUSION IN RADON ENTRY INTO HOUSES

by: Allan B. Tanner
U.S. Geological Survey
Reston, VA, 22092

ABSTRACT

Pressure-driven flow of radon-bearing soil gas is commonly accepted as the usual mechanism whereby radon moves from outside house foundations to cause elevated indoor radon concentrations. It is less clear how radon moves to the backfill-and-subslab zone just outside the foundation. Fourteen houses having elevated indoor radon concentrations were investigated by the U.S. Environmental Protection Agency and its contractors. The permeability of the ground to gas flow was measured next to and several meters from each house foundation. For 6 of the 14 houses none of the intrinsic permeability values exceeded 7.6×10^{-12} m^2, below which diffusion is likely to be the dominant mechanism of radon movement. Because it can be significant in unsaturated soils of moderate-to-low permeability, diffusion should not be ignored in considering radon movement to house foundations.

INTRODUCTION

Radon (^{222}Rn) in the ground moves by two principal mechanisms. In response to a gradient of radon concentration, there is a net movement of radon atoms in the direction of lessening concentration by the process of diffusion. In a porous medium such as soil, the effective diffusion coefficient, which characterizes the rate of diffusion, depends primarily on the degree of liquid saturation of the soil and secondarily on the porosity, pore sizes, adsorptive properties of the soil grains, and absorptive properties of the liquid phase. Diffusion can occur with or without soil-gas flow, which is caused by a pressure gradient in the soil. The rate of soil-gas flow is controlled mainly by the pressure gradient and the soil's permeability to gases. Permeability depends strongly on pore and grain size; like the diffusion coefficient, it decreases greatly as the fractional saturation of the soil by liquids increases.

It is generally accepted that where enough radon enters a house to cause concern, entry is usually due to pressure-driven flow of radon-bearing soil gas (1,2). Diffusion of radon through concrete slabs and walls is slow enough to reduce the radon concentration greatly by decay (3). Radon movement through local cracks, sumps, and utility openings by soil-gas flow is favored over diffusion if the air pressure within a house at the slab level is less than that in the soil, and if the zone comprising the backfill and subslab material is fairly permeable. Both conditions often exist, particularly if the house slab is laid on the layer of coarse aggregate required by many building codes. It is less clear to what degree each of the two mechanisms is responsible for radon movement from the soil to the foundation wall or to the underside of the slab. Presumably because of evidence that pressure-driven flow causes the actual radon entry, most modeling to date has assumed that diffusion can be neglected. I know of no study that justifies such an assumption for other than very permeable soils.

The purpose of this paper is to present the several factors most important to diffusion and flow, to relate them to various soil types and conditions, and to show that diffusion, rather than flow, is likely to be the dominant mechanism of radon movement to the foundations of some houses having moderately elevated indoor radon levels.

COMBINED DIFFUSION AND FLOW

The first equation for steady-state, one-dimensional radon movement incorporating both diffusion and flow velocity was derived by Grammakov (4). Clements (5) derived an equation for the steady-state radon flux density crossing the Earth's surface into the atmosphere. Multiplying the radon flux density by the mean life of radon (the reciprocal of the decay constant) yields the maximum amount of radon per unit area that can be sustained by steady migration from the source soil (6). Dividing that amount by the concentration of radon that would build up in the soil gas if there were no migration yields a distance, M, which is the volume of undepleted soil gas per unit surface area that would contain the amount of radon sustained externally. I call M the "mean migration distance." It is calculated as follows:

$$M = [1/(2L)][(-k/u)(dp/dx)+\sqrt{(-k/u)^2(dp/dx)^2+4eLD}], \quad (1)$$

where M is in meters, L is the radon decay constant, e is the soil porosity, k (m^2) is the soil's intrinsic permeability to gas, u is the viscosity of air (1.8×10^{-5} Pa-s at typical soil temperatures), dp/dx (Pa/m) is the pressure gradient, and D (m^2/s) is the (bulk) effective diffusion coefficient (see references 3 and 7), equal to the interstitial effective diffusion coefficient times the soil porosity.

The bulk effective diffusion coefficient can be estimated by the following equation (8):

$$D/e = 7 \times 10^{-6} \exp[-4(m-me^2+m^5)], \quad (2)$$

where m is the fractional water saturation of the soil.

Typical permeabilities of soils range from 10^{-16} m^2 for clays to 10^{-7} m^2 for clean gravels (7). Although the mean migration distance in clays is only of the order of 1 cm, diffusion is the dominant mechanism, and flow can be neglected. For even very low pressure gradients, flow is dominant in gravels and coarse sands. Because of their mixed grain sizes, most soils have permeability values between the extremes, and the relative contributions by flow and by diffusion depend not only on permeability and diffusion coefficient, but also on the pressure gradient.

Figures 1 through 4 are graphs computed from equation (1) in order to show the relative importance of diffusion and soil-gas flow for different values of permeability, porosity, diffusion coefficient, and pressure gradient. Because of interaction among the variables, the graphs should not be used to infer the effect of changing a single variable on the flux density of radon.

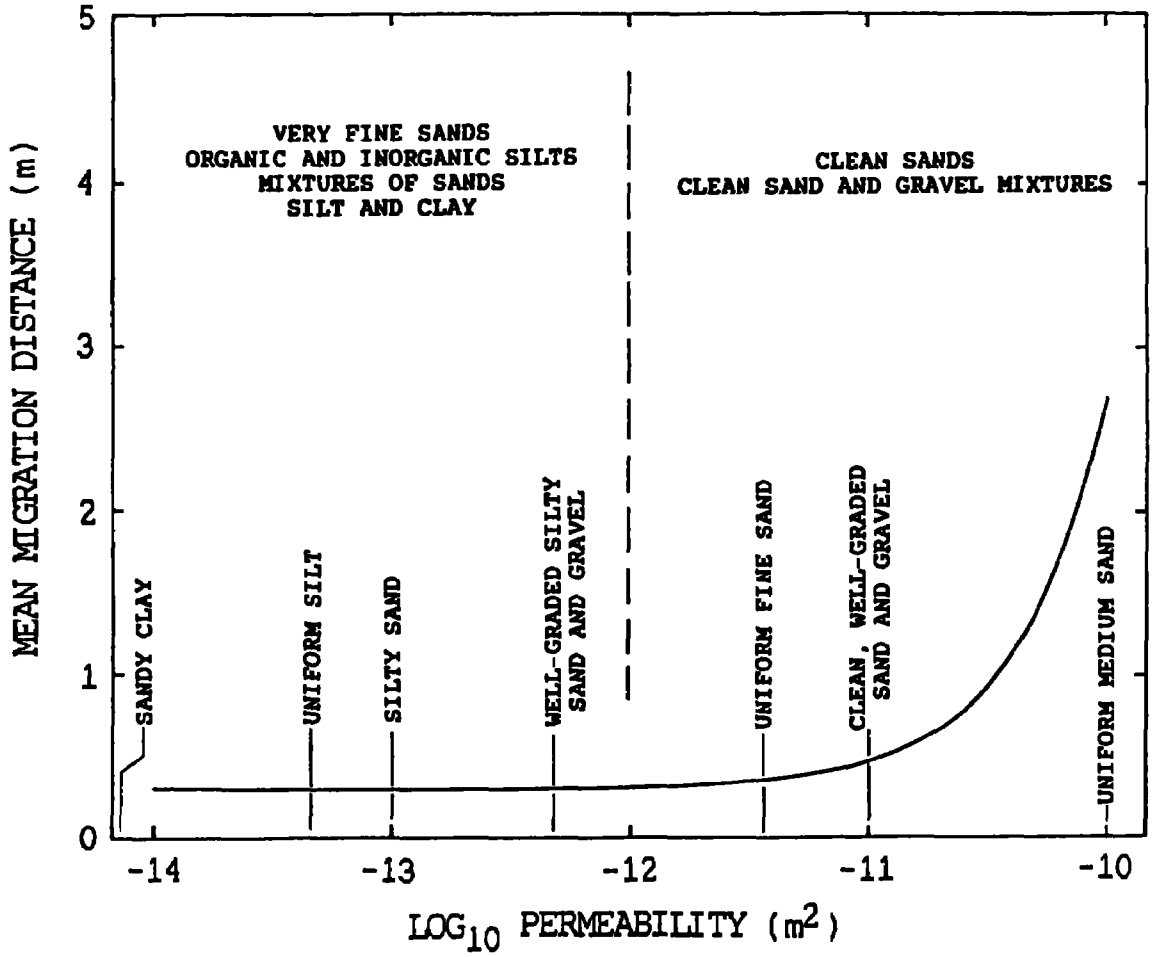

Figure 1. Mean radon migration distance for soils of 40 percent porosity, 50 percent water saturation, and -1 Pa/m pressure gradient. The correlations of soil types with permeability values or ranges are from reference (7).

Figure 1 has been computed for a soil porosity of 0.4, a pressure gradient of -1 Pa/m, a bulk effective diffusion coefficient of 4.8×10^{-7} m^2/s, corresponding to 50 percent water saturation, and the range of permeability extending from that of a sandy clay to that of a uniform medium sand. The permeability ranges of the soil types are taken from reference (7). Figure 1 shows that the mean interstitial migration distance is nearly independent of permeability below several times 10^{-12} m^2 under the specified conditions. Soil-gas flow should contribute little to radon migration in poorly graded soils containing substantial fractions of clay, silt, or fine sand. With well-graded grains and larger grain sizes, soil-gas flow is more important than diffusion.

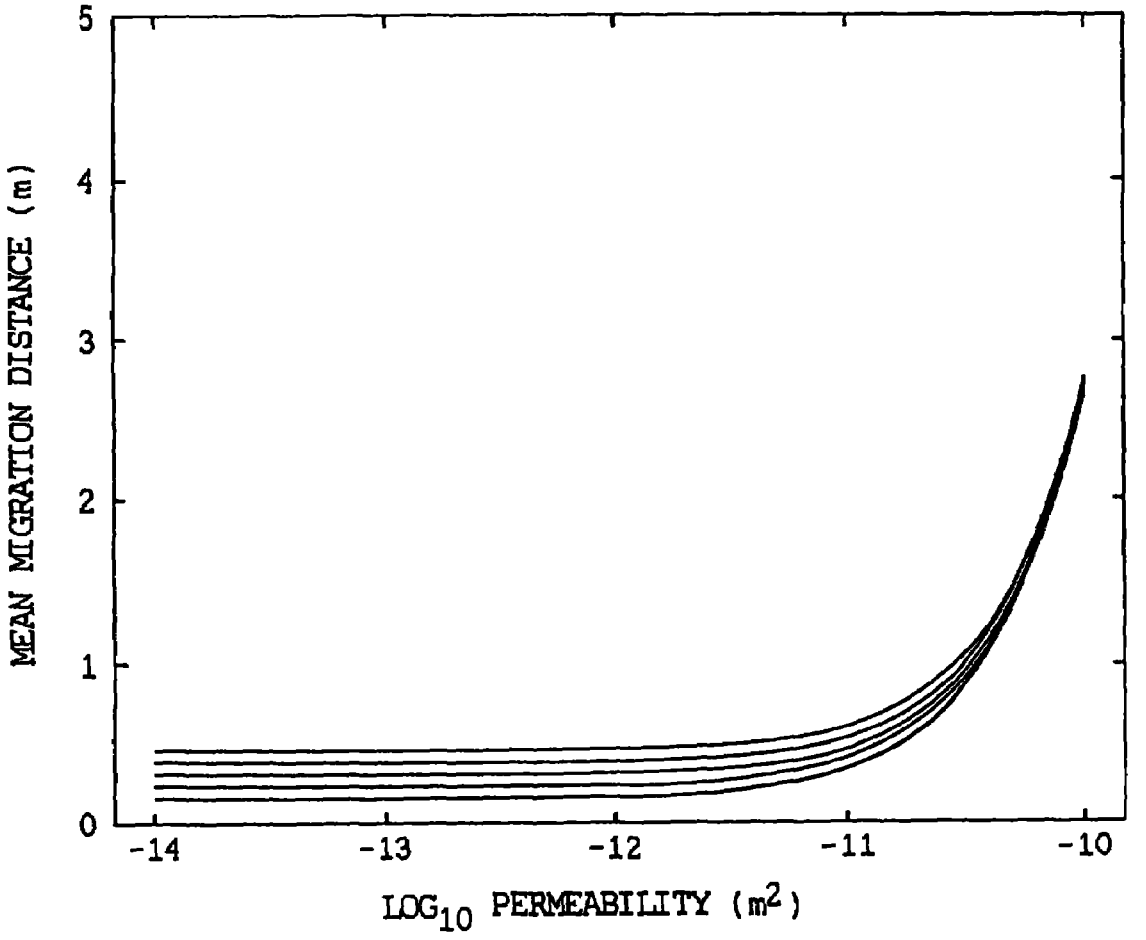

Figure 2. Mean radon migration distance for soil of 50 percent water saturation, -1 Pa/m pressure gradient, and porosities of 20, 30, 40, 50, and 60 percent (uppermost to lowest curves, respectively).

Figure 2 presents a family of curves computed for a pressure gradient of -1 Pa/m, a diffusion coefficient corresponding to 50 percent water saturation, and different values of porosity in the range from 20 to 60 percent. Soil-gas

flow is significant at slightly lower values of permeability in low-porosity soils than in high-porosity soils.

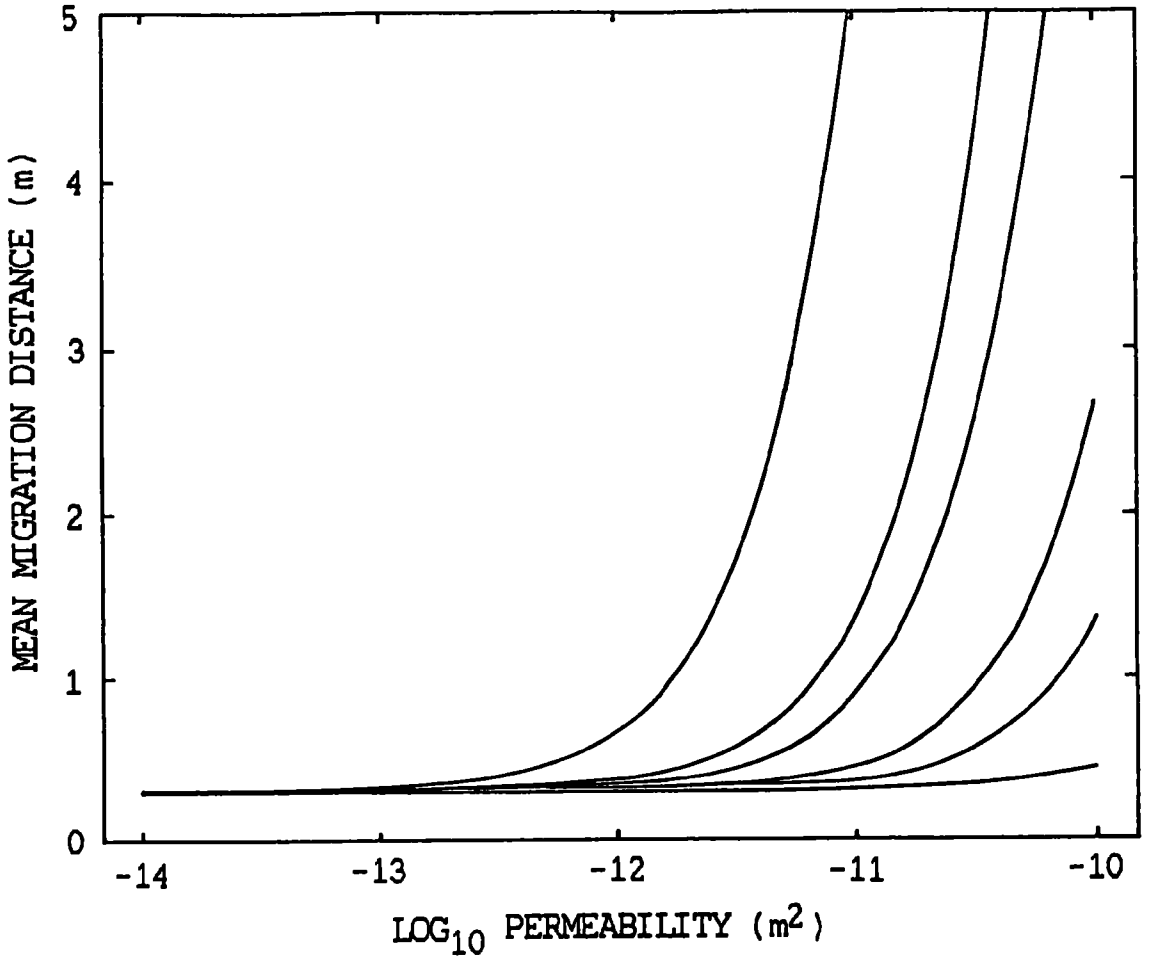

Figure 3. Mean radon migration distances for soils of 40 percent porosity, 50 percent water saturation, and pressure gradients of -20, -5, -3, -1, -0.5, and -0.1 Pa/m (uppermost to lowest curves, respectively).

Figure 3 presents a family of curves computed for soils of 40 percent porosity, a diffusion coefficient corresponding to 50 percent water saturation, and pressure gradients ranging from -20 to -0.1 Pa/m. Pressure differences of -5 Pa between U.S. houses and the soil are considered to be fairly high (9). If a -5 Pa difference were distributed over the typical radon diffusion length of about 1 m in soil, the resulting -5 Pa/m gradient should cause soil-gas transport of radon to be more important than diffusion in soils of permeability greater than about 10^{-12} m^2. Such gradients are likely where the radon flux converges at entry points such as cracks and utility openings, and the gradients decrease markedly with distance from the entry points. At a

house site where radon is effectively gathered from a zone several meters from the foundation, the gradients should be much less than 1 Pa/m. Where radon entry occurs over a broad front, such as through porous block walls or a distributed crack system, the one-dimensional migration regime discussed in this paper should be suitable.

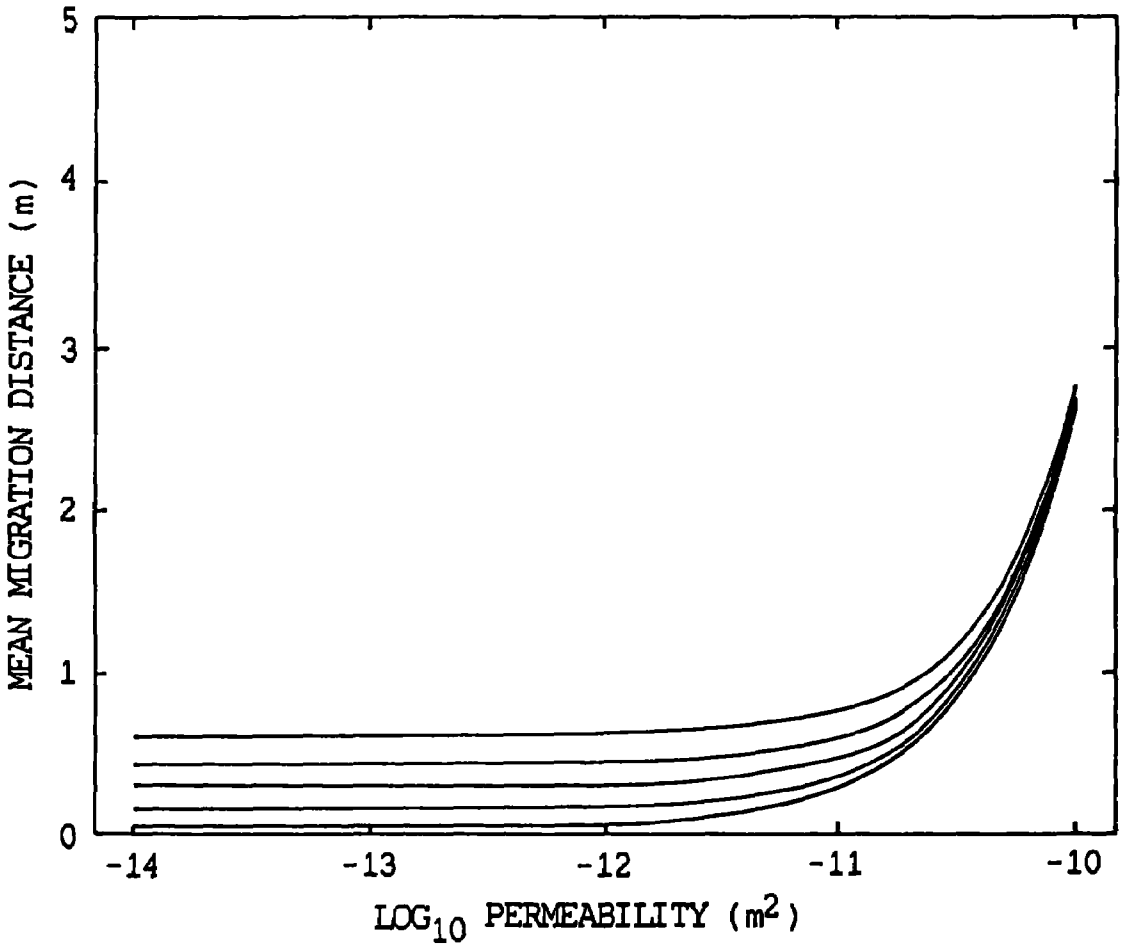

Figure 4. Mean radon migration distance for -1 Pa/m pressure gradient in soils of 40 percent porosity and 10, 30, 50, 70, and 90 percent water saturation (uppermost to lowest curves, respectively).

Figure 4 presents a family of curves computed for a pressure gradient of -1 Pa/m in soils of 40 percent porosity and 10, 30, 50, 70, and 90 percent water saturation. In the drier soils, soil-gas flow should be significant with permeability exceeding 10^{-11} m^2; in the wetter soils, soil-gas flow should be significant at somewhat lower values. Increasing saturation of a given soil reduces both its radon diffusion coefficient and its gas permeability.

I am not aware of studies of the effects of increasing saturation on both permeability and diffusion coefficient on the same material. However, Rogers and others (10) presented figures showing approximately 30-fold reduction of permeability from dry to saturated state and a three order-of-magnitude reduction of diffusion coefficient over the same range. Nazaroff and others (7) gave data indicating a decrease of gas permeability by a factor of 50 to 100 between the dry and saturated states of loamy sand. Because the diffusion coefficient enters into equation (1) to the 1/2 power, the effect of saturating soil on the mean migration distance in it by diffusion should be comparable with that for soil-gas flow.

Loureiro (11) included both diffusive and soil-gas flow mechanisms in modeling radon entry from dry soil via a slab-to-footing gap. He concluded that the diffusive mechanism was dominant for soils of permeability less than 10^{-12} m^2, and that the soil-gas flow mechanism was dominant above that value.

FIELD DATA

Two sets of field data were available that included soil permeability measurements for houses having indoor radon measurements exceeding the lowest action level. The first set was obtained as part of the U.S. Environmental Protection Agency's House Evaluation Program in work performed by Agency personnel and contractors. Radon in soil gas and the permeability of the ground close to and several meters from house foundations were measured by soil-probe methods at locations in Colorado Springs and Denver, Colorado, in northern Virginia, in Bartow and Lakeland, Florida, and in northern New Jersey. Of 14 different houses having indoor radon measurements exceeding the 148 Bq/m^3 (4 pCi/L) level, six had no measurement exceeding 7.6×10^{-12} m^2. The maximum values measured were 2.2×10^{-12}, 7.6×10^{-12}, 7.4×10^{-13}, 1.2×10^{-12}, 3.3×10^{-12}, and 6.4×10^{-12} m^2. Permeabilities at the sites typically ranged to values one to two orders of magnitude lower than the maximum. The greatest permeability was usually found in the backfill zone near the foundation wall.

I investigated three homesites that were included in the House Evaluation Program at the times of those tests. The three houses had indoor radon concentrations of about 800 Bq/m^3 (20 pCi/L) but are not included among the six houses discussed above because the House Evaluation Program permeability measurements exceeded 1×10^{-11} m^2 for those houses. By means of the procedure described in reference (6), I measured permeabilities ranging from 1.5×10^{-12} to 7×10^{-14} and from 2.2×10^{-12} to 1.2×10^{-13} m^2 at two of the houses; two measurements at different sites at the third house gave a value of 1.4×10^{-13} m^2. At two houses in northern New Jersey, both of which had indoor radon levels exceeding 7 kBq/m^3 (200 pCi/L), I measured permeabilities of 7×10^{-11} and 2×10^{-10} m^2, which were consistent with other observations of high permeabilities associated with severe indoor radon levels (12).

CONCLUSIONS

There is little doubt that severe indoor radon levels are very likely to be associated with highly permeable soils. However, moderately elevated indoor radon levels are sometimes associated with soils of low average permeability. At such sites, diffusion is probably the dominant mechanism of radon movement in the soil, particularly beyond the disturbed zone comprising the backfill and subslab aggregate.

ACKNOWLEDGMENTS

This study was supported in part by the Office of Health and Environmental Research of the U.S. Department of Energy under interagency agreement no. DE-AI05-87-ER60578. I thank R. Thomas Peake of the Office of Radiation Programs, U.S. Environmental Protection Agency, for making some of the House Evaluation Program data available.

The work described in this paper was not funded by the U.S. Environmental Protection Agency and therefore the contents do not necessarily reflect the views of the Agency and no official endorsement should be inferred.

REFERENCES

1. Åkerblom, G., Andersson, P., and Clavensjö, B. Soil gas radon--a source for indoor radon daughters. Radiation Protection Dosimetry. 7: 49, 1984.

2. Nero, A.V. and Nazaroff, W.W. Characterising the source of radon indoors. Radiation Protection Dosimetry. 7: 23, 1984.

3. Culot, M.V.J., Olson, H.G., and Schiager, K.J. Effective diffusion coefficient of radon in concrete, theory and method for field measurements. Health Phys. 30: 263, 1976.

4. Grammakov, A.G. On the influence of some factors in the spreading of radioactive emanations under natural conditions [in Russian]. Zhur. Geofiziki. 6: 123, 1936.

5. Clements, W.E. The effect of atmospheric pressure variation on the transport of ^{222}Rn from the soil to the atmosphere [Ph.D. dissertation]. New Mexico Inst. Mining and Technology, Socorro, N.M. 110 p.

6. Tanner, A.B. A tentative protocol for measurement of radon availability from the ground. Radiation Protection Dosimetry. 24: 79, 1988.

7. Nazaroff, W.W., Moed, B.A., and Sextro, R.G. Soil as a source of indoor radon: generation, migration, and entry. In: W.W. Nazaroff and A.V. Nero, Jr. (eds.), Radon and Its Decay Products in Indoor Air. John Wiley, New York, 1988. p. 57.

8. Rogers, V.C., Nielson, K.K., and Kalkwarf, D.R. Radon attenuation handbook for uranium mill tailings cover design. NUREG/CR-3533, U.S. Nuclear Regulatory Commission, Washington, D.C., 1984. 85 p.

9. Sextro, R.G. Oral communication, 1986.

10. Rogers, V.C., Nielson, K.K., and Merrell, G.B. Radon generation, adsorption, absorption, and transport in porous media. RAE-8810-1 and DOE/ER/60664-1, Rogers and Associates Engineering Corp., Salt Lake City, Utah. 48 p.

11. Loureiro, C. de O. Simulation of the steady-state transport of radon from the soil into houses with basements under constant negative pressure [Ph.D. dissertation]. LBL-24378, Lawrence Berkeley Laboratory, Berkeley, Calif. 278 p.

12. Sextro, R.G., Nazaroff, W.W., and Turk, B.H. Soil permeability and radon concentration measurements and a technique for predicting the radon source potential of soil. In: Proceedings of the 1988 Symposium on Radon and Radon Reduction Technology, Vol. 1, Symposium Oral Papers. EPA/600/9-89/006a. [U.S. Environmental Protection Agency] Radian Corp., Research Triangle Park, N.C., 1989. p. 5-61.

SOIL GAS AND RADON ENTRY POTENTIALS FOR SUBSTRUCTURE SURFACES

Bradley H. Turk
Rm. 109, 105 E. Marcy St.
Santa Fe, New Mexico 87501

Jed Harrison
U.S. EPA Office of Radiation Programs
Washington, D.C. 20460

Richard J. Prill
Washington Energy Extension Service
Spokane, Washington 99201

Richard G. Sextro
Indoor Environment Program
Lawrence Berkeley Laboratory
Berkeley, California 94720

ABSTRACT

Measurement techniques and parameters that describe the potential for areas of a building substructure to have high soil gas and radon entry rates have been developed. Flows and pressures measured at test holes in substructure surfaces while the substructure was intentionally depressurized were used in a highly simplified electrical circuit to model the substructure/soil network. Data from four New Jersey houses indicate that (1) the soil was a factor of two to six times more resistant to soil gas flow than substructure surfaces, (2) concrete slab floors, including perimeter gaps, cracks, and other penetrations, were approximately five times more resistant to soil gas movement than hollow block walls, and (3) radon entry potentials were highest for slab floors. These indices of entry potential may be useful for characterizing the relative leakiness of below-grade substructure surfaces and for determining the selection and placement of radon control systems.

INTRODUCTION

It is widely accepted that the pressure-driven flow of soil air into buildings is the most frequent cause of elevated indoor radon levels. Several studies have proposed techniques that define the ability of soil at a particular site to supply radon to a building structure via this convective flow (1,2,3,4,5). In some of these studies, the magnitude of the pressure field extending from a mechanically-depressurized house has also been mapped (6,7,8). The pressure coupling between the house and the soil location can be defined as the ratio of the pressure difference between the measurement location and the substructure to the depressurization of the substructure relative to outside. A small value for the pressure coupling indicates the existence of pathways connecting the house and soil location. The pathways

consist of openings through the substructure surfaces (cracks, holes, perimeter drains, etc.) and regions in the materials around the house that permit relatively unrestricted transport of soil air (permeable soil, gravel layers, and air gaps). Other work, some related to the control of indoor radon, has attempted to identify soil air pathways near substructures and to locate radon entry points in the building envelope (9,10,11,12).

Various measurements of the air permeability of the soil performed during many of the above studies are indicators of the mobility of soil gas in materials around a house. The air permeability can vary widely over both vertical and horizontal dimensions. High permeability zones were often found near substructures and were caused by less tightly-packed soil in the area disturbed by construction, layers of material provided for drainage (gravel), and air gaps below slab floors or near walls - some extended to the soil surface - created by expansion/contraction cycles and settling (4,13).

In this paper, we describe entry potentials for soil gas and radon through substructure surfaces that are based on the developments from the research mentioned above and on flows, pressures, and radon concentrations measured at the substructure/soil interface. This approach simplistically considers the below grade substructure surfaces, near-house materials, and nearby soils as elements of a "black box" whose aggregate characteristics assist in estimating the likelihood and relative magnitude of soil gas and radon entry. We do not include transport by diffusion. In addition, the analysis enables comparisons of the resistance of soil and of the below-grade substructure surfaces to air flow.

SOIL GAS AND RADON ENTRY POTENTIALS

Below grade, most houses are surrounded by a very complex matrix of soils, rock, and construction-related materials or structures, each having different capacities for radon production and soil gas and radon transport. In most situations, details of the geometry, characteristics, and interactions between these features and with the substructure cannot be known. Plus, the condition and construction details of the substructure surfaces in contact with these exterior materials are not fully known.

In order to account for these complexities without knowing their specifics, a method to integrate the flow and pressure characteristics is useful. If we assume a linear pressure dependence for air flow through soils and materials around the substructure (i.e., Darcy flow), the passage of soil gas through soil and into a substructure depends on the resistance of the flow path through the materials around the substructure and through the surfaces of the substructure. Therefore, a simplified electrical resistance analog of a typical basement/soil system can be created, as shown in Figures 1a and 1b, to simulate the flows, pressure drops, and resistances in the soils, near-house materials, and substructure surfaces.

A blower door that enhances depressurization in the substructure is represented by the battery in the circuit. The test holes drilled through the floor and walls permit measurements of air flows (current) and pressure drops (voltage) at various nodes in the circuit. While the blower is operating, the system is tested in two conditions: with the test hole closed and with the test hole open. With the test hole sealed, good pressure coupling between the interior of the substructure and the exterior at a test hole location (pathway with low effective resistance) may result from nearby cracks and openings in the substructure surfaces or from more distant openings through the substructure that are connected by high permeability pathways to the test

hole. Good coupling does not, however, necessarily mean that large quantities of soil gas will enter through the nearby openings. The soil, aggregate, or backfill material around the substructure must also be sufficiently permeable so that substantial quantities of soil gas can be transported to the openings. Therefore, with the test hole open (indicated in Figure 1b by the dotted lines representing the current, I_H, and resistance, R_H, of the test hole and flow measurement adaptor), a high air flow rate through the test hole suggests high permeability (low effective resistance) in the materials around the substructure and relatively rapid transport of soil gas to the nearby openings in the substructure surfaces. In general, when both good pressure coupling and high flow rates are measured at a test hole, then it is likely that significant amounts of soil gas will enter the house around that location.

A more quantitative interpretation of the data requires analysis of the analogous electrical circuit. Following are symbols and definitions (and the corresponding electrical parameters) used in the derivations. The subscript "C" identifies the condition with the test hole closed.

Q_H (I_H) = measured (corrected) flow through open test hole and flow adaptor (m^3/s),

Q_F (I_F) = defined flow through cracks and openings in below-grade substructure surfaces with test hole open (m^3/s),

Q_T (I_T) = defined total flow through cracks, openings, and test hole (m^3/s),

P_B (V_B) = measured pressure difference between inside of basement and outside, point a to c (Pa),

P_H (V_H) = calculated pressure drop across open test hole and flow adaptor, point a to b (Pa),

P_S (V_S) = pressure drop across soil paths between point b and outside with test hole open, $P_B - P_H$ (Pa),

R_H = defined resistance of open test hole and flow adaptor ($Pa\text{-}s/m^3$),

$R_{F\text{-}EFF}$ = calculated effective resistance that lumps resistances of cracks and openings in substructure surfaces and resistances of near-substructure materials surrounding the open test hole (R_{F1}, R_{F2}, R_{F3}, etc.) ($Pa\text{-}s/m^3$), and

$R_{S\text{-}EFF}$ = calculated effective resistance of soil paths to measurement point b (R_{S1}, R_{S2}, R_{S3}, etc.), with test hole open ($Pa\text{-}s/m^3$).

We assume that the complex network of resistances through the soil and substructure surfaces is represented approximately by the simplified circuit shown to the left in Figure 1b. With the test hole closed, a resistance ratio, Z (i.e., the resistance of the substructure surfaces and near-substructure materials divided by the resistance of the soil), can be defined as

$$Z = \frac{V_{HC}}{V_{SC}} = \frac{I_{TC} R_{FC\text{-}EFF}}{I_{TC} R_{SC\text{-}EFF}} = \frac{R_{FC\text{-}EFF}}{R_{SC\text{-}EFF}}, \quad \text{thus} \qquad [1]$$

$$R_{FC\text{-}EFF} = Z\left(R_{SC\text{-}EFF}\right). \qquad [2]$$

Using Kirchoff's rule for circuit analysis when the test hole is open, the following three independent equations are derived

$$V_B - I_H R_H - I_T R_{S\text{-}EFF} = 0 \,, \qquad [3]$$

$$I_F R_{F\text{-}EFF} - I_H R_H = 0 \,, \quad \text{and} \qquad [4]$$

$$I_T - I_F - I_H = 0 \,. \qquad [5]$$

If we assume that

$$R_{FC\text{-}EFF} \approx R_{F\text{-}EFF} \quad \text{and}$$

$$R_{SC\text{-}EFF} \approx R_{S\text{-}EFF}$$

then we can solve for $R_{S\text{-}EFF}$, using equations 2 through 5 and substituting for analogous air flow and pressure parameters, to obtain the effective soil resistance,

$$R_{S\text{-}EFF} = \frac{P_B - P_H\left(1 + \frac{1}{2}\right)}{Q_H} \,. \qquad [6]$$

$R_{F\text{-}EFF}$ is found by solving equation 2. These two resistance parameters enable comparisons of the resistance to air flow created by the soil and substructure surfaces.

Combining these resistances, we now define the entry potential of soil gas at a location, G (m^3/Pa-s), as the net conductance through the surrounding soil, near-substructure materials, and substructure surface materials from

$$I_T = \frac{V_B}{R_{S\text{-}EFF} + R_{F\text{-}EFF}} \,, \qquad \text{or} \qquad [7]$$

$$G = \frac{1}{R_{S\text{-}EFF} + R_{F\text{-}EFF}} \propto Q_T \,. \qquad [8]$$

Thus, larger values of either $R_{S\text{-}EFF}$ or $R_{F\text{-}EFF}$ result in a smaller soil gas entry potential.

Note that the area over which to apply the effective resistances and entry potential is not defined. In an ideal situation, where the subfloor materials are highly permeable (R_{F2} is small) and the substructure surfaces and surrounding soils are homogeneous - without discontinuities such as impermeable barriers or large short circuits, a single test hole location would suffice to calculate the total resistance of the substructure surfaces and of the soils. However, many of these discontinuities may exist around typical houses. Consequently, more than one measurement location is required to determine the local resistances at different locations. Unfortunately, in this situation with many test locations, it is difficult to know the distance from each test location over which the resistances are derived. Indeed, for those test locations in homogeneous materials such as subfloor gravel layers, identical conditions may be measured over a large area. While at the same house, measurements made at test locations in different materials could represent conditions very near to the test location.

The entry potential of radon, E (Bq/Pa-s), may be defined as the mass transfer of radon found near the substructure surfaces, C (Bq/m^3), with the prevailing pressure-normalized flow of soil gas into the building (soil gas entry potential):

$$E = GC \cdot \qquad [9]$$

Similar to the soil gas entry potential, the radon entry potential should indicate the likelihood that significant amounts of radon can enter a building through an area of the substructure surface. Both high soil gas entry rates (soil gas entry potential) and high radon concentrations at the exterior of the substructure will cause a higher radon entry rate (radon entry potential).

EXPERIMENTAL PROCEDURES

At four New Jersey houses, a blower door depressurized the substructure by -10 Pa to -37 Pa while air velocities and pressure differences were measured at indoor test holes. Measurements were made at up to three different pressures in two houses, LBL13 and LBL14C. By artificially depressurizing the building, the magnitude of most parameters was increased so that they were more easily measured and so that many environmental effects were minimized. All tests were conducted during June 1987. These houses were part of a larger research project investigating radon entry and control (14).

In each house, approximately 30 test holes (6 mm to 13 mm in diameter) had been drilled through substructure slab floors and hollow block walls, and into the block cavities of these walls (approximately 0.25 m above the floor) for a variety of measurement purposes. Some of the test holes through the floors penetrated only to the space or gravel layer directly below the slab, while at other holes, probes extended approximately 1 m into soil that was compacted before the slab was poured. At one location on each exterior wall, a probe completely penetrated the block wall to the soil.

In separate experiments conducted while the house was depressurized by the blower door, a pressure field map was made of the pressure coupling at some indoor test holes and at approximately 25 locations in the soil around the house. The soil probes were 13 mm OD and were placed at depths ranging from 0.2 m to 2.2 m and distances of 0.5 m to 3.5 m from the houses. The pressure coupling data for the soil probes provides an interesting comparison to those data measured at the test holes in the substructure surfaces.

Pressure differences were measured between each soil probe or exterior of each test hole, P_{HC} (test hole sealed), and the basement. All other test holes and soil probes were kept sealed. The basement depressurization, P_B, was measured relative to outside. All pressures were measured using an electronic micromanometer with a minimum resolvable pressure difference of 0.5 Pa and an accuracy of 1%.

Air velocities as small as 0.025 m/s at the open test holes were measured with a hot wire anemometer attached to a flow adaptor designed to mate with the various-sized holes (Figure 2). Where necessary, flow rates (I_B) were corrected for the effects of the size of the test hole. The pressure drop across the flow adaptor and test hole (P_B) was estimated using the engineering formula for laminar flow through a tube

$$\frac{P_H}{x} = \frac{8\mu Q_H}{\pi r^4} , \qquad [10]$$

where P_H = pressure drop (Pa),
x = length of the test hole plus flow adaptor (m),
μ = absolute viscosity of air, 1.8×10^{-5} kg/m-s, and
r = radius of the tube (in our case, we used the radius of the flow adaptor - 0.0045 m).

Estimated pressure drops in the test hole and flow adaptor ranged from 0.01 Pa to 3.5 Pa. In theory, a more accurate value for this pressure drop could be determined by direct measurement; however, the small pressure differences are difficult to measure in practice.

To determine the radon concentration in soil gas near the substructure, C, grab samples of soil gas from the test holes were collected in evacuated alpha scintillation flasks. The radon activity in the flasks was counted on a portable photomultiplier tube and scaler. Because grab samples were not always collected concurrently with measurements of flow and pressure difference, samples collected at other times during the study were used to compute average radon concentrations for the test holes. Uncertainties in the radon concentrations measured with this procedure are estimated to be ± 20 %.

RESULTS AND DISCUSSION

A total of 117 measurements were made at 75 test holes in the four houses. The average calculated effective resistances for soil ($R_{S\text{-}EFF}$) and substructure surfaces ($R_{F\text{-}EFF}$) are summarized in Table 1. The data are grouped according to location of the test hole. There is considerable variability in the resistances among test holes as indicated by the large standard deviations. By examining the geometric means, several patterns are apparent and statistically significant: 1) the effective soil resistance that is 'seen' by the test locations across the slab floors and in block wall cavities is similar, probably because large surface areas of soil (and for the block walls - wall areas exposed directly to the outside air) are accessible to the test holes; (2) the slab floors are approximately five times more resistant to soil gas movement than the interior surface of the porous block walls; and (3) for all locations, except those in the soil exterior to the walls, the substructure 'sees' the soil as being a factor of 2 to 6 times more resistant to soil gas flow than the substructure surfaces and the materials very near to the substructure. We also find that the entire thickness of a block wall is many times more resistant to soil gas flow than only the interior surface of the block - presumably because of the coatings and sealants that are applied to the exterior surface for waterproofing. These data support the view that the flow of soil gas into buildings depends to a lesser degree on the resistance of the building surfaces below grade than on the resistance of the surrounding soil and materials. It is important to recognize that low resistance values can result from low resistance in the materials near to the test locations or from the sum of many parallel resistances when the test location 'sees' a large area of soil and building material.

Average soil gas entry potentials, G, for each of the 75 test holes are shown on Figures 3 through 6. Pressure coupling ratios from the pressure field mapping tests are also shown so that comparisons can be made among the test locations. See Table 3 for a description of the symbols used on these figures. Values for G ranged from less than 0.01×10^{-6} $m^3/Pa\text{-}s$ to 3.2×10^{-6} $m^3/Pa\text{-}s$. These data are summarized in Table 2 by the same groupings as in Table 1. The geometric mean soil gas entry potential is highest for the hollow block walls, probably because of the high porosity (lower effective

resistance) of the block wall material and because the large exterior surface area exposed to soil and/or outdoor air is available to most entry locations on the interior surface via the interconnecting network of cavities. Similar conclusions were reached by Garbesi and Sextro (6).

For the two houses where G was calculated for different basement pressures, the mean coefficient of variation for replicates at 35 test holes was 49%. The entry potential did not appear to be biased by level of depressurization.

If we assume the average soil gas entry potential (0.73×10^{-6} m^3/Pa-s) is for an effective area of 1 m^2, then for a house with 175 m^2 of below grade surface area at a natural depressurization of 3 Pa, the soil gas entry rate is predicted to be 1.4 m^3/h. This soil gas entry rate is similar to the 1 m^3/h calculated by other researchers (6,15,16,17), and lower than that measured in houses on highly permeable soils (18).

Data for the radon entry potentials, E, at each house are also shown on Figures 3 to 6 and are summarized in Table 2. For 73 test holes, the geometric mean radon entry potential was highest for the test locations in subslab aggregate. Although the test holes into the block wall cavities had a slightly higher soil gas entry potential, the subslab test holes had greater concentrations of radon in the soil gas which compensated for their smaller soil gas entry potential. Calculated values of E ranged from less than 0.1×10^{-3} Bq/Pa-s to 1300×10^{-3} Bq/Pa-s.

When reviewing the radon entry potential plotted on Figures 3 to 6, we find that the areas of highest potential generally coincide with the locations where the pipes of successful subsurface ventilation-depressurization (SSD) radon control systems were placed through the slabs. For these houses, a 'high' radon entry potential would be considered greater than approximately 15×10^{-3} Bq/Pa-s. Since the entry potentials were calculated after installation of the SSD systems, these indices appear to provide a quantitative method for replicating the intuitive approach of successful mitigation contractors. House LBL12 is an exception, where it was difficult to bring indoor radon levels below the target concentration of 148 Bq/m^3. There were areas of high radon entry potential in this house that were not in proximity to an SSD pipe, and may have been the sources of inadequately controlled radon entry (Figure 4).

In general, the radon entry potential may indicate the preferred locations for SSD pipes, but will not provide information about the ability of a specific SSD system to reduce radon entry rates. The pressure field extension test that uses a vacuum cleaner or depressurizing blower remains the best technique to measure the extent to which a SSD system can reverse the natural pressure gradient around a substructure, and therefore control radon entry (10). Combining results from the pressure field extension test with identified areas of high radon entry potential may assist contractors deciding on the placement of SSD pipes. When the soil gas (and radon) entry potential is high for a particular location, but the pressure field extension or connection to the vacuum is poor, obstructions or high permeability short circuits are probably blocking or intercepting the pressure field from the vacuum. The problem then is to provide access to the areas of high radon entry potential.

The geometric mean radon entry potential for each of the four houses was compared with the average indoor radon concentration, measured between September 1 and May 1 and weighted by the volumes for various zones where indoor radon was measured. From the lowest to the highest average indoor radon concentration; 540, 620, 650, and 660 Bq/m^3, the geometric mean radon entry potentials were 6.4, 10, 7.2, and 18×10^{-3} Bq/Pa-s, respectively. Only

for the third house listed (LBL13), does the geometric mean radon entry potential fail to trend with increasing indoor radon concentrations. The geometric mean radon entry potential (assumed to be for an effective area of 1 m^2) can also be used in a mass balance equation along with actual surface areas and structure volumes and an assumed pressure difference of 3 Pa and ventilation rate of 0.5 h^{-1} to calculate a steady-state indoor radon concentration for each house. The correlation is poor between these calculated values (42, 39, 24, and 103 Bq/m^3, respectively) and the actual radon levels. And we see that using the radon entry potentials under-predicts actual radon levels by factors of 6 to 30.

LIMITATIONS

That the current development and application of these new parameters may still have weaknesses, is suggested in some of the data just presented. The electrical analog is imperfect since it assumes linear flow characteristics - which may not occur either under natural depressurization at entry locations or under the greater mechanically-induced depressurization at both entry locations and test holes. A more appropriate analogous circuit would also include capacitance to represent the storage and discharge of radon that is assumed to occur in spaces near the substructure in response to time-varying driving forces.

In addition, the assumptions, $R_{FC\text{-}EFF} = R_{F\text{-}EFF}$ and $R_{SC\text{-}EFF} = R_{S\text{-}EFF}$, are not exactly valid, since the paths for air flowing through the soil and building surfaces are different in the two measurement conditions. The effects of inhomogeneities in soils, near-house materials, and substructure surface materials on the assumption have not been examined. Although the derivation is generally not sensitive to the pressure drop across the test hole and flow adaptor (right hand term in the numerator of Equation 6), the term was occasionally as large as 55% of the substructure depressurization (P_B). This term has the greatest impact when the pressure drop across the test hole is large or when substructure surfaces are leaky (small Z). Since the test hole diameter will also have an important effect on the measured flow rate, all test holes should be drilled to the same size or corrections to a standard hole size (for this study, a 9 mm dia. hole) should be made. Then entry potentials may be more accurately compared between test holes and between houses.

The soil gas entry potential at a particular location is affected by all soils, materials, and openings in the below-grade surfaces around a building, but to a greater degree by those nearby or connected by a high permeability path. More study is required to determine the distance from a test hole over which the soil gas entry potential is applicable. For example, if R_{F2} in Figure 1b is small (i.e., highly permeable subfloor material), then the distance is large. If R_{F2} is large, then the entry potential is more localized. When these relationships are better understood, the test holes can be better placed to best represent the soil gas entry throughout the entire substructure.

The time-varying nature of many of the measured parameters may create difficulty in using a one-time determination of soil gas and radon entry potentials to represent typical entry potentials for a house. For example, the radon concentrations measured in grab samples collected from the test holes under natural conditions showed large variations. Repeated samples (between two and seven) were collected from 45 test holes at six houses over a 12-month period when radon control systems were not operating. The mean

coefficient of variation for the radon concentration at each test hole was 79%. Concentrations at the same test hole varied by up to a factor of 1000 from one sample to another. It is possible that these large variations in radon concentrations were caused by changes in wind, radon production in the soil, or soil gas flow rates into the houses. The radon concentration in grab samples from individual test holes collected during mechanically-induced depressurization can also be considerably different from concentrations during natural conditions. However, when concentrations measured at 99 test holes in seven houses during mechanically-induced depressurization were correlated with corresponding concentrations during natural conditions, we found a correlation coefficient (R) of 0.68 and that the means for the two conditions were not significantly different. This suggests that radon concentrations in samples collected during a brief period of mechanically-induced depressurization may, on average, be representative of concentrations under natural conditions.

In addition to variations in radon concentrations, it would not be surprising to also observe changes in the soil gas entry potential due to changes in soil permeability (for example, caused by precipitation or a moving water table). More study on the time-dependent variation of these parameters is required.

SUMMARY

A procedure has been described to determine the potential for soil gas and radon to enter a house at substructure surfaces by convective flow from the soil. The necessary field measurements of flow, pressure, and radon concentration are relatively simple and utilize commonly available equipment. These parameters for entry potential may be useful to: (1) identify areas in a substructure with the potential for comparatively high soil gas entry rates; (2) compare the relative leakiness of below-grade surfaces in different houses; (3) provide approximate measures of the resistance of the substructure surfaces and soils/materials around the substructure and provide a basis for establishing the relative importance of these features to radon entry; and (4) identify areas in a substructure with potentially high radon entry rates for placement of radon control systems.

Initial measurements in four houses indicate that the soils surrounding the houses are approximately three times more resistant to the transport of soil gas than the substructure surfaces and the materials near the substructure. Soil gas has approximately twice the entry potential at the surfaces of hollow block walls than at slab floors, but the slab floors have much higher radon entry potentials because of the greater radon concentrations below the slabs.

Modifications to the simple electrical resistance circuit used in this development to represent the substructure/soil system may improve the predictive capability of the procedure. In addition, determination of these new parameters in additional houses and under changing seasonal conditions is necessary to more fully examine their suitability as diagnostic and research tools.

ACKNOWLEDGMENTS

We appreciate the insightful comments of William Fisk, Ashok Gadgil, and Mark Modera; the program support of David Sanchez at AEERL, U.S. EPA; and the cooperation of the families of the seven New Jersey houses.

This work was supported by the Assistant Secretary for Conservation and

Renewable Energy, Office of Building and Community Systems, Building Systems Division; by the Director, Office of Energy Research, Office of Health and Environmental Research, Human Health and Assessments Division and Pollutant Characterization and Safety Research Division of the U.S. Department of Energy (DOE) under Contract No. DE-AC03-76SF00098; and by the U.S. Environmental Protection Agency (EPA) through Interagency Agreement DW89931876-01-0 with DOE. This paper has been reviewed in accordance with the U.S. EPA's peer and administrative review policies and approved for presentation and publication.

REFERENCES

1. Nazaroff, W.W. Predicting the rate of radon-222 entry from soil into the basement of a dwelling due to pressure-driven air flow. Radiation Protection Dosimetry. 24: 199-202, 1988.

2. Nazaroff, W.W. and Sextro, R.G. Technique for measuring the indoor ^{222}Rn potential. Environmental Science and Technology. 23: 451, 1989.

3. Schery, S.D. The design of accumulators and their use in determining the radon availability of soil. In: Proceedings of the 82nd Annual Meeting of the Air and Waste Management Association. 89-79.2, Anaheim, CA., 1989.

4. Sextro, R.G., Nazaroff, W.W., and Turk, B.H. Spatial and temporal variation in factors governing the radon source potential of soil. In: Proceedings of the U.S. EPA Symposium on Radon and Radon Reduction Technology. EPA-600/9-89/006a. pp. 5-61 to 5-74. Research Triangle Park, N.C., 1989.

5. Tanner, A. B. Measurement of radon availability from soil. In: M.A. Marikos and R.H. Hansman (eds.), Geologic Causes of Natural Radionuclide Anomalies, Proceedings of the GEORAD Conference, St. Louis, MO., April 21-22, 1987: Rolla, MO., Missouri Dept. Nat. Resources, Div. Geology and Land Survey Spec. Pub. No. 4, p. 139.

6. Garbesi, K., and Sextro, R.G. Modeling and field evidence of pressure-driven entry of soil gas into a house through permeable below-grade walls. Environmental Science and Technology. 23: 1481-1487, 1989.

7. Nazaroff, W.W., Lewis, S.R., Doyle, S.M., Moed, B.A., and Nero, A.V. Experiments on pollutant transport from soil into residential basements by pressure-driven airflow. Environmental Science and Technology. 21: 459, 1987.

8. Sextro, R.G., Moed, B.A., Nazaroff, W.W., Revzan, K.L., and Nero, A.V. Investigations of soil as a source of indoor radon. Chapter 2. In: P.K. Hopke (ed.), ACS Symposium Series No. 331, Radon and Its Decay Products: Occurrence, Properties, and Health Effects. pp. 10-29, American Chemical Society, New York, N.Y., 1987.

9. Figley, D.A. and Dumont, R.S. Techniques for measuring the air leakage characteristics of below grade foundation components. In: Proceedings of the 82nd Annual Meeting of the Air and Waste Management Association. 89-79.4, Anaheim, CA., 1989.

10. Gadsby, K.L., Hubbard, L.M., and Harrje, D.T. Rapid diagnostics: subslab and wall depressurization systems for control of indoor radon. In: Proceedings of the U.S. EPA Symposium on Radon and Radon Reduction Technology. EPA-600/9-89/006a. pp. 3-69 to 3-85. Research Triangle Park, N.C., 1989.

11. Matthews, T.G., Wilson, D.L., TerKonda, P.K., Saultz, R.J., Goolsby, G., Burns, S.E., and Haas, J.W. Radon diagnostics: subslab communication and permeability measurements. In: Proceedings of the U.S. EPA Symposium on Radon and Radon Reduction Technology. EPA-600/9-89/006a. pp. 6-45 to 6-66. Research Triangle Park, N.C., 1989.

12. Turk, B.H., Prill, R.J., Sextro, R.G., Harrison, J. Intensive radon mitigation research: lessons learned. In: Proceedings of the U.S. EPA Symposium on Radon and Radon Reduction Technology. EPA-600/9-89/006a. pp. 6-25 to 6-44. Research Triangle Park, N.C., 1989.

13. Turk, B.H., Harrison, J., Prill, R.J., and Sextro, R.G. Developing soil gas and ^{222}Rn entry potentials for substructure surfaces and assessing ^{222}Rn control diagnostic techniques. Submitted to Health Physics. Lawrence Berkeley Laboratory Report No. 27319, Berkeley, CA. 1989.

14. Sextro, R.G., Harrison, J., Moed, B.A., Revzan, K.L., Turk, B.H., Grimsrud, D.T., Nero, A.V., Sanchez, D. C., and Teichman, K.Y. An intensive study of radon and remedial measures in New Jersey homes. In: B. Seifert, H. Esdorn, M. Fischer, H. Ruden, and I. Wegner (eds.), Indoor Air '87: Proceedings of the 4th International Conference on Indoor Air Quality and Climate. Institute fur Wasser-, Boden- und Lufthygiene: Berlin. 2: pp. 295-299, 1987.

15. DSMA Atcon Ltd. Review of existing instrumentation and evaluation of possibilities for research and development of instrumentation to determine future levels of radon at a proposed building site. Report No. INFO-0096. Atomic Energy Board. Ottawa, Canada. 1983.

16. Fisk, W.J. and Mowris, R.J. The impacts of balanced and exhaust mechanical ventilation on indoor radon. In: B. Seifert, H. Esdorn, M. Fischer, H. Ruden, and I. Wegner (eds.), Indoor Air '87: Proceedings of the 4th International Conference on Indoor Air Quality and Climate. Institute fur Wasser-, Boden- und Lufthygiene: Berlin. 2: pp. 316-320, 1987.

17. Nazaroff, W.W., Feustel, H., Nero, A.V., Revzan, K.L., Grimsrud, D.T., Essling, M.A., and Toohey, R.E. Radon transport into a detached one-story house with a basement. Atmospheric Environment. 19: 31, 1985.

18. Turk, B.H., Prill, R.J., Grimsrud, D.T., Moed, B.A., and Sextro, R.G. Characterizing the occurrence, sources, and variability of radon in Pacific Northwest homes. Submitted to JAPCA, Journal of the Air and Waste Management Association. Lawrence Berkeley Laboratory Report No. LBL-26960, Berkeley, CA. 1989.

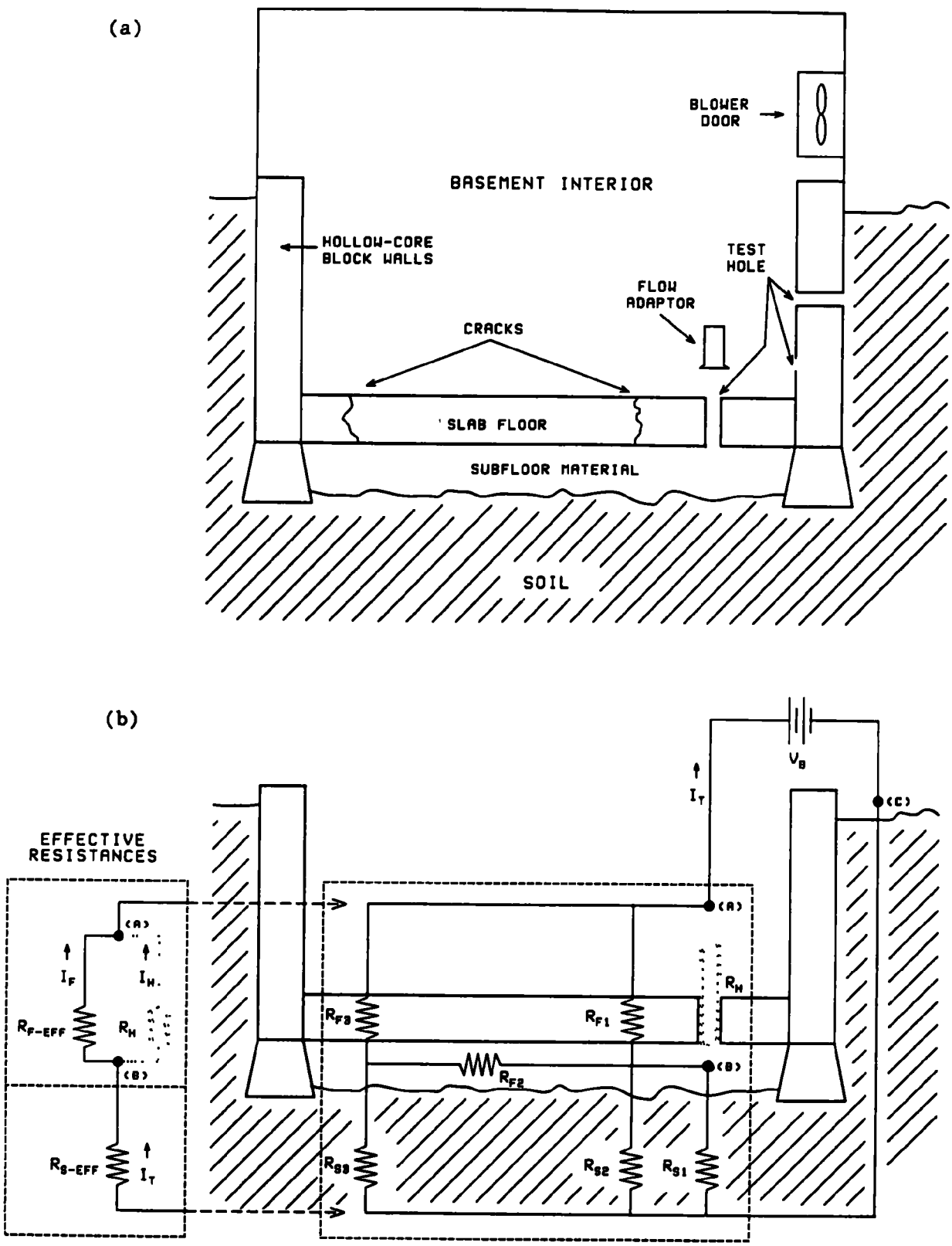

Figure 1. Drawing of substructure during pressure field mapping and basement depressurization (a). A simplified electrical analog of the various flows, pressure drops, and resistances during the test depicted in (a) is shown in (b). The dotted line indicates the variables associated with an open test hole. A further simplification is shown by the circuit on the left side of (b).

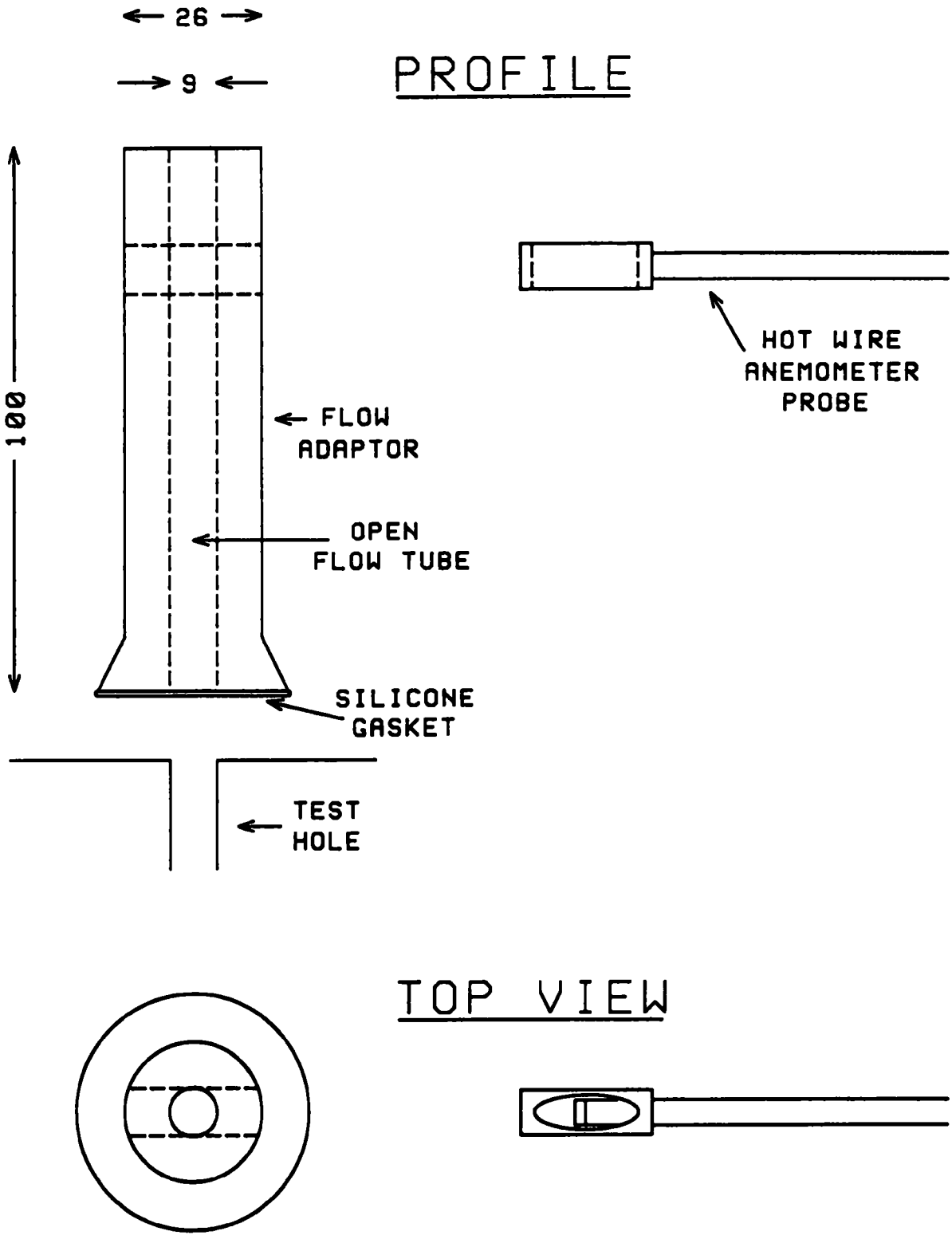

Figure 2. Flow adaptor device used to measure the flows through the test holes. The bottom opening of the adaptor seals against the test hole surfaces, while flows are measured with a hot wire anemometer probe placed inside the open end of the adaptor.

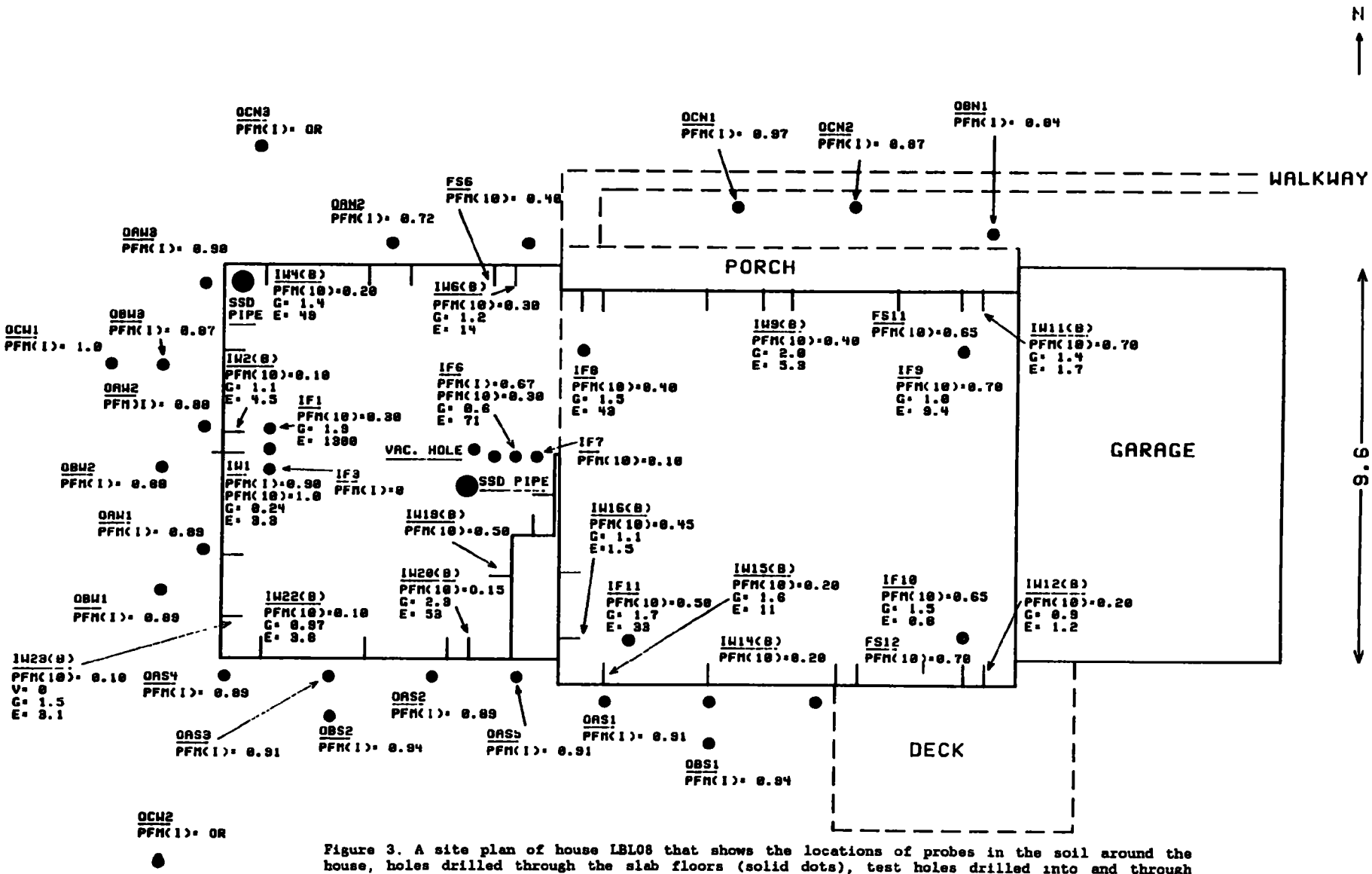

Figure 3. A site plan of house LBL08 that shows the locations of probes in the soil around the house, holes drilled through the slab floors (solid dots), test holes drilled into and through hollow block walls (vertical and horizontal lines), and the pipes for the radon control systems. Data for pressure coupling ratios during pressure field mapping tests (PFM), and for soil gas (G) and radon (E) entry potentials are placed under the identification code for the test holes. See Table 3 for more complete descriptions of the codes and symbols that are used.

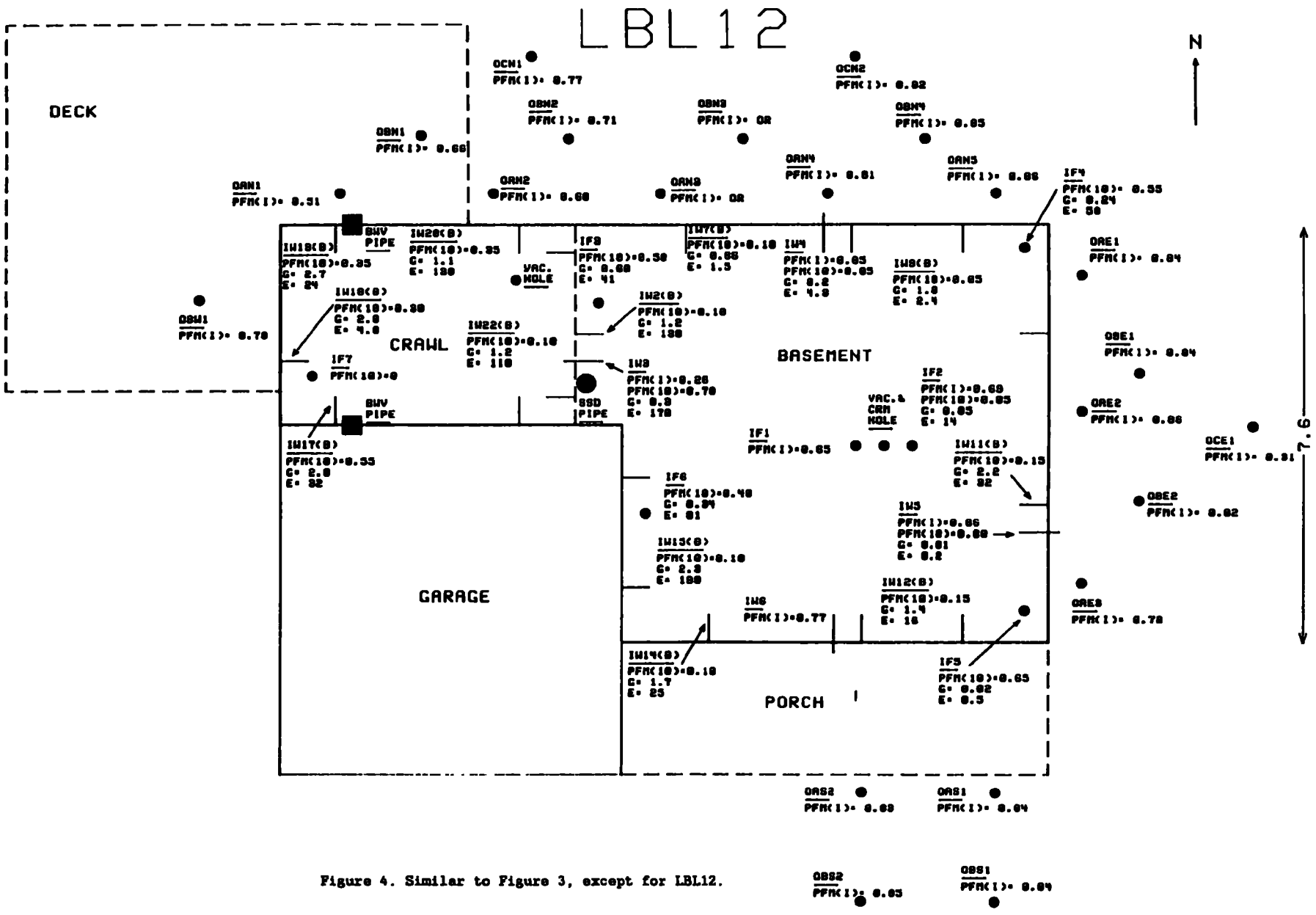

Figure 4. Similar to Figure 3, except for LBL12.

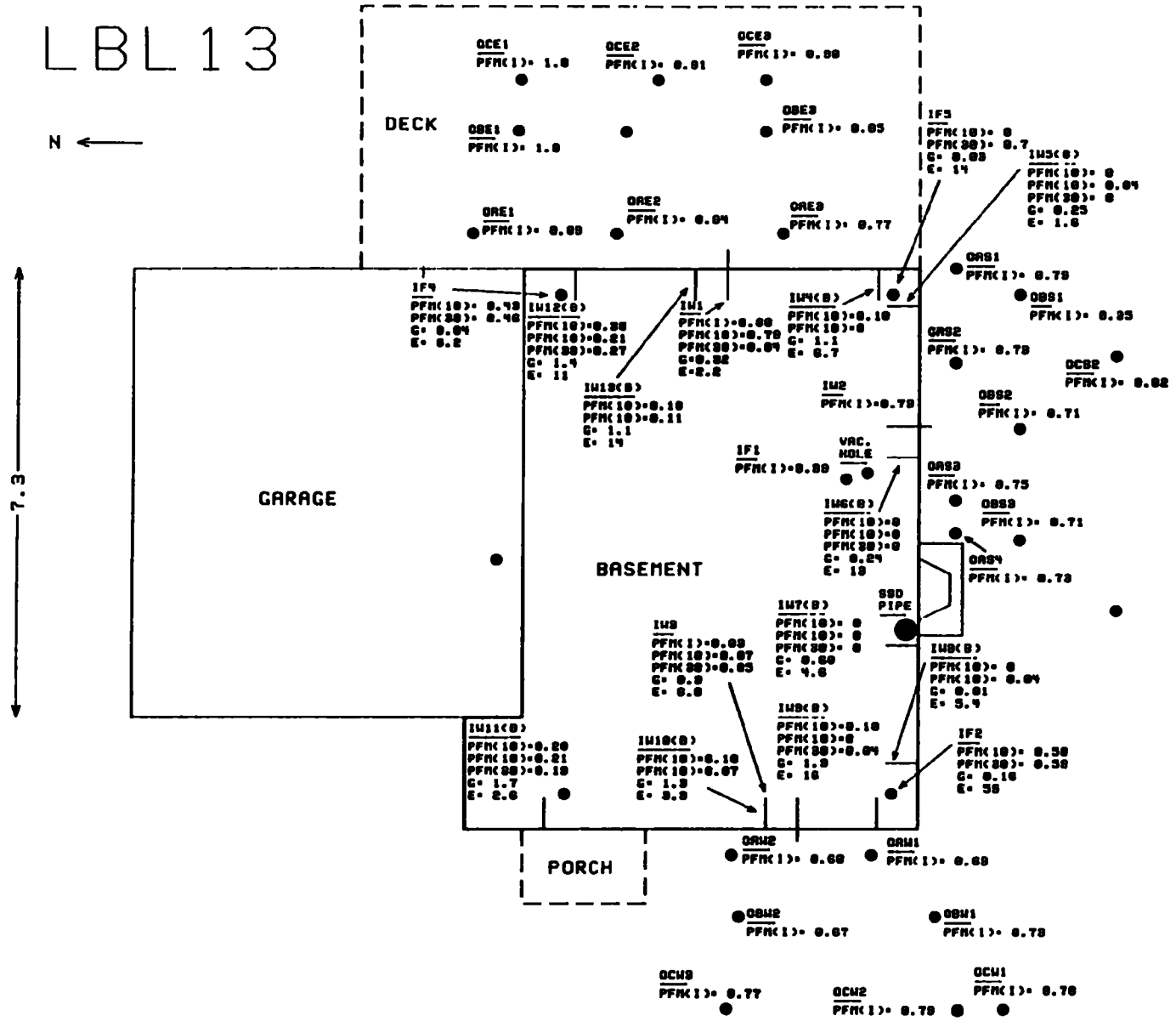

Figure 5. Similar to Figure 3, except for LBL13.

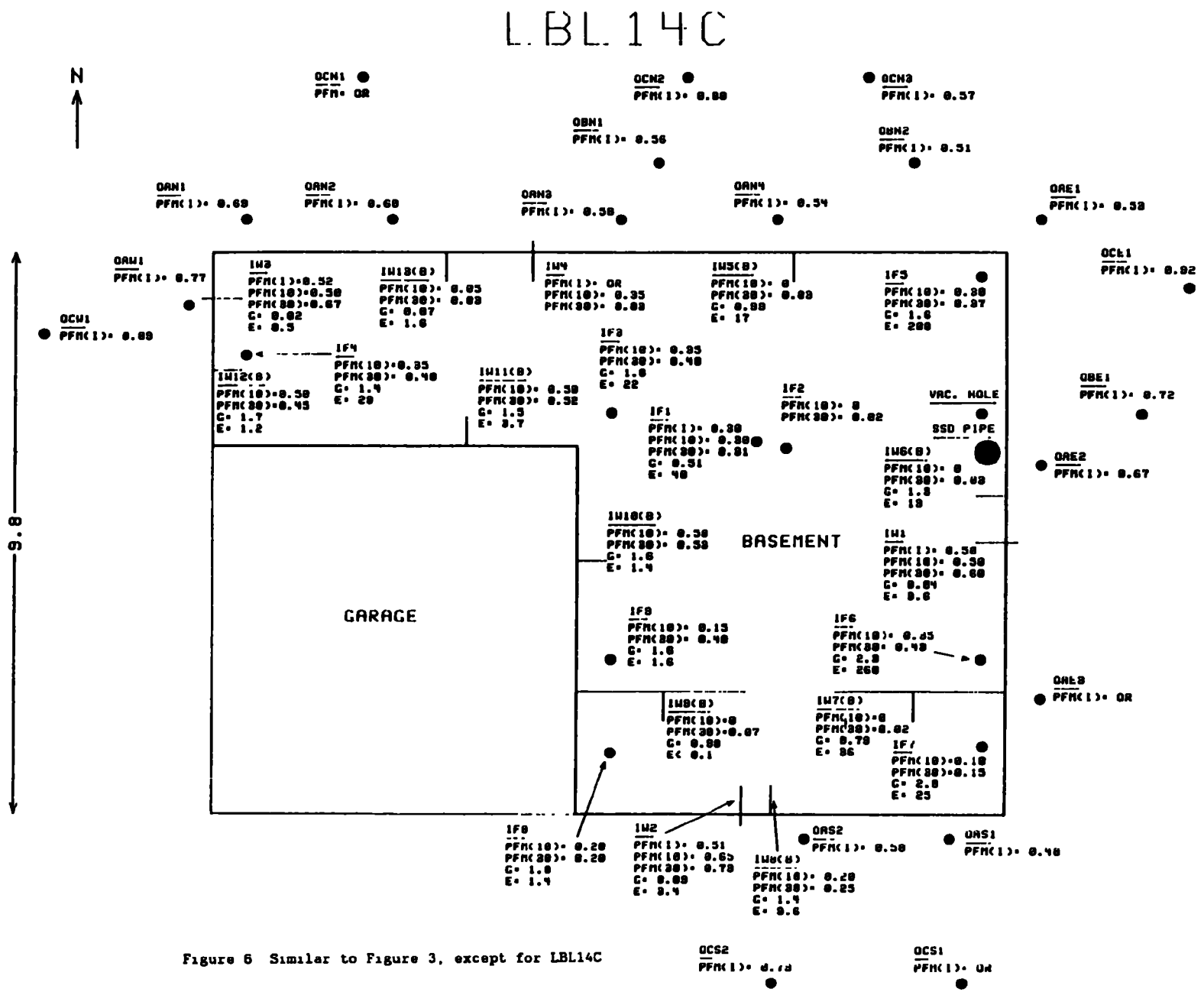

Figure 6 Similar to Figure 3, except for LBL14C

Table 1. Statistical Summary of Effective Resistances for Soils and Substructure Surfaces from Four Houses

Material Category	Test Hole Location: Below Slab Gravel	Block Wall Cavity	Wall Exterior	All Locations
Soils, $R_{S\text{-}EFF}$ (10^6 Pa-s/m^3)				
Geom. Mean	1.2	0.68	2.5	0.93
Geom Std Dev	5.0	2 2	5.8	3 6
Arith Mean	5.3	1.1	8.1	3.2
Arith Std Dev.	11	2.1	12	7.7
Number	22	44	9	75
Substructure Surfaces, $R_{F\text{-}EFF}$ (10^6 Pa-s/m^3)				
Geom Mean	0 65	0.12	5.7	0.32
Geom Std Dev.	4 8	2.1	7 8	6.0
Arith Mean	3 0	0.16	19	3.2
Arith Std Dev	7.7	0.12	26	11
Number	22	44	9	75

Table 2 Statistical Summary of Soil Gas and Radon Entry Potentials from Four Houses

Entry Potential	Test Hole Location: Below Slab Gravel	Block Wall Cavity	Wall Exterior	All Locations
Soil Gas Entry Potential, G (10^{-6} m^3/Pa-s)				
Geom. Mean	0.5	1.2	0.11	0 73
Geom Std Dev	4 8	1.6	4 3	3 6
Arith Mean	1.1	1.4	0.24	1.1
Arith Std Dev	0.85	0.52	0.28	0.70
Number	22	44	9	75
Radon Entry Potential, E (10^{-3} Bq/Pa-s)				
Geom. Mean	23	7.9	3.2	9.7
Geom Std. Dev.	6 7	5.1	6.4	6.2
Arith Mean	110	24	21	48
Arith Std Dev.	280	42	54	160
Number	22	42	9	73

Table 3. Key to Symbols for Figures 3 to 6

LOCATIONS

I = Indoor
- W = Wall
  - (B) = Into block wall cavities
  - Blank = Through wall, into soil
  - Top = Opening into block at top of wall
- F = Through floor

FS = Floating slab

O = Outdoor
- A ≈ 0.5 m from house
- B ≈ 1.5 m from house
- C ≈ 3.0 m from house
- N,E,W,S = Orientation to compass direction

1,2,3,... = Arbitrary sample location number

SSD PIPE = Subsurface depressurization pipe for radon control system

BWV PIPE = Block wall ventilation pipe for radon control system

VAC. HOLE = Test hole where vacuum was placed for pressure field extension tests

MEASUREMENTS AND DATA

PFM = Pressure field map coupling ratio $\left(\frac{\Delta P_{TESTHOLE}}{P_{OUTSIDE} - P_{BASEMENT}}\right)$
- I = Initial test, basement depressurized to -30 Pa
- 10 = Basement depressurized to -10 Pa
- 30 = Subsequent tests with basement depressurized to approx. -30 Pa
- OR = Over range

G = Soil gas entry potential (10^{-6} m^3/Pa-s)

E = Radon entry potential (10^{-3} Bq/Pa-s)

MEASUREMENTS AND MODELLING OF RADON INFILTRATION INTO A DWELLING*

by: P. Stoop, F.J. Aldenkamp, E.J.T. Loos, R.J. de Meijer and L.W. Put
Kernfysisch Versneller Instituut
Rijksuniversiteit Groningen, Zernikelaan 25, 9747 AA Groningen, the Netherlands

In situ measurements in a Dutch test dwelling of radon exhalation of walls, floor and soil in and under the dwelling are interpreted in terms of source strengths. Continuous measurements of radon concentration in various compartments (e.g. crawl space and living room) of the same dwelling together with measurements of leakage parameters, temperature, pressure differences between compartments and ground-water table are used to obtain information on the dynamic aspects of the radon infiltration. Source strengths and dynamic variables are used as input for a multi-room model to describe the variations and interrelations of radon concentrations in various compartments. Despite the relatively low radon concentration in the soil gas (~ 10000 $Bq.m^{-3}$) and the low permeability of the soil, preliminary analyses suggest pressure driven flow through the soil to the crawl space to be an important radon source. A possible influence of precipitation on this flow and on the source strength for the soil of the crawl space is discussed.

*) Research supported in part by the Dutch Government and the Commission of the European Communities.

1. INTRODUCTION

Radon being a noble gas has the property to move from its location of birth by two physical processes: diffusion and pressure driven flow. Diffusion is the process by which radon is transported due to concentration differences. Pressure differences cause transport through e.g. porous materials and openings in walls. The importance of the transport is determined by the product of current and concentration; a low current with a high concentration may be equally important as a high current with a low concentration.

To design effective countermeasures against elevated radon concentrations, source strengths, entry routes and driving forces have to be known. Source strengths can be estimated for a dwelling by measuring *in situ* the exhalation rate of various components of a dwelling. Entry routes and driving forces may be determined from measurements of radon concentrations simultaneously with other relevant physical parameters.

The dynamic aspects have been measured in houses in New Jersey by the groups of Berkeley and Princeton-Oak Ridge. So far, to our knowledge, no results have been published in the open literature. Also in Finland continuous measurements of radon have been made by Arvela *et al.* (1). They compare the variation in measured radon concentrations of 33 houses with variations calculated with a model which relates indoor radon concentrations to radon entry rate, air infiltrations and meteorological factors. In houses with a slab on ground the measured seasonal variations are often explained almost entirely by pressure driven flow. Diffusion is according to ref. (1) a significant source in case of large porous concrete walls against the soil. According to their measurements and calculations the diurnal maximum in the radon concentrations occurs in the morning and is caused by pressure driven flow.

Median radon concentrations in the Netherlands (2-3) are comparable to values found in the Federal Republic of Germany and England. However, due to the absence of rock near the surface, except for the far south eastern tip, the percentage of dwellings with high concentrations is smaller. In the absence of the need for immediate mitigation an investigation of radon entry and transport for a "typical" house may provide knowledge which leads to reduction of the population dose due to exposure to radon.

In the present investigation measurements are carried out in a test dwelling in Roden in the northern part of the Netherlands. As most Dutch dwellings it has a crawl space which is the result of excavating a part of the soil and refilling it partly with sand. The soil in the 50 cm high crawl space is uncovered. Radon concentrations in the crawl space and the living room have been monitored with time-integrating detectors since 1980.

Unexpected variations (4) were observed in the year average radon concentrations, which are likely due to fluctuations in the ground water level often inundating the crawl space.

The aim of the present investigation is to obtain better understanding of the behaviour of radon concentrations in dwellings. This goal is thought to be achieved by developing a dynamic model in which the radon concentrations are calculated from static source strengths and air currents. For the source strengths the exhalation by walls, floors, ceilings and soil were measured; air currents were deduced from measured pressure differences and measured or estimated leak sizes. Moreover a number of possibly relevant parameters as ground water level, relative humidity, temperature, barometric pressure, and precipitation rate were measured and ventilation rates were deduced.

In this paper we present measurements and calculations for two periods of one week with different characteristics. An hypothesis is formulated in which rainfall plays an important role in changes of values of exhalation rate, source strength and pressure driven flow.

2. TEST DWELLING AND EXPERIMENTAL PROCEDURES

2.1. TEST DWELLING

The test house is located in Roden, southwest of the city of Groningen in the northern part of the Netherlands. It is located on the edge of the "Drents Plateau"; the local soil consists of silty fine sand with intercalations of boulder clay upon "pot clay". The impermeability of the pot clay causes large and rapid variations in the groundwater level. Prior to the installation of a water drainage system in February 1989 the groundwater levels often almost reached the soil surface. Such situations are not uncommon for recently build houses in various parts of the Netherlands.

The dwelling is a single family house, built in 1973. It has a rectangular floor shape with a wall extending from the crawl space to the roof, which divides the house into a northern and southern part which can be regarded as reasonably independent. In the present investigation only the southern part is investigated. This part consists of a crawl space and a high loft living room, with an "open kitchen", directly covered by the roof. The ceiling of the crawl space consists of prefab hollow concrete bars which are covered by a layer of a few centimeters cement; in the living room this layer is covered with ceramic tiles. The outside walls are cavity walls consisting of masonry (about 10 cm thick); the cavity has been filled in 1976 with a polyurethane foam for thermal insulation. The floor of the crawl space consists of uncovered sand and is situated at about 40 cm below the

surrounding soil of the yard. Around the house, at a distance of 1 to 1.5 m, a ring type drain has been installed in February 1989 at a depth of 70-90 cm below the surface. The dividing wall in the crawl space has two crawl openings in addition to feed throughs for central heating (water) and utilities. In June 1989 these openings have been closed by 5 cm thick foam board. All remaining openings in the wall were sealed with caulk. In October 1989 a 20 cm diameter ventilation duct plus fan was installed in order to (de)pressurize the southern part of the crawl space. Natural ventilation of the crawl space occurs via ventilation shafts to the outside air; in principle these shafts should have no connection with the cavity wall.

2.2. EXPERIMENTAL TECHNIQUES

Radon exhalation rates were measured with a device developed from a prototype designed by Ackers (5). A description of the modified version and its collection properties is given in ref. (6). For a measurement the device is placed on a surface; soft-rubber rings at the ends of the two coaxial cylinders are supposed to fit air-tight to the surface. For rough surfaces caulk is applied to the surface and the outer ring after the device has been mounted. For measurements in soil a 30 cm long cylinder with a flat and smooth top surface is placed in the soil on which the device is mounted. Prior to each measurement the device is flushed with dry nitrogen.

The exhalation rate, E, is determined from a fit to the growth curve for the radon concentration C

$$C(t) = \frac{E \cdot A}{V \cdot \lambda} (1 - e^{-\lambda t}). \qquad (2.1)$$

In this equation A is the area covered by the inner cylinder and V is the measuring volume. The quantity λ is the effective decay constant and is the sum of the nuclear decay constant of radon and a constant associated with leakage by diffusion from the measuring volume to its surrounding.

Radon concentrations were measured with a radon meter based on the Lucas cell principle. The device is designed for low background, high efficiency and short measurement time. The efficiency for radon with respect to radon daughters was optimized by segmenting a 13 cm diameter, 30 cm long cylindrical cell into 8 longitudinal sections. The cell and segment wall are covered by ZnS(Ag) except for the side where the cell is mounted onto a 13 cm diameter, low background photo multiplier tube. Due to this geometry a high efficiency for radon is obtained: about 50%. The efficiency for each of the two α-emitting radon daughters is about 60%.

The setup was operated in a quasi-continuous mode: a sample is taken by flushing the cell over a filter and a drying column for five minutes; subsequently the sample is counted for 25 minutes and the number of counts

is stored in the memory of a data logger. Simultaneously the values of the following parameters averaged over 25 minutes are stored in the memory: pressure differences between the outside air at three sides of the dwelling at the crawl space ventilation openings, the pressure difference between living room and crawl space, temperature and relative humidity of outside air, air in the living room and in the crawl space, temperature of the soil near the house and in the yard and barometric pressure.

After transfer of the data to the central computer the counts from the radon meters were converted to radon concentrations after corrections for daughter activity and background.

3. RESULTS

3.1. EXHALATION RATES

TABLE 1. EXHALATION RATES (E), EFFECTIVE DECAY CONSTANT (λ_{eff}), AND SURFACE AREA (A), FOR WALLS, FLOOR AND SOIL OF THE CRAWL SPACE AND LIVING ROOM IN THE SOUTHERN PART OF THE TEST DWELLING.

	E ($Bq.m^{-2}.h^{-1}$)	λ_{eff} (h^{-1})	A (m^2)	E.A ($Bq.h^{-1}$)
crawl space (V=26 m^3)				
soil d = 58 [1]	1.78 ± 0.08	0.014	48	85
" d = 48	0.88 ± 0.06	0.011		42
" d = 46	1.02 ± 0.06	0.011		49
inner wall	2.44 ± 0.06	0.11	10	24
outer wall	1.96 ± 0.04	0.043	15	29
ceiling[2]	3.40 ± 0.05	0.054	48	173
living room (V=208 m^3)				
floor	1.34 ± 0.04	0.032	48	65
wall	0.26 ± 0.05	0.074	97	25

[1] water level relative to the soil surface, averaged over the measuring period

[2] taken identical to the value of the floor in the study

Table 1 lists exhalation rates, effective decay constants and surface areas for the perimeters in the crawl space and living room. The exhalation rate for the ceiling is taken equal to the value obtained for the floor in the study because the value for the ceiling could not be measured directly due to its curved surface. In the study the prefab concrete bars are covered by a few centimeters of cement. In the table three measurements are reported taken at different levels of the ground-water in the crawl space. Here one notes a decreasing exhalation rate with a decreasing thickness of the sand layer between the exhalation meter and the ground-water. In the crawl space the exhalation rate of the soil is a factor of two to three smaller than of the walls and the ceiling. The product of surface area and exhalation rate makes that the ceiling yields the largest contribution to the diffusive source strength in the crawl space. From the values of λ_{eff} one notices the large value for the inner wall. This value indicates the roughness of the surface which made it difficult to mount the device leak-tight.

3.2. QUASI-CONTINUOUS RADON MONITORING

Fig. 1 shows from top to bottom four pressure differences $P_i - P_{cs}$ with i=west, south, east and living room, respectively, and P_{cs} is the pressure in the crawl space, the deduced ventilation rate, the radon concentration in the crawl space, and the barometric pressure in week 24 (June 11^{th} - 17^{th}) of 1989. This week was characterized by absence of wind, high temperatures during day time and cool nights. In the figure one notices that during the night time the living room is at a lower pressure than the crawl space and the crawl space is at lower pressure than the outside air. This is attributed to the temperature difference between living room and outside air. In the absence of wind or forced ventilation this stack effect is considered the driving force for the pressure difference between crawl space and living room. The ventilation rate is calculated from conservation of air mass and the flow calculated from the pressure differences and the measured leak of the crawl space ventilation shafts. From the figure one notices that both ventilation rate *and* radon concentration in the crawl space are in phase with each other and the pressure differences over the wall.

Fig. 2 shows the time dependence of a number of parameters during week 31, 1989. In this week there has been almost continuously wind from the southwest, resulting in over pressure at the south and west walls and under pressure in the living room, all with respect to the crawl space. Heavy rain fall occurs on Sunday afternoon and evening as showers. No obvious effect on the radon concentration is observed. On Tuesday and Wednesday evening the open fire was lit causing a sharp increase in the pressure difference between living room and crawl space. Surprisingly no effect of this increased under pressure is observed on either radon concentrations and/or pressure difference of the crawl space with the outside world. The radon

concentration in the crawl space shows the diurnal cycle similar to the one in fig. 1. Also in the pressure differences such a cycle is noticeable. The difference with fig. 1, however, is that the maxima in the crawl space radon concentration are more pronounced and that for Tuesday, Wednesday and Thursday they coincide with the minima in the ventilation rate. However, they are more pronounced than the variations in the ventilation rate. The overall trend of the crawl space radon concentration is decreasing towards the middle of the week and increasing afterwards. For the radon concentration in the living room no diurnal cycle is observed; the concentration diminishes somewhat on Wednesday and Thursday.

4. ANALYSIS AND INTERPRETATION

4.1. STATIC VENTILATION MODEL

In the extremely simplified model for the radon concentration in a room which is ventilated with radon-free air one considers constant static sources and a constant ventilation rate. For the equilibrium situation one may write for the radon concentration C in a room with ventilation rate λ ($\lambda \gg \lambda_{Rn}$) and volume V:

$$C = \frac{1}{\lambda V} \sum_i E_i A_i, \qquad (4.1)$$

where the summation is over all radon exhaling surfaces indicated by i with exhalation rate E_i and surface area A_i. Here it is assumed that the radon concentration in the incoming ventilation air may be neglected.

For the crawl space with volume V=26 m^3, a ventilation rate λ=0.5 h^{-1} (based on the average value in fig.2e) and E_i and A_i taken from table 1 one obtains a value of C=21 and 17 $Bq.m^{-3}$ for a dry soil (d=46 cm) and a barely inundated (d=0 cm) crawl space, respectively. In the latter case the contribution from the soil has been neglected. In the period 1980-1987 time averaged radon concentrations were measured (4); the average value was 50±20 $Bq.m^{-3}$. The large uncertainty in this value is due to large fluctuations in the radon concentration, presumably due to variations in the ground-water level (4).

From the numbers one may conclude that based on the exhalation measurements the radon concentration in the crawl space is two to three times higher than expected on diffusion from the materials. This discrepancy indicates another source of radon which, for this crawl space, is equally or even more important.

A similar simplified model yields for the living room with constant source terms and a constant ventilation with a constant fraction, α, of air from the crawl space:

$$C_{lr} = \alpha C_{cs} + (1-\alpha) C_0 + \frac{1}{\lambda V} \sum_i E_i A_i . \qquad (4.2)$$

Substituting C_{lr}=22 Bq.m^{-3} (ref. 4), C_{cs}=50 Bq.m^{-3}, C_0=3 Bq.m^{-3}, λ_{lr}=0.5 and E_i and A_i from table 1 one obtains α=0.4. This value would correspond to a crawl space ventilation rate of at least 3 h^{-1} and hence a discrepancy between the radon contribution calculated from static sources and the observed value for the crawl space of a factor of 15.

4.2. DYNAMIC VENTILATION MODEL

A dwelling is considered with N rooms, each having a radon concentration $C_i(t)$ and a volume V_i; outdoor parameters are indicated by N+1. The radon concentration in room i is determined by the total strength of radon sources in the room, S_i, and the transport of radon by air currents. If q_{ik} denotes the air current from room k into room i the following mass-balance equation for room i can be written:

$$V_i \frac{dC_i(t)}{dt} = - \lambda_{Rn} V_i C_i(t) + \sum_{k=1}^{N+1} (q_{ik} C_k(t) - q_{ki} C_i(t)) + S_i . \qquad (4.3)$$

Defining $\lambda_i = \frac{1}{V_i} \sum_{k=1}^{N+1} q_{ki}$ as the ventilation rate of room i and $\Psi_{ik} = \frac{q_{ik}}{V_i}$,

eq. (4.3) transforms into:

$$\frac{dC_i(t)}{dt} = - (\lambda_{Rn}+\lambda_i) C_i(t) + \sum_{k=1}^{N+1} \Psi_{ik} C_k(t) + S_i/V_i \qquad (4.4)$$

Eq. (4.4) can be written for each of the N rooms, giving a system of N coupled linear non-homogeneous differential equations. The set of equations can be described more comprehensively using vector and matrix notation. In principle the equations can be solved analytically, in practice, however, instabilities occur and a numerical solution is preferred. The algorithms have been implemented in a computer programme (CARACO).

Essential for the calculation are the input parameters: the currents q_{ik} and the source strengths S_i. The currents q_{ik} have been deduced from the pressure difference between room i and k, $\Delta p_{ik}=p_k-p_i$, and the air transparency of a barrier between the compartments i and k, T_{ik}.

$$q_{ik} = T_{ik} \left(\frac{\Delta p_{ik}}{1\ Pa} \right)^n \qquad (4.5)$$

The values of T_{ik} and n are taken from a previous study on the air leaks in this test dwelling (7). For the source term in the crawl space a pressure driven flow term (S_{pdf}) was added to the static sources (S_{st}) as discussed in sect. 4.1. This pressure driven flow stems from the pressure difference between the outside and the crawl space and causes a small, Darcy-type flow, through the soil (and the walls of the crawl space). This flow becomes important due to the relatively high concentration of radon in soil. The relative intensity of this term depends on the permeability of the soil (and walls), the radon concentration in the soil and the length of the crawl space perimeter. As starting values were taken: for the permeability 5.10^{-12} m^2, the value for fine sand, and for the radon concentration in the soil gas 10^4 $Bq.m^{-3}$.

Fig. 3 shows the radon concentration in the crawl space measured during week 24, 1989. The dashed curve is the calculated concentration based on measured leakage parameter, measured S_{st} and a pressure driven flow (PDF) term with a strength 40 times the estimated value of S_{pdf} based on the starting parameters. Without the adjustment of S_{pdf} the magnitude of the concentration is a factor of three too low and the oscillations are out of phase. For the radon concentration in the living room (not measured during that week) a value of about 75 $Bq.m^{-3}$ was assumed at the rare moments that the flow was from the living room to the crawl space. The results indicate that the missing radon concentration in the crawl space may be accounted for by a values of the S_{pdf} which is almost two orders of magnitude larger than estimated from rather arbitrary starting parameters.

Fig. 4 shows radon concentrations in the living room (top) and crawl space (bottom) measured during week 31, 1989. The dashed curves represent the concentrations calculated with a two-room model. First the crawl space concentration was optimized by starting from values for parameters as found for week 24, 1989. The result in the bottom part of fig. 4 is obtained with a seven times larger value than the measured value of S_{st} and a value for S_{pdf} equal to the value estimated from the original starting parameters. With these values of S_{st} and S_{pdf} the average concentration in the crawl space is reproduced; in the living room the concentration is a factor of two

too low. The larger static source term is necessary to reproduce the dips in the crawl space radon concentration at times of increased ventilation; the smaller S_{pdf} to obtain the correct average values.

At first sight it seems rather strange that the size of the terms changes in time and one may argue that the infiltration of radon is still a large puzzle. Without trying to reduce such a conclusion one could think of a possible explanation. During week 31 the ground-water level reached one of its lowest values of the year (d=58 cm). The exhalation of the soil in this period, measured at one location increases sharply (d=58 cm in table 1). The increase of the exhalation rate is larger than expected on basis of difference of water level at d=48 and 46 cm.

As a hypothesis we propose a role to rainfall to qualitatively account for both the increase in exhalation rate and the reduction of the PDF-term. The concentrated precipitation did hardly change the ground-water level until the latter part of the week. This means that the percolating rain has been forming a type of piston on the soil closing of pores in air with water thereby reducing the porosity and permeability of the soil. The slowly moving piston blocks the diffusion of radon to the outdoor soil and thus causes an increase of the radon in the soil gas below the piston. This will enhance the exhalation of the soil in the crawl space, especially near the perimeters (the measurement of the exhalation was made close to the centre). Moreover the reduction of permeability will reduce the PDF-term. It should be stressed again that this is only a hypothesis, which qualitatively accounts for these rather large changes.

CONCLUSIONS

Radon concentrations in crawl spaces and living rooms are larger than calculated from measured static source strengths. Time evolution of radon concentrations measured simultaneously with pressure differences indicates that pressure driven flow may account for the missing contribution to the concentration as well in the crawl space as the living room. This is the result of the preliminary analysis of two weeks in the summer of 1989 with different weather characteristics.

From this analysis we conclude that the effective strength of diffusive and pressure driven terms are not constant in time. It is proposed as a hypothesis that changes in water content of the soil due to precipitation may temporarily increase the radon concentration below the wetted layer and that the increased water content may reduce the pressure driven flow.

Although we are still at the beginning of the analysis of the data and our hypothesis may be replaced by others we would be tempted to state that

understanding radon infiltration into dwellings is not so much a problem of transport in the dwelling than it is a problem of radon transport of soil. In our present opinion the way to better understanding is a combination of analysing measurements, as described in this paper, over a longer period of time to identify possible important parameters and investigations of these parameters under controlled conditions in the laboratory.

This work is part of the research programme of the Environmental Radioactivity Research Group at the KVI and has been financed by the Dutch Government, as part of the National Research Programme RENA, and by the Commission of the European Communities, as part of the 1985-1989 Radiation Protection Programme.

REFERENCES

1. Arvela, H., Voutilainen, A., Mäkeläinen, I., Castren, O. and Winquist, K. Comparison of predicted and measured variations of indoor radon concentration. Radiat. Prot. Dosim. 24: 231-235, 1988.

2. Put, L.W., de Meijer, R.J. and Hogeweg, B. Survey of radon concentration in Dutch dwellings. Sci. Total Environ. 45: 441-448, 1985.

3. Put, L.W., de Meijer, R.J. and Bošnjaković, B.F.M. Radon in the Netherlands. In: Indoor RADON II. Proc. 2nd APCA. Int. Spec. Conf. Cherry Hill, APCA, Pittsburgh, U.S.A., pp. 107-119, 1987.

4. Put, L.W., de Meijer, R.J. Variation of time-averaged indoor and outdoor radon concentrations with time, location and sampling height. Radiat. Prot. Dosim. 24: 317-320, 1988.

5. Ackers, J.G. Direct measurements of radon exhalation from surfaces. Radiat. Prot. Dosim. 7: 199-201, 1984.

6. Aldenkamp, F.J., de Meijer, R.J., Put, L.W. and Stoop, P. Removal processes for charged radon decay products, submitted to Radiat. Prot. Dosim.

7. Phaff, J.C., de Gids, W.F. and Knoll, B. Ventilatie van gebouwen. Metingen van de luchtlekken en voorspelling van de ventilatie van een woning in Roden, IMG-TNO Technical Report C535, Sept. 1983, TNO-Delft.

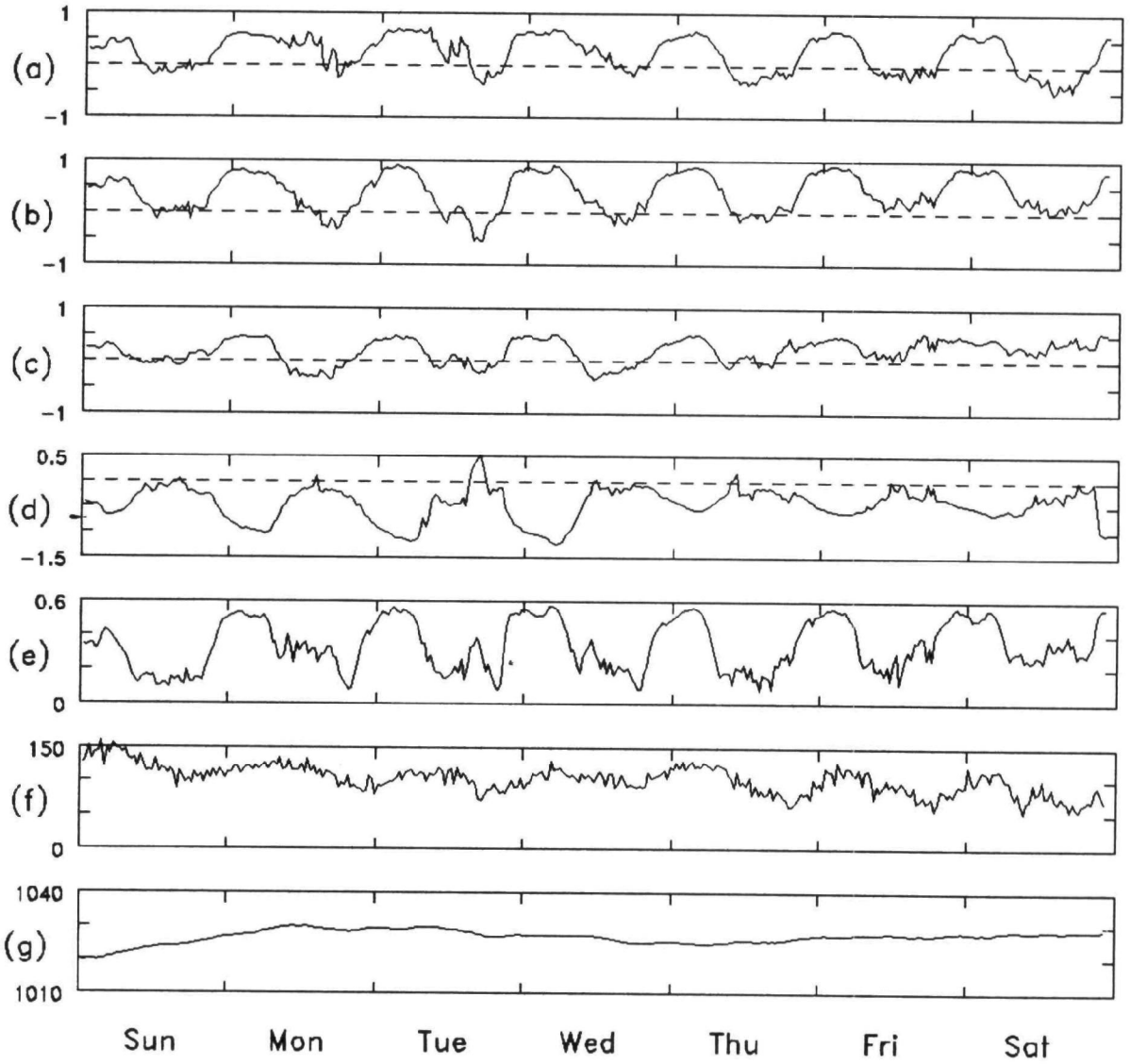

Fig. 1 Pressure differences P_i-P_{cs}(Pa) with P_i being the pressure at the west (a), south (b) and east (c) outside wall and in the living room (d) and with P_{cs} being the pressure in the crawl space. The calculated ventilation rate (h^{-1}) of the crawl space and the measured radon concentration ($Bq.m^{-3}$) and the barometric pressure (hPa) are presented in parts (e), (f) and (g), respectively. All data were collected in week 24, 1989 (June 11-17).

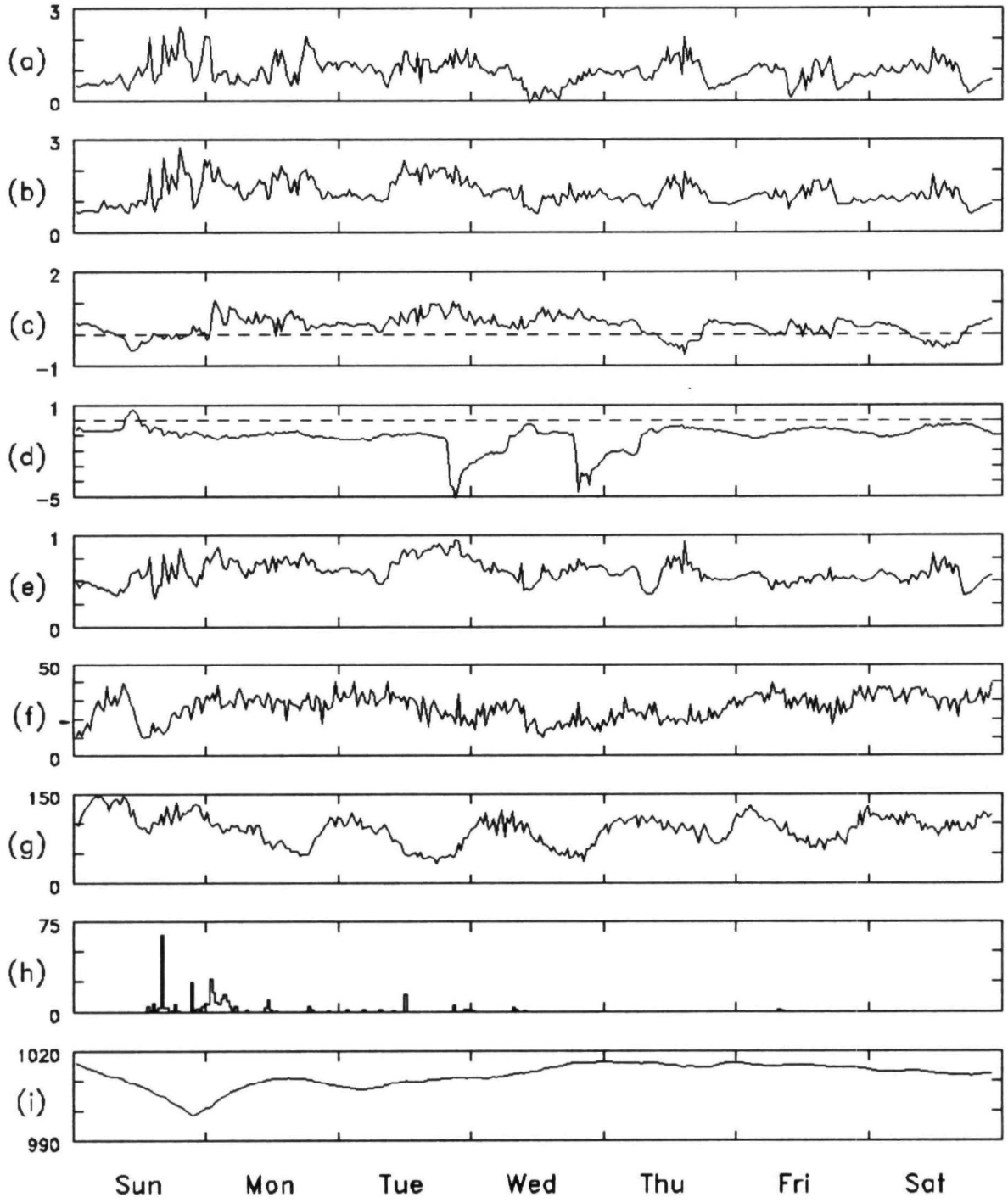

Fig. 2 Pressure differences $P_i - P_{cs}$ (Pa) with P_i being the pressure at the west (a), south (b), and east (c) outside wall and the living room (d), the calculated ventilation rate (h^{-1}) of the crawl space, part (e) the measured radon concentrations($Bq.m^{-3}$) in living room (f) and crawl space (g), precipitation rate ($mm.h^{-1}$) in part (h), and barometric pressure (hPa) in the bottom part. All data are collected in week 31, 1989 (July 30 - August 5).

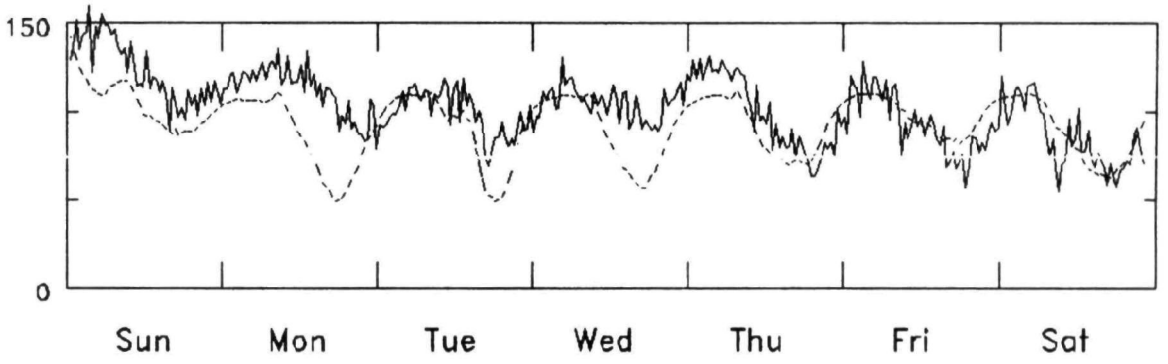

Fig. 3 Radon concentration in the crawl space of the test dwelling in Roden during week 24, 1989 (June 11-17). The solid curve represents the measurement, the dashed curve the calculated concentration with a dynamic model. Multiplication factors for the measured S_{st} and estimated S_{pdf} are 1

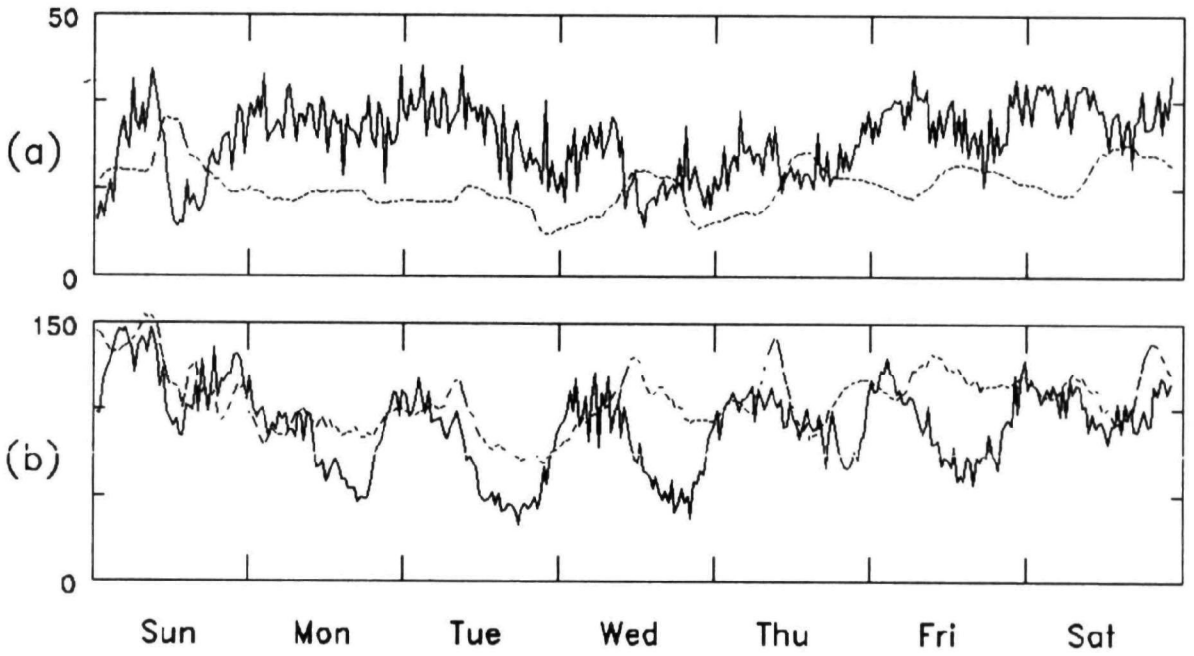

Fig. 4 Radon concentration in the crawl space and living room of the test dwelling in Roden during week 31, 1989 (July 30 - August 5). (See fig. 3). Multiplication factors for the measured S_{st} and estimated S_{pdf} are 7 and 1, respectively.

Session VI:

Radon in the Natural Environment

BENCHMARK AND APPLICATION OF THE RAETRAD MODEL

by: V.C. Rogers
K.K. Nielson
Rogers and Associates Engineering Corporation
Salt Lake City, Utah 84110-0330

ABSTRACT

Field measurements were used to benchmark a simple new predictive correlation between soil gas permeability and soil grain size, moisture, and porosity. The correlation was incorporated with a previous diffusion correlation into the new RAETRAD code, that calculates radon generation and two-dimensional transport in soils, and radon entry into structures. RAETRAD generalizes the one-dimensional RAETRAN model, combining advective and diffusive radon transport with radon emanation, decay, absorption, and adsorption. RAETRAD calculations suggest 0.03 percent radon entry efficiency for slab-on-grade homes on low-permeability soils ($<10^{-8}$ cm^2), increasing to 0.1 percent for sandy soils. Soil or fill properties in the first few feet dominate radon entry efficiency and limiting radium concentrations for prescribed indoor radon levels. For indoor radon concentrations of 2 pCi/liter, sandy soils may contain only 2-3 pCi/g radium compared to 10-20 pCi/g for more clayey soils.

This paper has been reviewed in accordance with the U.S. Environmental Protection Agency's peer and administrative review policies and approved for presentation and publication.

INTRODUCTION

Radon generation and transport in soils and its subsequent entry into dwellings is a complex process requiring characterization of the soil conditions, meteorological conditions, and the structure. Radon emanates from radium-bearing minerals into the soil pore space, followed by diffusive and advective transport in both liquid and gas phases into the dwelling, entering via cracks, sumps, porous building materials, and other routes. The RAECOM (Radon Attenuation Effectiveness and Cover Optimization with Moisture) (1) multiregion, one-dimension radon generation and transport code has been used widely to predict radon migration through porous media. RAETRAN (RAdon Emanation and TRANsport) (2) provides similar capabilities, but also includes advective transport mechanisms. These codes are easy to use and require very little input data; however, because they are one-dimensional, they have limited application for radon entry into structures.

The mathematics of the RAETRAN code have been extended to two dimensions. In addition, the pressure-driven flow equation now is solved in the code instead of externally as required with RAETRAN. The resulting position-dependent velocities have corresponding boundary conditions to those used for the radon generation and transport calculations. The resulting code, called RAETRAD (RAdon Emanation and TRAnsport into Dwellings) (3), retains the general simplicity of operation and minimal input requirements as the earlier RAECOM and RAETRAN codes. However, it provides a more detailed description of radon movement through porous materials such as soil and concrete and subsequent radon entry into structures coupled to the soils.

Key factors in the simplicity of the RAETRAD input data are the simple correlations for predicting gas permeabilities and radon diffusion coefficients for the porous materials. These correlations and their use are discussed in the next section. After that the RAETRAD code is briefly described, and finally is applied to typical Florida soils and structures to obtain radon entry efficiency factors and radon entry rates into dwellings, and to estimate example maximum soil radium concentrations for foundation fill materials.

AIR PERMEABILITY AND RADON DIFFUSION COEFFICIENT CORRELATIONS

Radon migration through soils and entry into dwellings depend strongly on values of radon diffusion coefficients and air permeabilities for the soils and for the applicable house construction materials. Simple correlations for the radon diffusion coefficient have been developed and have been widely used (4-5). The diffusion coefficient correlation that is incorporated in RAETRAD is (6-7):

$$D = \frac{3p(1+p)d_g}{8(2+\pi d_g)} \exp\left[\frac{7p(1+p)d_g}{2+d_g} m - 7m^5\right], \quad (1)$$

where

- D = pore average radon diffusion coefficient ($cm^2 s^{-1}$)
- p = soil porosity
- d_g = geometric mean particle diameter (μm)
- m = fraction of moisture saturation.

Predictive correlations for gas permeability have been proposed previously (7-8). A recently improved permeability correlation for shallow soils (9) was incorporated into RAETRAD:

$$K = p\left(\frac{1-m}{200}\right)^2 d_a^{4/3}, \quad (2)$$

where

- K = air permeability in porous material (cm^2)
- d_a = arithmetic average particle diameter (cm).

Equations (1) and (2) reveal that soil gas permeability and radon

diffusion coefficients both can be estimated from soil moisture, porosity, and particle diameter averages d_g and d_a. In turn, the particle diameter averages can be estimated from standard soil classifications such as the 12 categories used by the U.S. Soil Conservation Service (SCS) (10). Furthermore, the appropriate soil moisture near a dwelling can be estimated from the soil classification and soil matric potential (11).

As an example of the above methodology, measurements were made of the in-situ moisture, gas permeability, porosity, and soil particle sizes for several soils in Florida. Soil samples were obtained at depths of 60 to 75 cm from several locations around the state. The data for the soils are given in Table 1. The soil gas permeabilities were estimated from Equation (2) using the field soil data. The resulting correlation-predicted permeabilities and measured field permeabilities are also given in Table 1. In general, the agreement is within the experimental uncertainties. Two-thirds of the predictions were within a factor of 2 of the field-measured gas permeabilities.

From the particle size and moisture information in Table 1, soil matric potentials were estimated using the methodology described in Reference 11. The estimated matric potentials ranged from $1x10^4$ Pa to $3.4x10^4$ Pa. A matric potential of $5x10^4$ Pa was selected as a reasonably conservative dry-side average for conditions in the locations sampled in Florida. Using the $5x10^4$ Pa matric potential and soil particle size distribution parameters from the soil samples, soil moisture, permeabilities, and diffusion coefficients were estimated for the broader range of soils defined by the U.S. Soil Conservation Service classifications (10). These data are given in Table 2, and were used in the example radon migration and house entry analyses performed by RAETRAD.

TABLE 1. COMPARISON OF IN-SITU SOIL GAS PERMEABILITIES WITH CALCULATED VALUES

Location	Clay wt.%	Silt wt.%	Sand wt.%	Density (g/cm^3)	Moist. Sat'n.	Measured Permeability (cm^2)	Calculated Permeability (cm^2)	Ratio of Calc.Perm./ Meas.Perm.
Ocala	5.9	7.4	86.7	1.54	0.17	$8.5x10^{-8}$	$5.4x10^{-8}$	0.63
Leesburg	74.6	24.8	0.6	1.45	0.86	$3.6x10^{-12}$	$1.3x10^{-11}$	3.52
Leesburg	1.7	5.4	92.9	1.51	0.12	$1.2x10^{-7}$	$8.0x10^{-8}$	0.66
E Orlando	2.0	3.9	94.0	1.48	0.12	$1.0x10^{-7}$	$6.5x10^{-8}$	0.65
N Orlando	1.9	3.0	95.1	1.50	0.19	$2.4x10^{-7}$	$4.4x10^{-8}$	0.18
SW Orlando	2.1	3.1	94.8	1.75	0.49	$4.2x10^{-8}$	$2.1x10^{-8}$	0.51
SW Orlando	1.2	2.2	96.5	1.52	0.13	$9.0x10^{-8}$	$6.6x10^{-8}$	0.73
Kissimee	0.9	1.9	97.2	1.52	0.15	$7.2x10^{-8}$	$7.6x10^{-8}$	1.05
Lakeland	2.2	2.9	94.9	1.56	0.10	$6.8x10^{-8}$	$6.3x10^{-8}$	0.93
NE Tampa	2.2	5.1	92.7	1.69	0.40	$1.1x10^{-7}$	$3.0x10^{-8}$	0.27
Tampa	2.0	5.7	92.3	1.67	0.73	$4.5x10^{-10}$	$4.1x10^{-9}$	9.21
S Tampa	3.2	4.9	92.0	1.52	0.13	$8.6x10^{-8}$	$6.7x10^{-8}$	0.78

TABLE 2. MOISTURES, DIFFUSION COEFFICIENTS, AND PERMEABILITIES OF STANDARD SCS SOILS AT 0.5-BAR MATRIC POTENTIAL*

SCS Soil Classification	Moisture Saturation Fraction	Radon Diffusion Coefficient† (cm^2/s)	Soil Gas Permeability‡ (cm^2)
Sand	0.073	5.1×10^{-2}	1.6×10^{-7}
Loamy Sand	0.196	3.1×10^{-2}	1.4×10^{-7}
Sandy Loam	0.377	1.5×10^{-2}	6.1×10^{-8}
Sandy Clay Loam	0.411	1.3×10^{-2}	5.1×10^{-8}
Sandy Clay	0.488	9.4×10^{-3}	3.2×10^{-8}
Loam	0.576	5.0×10^{-3}	1.7×10^{-8}
Clay Loam	0.664	2.7×10^{-3}	7.5×10^{-9}
Silt Loam	0.780	5.4×10^{-4}	1.7×10^{-9}
Clay	0.813	7.9×10^{-4}	1.0×10^{-9}
Silty Clay Loam	0.900	7.2×10^{-5}	1.2×10^{-10}
Silty Clay	0.932	4.8×10^{-5}	3.3×10^{-11}
Silt	0.938	1.4×10^{-5}	1.8×10^{-11}

*At 1.6 g/cm^3 bulk dry density; 0.407 porosity.
†Estimated from Equation 1.
‡Estimated from Equation 2.

THE RAETRAD CODE

RAETRAD solves the-two dimensional radon balance and air pressure balance equations in cylindrical geometry. The two-dimensional rate balance equation for radon in the gas component of the soil pore space is given by:

$$D_a \left(\frac{d^2 C_a}{dr^2} + \frac{1}{r} \frac{dC_a}{dr} + \frac{d^2 C_a}{dz^2} \right) - \lambda C_a - \frac{k_a \rho \lambda}{(1-m)} C_a + \frac{K_p}{p(1-m)} \left(\frac{dP}{dr} \frac{dC_a}{dr} + \frac{dP}{dz} \frac{dC_a}{dz} \right) + \frac{R \rho \lambda E_{air}}{p(1-m)} R \frac{m\lambda}{(1-m)k_d} + T_{wa} = \frac{dC_a}{dt} \quad (3)$$

where

D_a = radon diffusion coefficient in air, including tortuosity
C_a = radon concentration in the air-filled pore space

r - radial distance from center of house
z - vertical depth from ground surface
λ - radon decay constant
k_a - air-surface adsorption coefficient for radon
ρ - bulk dry density
m - fraction of moisture saturation
K_p - pore gas permeability
p - total porosity
P - pore gas pressure
R - radium concentration in the solid matrix
E_{air} - component of emanation coefficient that is a direct pore air source of radon
k_d - equilibrium distribution coefficient for radium in solid-to-pore-liquid
T_{wa} - transfer factor of radon from pore water to pore air

The T_{wa} transfer factor from pore water to pore air is obtained from combining Equation (3) with a similar rate balance equation for radon in pore water (6). The derivatives of the atmospheric and soil air pressures are obtained by solving the following equation using the same approach as for the radon transport equation:

$$K\left[\frac{d^2P}{dr^2} + \frac{1}{r}\frac{dP}{dr} + \frac{d^2P}{dz^2}\right] = \frac{dP}{dt} \qquad (4)$$

The boundary conditions for Equation (4) are the indoor air pressure applied to the inside surface of the dwelling floor, and the outdoor air pressure (typically averaging zero) applied to the outdoor soil surface. If the dwelling is at a negative pressure compared to the outdoors, then air movement proceeds from the outdoor soil surface downward through the soil and then inward and upward towards the structure as shown in Figure 1. Radon entry into the slab-on-grade dwelling in Figure 1 is assumed to be through a perimeter crack, such as may occur between the slab and foundation footings.

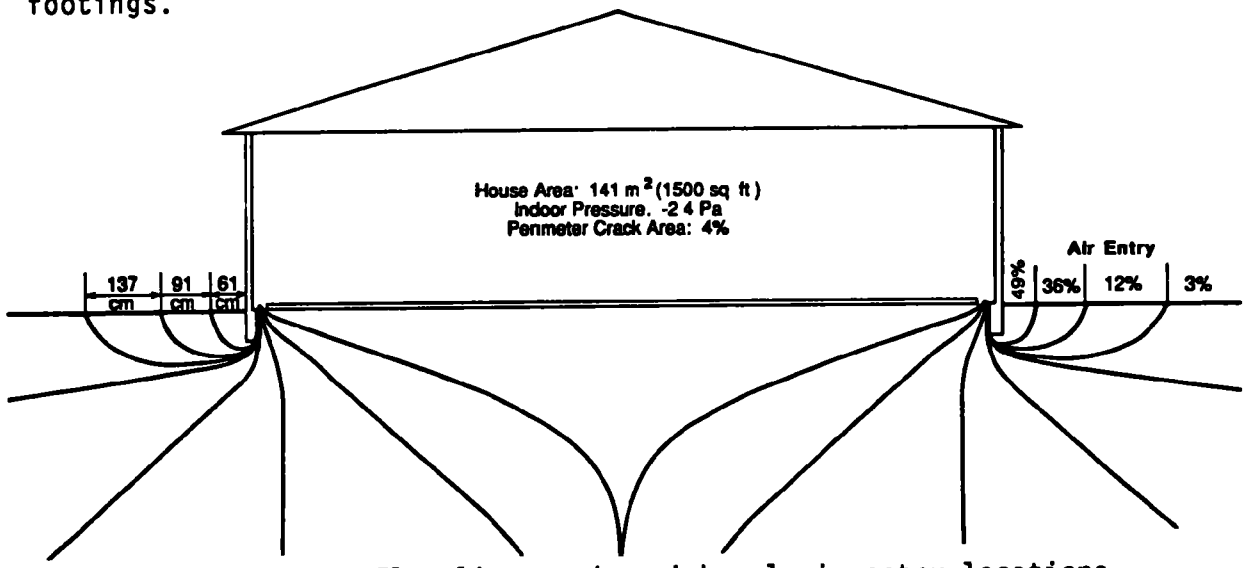

Figure 1. Flow lines and peripheral air entry locations for a structure on a 61-cm deep foundation in sandy soil ($K = 1.7 \times 10^{-7}$ cm^2).

After the pressure field is determined, RAETRAD solves the radon generation and transport equations to obtain values for the following parameters (3):

1. Radon concentration in soil air pores as a function of position.
2. Average radon concentration under the dwelling slab (if applicable).
3. Diffusive, advective, and total surface radon fluxes.
4. Radon entry rates through dwelling floors, walls, and cracks in contact with the soil.
5. Air entry rates from the soil.
6. Radon entry efficiency factors for the dwelling-soil system.

The radon entry efficiency factor is defined as the average indoor radon concentration divided by the area-weighted average sub-slab radon concentration in the soil pores.

APPLICATION OF RAETRAD

The RAETRAD code was applied to the soils and soil conditions given in Table 2. A slab-on-grade structure was coupled to the soils as shown in Figure 1, and it was assumed that radon entered the dwelling through a perimeter crack between the 10-cm thick concrete slab and a 60-cm deep foundation footing. The dwelling is assumed to be at a -2.4 Pa pressure compared to the atmosphere. The radon emanation coefficient of the soil is 0.25. Other parameters used in the analyses are shown in Figure 1.

Radon entry efficiency factors computed by RAETRAD for the dwelling on each of the SCS soils are shown in Figure 2. They increase with increasing soil permeability mainly for coarse-grained soils. The entry efficiency factor becomes less dependent on permeability for permeabilities less than about 10^{-8} cm^2, because diffusion processes dominate the radon entry rate into the dwelling for the low-permeability soils. For these examples, the entry efficiency varies from about 0.025 to 0.1 percent. The radon entry efficiency factors are determined from the radon entry rates, dwelling air volumes, and air exchange rates. The average air exchange rate can be either input directly or estimated from procedures published by the American Society of Heating, Refrigerating and Air-Conditioning Engineers (12). The present example used an air exchange rate of 1 hr^{-1}.

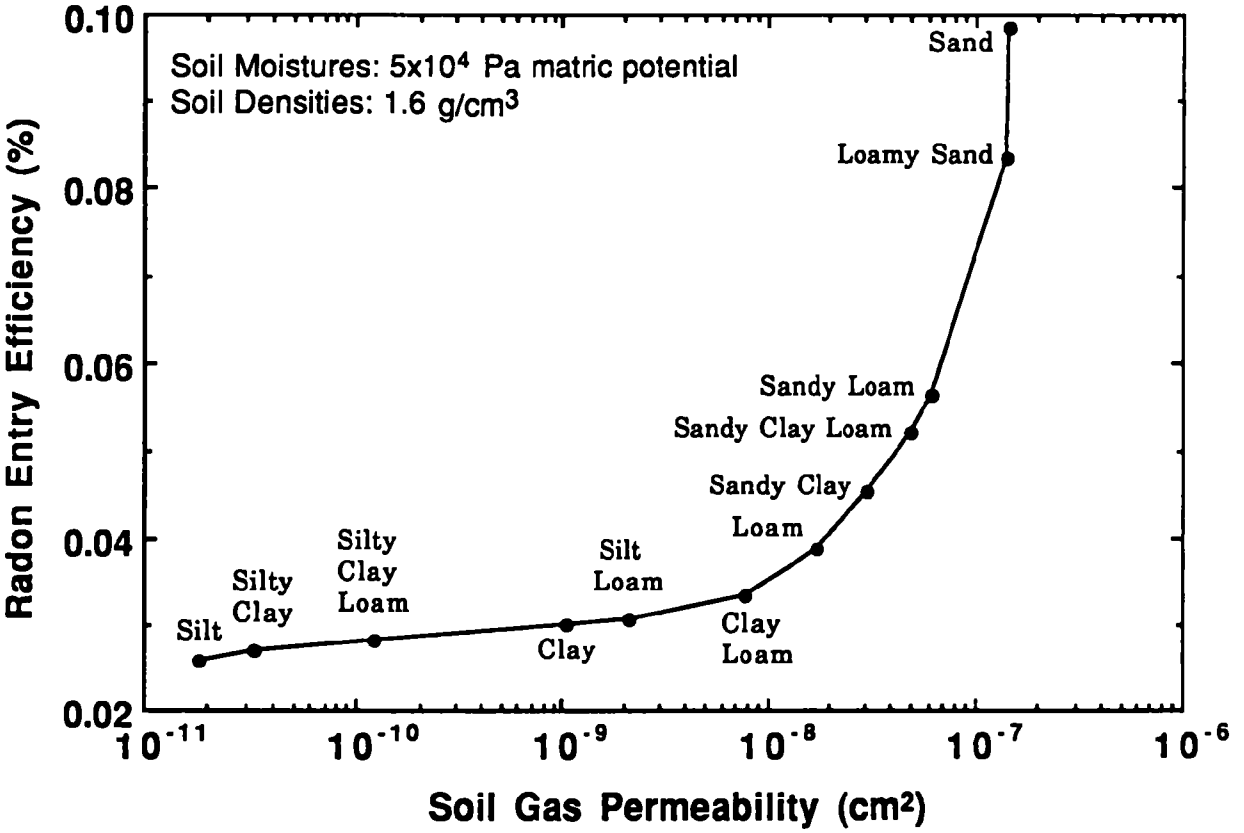

Figure 2. Radon entry efficiencies computed by RAETRAD for a slab-on-grade structure (Figure 1) on uniform soils defined in Table 2.

Maximum soil radium concentrations can also be determined from the example analyses by assuming a maximum indoor radon concentration guideline. A guideline of 2 pCi/liter applied to the example calculations gives the maximum soil radium concentrations shown in Figure 3. The maximum soil radium increases with decreasing soil permeability. Calculations were also made of the maximum soil radium concentrations for a layer of foundation fill material placed over the natural soil. Fill material properties generally obscured effects from the underlying soils when the fill layer thickness exceeded approximately 1 m. For thinner fill layers, high or low radium contents in the underlying soil affected the acceptable radium content of the fill material. As shown in Figure 3, the maximum soil radium for the fill material also becomes insensitive to the natural soil conditions for low-permeability fill materials (less than about 10^{-8} cm^2 permeability). Sandy soils permitted only 2-3 pCi/g radium before exceeding the 2 pCi/liter indoor radon concentration, while finer-grained soils could have 10-20 pCi/g due to their lower permeabilities and diffusion coefficients (Figure 3).

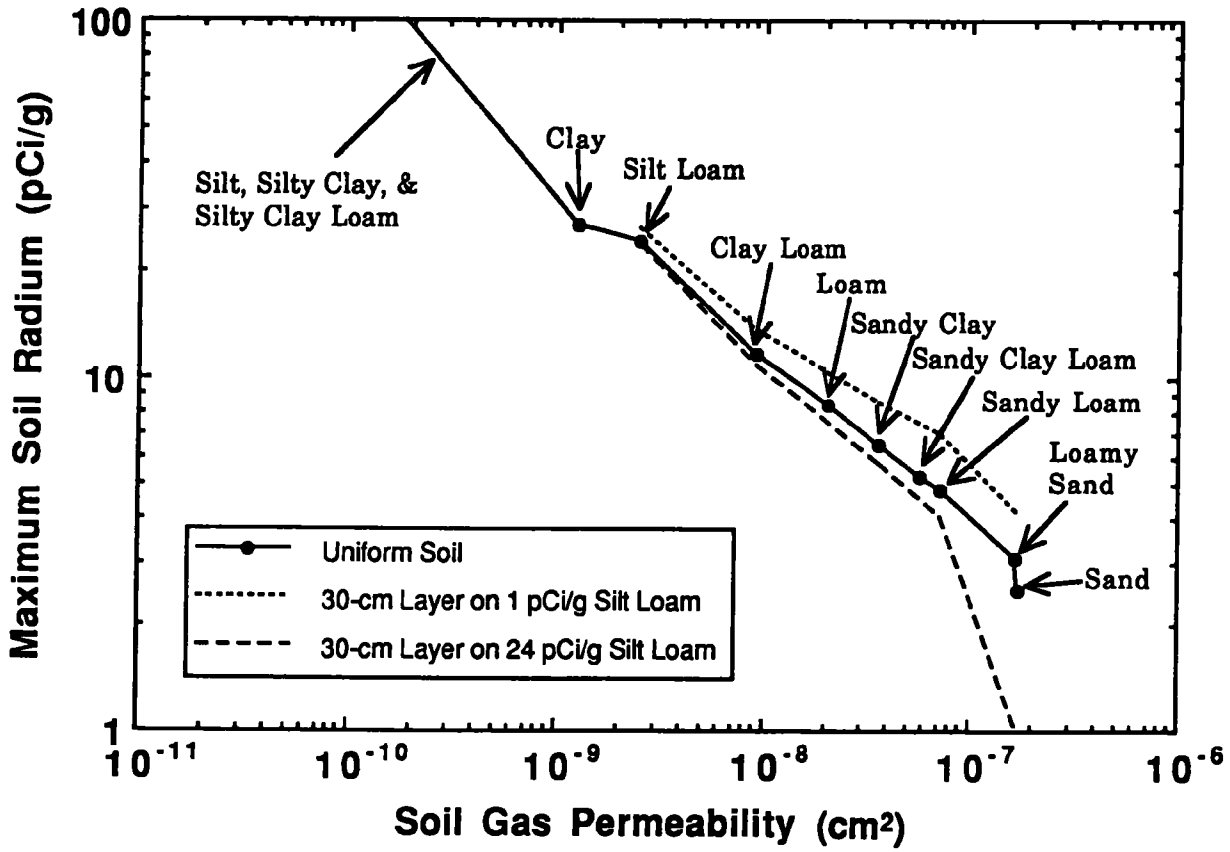

Figure 3. Maximum soil radium concentrations to maintain 2 pCi/liter radon in a slab-on-grade structure (Figure 1) on SCS soils that are uniform (solid line) or used for a 30 cm fill layer over a silt-loam base soil (broken lines). Soil properties are defined in Table 2.

Radon entry efficiency factors and maximum soil radium concentrations also vary according to the perimeter crack width. Figure 4 shows the variation of the entry efficiency factor with the perimeter crack area for a sandy soil. The perimeter crack area is expressed as a percentage of the total slab area, and also may be used to approximate the effects of perimeter utility penetrations through the slab.

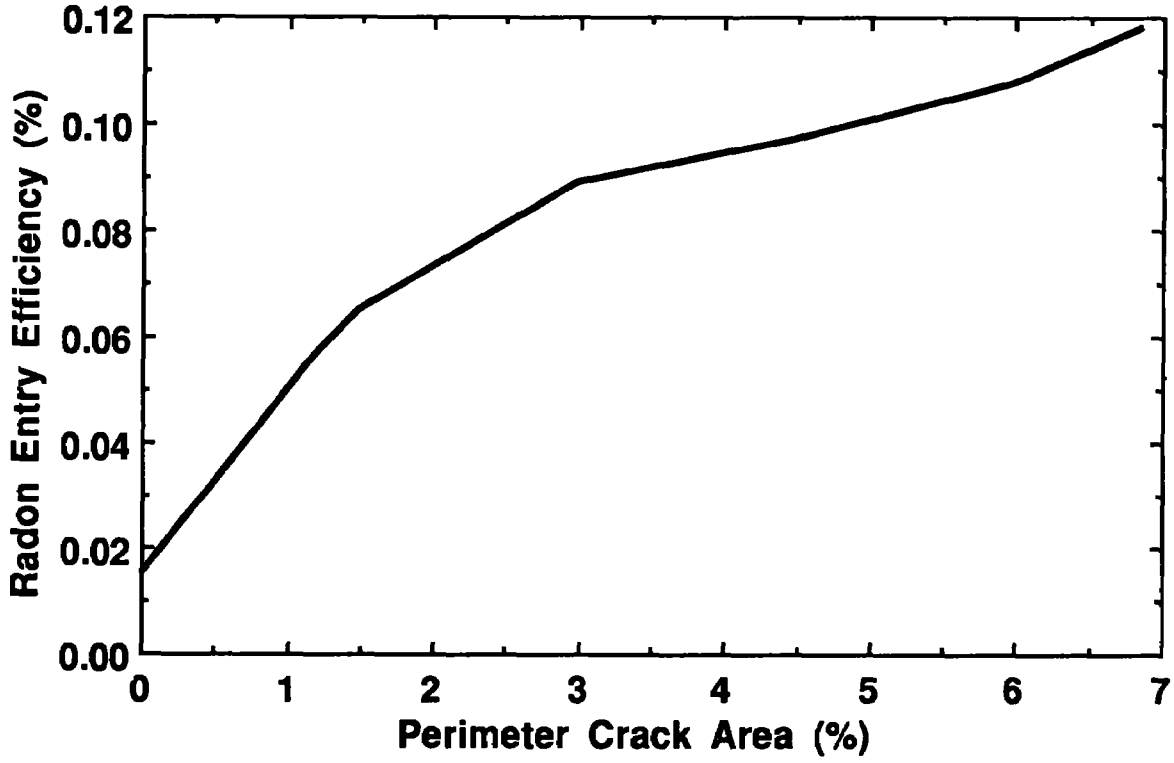

Figure 4. Variation of radon entry efficiencies with the size of perimeter crack for the slab-on-grade structure (Figure 1) on SCS sandy soil.

As a benchmark for RAETRAD, an analysis was performed for a house-soil system in Florida for which some field data are available. The indoor radon concentration for a 203 m^2 slab-on-grade dwelling was measured to average about 10 pCi/liter.

The radium concentration in the top 30 cm of subslab soil is about 0.9 pCi/g, the soil moisture is about 15 percent of saturation, and the measured permeability is 8×10^{-7} cm^2. A subslab radon concentration of 4,200 pCi/liter indicates the presence of a deeper soil layer with elevated radium. This is represented by a 5 pCi/g soil radium layer beneath the top 31 cm layer characterized above. A radon emanation coefficient of 0.25 is also used in the analysis. The RAETRAD calculation gives a subslab radon concentration of 4,000 pCi/liter and an indoor radon concentration of 7 pCi/liter, for a house pressure differential of 1.0 Pa. The estimated indoor concentration is within 30 percent of the measured value of 10 pCi/liter.

ACKNOWLEDGEMENT

This work was supported in part by U.S. Department of Energy grant DE-FG02-88ER60664 and in part under subcontract IAG-RWFL933783 to the U.S. Environmental Protection Agency.

REFERENCES

1. Rogers, V.C., and Nielson, K.K., "Radon Attenuation Handbook for Uranium Mill Tailings Cover Design," U.S. Nuclear Regulatory Commission report NUREG/CR-3533, April 1984.

2. Nielson, K.K., and Rogers, V.C., "Radon Generation, Absorption and Transport in Porous Media -- The RAETRAN Model," *EOS*, 70, 497 (1989).

3. Nielson, K.K., and Rogers, V.C., "A Mathematical Description of Radon Generation, Transport and Entry Into Structures," in preparation.

4. Nielson, K.K., Rogers, V.C., and Gee, G.W., *Soil Science Society of America Journal* 52, 898 (1988).

5. U.S. Nuclear Regulatory Commission Regulatory Guide 2.64, "Calculation of Radon Flux Attenuation by Earthen Uranium Mill Tailings Covers," June 1989.

6. Rogers, V.C., Nielson, K.K., and Merrell, G.B., "Radon Generation, Adsorption, Absorption, and Transport in Porous Media," U.S. Department of Energy report DOE/ER/60664-1, May 1989.

7. Rogers, V.C., and Nielson, K.K., "Radon Emanation and Transport in Porous Media," in Proceedings: The 1988 Symposium on Radon and Radon Reduction Technology, Volume 1, EPA-600/9-89/006a (NTIS PB89-167480), March 1989.

8. Shepherd, R.G., "Correlations of Permeability and Grain Size," *Groundwater* 27, 633-638, 1989.

9. Rogers, V.C., and Nielson, K.K., "Predictive Correlations for Air Permeabilities and Radon Diffusion Coefficients in Porous Media," in preparation.

10. Dunn, I.S., Anderson, L.R., and Kiefer, F.W., *Fundamentals of Geotechnical Analysis*, New York: Wiley & Sons, 1980.

11. Nielson, K.K., and Rogers, V.C., "Moisture, Radon Diffusion and Air Permeability Characteristics of SCS Soil Classifications," in preparation.

12. *Fundamentals Handbook*, "Ventilation and Infiltration," American Society of Heating, Refrigerating and Air-Conditioning Engineers (1981).

GEOLOGIC CONTROLS ON RADON OCCURRENCE IN GEORGIA

L.T. Gregg
Atlanta Testing & Engineering, Inc.
11420 Johns Creek Parkway
Duluth, Georgia 30136

Gene Coker
United States Environmental Protection Agency
345 Courtland Street, N.E.
Atlanta, Georgia 30365

ABSTRACT

Through a combination of geologic models and field measurements, each of the four geologic provinces of Georgia can be characterized for radon concentration. The combinations of bedrock lithology and soil characteristics most likely to exhibit higher radon concentration in Georgia are granites, granodiorites, granite gneisses, pegmatites, mylonites, carbonaceous shales, phosphates, and monazite/heavy mineral placers, coupled with high to medium permeability soils such as gravels, sands, and uniformly-graded silts and sandy silts. Saprolite and surficial soil may either enhance or impede radon migration, as may hydrogeologic characteristics and rock structures such as faults and joint/fractures.

INTRODUCTION

The four radioisotopes considered in this paper are uranium, thorium, radium, and radon. The principal uranium isotope is U^{238}, which decays to Ra^{226}. Radium-226 decays to Rn^{222}, which decays to polonium, bismuth and finally lead. The principal thorium isotope is Th^{230}, which decays to Ra^{228}, then to Rn^{220}, polonium, bismuth and finally lead. Because of its half-life of 3.8 days, Rn^{222} is of much more concern and interest from an environmental standpoint than Rn^{220} (56 seconds half-life).

The basic properties of radon are: it is gaseous and therefore highly mobile, it is an alpha and gamma emitter so its presence can be measured (usually with an alpha-particle measuring device), it is a daughter or decay product of radium, it is moderately soluble in water and its solubility decreases with increasing temperature, and it does not readily combine chemically with other elements. These properties form the framework for our understanding of radon generation, occurrence and migration in rocks, soils, and groundwater.

In considering the geologic setting of Georgia and the Southern Appalachians, the major structural and lithologic trends run from northeast to southwest. The principal rock types in the Cumberland Plateau and the Valley and Ridge Provinces are limestones, dolomites, shales, and sandstones, in the Blue Ridge and Piedmont Provinces igneous and metamorphic rocks such as granites, gneisses, and schists, and in the Coastal Plain limestones, sandstones, phosphates, and unconsolidated sediments.

URANIUM GEOCHEMISTRY

Uranium abundance typically ranges from 2 to 5 parts per million (ppm) in granites to as high as 9 ppm in nepheline syenites, from 0.5 to 2 ppm in the andesites and mafic rocks and much less in the ultramafic rocks, to as high as 34 ppm in the Marcellus Shale (an analog of the Chattanooga Shale) and 120 to 140 ppm in the phosphates and phosphorites. Thorium shows similar ranges, as high as 50 ppm in granites.

Why is uranium so widely distributed? Uranium is polyvalent, with the three principal ions being +4, +5, and +6. It has a large atomic radius of 0.8 to 0.97 angstroms; it is highly active chemically and forms strong complexes with many ligand species; and the hexavalent compounds are more soluble than the tetravalent compounds, the latter being isomorphic with Ca, Th, Zr, W, Mo, and so forth. This suite of properties results in a complex geochemistry.

During magmatic differentiation, uranium does not seem to form separate mineral precipitates. There is isomorphic substitution in some rock-forming minerals. Uranium tends to concentrate in late stage crystallization in acidic rocks and minerals such as granites and felsic volcanics, and through hydrothermal action in pegmatite dikes and veins. This is primarily due to its large atomic radius and to its affinity for late forming members in the reaction sequence such as quartz, potassium feldspar and muscovite. In igneous rocks, the petrofabrics play an important role in uranium concentration (or enrichment). The petrofabrics provide microstructural control of uranium movement and deposition such as coatings around mineral grains, and within microfractures and along crystal cleavage planes (which provide a type of porosity for the uranium bearing waters). In felsic volcanics, both acidic and alkalic, uranium may be highly dispersed and thus readily leachable. Some concentration of uranium has been observed in ashes and tuffs and in cross-cutting dikes and veins.

In sedimentary rocks, uranium concentration is more dependent upon the geochemical cycle, including such mechanisms as oxidation-reduction, absorption, adsorption by substrates such as iron oxide, silica, and organic material, formation of fluoride, sulfate, phosphate, carbonate, and organic complexes, the relative mobility of the hexavalent and tetravalent ions, and the weathering and solution of the uranium source and the transport, precipitation and deposition of the weathered uranium. Figure 1 shows the processes

controlling the occurrence of syngenetic uranium in the sedimentary environment. Through various mechanisms - oxidation, reduction, adsorption, ionic substitution, and evaporation - uranium concentrates in different sedimentary rocks. Figure 2 shows the processes controlling epigenetic uranium deposition. Concentration mechanisms here are primarily adsorption, precipitation, evaporation, and changes in redox potential and pH.

Figure 3 shows an idealized sequence of the processes that control uranium concentration in metamorphic rocks, where recrystallization may cause a grain size increase, porosity reduction, and liquid-gas expulsion, resulting in uranium movement into fractures, shear zones, and lower pressure zones and concentration in them.

To summarize, the principal factors in uranium mobility and concentration are the long half-life, ionic size, polyvalence, mineralogy and uranium content of the source, petrofabric, and geochemical conditions such as the amount and rate of circulating water, climatic factors, pH and Eh, the presence or absence of complexing agents, and the presence or absence of sorptive materials.

RADIONUCLIDE MOBILITY

Uranium is more mobile than its daughter product radium. Generally, uranium may be considered much more mobile in oxidizing environments than in reducing environments, whereas radium is most mobile in chloride-rich reducing environments. Radium tends to behave chemically somewhat similar to the alkaline earths such as calcium and may complex with sulfate, carbonate, or chloride.

Since radon is a gas, the oxidation-reduction environment is immaterial. Radon has two principal components to its movement: diffusion, which is generally thought to be a minor component (probably an average of about 1 meter from its radium parent source), and convection, which is the major component. Radon can move many meters by convection, but it has to be carried in some type of "geo-gas" that can be either a mixture of helium, nitrogen, methane, CO_2, and so forth, or groundwater, or both.

Once radon is liberated (or "emanates") from its radium parent source, within rock, soil, or water, it will tend to migrate by diffusion and convection to zones of lower pressure, for example vertically toward the surface. A high permeability soil will allow radon to more readily permeate upward to the surface than will soils high in the clay minerals that have resultant high porosity but low permeability. Figure 4 shows an idealized cross-section of the Piedmont from surface soils down through massive saprolite, structured saprolite, partially weathered rock and fresh bedrock. Circulating meteoric waters near the surface should more actively dissolve and transport leachable uranium than at greater depths, where these waters may concentrate iron, silica, and clay substrates which would tend to act as scavengers to concentrate uranium. Relict structures within the

structured saprolite such as joints, fractures, faults, mineral veins, and foliation planes would provide pathways for percolating waters and deposition of substrates and organic material, resulting in sites for precipitation of radionuclide complexes and concentration of uranium, thorium, and radium. These relict structures should also act as conduits for radon migration, through diffusion and convection, toward the surface.

NURE STREAM SEDIMENT DATA

Under the NURE Program, uranium and thorium were measured in stream sediments. The mean in Georgia stream sediments for uranium was 11.62 ppm and 56.62 ppm for thorium. The average upper continental crustal abundances are 2.5 ppm and 10 ppm for uranium and thorium respectively. Thus, the ratio of the mean to the crustal abundance in Georgia is about 4.5 for uranium and 5.5 for thorium.

Figure 5 shows the NURE stream sediment data for uranium (1). The outlined zones include the two highest concentrations of uranium, ranging from 6.1 ppm to 426 ppm. Note the trends from northeast to southwest. The NURE thorium data in stream sediments is almost a perfect overlay of the uranium data, which is not too surprising if one considers the location of the so-called monazite belt as it traverses the Carolinas and Georgia. However, it should be noted that heavy minerals, as they are weathered and eroded from host rocks, tend to concentrate in stream sediments at highly variable transport distances. Thus uranium and thorium stream sediment concentrations are at best an imperfect indicator of adjacent host rock concentrations.

GEOLOGIC CONTROLS IN THE PIEDMONT PROVINCE

We have categorized the geologic factors controlling radon occurrence in the Piedmont Province as bedrock, saprolite, soil, groundwater, and surface processes.

Obviously these factors must interact with one another, but the degrees and types of interaction are not well known, except in a few instances. In examining bedrock, we must consider the lithology and mineralogy, the mobility of radium in either an oxidizing or reducing environment, the amount and continuity of near-surface jointing and fracturing, the proximity of major faults and shear zones, the depth of the water table, and the proximity of pegmatite dikes and veins. Radon concentration and migration in saprolite is influenced by the lithology of the parent rock, the amount and degree of jointing and fracturing and interconnection, the degree of water saturation, permeability and porosity, thickness, zonation (whether the saprolite is structured or massive), and the distribution and extent of nanopores (pores less than one micron in width). In surface and near surface soil the principal influences are thickness, zonation (A, B, and C zones), moisture content (8 to 15 percent has been suggested (2) as optimum for radon emanation), permeability and porosity of the soil, and finally the temperature gradient from the surface,

which determines the water vapor pressure of the soil. The major groundwater influences are the recharge area, the flow directions and flow rates, seasonal fluctuations and the presence of water supply wells (both of which cause a pumping effect), and the infiltration of surface precipitation. Finally, there are meteorologic and topographic effects on radon migration that can be enumerated but are not well understood. Meteorologic controls on soil-gas transport that have been identified are temperature, humidity, precipitation, barometric pressure, presence or absence of snow cover, and wind speed and direction. Topographic effects are primarily the varying thickness of soil cover on ridge tops and hillsides versus that in valleys.

RADON OCCURRENCE IN GROUNDWATER

Until recently, radon occurrence in groundwater has in general been the subject of less research than in soil and bedrock, although there is a fairly large body of empirical groundwater data for the U.S. and some quantitative analysis of that database. There have been several published physical models of radon release from soil and rock into groundwater and transport through aquifers into pumping wells. Together with aquifer lithology, the width and frequency of fractures and pores/nanopores in the aquifer are key determinants of both radon release and transport.

Aquifer lithology has been shown (3) to be a useful and relatively accurate predictor of radon concentrations in groundwater across a wide suite of rock types in North Carolina: granite, metasediments and metavolcanics, gneisses and schists, mafics, nonmarine and marine clastic sediments. The average radon concentrations measured in each of these rock types were generally consistent with relative abundances of uranium in these rocks.

EPA GROUNDWATER SAMPLING PROGRAM

In recognition of the need for additional research, EPA initiated a groundwater sampling program in 1988 in Georgia and Tennessee (4). In Georgia, nine aquifer units or rock types, with more or less homogeneous geologic conditions, were selected for sampling. These nine units or sampling cells are somewhat representative of portions of the four geologic provinces in Georgia. Within each sampling cell, ten private well sample sites were located and sampled. The sampling protocol required continuous pumping and measurements every five minutes of temperature, specific conductance, dissolved oxygen, and pH until these parameters stabilized. After purging and stabilization, the water sampling took place at the faucet nearest the wellhead. For each sample, a total of forty-eight chemical parameters and fourteen radionuclide parameters, including radon and uranium, were analyzed by EPA analytical laboratories.

Some preliminary results from the EPA groundwater sampling program in Georgia

show a range of radon in groundwater in a Piedmont granite gneiss from 3,160 to 268,500 picocuries per liter (pCi/l) with an average of nearly 82,000 pCi/l. In the Blue Ridge, as expected, the minimums, maximums and average are much lower, as is the case in the Valley and Ridge and the Coast Plain.

SUMMARY

The most suspect terranes for radon occurrence in Georgia are granite, granodiorite, granitic gneiss, pegmatites, mylonites and other cataclastics, carbonaceous shales, phosphates and phosphorites, and monazite/heavy mineral placers, which are overlain by high to medium permeability soils and which have conduits for radon migration from the source to the surface, such as joints, fractures, faults, bedding planes and foliation planes.

Much research remains to be done. The E.P.A. groundwater sampling program currently underway will be an important contributor to understanding radon occurrence in groundwater in the Southeast.

The work described in this paper was not funded by the U.S. Environmental Protection Agency and therefore the contents do not necessarily reflect the views of the Agency and no official endorsement should be inferred.

REFERENCES

1. Koch, George S., Jr., A Geochemical Atlas of Georgia, Georgia Geologic Survey, Geologic Atlas 3, 1988.

2. Otton, James K., et al, Map Showing Radon Potential of Rocks and Soils in Fairfax County, Virginia, U.S. Geological Survey, Miscellaneous Field Studies Map MF-2047, 1988.

3. Loomis, Dana P., Aquifer Lithology As a Predictor of Radon Concentration in Groundwater: Research Results in North Carolina, U.S. E.P.A. Conference on Indoor Radon, EPA 904/9-87 145, 1987.

4. Coker, Gene and Olive, Robert, Radionuclide Concentrations from Waters of Selected Aquifers in Georgia, U.S. Environmental Protection Agency, Region IV, 1989.

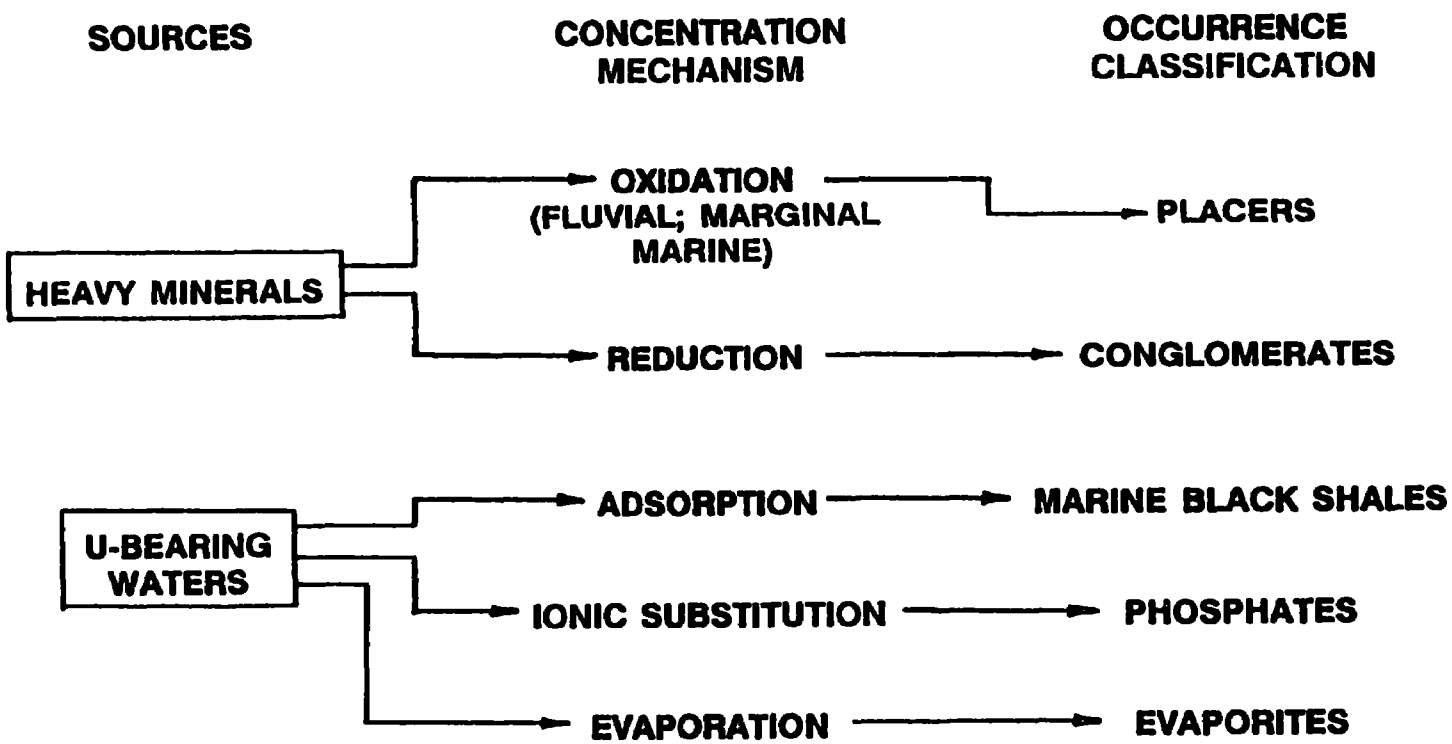

FIGURE 1. SYNGENETIC URANIUM IN SEDIMENTARY ENVIRONMENTS

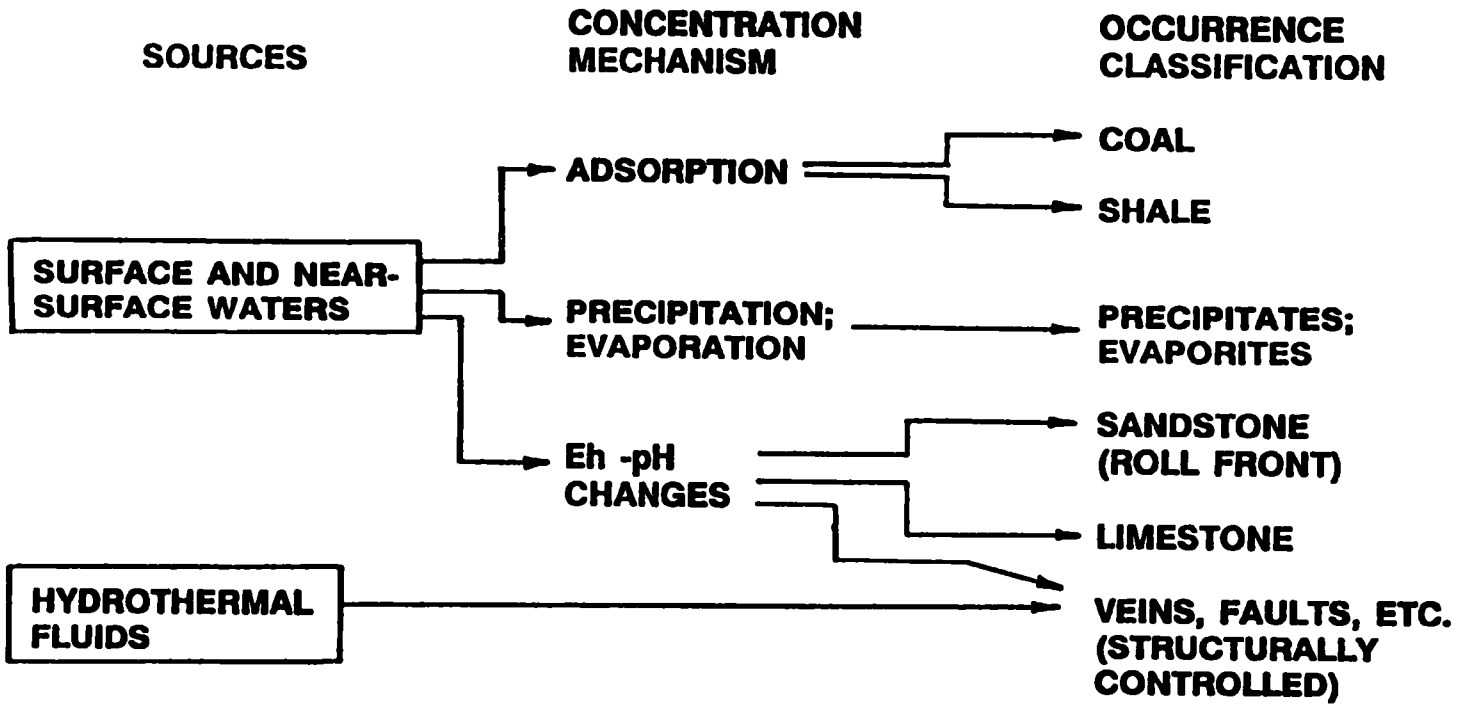

FIGURE 2. EPIGENETIC URANIUM IN SEDIMENTARY ENVIRONMENTS

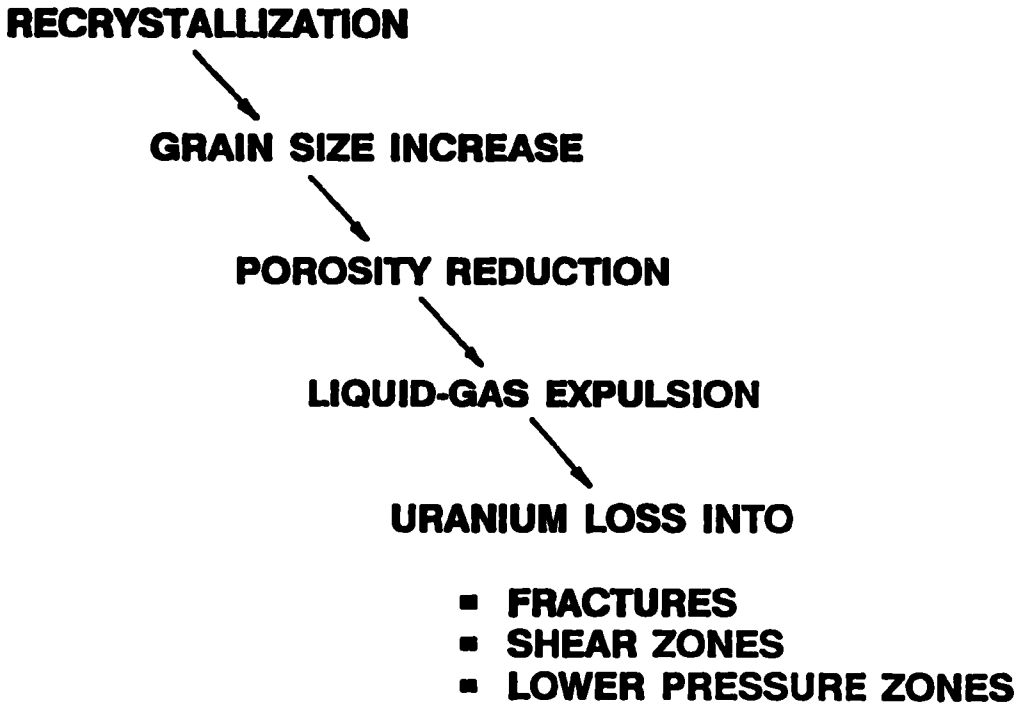

FIGURE 3. URANIUM IN METAMORPHIC ROCKS

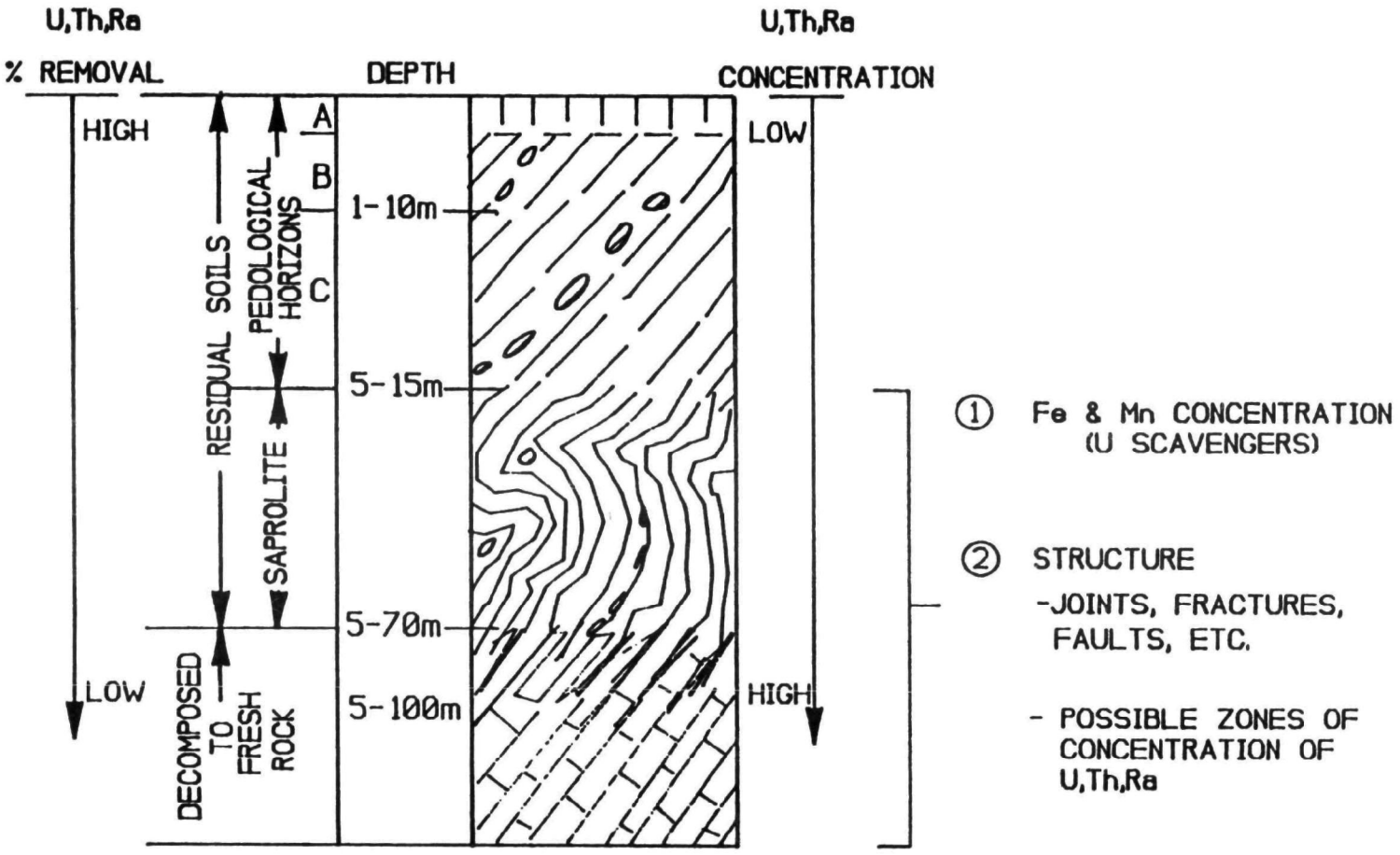

FIGURE 4. IDEALIZED PIEDMONT SUBSURFACE MODEL

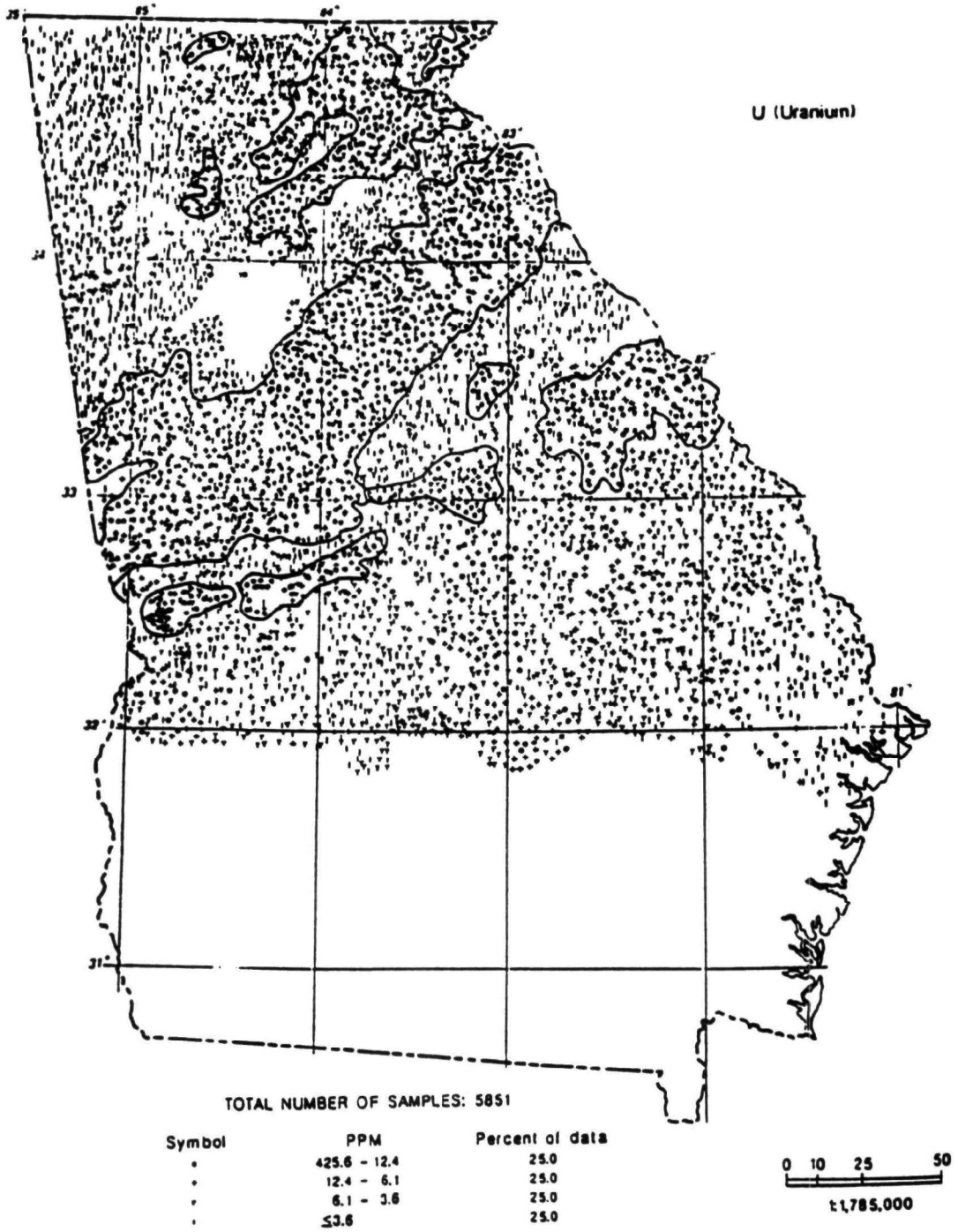

FIGURE 5. NURE STREAM SEDIMENT DATA

CORRELATIONS OF SOIL-GAS AND INDOOR RADON WITH GEOLOGY IN GLACIALLY DERIVED SOILS OF THE NORTHERN GREAT PLAINS

R. Randall Schumann[1], R. Thomas Peake[2], Kevin M. Schmidt[3], and Douglass E. Owen[1]
[1]U.S. Geological Survey, MS 939 Denver Federal Center, Denver, CO 80225-0046
[2]U.S. EPA, 401 M St. SW, Washington, DC 20460
[3]USGS, 345 Middlefield Rd., Menlo Park, CA 94025

ABSTRACT

A higher percentage of homes in parts of the northern Great Plains underlain by soils derived from continental glacial deposits have elevated indoor radon levels (greater than 4 pCi/L) than any other area in the country. Soil-gas radon concentrations, surface radioactivity, indoor radon levels, and soil characteristics were studied in areas underlain by glacially-derived soils in North Dakota and Minnesota to examine the factors responsible for these elevated levels. Clay-rich till soils in North Dakota have generally higher soil-gas radon levels, and correspondingly higher indoor radon levels, than the sandy till soils common to west-central Minnesota. Although the proportions of homes with indoor radon levels greater than 4 pCi/L are similar in both areas, relatively few homes underlain by sandy tills have screening indoor radon levels greater than 20 pCi/L, whereas a relatively large proportion of homes underlain by clayey tills have screening indoor radon levels exceeding 20 pCi/L. The higher radon levels in North Dakota are likely due to enhanced emanation from the smaller grains and to relatively higher soil radium concentrations in the clay-rich soils, whereas the generally higher permeability of the sandy till soils in Minnesota allows soil gas to be drawn into structures from a larger source volume, increasing indoor radon levels in these areas.

This paper has been reviewed in accordance with the U.S. Environmental Protection Agency's peer and administrative review policies and approved for presentation and publication.

INTRODUCTION

Preliminary testing by the U.S. Environmental Protection Agency (EPA) as part of the EPA/State Indoor Radon Survey (1) indicates that a large proportion of homes built on soils derived from continental glacial deposits have screening indoor radon concentrations greater than EPA's recommended action level of 4 pCi/L. Although a correlation between highly permeable glacial deposits and elevated indoor radon levels has been documented by previous researchers, notably in northern Europe (2, 3, 4), the magnitude of the problem in the northern Great Plains States (Table 1) was unexpected because the deposits have low to moderate permeability and low surface gamma radioactivity signatures.

A regional-scale correlation between radon potential and surface gamma radioactivity of areas underlain by bedrock or soils derived from underlying bedrock (5, 6, 7, 8) allows preliminary predictions of radon potential to be made from equivalent uranium or radium data calculated from gamma radioactivity, one of the best sources of which is the map of NURE aerial radioactivity data for the conterminous United States compiled by the U.S. Geological Survey

(USGS) (9). However, the number of homes in North Dakota, Minnesota, and Iowa with elevated indoor radon levels (Table 1) is disproportionately high compared to the generally low aerial radiometric signature of the area. Glacial drift derived largely from the Pierre Shale in North Dakota and from crystalline rocks of the Canadian Shield in Minnesota generate elevated indoor radon levels in a large number of homes in those States. Soils in the area are not necessarily highly permeable; in fact, some of the highest indoor radon levels in North Dakota were measured in homes in the Red River Valley along the eastern border of the State, which is underlain primarily by silty-clay lacustrine deposits of glacial Lake Agassiz (10, 11).

As part of the EPA-USGS joint effort to identify and characterize the radon potential of the United States, a field investigation was initiated to quantitatively identify and describe the geologic factors responsible for anomalous indoor radon concentrations in the northern Great Plains and Great Lakes States underlain by continental glacial deposits. This report presents preliminary observations from field investigations in North Dakota and Minnesota.

GLACIAL GEOLOGY

Most of North Dakota and Minnesota are underlain by Wisconsin-age continental glacial deposits, except for the southwest corner of North Dakota, which is unglaciated and underlain by Tertiary and Upper Cretaceous sandstones and shales (Figure 1), and the southeast corner of Minnesota, which is underlain by pre-Wisconsin glacial drift (Figure 2). In North Dakota, ice advanced from the north and northwest in six separate glacial advances during Wisconsin time (Figure 1). The tills of all the ice advances are lithologically similar and are derived primarily from Tertiary and Upper Cretaceous shales, siltstones, and sandstones that comprise the underlying bedrock in North Dakota and southwestern Manitoba. Some of the deposits in the northeastern part of the State also include carbonate-rich till derived from Paleozoic limestone and dolomite in southern Manitoba (11). Most of the tills consist of nearly equal parts sand, silt, and clay (12, 13). Lacustrine deposits of glacial Lakes Agassiz, Souris, and Devil's Lake (Figure 1) are composed primarily of silty clays and clays, and are commonly interbedded with tills. The unoxidized tills are generally dark olive gray to bluish gray. Iron oxidation and accumulation of calcium carbonate are common weathering effects (14); both were noted in nearly all of the soils sampled in the study area.

Wisconsin-age glacial drift covers most of Minnesota. The drift can be classified into deposits of four major ice lobes that advanced at different times and in different directions, from areas with different source lithologies (Figure 2). Each lobe experienced multiple phases of ice advance, some of which overlapped other lobes in time and space. In order of roughly decreasing age, the major lobes are the Wadena, Rainy, Superior, and Des Moines (15). Drift of the Wadena lobe is exposed only in central Minnesota (Figure 2). The Wadena lobe advanced southward from the north and northwest, moving in a generally north-south direction in central Minnesota. Wadena drift is dominantly gray to buff-colored, sandy, calcareous till derived from carbonate rocks of southern Manitoba. The Rainy lobe moved from northeast to southwest. Rainy lobe drift covers parts of northeastern and central Minnesota and varies in both color and constituent lithology. In the northeast the drift is derived primarily from gabbro and basalt, giving it a gray color. Further west the drift is light gray to light brown, reflecting a dominantly granite source. In central Minnesota, Rainy lobe drift is derived mostly from metamorphic rocks and has a brown color resulting from oxidation of the initially gray metamorphic rock fragments.

The Superior lobe advanced from northeast to southwest in the eastern part of the State, roughly parallel to the Rainy lobe. It carried generally sandy red till containing sandstone and slate pebbles. Drift of the Des Moines lobe was primarily derived from Upper Cretaceous shales of

southern Manitoba, eastern North Dakota, and western Minnesota. Sublobes of the Des Moines lobe moved eastward across northern Minnesota and southward to central Iowa. Till derived from the Des Moines lobe is generally gray to buff, calcareous, silty to clayey (16). Silty and clayey lacustrine deposits of Lake Agassiz cover much of the Red River Valley in the northwestern part of the State (Figure 2).

METHODS

Field sampling was conducted at 132 locations along four traverses, each 100-150 km long, along highway rights-of-way (Figure 1, 2). Sample stations were spaced about 4 km apart. The field measurements were made during two weeks in August, 1989 during which the weather was mostly warm and dry, so any variations in measured values due to climate or weather-related effects are estimated to be negligible compared to variations caused by geologic factors. At each station, soil-gas radon was sampled at 1 m depth using the method of Reimer (17) and surface gamma radioactivity was measured with a portable gamma-ray spectrometer. The gamma-ray spectrometer gives an estimate of the concentrations of uranium, radium, thorium, and potassium in the upper 30 cm of soil. At alternate stations, an additional soil-gas sample was collected and soil permeability was estimated using soil-gas probes and equipment developed by V.C. Rogers and Associates (18), and soil profiles were examined, described, and sampled with a bucket auger. Soil samples were collected at the surface and at 1 m at alternate stations. Laboratory analyses of these samples were not completed at the time of this writing.

PRELIMINARY FIELD DATA

Results of field sampling of soil gas, permeability, and surface radioactivity are summarized in Table 2. Each traverse generally characterizes a specific glacial lobe or group of similar lobes. Traverse ND-1 crosses deposits of advances 2, 3, and 4. Most of traverse ND-2 characterizes deposits of advances 5 and 6, except for those samples at the eastern end of the traverse, which were collected in sediments of glacial Lake Agassiz, and which are treated separately from the rest of ND-2 (Figure 1; Table 2). In Minnesota, traverse MN-1 crosses deposits of the Wadena and Rainy lobes, and traverse MN-2 primarily crosses deposits of the Des Moines lobe (Figure 2).

Average soil-gas radon concentrations, equivalent uranium (eU), and permeabilities for each transect are compared in Figure 3 and Table 2. Soil-gas radon concentrations and eU are generally higher in North Dakota than in Minnesota,. The highest soil radon and eU concentrations and lowest permeabilities were measured in soils derived from sediments of glacial Lake Agassiz. A good correlation exists between eU measured at the surface and soil radon measured at 1 m (Figure 4a). Average ratios of eU to soil-gas radon concentration are significantly lower in this study than for similar ratios in unglaciated areas, such as those reported by Gundersen (19) and Gundersen and others (6).

Permeability appears to exhibit a weak inverse correlation with soil-gas radon concentration (Figure 4b), although the range of permeability values is relatively small; all the average values are between 2×10^{-8} and 9×10^{-8} cm^2, and all 39 permeability measurements fall between 10^{-10} and 10^{-7} cm^2. It was expected that the Minnesota soils, especially the sandy and silty soils derived from Wadena and Rainy lobe deposits (traverse MN-1), would have higher permeabilities than were measured (U.S. Soil Conservation Service soil surveys for the area describe many of the soils as moderately to rapidly permeable). The lower measured values may have been due to localized wet soil conditions, or to better development of the B horizon, which is generally a zone of

accumulation of fines and therefore less permeable than over- or underlying horizons, in the older Wadena and Rainy lobe soils. Soils sampled along the Minnesota transects have somewhat higher and generally more variable permeability than those sampled in North Dakota (Figure 3).

DISCUSSION

The physical, chemical, and drainage characteristics of soils formed on glacial deposits vary according to source bedrock type and the glacial features on which they are formed. Although the effects of glaciation have modified the relationship between the bedrock source and the soil's radon generation and transport characteristics, source rock lithology exerts a major control on radon potential because it determines the initial uranium and/or radium concentrations in the glacial drift and the type of soil (clayey or sandy, for example) that develops. Soils formed on ground or stagnation moraine deposits, which underlie most of the study area, tend to be more poorly drained and contain more fine-grained material than soils formed on outwash or eskers, which are generally coarser and well drained.

In general, soils developed from glacial deposits are moderately to highly permeable and rapidly weathered, because crushing and grinding of the rocks by glacial action may enhance and speed up soil weathering processes (20). Grinding of the rocks increases the radionuclide mobility in the resulting soils by exposing the uranium and radium at grain surfaces, where they are more easily leached and moved downward through the soil profile with other mobile ions. Accumulations of $CaCO_3$ and iron oxides were observed below about 75 cm in most soils in the study area. $CaCO_3$ and iron oxides form soil-grain coatings or concretions that sorb or associate with uranium (21, 22), providing a possible mechanism for uranium accumulation and enhanced radon emanation in deeper soil horizons. The low surface radioactivity and comparatively high soil radon concentrations of the glacial soils suggests that radionuclides have been removed from the upper soil layers and are probably concentrated in deeper horizons. This may explain why preliminary radon potential predictions based primarily on aerial gamma-ray data typically provide an underestimate of the number of homes with indoor radon problems in some areas underlain by glacial drift.

Clayey till soils, such as those underlying most of North Dakota, have high emanation coefficients (23) and usually have low to moderate permeability, depending on the degree to which the clays are mixed with coarser sediments. Soils formed on tills consisting of mostly coarse material, such as the sandy tills that underlie much of Minnesota, tend to emanate less radon because the larger grains have lower surface area-to-volume ratios, but because these soils have generally higher permeability, radon transport distances are longer, so buildings constructed in these materials are able to draw soil air from a larger source volume, and moderately elevated indoor radon concentrations may be achieved from comparatively lower radioactivity soils (24, 25). In till soils with extremely high permeability, atmospheric dilution may become significant, so elevated indoor radon levels are less common.

Two general classes of glacial soils can be identified from this study: 1) clay-rich soils with lower permeability and higher emanation coefficients, and 2) coarser-grained soils with lower emanation coefficients and higher permeability. The effect of this difference in soil characteristics can be clearly seen by comparing the distributions of indoor radon levels in North Dakota (Figure 5) and Minnesota (Figure 6). Although both types of soils can generate indoor radon levels greater than 4 pCi/L, till soils with high emanation coefficients can generate a significant number of indoor radon levels greater than 20 pCi/L (Figure 5), whereas soils with high permeability tend to generate few indoor radon levels greater than 20 pCi/L (Figure 6).

SUMMARY

A comparison of glacial geology, soil-gas radon and gamma radioactivity data, and indoor radon data for Minnesota and North Dakota indicates that glaciation modifies the relation among source bedrock, soils, and their resulting radon emanation and transport characteristics, but radon potential predictions are possible if the nature of these modifications is understood. The preliminary observations presented in this paper suggest that two factors are important to consider when predicting radon potential in glaciated terranes. 1) Glaciers transport and redistribute bedrock, so a bedrock geologic map may not accurately reflect the parent material lithology of glacially-derived soils, but knowledge of source rock lithology (or lithologies, as glaciers may also mix rocks from several sources together) will aid in determining the radon emanation and transport characteristics of the derivative tills. 2) Grinding of the rocks by glaciers reduces grain size and therefore increases grain surface area, enhancing radon emanation by exposing more radium at grain surfaces than in coarser-grained soils. Glacial mixing and crushing also speeds up the weathering process, so radionuclides may be leached from shallow horizons of till soils more rapidly than in soils developed on untransported bedrock, thus giving a surface gamma radioactivity reading that may underestimate the uranium and radium concentrations at depth.

ACKNOWLEDGEMENTS

This study was conducted in cooperation with, and funded in part by, the U.S. Environmental Protection Agency under Interagency Agreement DW14933884-0. Thanks are due to S.S. Agard and G.M. Reimer for reviewing the manuscript and to L.C.S. Gundersen for helpful discussions.

REFERENCES

1. Ronca-Battista, M., Moon, M., Bergsten, J., White, S.B., Holt, N., and Alexander, B., Radon-222 concentrations in the United States--Results of sample surveys in five states. Radiation Protection Dosimetry 24: 307-312, 1988.

2. Åkerblom, G., Andersson, P., and Clavensjo, B., Soil gas radon—A source for indoor radon daughters. Radiation Protection Dosimetry 7: 49-54, 1984.

3. Castrén, O., Mäkeläinen, I., Winqvist, K., and Voutilainen, A., Indoor radon measurements in Finland: A status report. In: Hopke, P.K. (ed.), Radon and Its Decay Products. American Chemical Society Symposium Series 331: 97-103, 1987.

4. Stranden, E, Radon-222 in Norwegian dwellings. In: Hopke, P.K. (ed.), Radon and Its Decay Products. American Chemical Society Symposium Series 331: 70-83, 1987.

5. Duval, J.S., Use of aerial gamma-ray data to estimate relative amounts of radon in soil gas. In: Gundersen, L.C.S., and Wanty, R.B. (eds), Field studies of radon in natural rocks, soils, and water. U.S. Geological Survey Bulletin, in press.

6. Gundersen, L.C.S, Reimer, G.M., Wiggs, C.R., and Rice, C.A., Map showing radon potential of rocks and soils in Montgomery County, Maryland. U.S. Geological Survey Miscellaneous Field Studies Map MF-2043, scale 1:62,500, 1988.

7. Peake, R.T., and Schumann, R.R., Regional radon characterizations. In: Gundersen, L.C.S., and Wanty, R.B. (eds), Field studies of radon in natural rocks, soils, and water. U.S. Geological Survey Bulletin, in press.

8. Schumann, R.R., and Owen, D.E., Relationships between geology, equivalent uranium concentration, and radon in soil gas, Fairfax County, Virginia. U.S. Geological Survey Open-File Report 88-18, 1988, 28 p.

9. Duval, J.S., Jones, W.J., Riggle, F.R., and Pitkin, J.A., Equivalent uranium map of the conterminous United States. U. S. Geological Survey Open-File Report 89-478, 1989.

10. Clayton, Lee, Moran, S.R., and Bluemle, J.P., Explanatory text to accompany the geologic map of North Dakota. North Dakota Geological Survey Report of Investigation 69, 1980, 93 p.

11. Moran, S.R., Arndt, M., Bluemle, J.P., Camara, M., Clayton, L., Fenton, M.M., Harris, K.L., Hobbs, H.C., Keatinge, R., Sackreiter, D.K., Salomon, N.L., and Teller, J., Quaternary stratigraphy and history of North Dakota, southern Manitoba, and northwestern Minnesota. In: Mahaney, W.C. (ed.), Quaternary stratigraphy of North America. Stroudsburg, Pennsylvania, Dowden, Huchinson, and Ross, 1976, p. 133-158.

12. Lemke, R.W., Geology of the Souris River area, North Dakota. U.S. Geological Survey Professional Paper 325, 1960, 138 p.

13. Winters, H.A., Geology and ground water resources of Stutsman County, North Dakota, Part I: Geology. North Dakota Geological Survey Bulletin 41, 1963, 84 p.

14. Lemke, R.W., Laird, W.M., Tipton, M.J., and Lindvall, R.M., Quaternary geology of the northern Great Plains. In: Wright, H.E., Jr., and Frey, D.G. (eds), The Quaternary of the United States. Princeton, NJ, Princeton University Press, 1965, p. 15-27.

15. Hobbs, H.C., and Goebel, J.E., Quaternary geologic map of Minnesota. Minnesota Geological Survey Map S-1, scale 1:500,000, 1982.

16. Wright, H.E., Jr., and Ruhe, R.V., Glaciation of Minnesota and Iowa. In: Wright, H.E., Jr., and Frey, D.G. (eds.), The Quaternary of the United States. Princeton, NJ, Princeton University Press, 1965, p. 29-41.

17. Reimer, G.M., Simple techniques for soil-gas and water sampling for radon analysis. In: Gundersen, L.C.S., and Wanty, R.B. (eds), Field studies of radon in natural rocks, soils, and water. U.S. Geological Survey Bulletin, in press.

18. Nielson, K.K., Bollenbacher, M.K., Rogers, V.C., and Woodruff, G., Users guide for the MK-II radon/permeability sampler. U.S. Environmental Protection Agency report, in press.

19. Gundersen, L. C. S., Anomalously high radon in shear zones. In: Osborne, M., and Harrison, J., symposium cochairmen, Proceedings of the 1988 Symposium on Radon and Radon Reduction Technology, Volume 1, oral presentations. U.S. Environmental Protection Agency publication EPA/600/9-89/006A, 1989, p. 5-27 to 5-44.

20. Jenny, H., The clay content of the soil as related to climatic factors, particularly temperature. Soil Science 40: 111-128, 1935.

21. Hansen, R. O., and Stout, P. R., Isotopic distributions of uranium and thorium in soils. Soil Science 105: 44-50, 1968.

22. Nash, J. T., Granger, H. C., and Adams, S. S., Geology and concepts of genesis of important types of uranium deposits. Economic Geology, 75th Anniversary volume: 63-116, 1981.

23. Grasty, R. L., The relationship of geology and gamma-ray spectrometry to radon in homes. EOS 70: 496, 1989.

24. Duval, J.S., Otton, J.K., and Jones, W.J., Estimation of radon potential in the Pacific Northwest using geological data. U.S. Department of Energy, Bonneville Power Administration report DOE/BP-1234, 1989.

25. Kunz, C., Laymon, C. A., and Parker, C., Gravelly soils and indoor radon. In: Osborne, M., and Harrison, J., symposium cochairmen, Proceedings of the 1988 Symposium on Radon and Radon Reduction Technology, Volume 1, oral presentations. U.S. Environmental Protection Agency publication EPA/600/9-89/006A, 1989, p. 5-75 to 5-86.

TABLE 1. PERCENT OF HOMES IN THE EPA/STATE INDOOR RADON SURVEY WITH SCREENING INDOOR RADON MEASUREMENTS GREATER THAN 4 PCI/L FOR STATES UNDERLAIN PRIMARILY BY GLACIAL DEPOSITS

STATE	PERCENT > 4 pCi/L	# OF HOMES TESTED
Iowa	71	1381
Michigan	12	1989
Minnesota	47	919
North Dakota	65	1596
Wisconsin	27	1191

(data from EPA press releases, 1987-89)

TABLE 2. RADON IN SOIL GAS, GAMMA RADIOACTIVITY, AND PERMEABILITY DATA FOR 132 SAMPLE LOCATIONS IN MINNESOTA AND NORTH DAKOTA

See figures 1 and 2 for locations of sampling traverses. Rn=soil-gas radon concentration at 1m, eU=equivalent uranium measured at the surface by gamma spectrometer, S.D.=sample standard deviation, n=number of measurements.

	ND-1	ND-2	Lake Agassiz	MN-1	MN-2
Rn (pCi/L)					
MINIMUM	310	400	570	120	170
MAXIMUM	2325	3750	2865	1485	2700
MEAN	883	1357	1739	416	832
MEDIAN	792	1065	1527	270	687
S.D.	440	900	738	359	567
n	29	21	11	35	35
eU (ppm)					
MINIMUM	1.1	0.7	1.2	0.1	0.3
MAXIMUM	2.3	2.2	3.0	1.2	2.7
MEAN	1.7	1.5	2.0	0.4	1.2
MEDIAN	1.7	1.6	0.6	0.4	1.2
S.D.	0.4	0.4	2.2	0.3	0.5
n	29	22	11	35	35
PERMEABILITY (cm^2)					
MINIMUM		7.5×10^{-9}	2.6×10^{-9}	2.3×10^{-9}	2.7×10^{-10}
MAXIMUM		1.2×10^{-7}	2.9×10^{-8}	2.1×10^{-7}	1.8×10^{-7}
MEAN		4.6×10^{-8}	1.7×10^{-8}	3.1×10^{-8}	8.3×10^{-8}
MEDIAN		3.0×10^{-8}	1.9×10^{-8}	1.4×10^{-8}	9.5×10^{-8}
S.D.		4.5×10^{-8}	1.3×10^{-8}	5.7×10^{-8}	5.6×10^{-8}
n		6	3	12	18

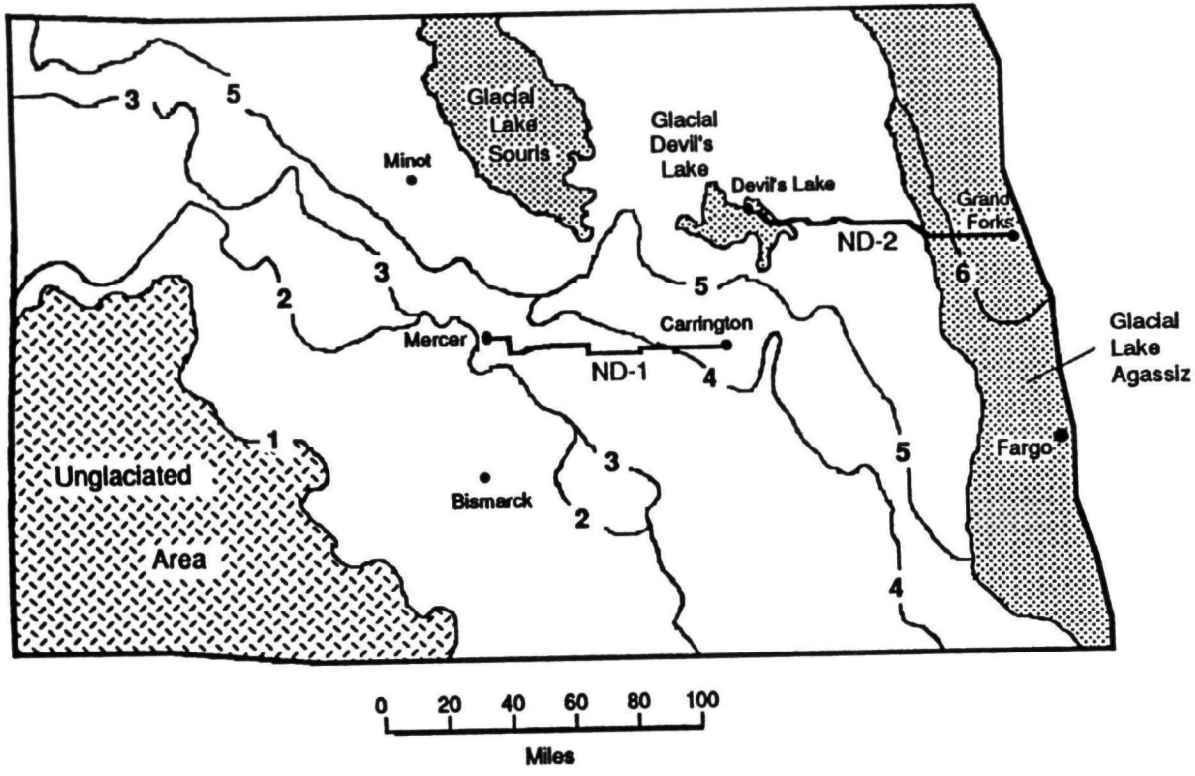

Figure 1. Map of North Dakota showing Wisconsin-age glacial deposits and locations of sampling traverses (ND-1 and ND-2). Numbered lines indicate maximum extent of each glacial advance. Modified from (14).

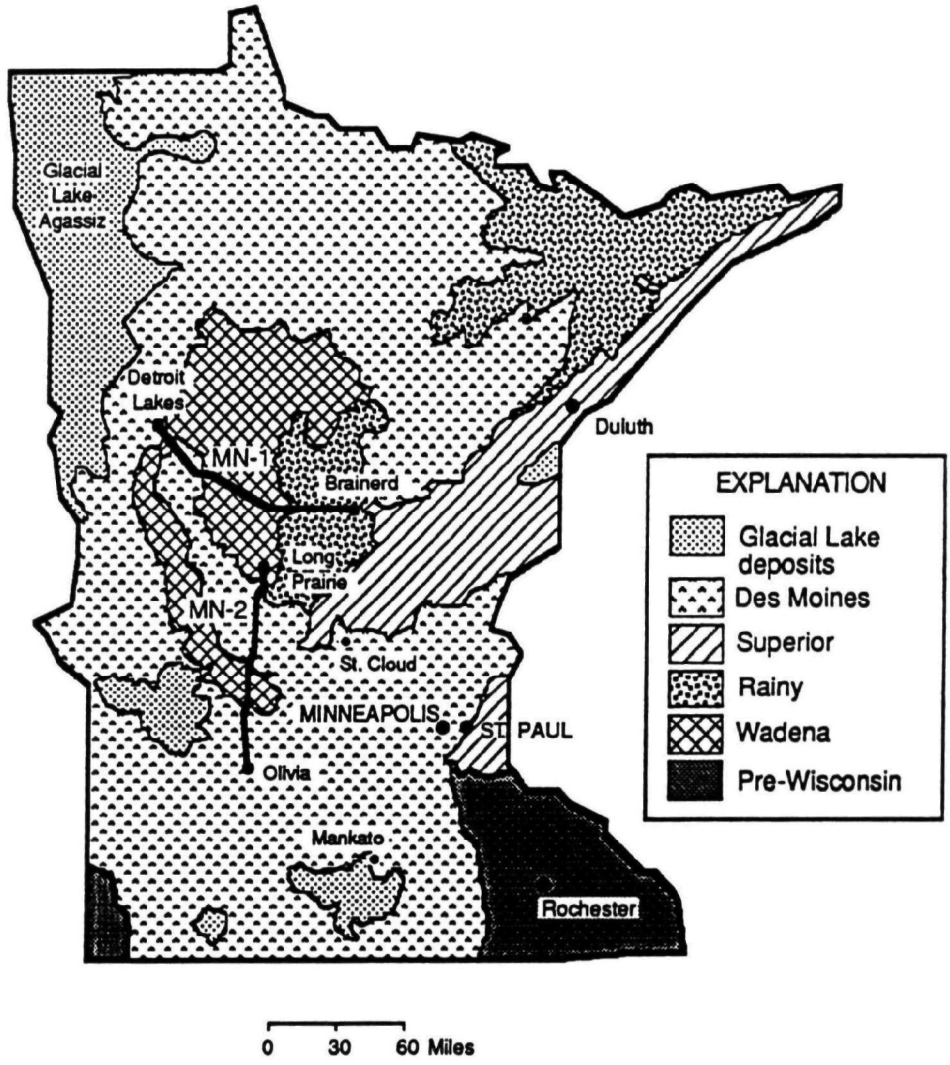

Figure 2. Map of Minnesota showing Wisconsin-age glacial deposits and locations of sampling traverses (MN-1 and MN-2). Patterned areas indicate deposits of named glacial lobes, as indicated in map legend. Modified from (15).

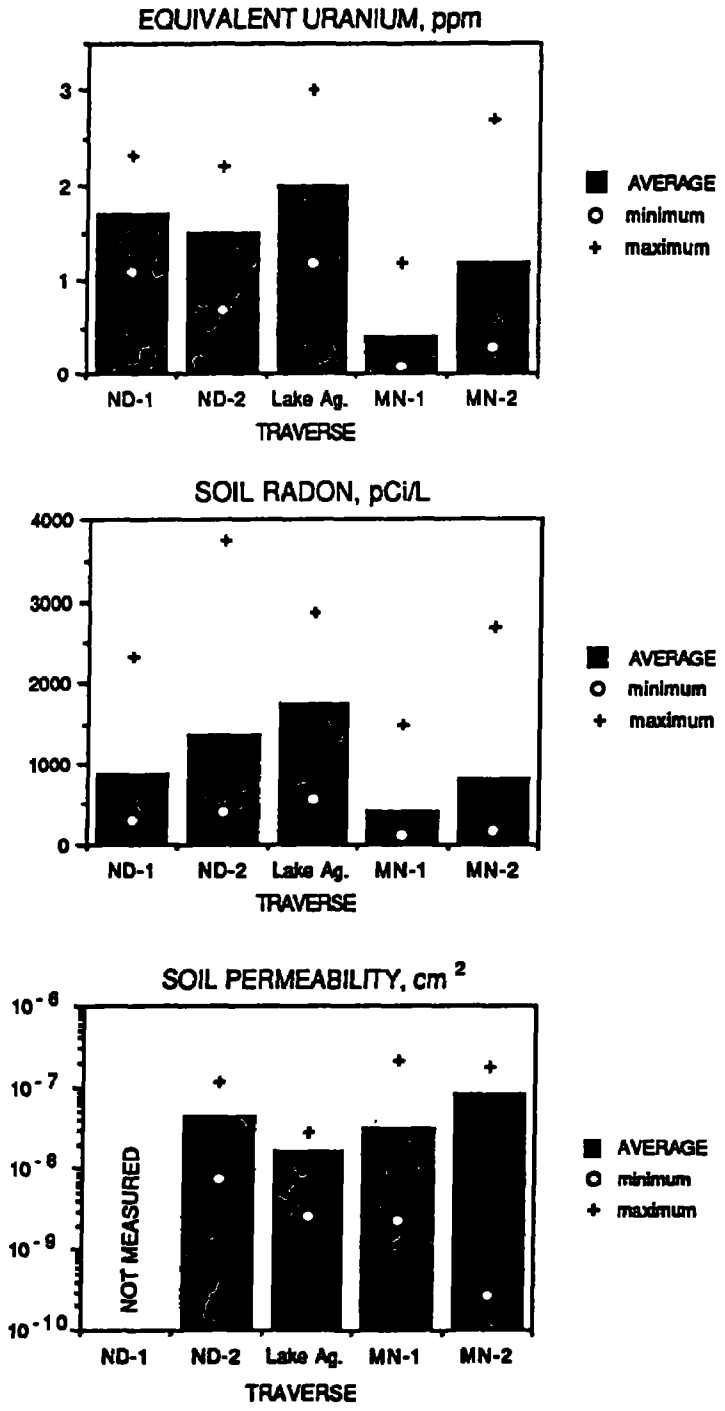

Figure 3. Average, minimum, and maximum equivalent uranium (eU), soil-gas radon, and permeability for soils in the study area. See Figures 1 and 2 for locations of traverses.

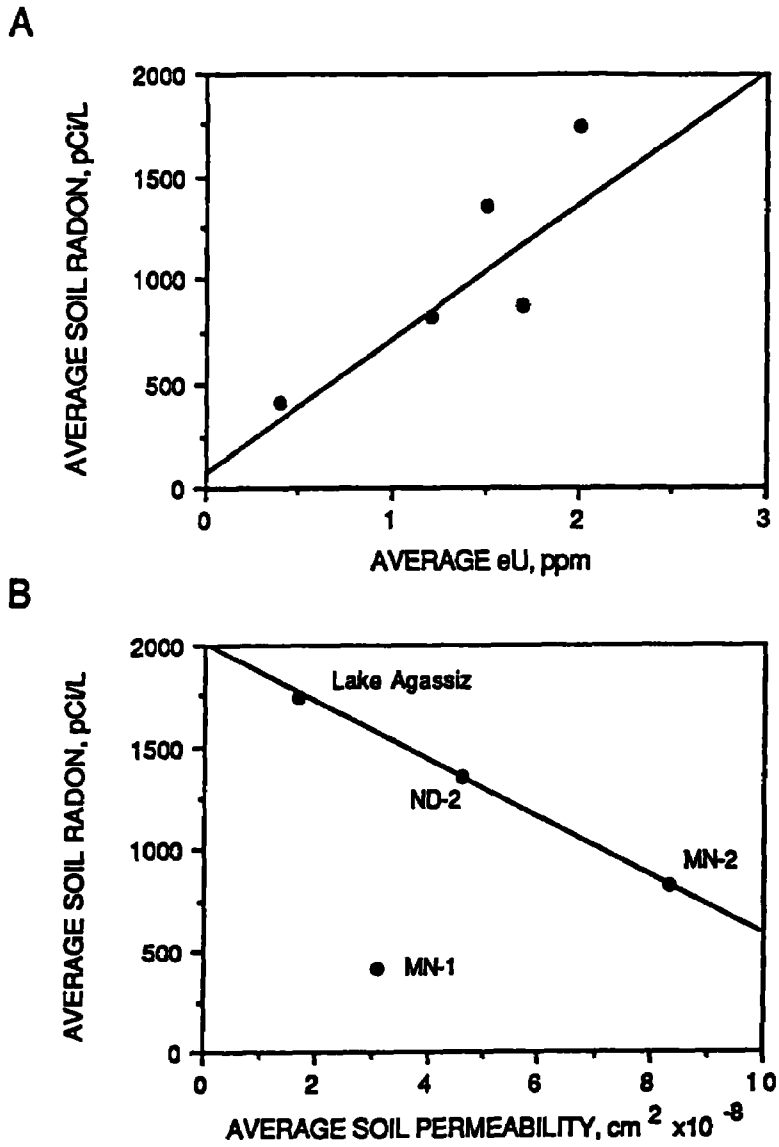

Figure 4. a) eU versus soil radon. Each point represents the average for one traverse. R^2=0.73. b) Permeability versus soil radon. Each point represents the average for one traverse. Line fitted visually, excluding the point representing MN-1.

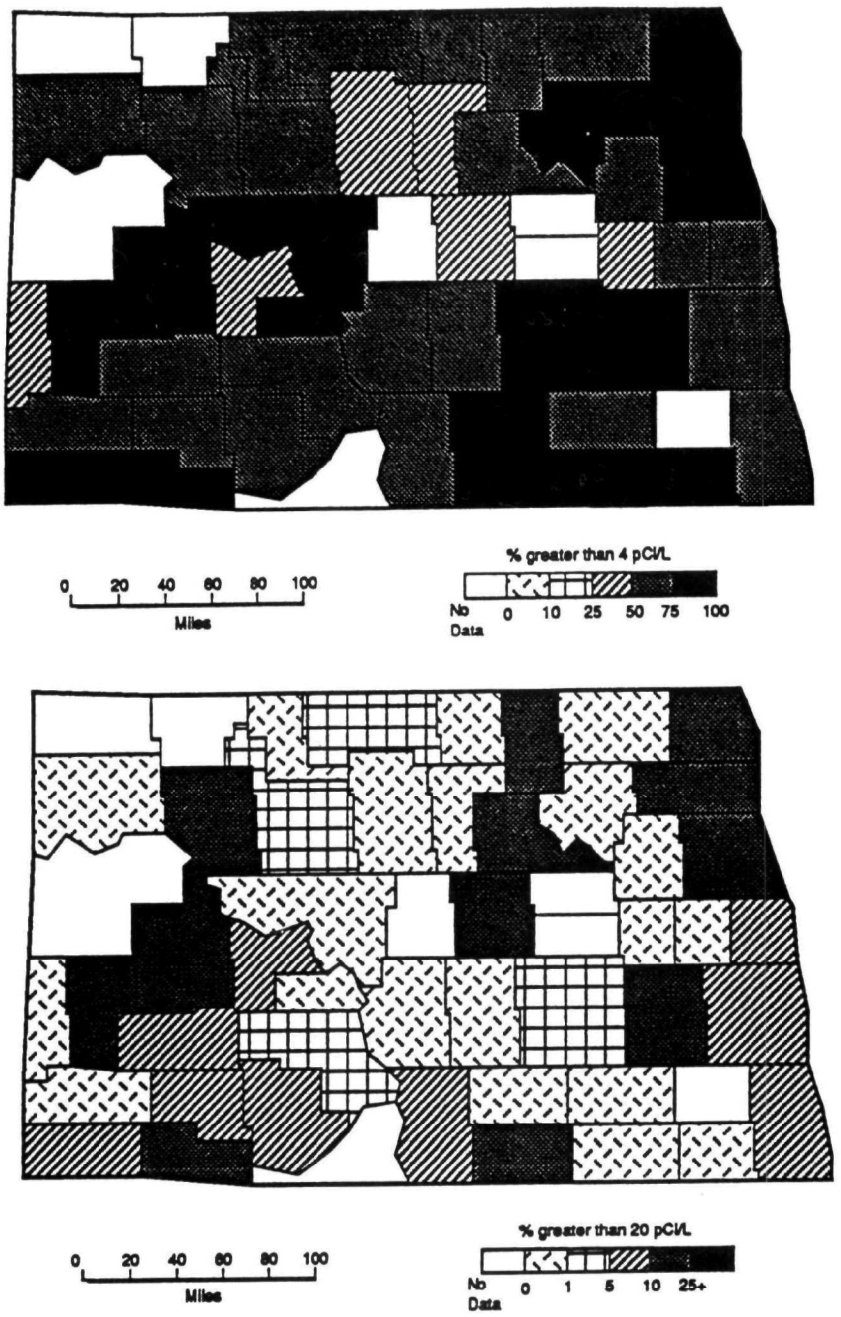

Figure 5. Percent of homes tested in the State/EPA Indoor Radon Survey with basement screening indoor radon values in excess of 4 pCi/L and 20 pCi/L in North Dakota, by county.

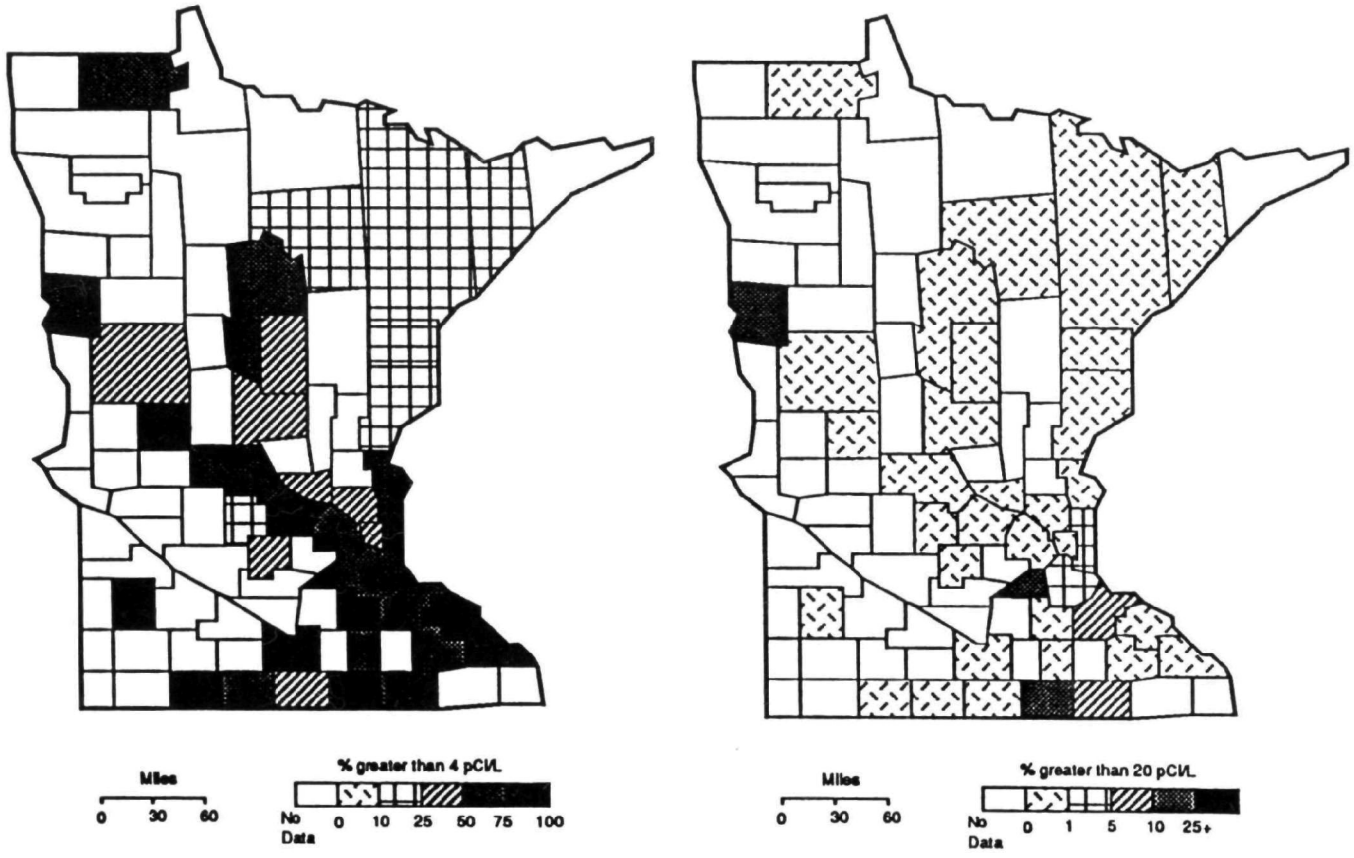

Figure 6. Percent of homes tested in the State/EPA Indoor Radon Survey with basement screening indoor radon values in excess of 4 pCi/L and 20 pCi/L in Minnesota, by county.

GEOLOGIC FACTORS AND HOUSE CONSTRUCTION PRACTICES AFFECTING INDOOR RADON IN ONONDAGA COUNTY, NEW YORK

by: Charles Laymon and Charles Kunz
Wadsworth Center for Laboratories and Research
New York State Department of Health
Albany, New York 12201-0509

ABSTRACT

Indoor radon in Onondaga County, New York is largely controlled by bedrock and surficial geology. At more local scales, these alone are insufficient to characterize indoor radon potential. A detailed study of the concentration of indoor radon, soil radium, soil-gas radon, soil and bedrock type, permeability, and home construction practices indicates that above-average indoor radon concentrations are associated with gravelly moraine and glaciofluvial deposits, the radium-bearing Marcellus Shale, and high permeability zones around the substructure of houses built into limestone bedrock.

INTRODUCTION

Indoor radon[1], produced by the radioactive decay of radium-226 in rocks and soil, is the product of a complex system of interrelated variables. Because of the inherent relationship between geology and indoor radon, geologists have been challenged in recent years with the problems of identifying areas of potential public health risk and developing protocols for evaluating indoor radon potential prior to new house construction. It is recognized that many factors affect indoor radon, but the importance of these factors at different scales is not well understood. New York is geologically very diverse and the New York State Department of Health has been actively involved in trying to better understand the geologic controls on indoor radon. Onondaga County in central New York is one of several counties in the state that has received special attention.

---

[1]Radon occurs in three forms, Rn-119, Rn-220, and Rn-222. The longest-lived isotope, Rn-222, is the most important with regard to public health and will be referred to exclusively in this paper.

For the past several years, the New York State Department of Health has provided activated charcoal canister radon detectors to state residents at a minimal cost. Over 4300 measurements have been made in Onondaga County as part of this program. In this paper, we examine the county-wide distribution of indoor radon and the radon problem at several local areas. Results of this investigation demonstrate that bedrock and surficial geology are adequate to characterize indoor radon potential at the county-wide scale, but at smaller scales of a few square kilometers or less, many other characteristics need to be considered. Particularly important is an understanding of the variability within the major controls and how homes within the area interface with their environment.

GEOLOGIC SETTING

PHYSIOGRAPHY

Onondaga County is centrally located in New York State and at the northeastern edge of the Finger Lakes Region (Figure 1). The county spans the border between two physiographic provinces, the Erie-Ontario Lowland to the north and the Appalachian Upland to the south. The Erie-Ontario Lowland encompasses the relatively low, gently undulating plain lying south of Lakes Erie and Ontario. Glacial scour has produced numerous ridges of till and rock, which are surrounded by extensive and thick deposits of stratified glaciolacustrine sand and mud (3).

Onondaga County is underlain by Upper Silurian to Upper Devonian shales, limestones, and minor sandstones that are exposed in east-west trending bands and dip slightly to the south beneath progressively younger strata (1,2). Differing resistance of the bedrock to weathering processes has produced a scarp at the northern edge of the Appalachian Upland that rises sharply to the south more than 300 m in elevation (Figure 1). The scarp is comprised of several benches formed primarily on the Onondaga and Helderberg Limestones and is, therefore, referred to as the Onondaga or Helderberg Escarpment (2,4,5).

The Appalachian Upland is characterized by greater relief as a result of fluvial dissection of the uplifted bedrock. The northern edge of the upland is cut by the Finger Lakes and adjacent through valleys, which are glacially modified valleys of preglacial river drainage. A segment of the largest moraine in New York, the Valley Heads Moraine, crosses the southern end of Onondaga County (3,6). Thick sequences of gravelly outwash fill the deeply cut through valleys of the upland and thin till covers the upland interfluves between the valleys (3).

The dominant soils in Onondaga County are derived from glacial deposits containing varying amounts of limestone, shale, and sandstone. For the most part these soils are deep, medium-textured, well drained to moderately well drained, and medium to high in lime content (7).

BEDROCK LITHOLOGIES OF THE ONONDAGA ESCARPMENT

Before discussing the geologic controls on indoor radon along the Onondaga Escarpment, a review of the bedrock lithologies found on the

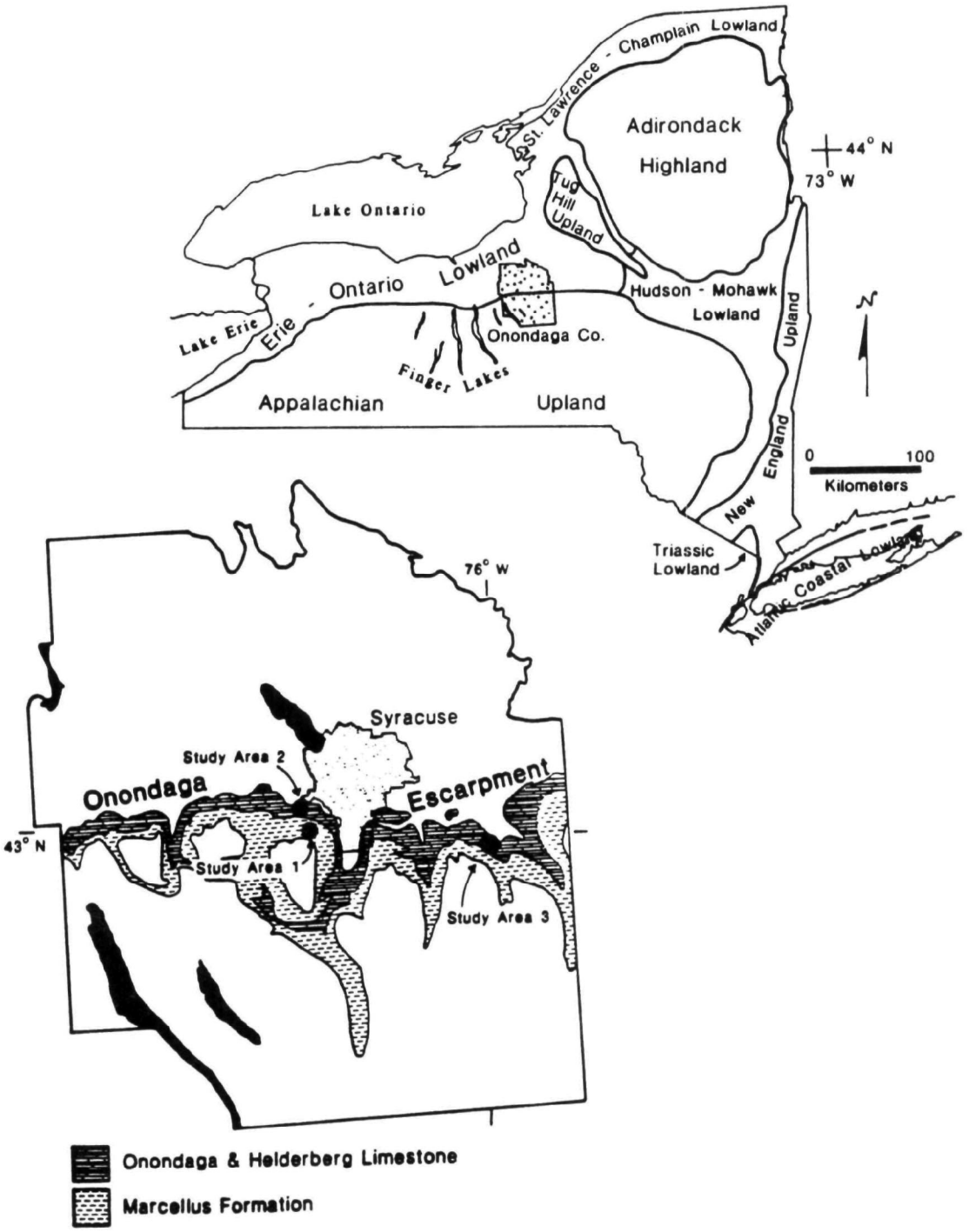

Figure 1. Maps showing the physiographic provinces of New York State and location of Onondaga County, and the study areas along the Onondaga Escarpment.

escarpment is beneficial. The Upper Silurian Rondout Dolostone is a poorly exposed gray dolostone at the base of the escarpment (5). The Rondout Dolostone grades upward into the overlying Lower Devonian Helderberg Group, which consists of about 45 m of limestone and generally forms the middle part of the escarpment (4,5). The Middle Devonian Oriskany Sandstone overlies the Helderberg Group. This sandstone is absent from the western part of the county, but increases in thickness from about 1 cm southwest of Syracuse (Figure 1) to about 5 m on the eastern edge of the county (5). Although the Oriskany Sandstone is relatively thin, it is notable for containing radium-bearing, black nodules of calcium phosphate such that it is readily detected in gamma-ray logs from wells (4,8,9) (Figure 2). Despite this, indoor radon has not been attributed to the nodules. The Onondaga Limestone, which is about 24 m thick, overlies the Oriskany Sandstone and is the most durable rock in the escarpment, cropping out at or near the top (5).

Immediately overlying the Onondaga Limestone are thick beds of black, bituminous, argillaceous shale collectively known as the Marcellus Formation (5,9). This formation increases in thickness from about 30 m at the western edge of the county to about 90 m at the eastern edge (9). The Marcellus Formation is most noted in New York State for its radioactivity and it is consequently easily recognized in gamma-ray logs of wells (8,9,10) (Figure 2). In general, radioactivity of the Marcellus Formation is greatest at the base and decreases progressively upward to the top with the exception of a 1 m thick limestone bed of relatively low activity about 5 m above the base of the formation.

Results of whole-rock gamma spectrometry analysis of the Marcellus Formation are given in table 1. Similar results for the Onondaga and Helderberg Limestones are also given in table 1 for comparison. It is apparent from these results that the Marcellus Formation shales are enriched in uranium and radium compared to the underlying limestone units. In addition, the uranium-to-radium ratio is nearly one to one for both rock types (taking analytical error and the geometric standard deviation into account) suggesting that the radium is in equilibrium with the uranium and there is no evidence of preferential removal of radium by solution.

TABLE 1. RADIONUCLIDE CONTENT OF BEDROCK

	^{238}U	^{226}Ra	^{232}Th
Marcellus Formation			
Geom. Mean	3.5	2.6	1.2
Geom. Std. Dev.	1.4	1.2	1.1
n	10	10	10
Onondaga and Helderberg Limestones			
Geom. Mean	0.3	0.3	0.1
Geom. Std. Dev.	1.8	1.6	1.8
n	31	32	32

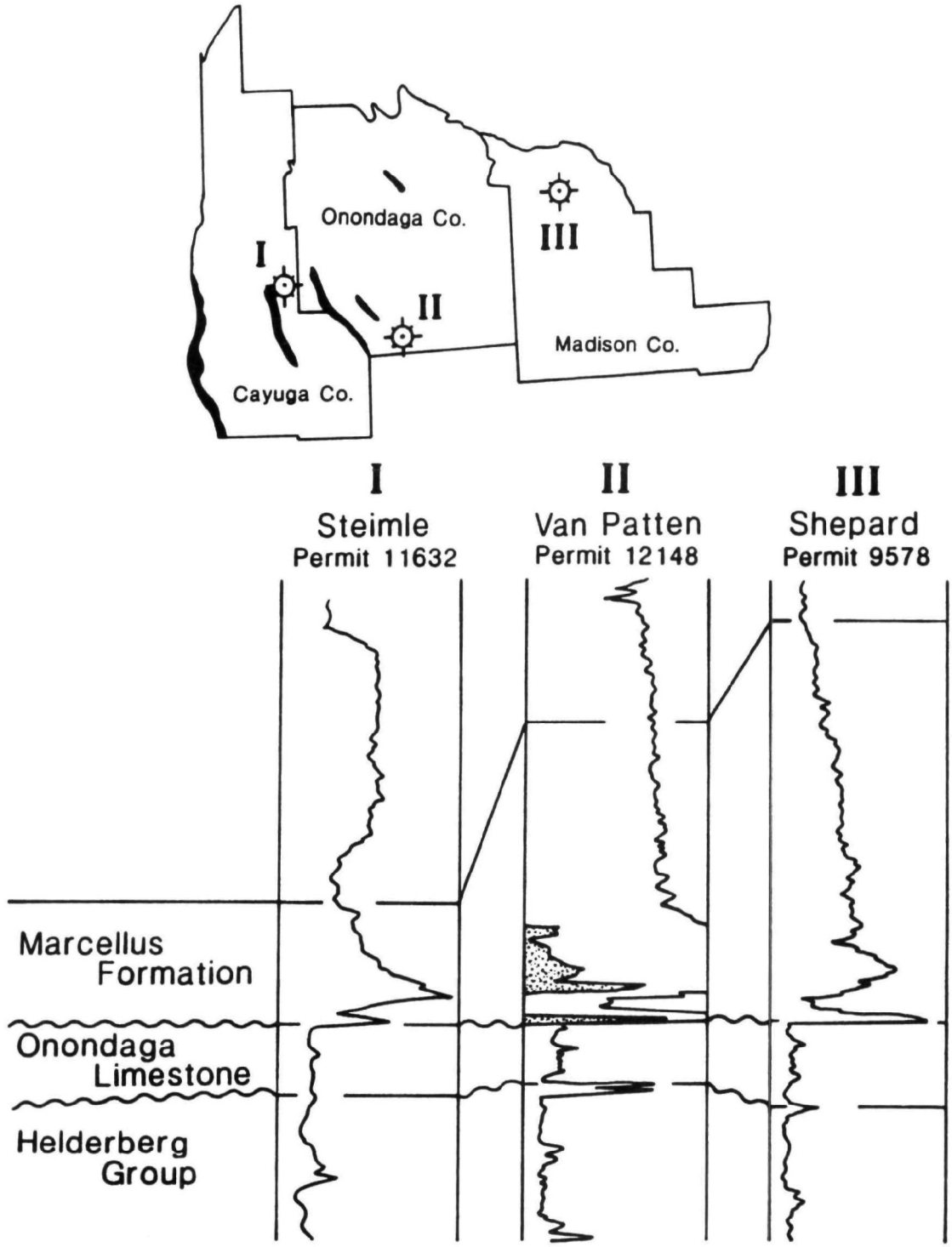

Figure 2. Gamma-ray logs of the Marcellus Formation, Onondaga Limestone, and upper Helderberg Group from three wells in and adjacent to Onondaga County.

METHODS

INDOOR RADON

Indoor radon survey results reported in this paper are based on volunteered two or four day screening measurements primarily in the basement using activated charcoal canister detectors. Measurements were made at any time of the year, but most were made during the fall, winter, and spring. Follow-up measurements were made in homes with screening results greater than 20 pCi/L.

SOIL-GAS RADON

Soil-gas samples were collected by driving a 2.5 cm diameter steel pipe into the soil to bedrock or a depth of 120 cm (11). Soil gas was withdrawn through perforations at the tip of the pipe and the concentration of radon was measured by alpha scintillation using Lucas cells.

PERMEABILITY

Permeability is measured using the same apparatus used to sample soil gas. Soil gas is withdrawn from the ground at a fixed flow rate while the pressure differential required to maintain that flow is measured (11). Permeability can then be calculated using a standard equation (11,12).

SOIL AND ROCK CHEMISTRY

Soil samples were prepared for radionuclide analysis by placing approximately 100 g of air-dried soil less than 2 mm in diameter in a sealed polyethylene bottle and set aside for three weeks to allow the radon and radon daughters to obtain equilibrium with the radium of the sample. Approximately 100 g of each rock sample was crushed and ground to a powder and similarly sealed in a bottle and set aside for three weeks. The uranium-238, radium-226, and thorium-232 concentrations were determined after measuring the rate of gamma emissions by spectroscopy with a Ge(Li) detector.

RESULTS AND DISCUSSION

COUNTY-WIDE DISTRIBUTION OF INDOOR RADON

Over 4300 indoor radon screening measurements in Onondaga County yield a mean and geometric mean of 10.1 and 4.4 pCi/L, respectively. Examination of the distribution of indoor radon survey results grouped by zip code area can be helpful in identifying large-scale geologic controls on indoor radon (13). Indoor radon in the Erie-Ontario Lowland physiographic province is generally below 4 pCi/L (Figure 3). This can be attributed to the low concentration of uranium and radium in the bedrock (9) and an extensive and thick cover of glacial lacustrine sediments (3) (Figure 3). These sediments are generally fine-grained and well sorted with almost no gravel-size clasts, resulting in moderate to low permeability for gas flow (7). Much of the area covered by these sediments is poorly drained, resulting in large swamps. Only a few

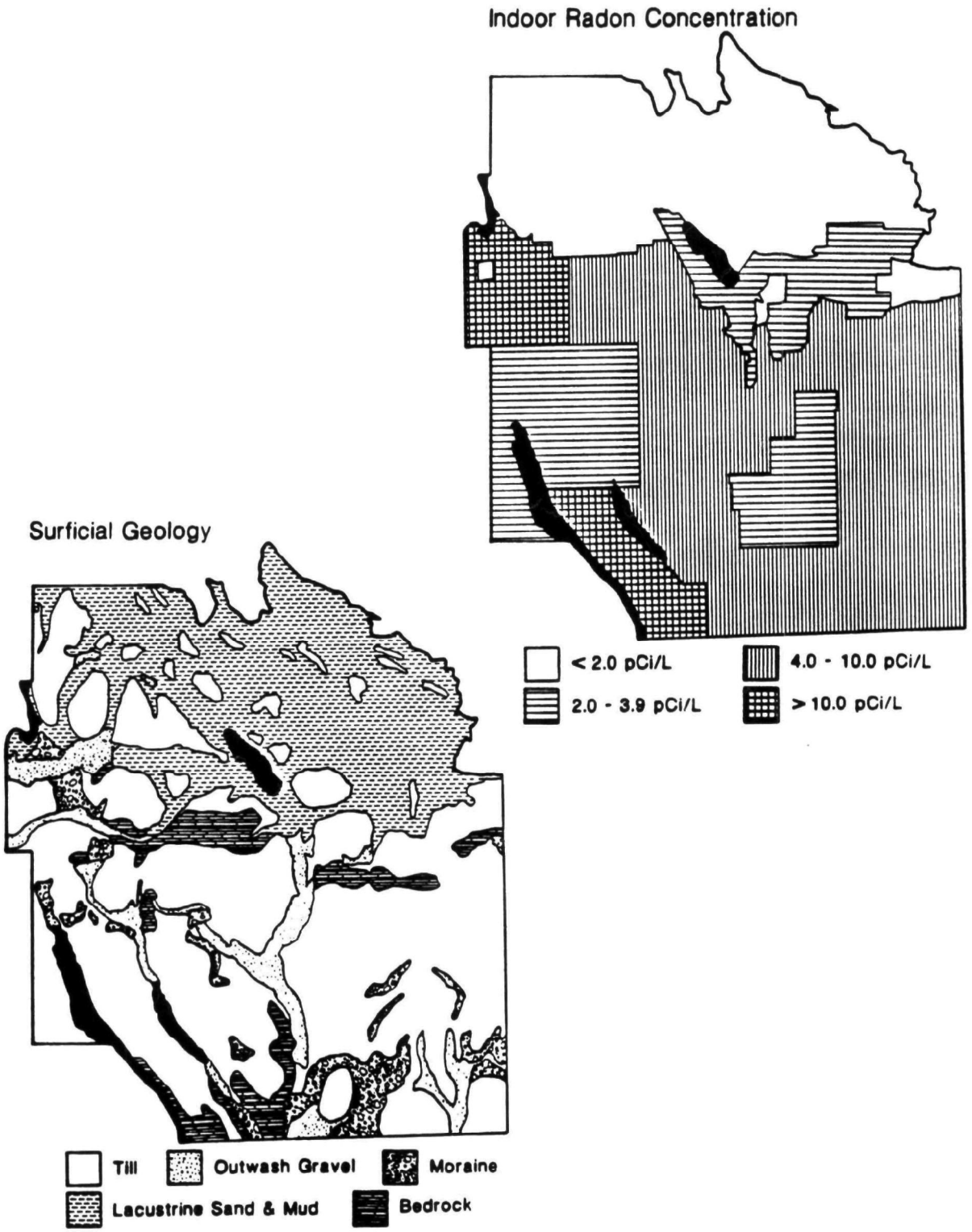

Figure 3. Maps of Onondaga County showing indoor radon concentrations and surficial geology

drumlins and areas covered with gravelly loamy till remained above the ice marginal lake levels and were not covered with glaciolacustrine sediments (3). In spite of the gravel component of the till, the fine-grained nature of its matrix restricts permeability to moderate or lower.

In the southern part of the county, including the Onondaga Escarpment, indoor radon concentrations greater than 4 pCi/L are more common (Figure 3). These higher concentrations are attributed to a) the radium-bearing, black Marcellus Shale, b) building practices in the limestone bedrock, and c) the highly permeable moraine and glaciofluvial deposits. Almost the entire Appalachian Upland of Onondaga County is covered by till, outwash, or moraine deposits (3) (Figure 3). Numerous permeability measurements in these deposits throughout New York State show variability depending on the texture and degree of sorting, but in general, demonstrate relatively high permeability for gas flow ranging between 10^{-8} and 10^{-11} m^2 (11). Above-average concentrations of indoor radon are often associated with permeable surficial deposits, even in the absence of above-average concentrations of radium in the soil and bedrock (11,14,15). We attribute many of the elevated concentrations of indoor radon in southern and central Onondaga County to the highly permeable nature of these glacial deposits.

Many homes with indoor radon concentrations greater than 4 pCi/L occur along a narrow east-west trending band across the central part of the county corresponding to the Onondaga Escarpment. Although some of the elevated indoor radon concentrations can be attributed to the Marcellus shale, detailed field investigations with laboratory analyses reveal that many homes along the escarpment underlain by Onondaga or Helderberg Limestone also possess elevated concentrations of indoor radon. Hand and Banikowski (16) attributed elevated indoor radon concentrations on, and north of, the Onondaga Escarpment to redistribution of uranium from the Marcellus Formation into subjacent limestones by ground water. No direct evidence for this has been observed. Below, we present results from several small study areas along the escarpment that illustrate the complex nature of the association between topography, bedrock, erosion and transport processes, soils, and home construction practices that occur along the Onondaga Escarpment leading to elevated radon levels.

STUDY AREA 1

This study area is located on the Marcellus Formation and forms the basis for comparison with the other study areas located on the underlying limestones (Figure 1). Indoor radon concentrations in 19 single-family homes located within the study area yield a mean and geometric mean of 8.5 and 6.0 pCi/L, respectively. The soil derived from rapidly weathered Marcellus shale is silt loam with shale fragments and is typically less than one-meter thick and poorly drained (7). Permeability of the soil is generally moderate to high, ranging from 5×10^{-12} to 1×10^{-9} m^2, and in most cases, it is fairly consistent with depth (Figure 4). The soil contains above-average concentrations of uranium and radium (Table 2). Soil-gas radon concentrations range up to 5300 pCi/L. The mean soil-gas radon concentration near the foundation of homes is about 1650 pCi/L, whereas in less disturbed soil in the yard away from the homes it averages about 2200 pCi/L.

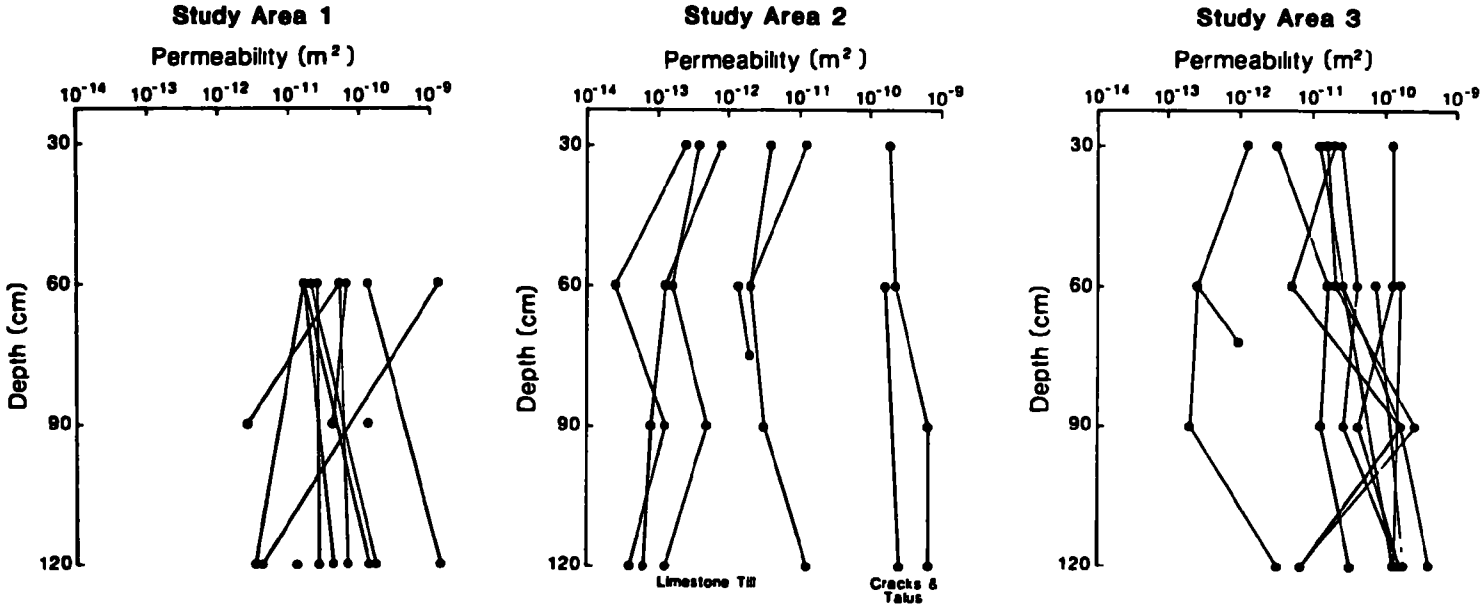

Figure 4. Permeability profiles for each study area.

TABLE 2. RADIONUCLIDE CONTENT OF SOIL

	^{238}U	^{226}Ra	^{232}Th
Study Area 1 (n=47)			
Geom. Mean	2.5	2.0	1.1
Geom. Std. Dev.	1.4	1.4	1.2
Study Area 2 (n=14)			
Geom. Mean	1.1	0.7	0.6
Geom. Std. Dev.	1.3	1.3	1.2
Study Area 3 (n=16)			
Geom. Mean	2.1	2.0	0.9
Geom. Std. Dev.	1.5	1.8	1.3

STUDY AREA 2

This study area is located on the Onondaga and the Helderberg Limestones on the escarpment downslope from Study Area 1 (Figure 1). Indoor radon concentrations in 39 homes have a mean and geometric mean of 12.7 and 7.4 pCi/L, respectively. The overburden in this area is variable in thickness and ranges in texture from gravelly loam to silty clay loam reflecting its multiple sources (7). Some of the overburden in this area is calcareous till derived from limestone and shale bedrock to the north that was transported southward over the escarpment. Elsewhere, there is evidence that Marcellus shale has been transported northward over some parts of the area by slope wash and fluvial processes. Disturbance of the overburden during home construction has made it difficult to separate soils derived from both of these sources. The radionuclide content of the till is average to slightly below average for soils (Table 2). In general, permeability of the till is low to moderate, ranging from 5×10^{-14} to 1×10^{-11} m^2, but permeability of the soil in cracks between limestone blocks and buried limestone talus is higher, approximately 5×10^{-10} m^2 (Figure 4). The radon concentration of several soil-gas samples from undisturbed soil in these cracks and buried talus range from about 1400 to 1700 pCi/L. For homes built into the limestone bedrock, permeability is slightly higher adjacent to the home in the backfilled area around the basement than it is in the undisturbed soil nearby.

STUDY AREA 3

This study area also is located downslope from the Marcellus Formation on Onondaga and Helderberg Limestones (Figure 1). Indoor radon concentrations in 56 homes yield a mean and geometric mean of 46.0 and 20.8 pCi/L, respectively. The soil is shaly loam or silt loam, often less than one-meter thick (7), and contains above-average concentrations of uranium and radium (Table 2). Permeability of the soil is generally moderate to high, ranging from

5×10^{-12} to 5×10^{-10} m^2, and in general, is fairly consistent with depth (Figure 4). As in Study Area 2, permeability is higher in the backfilled area adjacent to homes than in the undisturbed soil farther away. Soil-gas radon concentrations range from about 400 to 5000 pCi/L. The mean soil-gas radon concentration near the foundation of homes is about 1600 pCi/L, whereas less disturbed soils in the yard away from the home have a mean of about 1900 pCi/L.

It has become increasingly clear after intensive study that several important factors are acting together to increase the radon potential of homes in this area. Even though these homes are built on limestone that possesses very little radon source potential (Table 1), the overlying soil, which infiltrates joints and solution cavities in the limestone bedrock provides a sufficient source of radium for radon production. From the texture of the soil, abundance of shale fragments, and similar radionuclide content to the Marcellus shale and corresponding soil, it is clear that much of the soil in this area is derived from the Marcellus Formation and not the underlying limestone bedrock. It is unclear if the Marcellus shale was incompletely eroded by glaciers from the Onondaga Limestone, or if it was transported beyond its bedrock limits and over both the Onondaga and the Helderberg Limestones by mass movement or fluvial processes. Inconclusive evidence exists for both mechanisms.

The choice of home construction practices by builders in Study Area 3 also influences indoor radon potential. Most homes in the area are two-story, colonial, single-family homes between 10 and 30 years old with full basements or combination basements and crawl spaces. Most of these homes are heated by forced air from gas furnaces located in the basement. Basement walls were made with cement blocks, open at the top, and penetrated by the utilities. Slabs were poured up to the wall and now slab-wall separations occur in at least 50 percent of the homes examined. Floor drains, rather than sump holes, were used almost exclusively, and floor cracks are common.

Indoor radon measurements on the first floor and in the basement of homes in Study Area 3 shows that radon concentrations on the first floor are on average 18 percent of the concentration in the basement. Radon concentrations in crawl spaces are about 50 percent higher than in the adjacent basement. Radon concentrations in the block walls are about the same or slightly higher than in the basement, and concentrations below the slab, as indicated by grab samples from floor drains, cracks, and slab-wall separations, are about 100 percent higher than in the basement.

HOME BUILDING IN LIMESTONE BEDROCK

Excavation of limestone bedrock is a difficult, time-consuming, and expensive task for the home builder, particularly when drilling and blasting are required. Consequently, builders are forced to either build a split-level home partially below grade, build the home with a full basement only partially below grade, or build combination partial basements with crawl spaces. Below-grade combinations seem to be more common in the limestone bedrock terrain along the Onondaga Escarpment. Basement and crawl space slabs were poured directly on the underlying limestone bedrock and rubble that was generated in the excavation process or over an intervening gravel

bed. In either case, sub-slab communication is excellent and the sub-slab area becomes a part of a large network of interconnected joints and solution cavities in the limestone bedrock underlying and surrounding the house.

Joints developed in most beds of the limestone bedrock are widely spaced, resulting in large blocks commonly more than one meter to a side. Large numbers of these boulders are excavated for basement construction. In the absence of much overburden on the limestone bedrock along the escarpment, backfilling around the below-grade foundation with the excavated material produces a poorly compacted zone with void spaces. One builder, who needed to import top soil to cover the bedrock around some homes that were built into the limestone bedrock, stripped top soil from its source along with the brush that was growing on it to help prevent the top soil from infiltrating the cracks and cavities. In Study Area 3, soil derived from Marcellus shale was incorporated in the backfill, adding a fine-grained, radium-bearing component to the matrix of the gravelly limestone backfill. The result of these practices is the formation of a highly permeable zone around the foundation of the homes that may even be interconnected with the network of joints and solution cavities in the bedrock. The potential soil-gas collection area of these homes is so large that, even in the absence of a substantial radon source, indoor radon concentrations can become very high.

SUMMARY AND CONCLUSIONS

The radium content of bedrock and permeability of surficial materials are the primarily factors controlling indoor radon in Onondaga County. However, at smaller scales, additional factors also affect indoor radon to the same extent. The most important of these factors is how each house interfaces with its environment. Along the Onondaga Escarpment, where overburden is thin and many homes are built into limestone bedrock and surrounded by a highly permeable zone, there is a high potential for these homes to have elevated levels of indoor radon even though the radium content of the bedrock is well below average. The effectiveness with which a home draws soil gas from this zone is dependent on many design characteristics. Other factors affecting indoor radon in Onondaga County include dispersal of radium-bearing rock or soil by glacial, mass movement, and fluvial processes. These processes extend the effect of the radon source rock beyond the mapped limits of its bedrock source. Consequently, identification of radon risk based on geologic contacts can greatly underestimate the area affected. The complexities of the radon system identified in this paper are not unique to Onondaga County. They most certainly occur elsewhere in New York State and may be prevalent throughout much of the eastern U.S., particularly in the Appalachian Mountain region.

The work described in this paper was not funded by the U.S. Environmental Protection Agency and therefore the contents do not necessarily reflect the views of the Agency and no official endorsement should be made.

ACKNOWLEDGEMENTS

Funding for this research was provided by the New York State Department of Health Radon Program and the New York State Energy Research and Development Authority. We are grateful for the field and laboratory assistance of R. Mahoney, C. Parker, M. Reynolds, and D. Gordon.

REFERENCES

1. Broughton, J.G., Fisher, D.W., Isachsen, Y.W. and Rickard, L.V. Geology of New York. New York State Museum and Science Service, Educational Leaflet 20, Albany, New York, 1966, 49 pp.

2. Rickard, L.V. and Fisher, D.W. Geologic map of New York, Finger Lakes sheet. 1:250,000. New York State Museum and Science Service, Map and Chart Series No. 15. 1970.

3. Muller, E.H. and Cadwell, D.H. Surficial geologic map of New York, Finger Lakes sheet. 1:250,000. New York State Museum and Science Service, Map and Chart Series No. 40. 1986.

4. Clarke, J.M. and Luther, D.D. Geologic map of the Tully Quadrangle. New York State Museum, Bulletin 83. 1905. 70 pp., map.

5. Hopkins, T.C. The geology of the Syracuse quadrangle. New York State Museum, Bulletin 171. 1914. 80 pp., map.

6. Muller, E.H. Surficial geology of the Syracuse field area. In: J.J. Prucha (ed.), Guidebook, New York State Geological Association, 36th Ann. Mtg., May 8-10, 1964. p. 25.

7. Hutton, Jr., F.Z. and Rice, C.E. Soil survey of Onondaga County, New York. U.S. Department of Agriculture, Soil Conservation Service and Cornell University Agricultural Experiment Station, 1977. 235 pp., maps.

8. Vickers, R.C. A radioactivity study of the sedimentary rocks of central New York State and a description of the methods and apparatus used. M.Sc. Thesis, Syracuse University. Syracuse, New York. 1951. 39 pp.

9. Rickard, L.V. Stratigraphy of the subsurface Lower and Middle Devonian of New York, Pennsylvania, Ohio and Ontario. New York State Museum, Map and Chart Series, No. 39. 1989. 59 pp., maps.

10. Leventhal, J.S., Crock, J.G. and Malcolm, M.J. Geochemistry of trace elements and uranium in Devonian shales of the Appalachian Basin. U.S. Geological Survey Open-File Report 81-778. 1981. 72 pp.

11. Kunz, C., Laymon, C.A. and Parker, C. Gravelly soils and indoor radon. In: Proceedings of the 1988 Symposium on Radon and Radon Reduction

Technology. U.S. Environmental Protection Agency, Denver, CO. 1988.

12. DSMA, Atcon, Ltd. Review of existing instrumentation and evaluation of possibilities for research and development of instrumentation to determine future levels of radon at a proposed building site. Report for the Atomic Energy Control Board, Ottawa, Ont. 1983.

13. Mose, D.G., Chrosniak, C.E. and Mushrush, G.W. State-size radon hazard maps based on zip code compilations. In: Abstracts with Programs, Geological Society of America. 1989. p. A143.

14. Grace, J.D. Radon anomalies in southern Michigan. In: Abstracts with Programs, Geological Society of America. 1989. p. A144.

15. Smith, G.W., Mapes, R.H., Hinkel, R.J. and Darr, R.L. Radon hazards associated with glacial deposits in Ohio. In: Abstracts with Programs, Geological Society of America. 1989. p. A144.

16. Hand, B.M. and Banikowski, J.E. Radon in Onondaga County, New York: Paleohydrogeology and redistribution of uranium in Paleozoic sedimentary rocks. Geology 16: 775, 1988.

GEOLOGIC CONTROLS ON INDOOR RADON IN THE PACIFIC NORTHWEST

by: James K. Otton
Joseph S. Duval
U. S. G. S.
Reston, VA 22092

ABSTRACT

Indoor radon data for some townships in the Pacific Northwest (Washington, Oregon, Idaho, western Montana and western Wyoming) have been compared with aerial gamma-ray data which show the radium content of surface materials. Surface radium measurements provide a first-order estimate of the average levels of indoor radon where soils have low to moderate intrinsic permeability. Areas with significantly higher average indoor radon are almost all characterized by soils that have higher permeabilities, based on county soil descriptions. The permeability effect is greatest in the dry areas (less than 50 cm annual precipitation) in the eastern part of the study area. In the wet Puget lowland, elevated indoor radon levels occur only in houses on soils with extremely high permeability. Some of the areas above the general trend are also characterized by steep slopes.

Session C-V:

Radon Entry Dynamics—POSTERS

SUB-SLAB SUCTION SYSTEM DESIGN FOR LOW PERMEABILITY SOILS

by: David E. Hintenlang, Ph.D.
Department of Nuclear Engineering Sciences
University of Florida
Gainesville, FL 32611

Richard A. Furman
School of Building Construction
University of Florida
Gainesville, FL 32611

ABSTRACT

Soils having permeabilities in the range of 10^{-11}-10^{-10} m^2 have sometimes proven to be difficult subjects for the successful implementation of radon-mitigating sub-slab suction systems. The characteristics of soils having permeabilities in this range have been studied and a model developed that describes the pressure fields and airflows that may be expected due to sub-slab suction points. The model has been computerized to permit its use as a design tool for a variety of slab and sub-slab suction system configurations. Methods of using this model to help optimize sub-slab suction system design and the effectiveness of mitigation will be presented. Pressure-field and airflow predictions that have been made using this technique, as well as the resulting decreases in indoor radon concentrations, will be compared with measurements made on the University of Florida Test Slabs and for whole-house installations.

Funding Statement. Research sponsored by the Environmental Protection Agency (CR 814-925-010) and the State of Florida Board of Regents State University System Radon Research Program. This paper has been reviewed in accordance with the U.S. Environmental Protection Agency's peer and administrative review policies and approved for presentation and publication.

INTRODUCTION

Sub-slab depressurization systems have proven to be an effective means of reducing indoor concentrations of radon-222 gas in single-family houses. Their effectiveness has been demonstrated in the northeast portion of the United States, and these systems are now being implemented in other areas of the country

that may utilize different construction techniques and materials. The performance of sub-slab depressurization systems is strongly dependent on the characteristics of specific construction features and,in particular, the sub-slab medium. In order to adapt these systems to the conditions that may be encountered in different geographical areas, it is imperative to develop a precise understanding of the operation of these systems and their interactions with the house/soil system in which they are located.

The development of a complete understanding of sub-slab depressurization systems is also necessary for the practical aspects of optimizing the design and installation procedures for these systems. Some considerations encountered when optimizing these mitigation systems are the minimization of the number of suction points, accounting for the limited availability of locations to install the suction points, and the optimization of ventilation pipe and mitigation fan sizes.

In order to address some of these issues, a mathematical/computer model that simulates the performance of sub-slab depressurization systems has been developed and applied to buildings of slab-on-grade construction type, including slab-on-stemwall and monolithic poured slabs. These types of construction represent the dominant construction types in Florida. This area also utilizes sandy, sub-slab fill materials almost exclusively. The mathematical/computer model is, therefore, specifically designed to accommodate these conditions but may be applied equally well in any region where the sub-slab materials are homogeneous and the air velocities in the sub-slab materials induced by the ventilation system are sufficiently low to avoid turbulent flow.

THEORY

Sub-slab depressurization systems contribute to reduced indoor radon concentrations through two mechanisms: 1) they may provide sufficient airflow and dilution of the soil gas immediately underneath a slab so that the radon gas concentrations at that point are significantly reduced, or 2) they may eliminate or reverse the direction of pressure-driven flow of radon containing soil gas by reversing the sub-slab pressure differentials. Source strengths are frequently strong enough, and the airflow rates small enough (for sub-slab materials having air permeabilities less than about 5×10^{-10} m^2), that mechanism 2) is frequently dominant. This results in the necessity of ensuring that any installed sub-slab depressurization system can, in fact, depressurize a significant area under a slab, relative to the above-slab pressure.

Airflow through porous media, such as the fill encountered below a slab, is governed by several fundamental laws (1). These are the conservation of mass for a fluid moving through porous media,

$$\nabla(\rho \cdot V) = 0 \qquad (1)$$

where ρ is the fluid density, V is the fluid velocity and Darcy's Law,

$$V = -\frac{k}{\mu} \nabla \cdot p \qquad (2)$$

where k is the air permeability of the porous medium, μ is the fluid viscosity, and $\nabla \cdot p$ is the applied pressure gradient. The simultaneous solutions of these equations for appropriate boundary conditions describe the airflow and pressure fields developed by a sub-slab depressurization system.

Substituting Darcy's Law into the equation of mass conservation, assuming that the fluid (air) is incompressible, yields:

$$\nabla \cdot (K \nabla \cdot P) = 0 \qquad (3)$$

which must then be solved for appropriate boundary conditions.

In order to obtain solutions for a wide variety of boundary and sub-slab conditions in three dimensions, a computer solution utilizing finite difference methods was developed. The methodology of this approach involves dividing the sub-slab volume into a number of small discrete volumes, referred to as cells. Each cell is permitted to communicate (have a flow of air) with its nearest neighbor cells. The program iterates a series of steps where the flow of soil gas from cell to cell is governed by equation (3). The iterative process continues until steady-state conditions are achieved; i.e., the flow into the sub-slab volume is equal to the flow out of the sub-slab volume.

Boundary conditions that govern the generic operation of sub-slab ventilation systems are determined by the presence of sources and sinks for the air current. In practical sub-slab depressurization systems, air must be drawn into the sub-slab volume to replace the air that is forced out of that volume by the suction fan. The precise sources of this replacement air vary according to the physical conditions unique to that site. For slab-on-grade construction, there are several common sources for this replacement air. Cinderblock stemwalls frequently provide a dominant source, since they have permeabilities equal to, or larger than, those of the soils of interest and allow outdoor air to be pulled into the sub-slab volume. Where the block stemwalls are well sealed, air must be pulled into the soil around the building from the outdoor air. This air is then transported below the stemwalls and footings to the sub-slab volume. Cracks in and around the concrete slab also allow indoor air to be transported to the sub-slab volume. The primary sink for sub-slab depressurization systems is the suction pressure applied to the sub-slab materials, either in the form of a suction pit or an extended suction scheme such as a drainage mat.

The boundary conditions that characterize each of these sources or sinks may be specified as a pressure measured relative to atmospheric pressure. The pressures at boundaries that permit the infiltration of outdoor air are therefore equal to atmospheric pressure, and the pressures at the suction points simply become the applied suction pressures.

The implementation of this technique for computer solutions requires the complete specification of all boundary conditions. These correspond to physical quantities such as slab dimensions, construction type and geometry, the sizes and locations of cracks, and the number, location, and size of the suction points. Following the specification of these parameters, the finite difference

methods discussed previously are utilized to obtain a three-dimensional simulation of the pressure and velocity fields present in the sub-slab volume.

Although the calculations are performed in full three dimensions, it is usually most effective to present the data in the form of a two-dimensional slice (vertical or horizontal) in which the pressure or velocity field contours may be easily evaluated. For the purposes of designing and evaluating sub-slab depressurization systems for radon mitigation, the pressure fields of primary interest are those in the horizontal plane immediately below the concrete slab. The pressure fields generated for this location also lend themselves well to experimental measurements for verification of the computer simulations.

EXPERIMENTAL

Experimental evaluations of the pressure fields in the plane immediately below the concrete slab have been made on a number of different slabs for comparison with the computer predictions. These tests have been performed both at houses where active sub-slab depressurization systems have been installed and at the University of Florida Test Slab Site. The Test Slab Site was explicitly built to investigate the performance of and changes associated with sub-slab depressurization systems under a variety of conditions (2). The University of Florida Test Slab site consists of four test slabs built with the slab-in-stem-wall construction technique using standard construction practices. Each slab has dimensions of 24 ft x 48 ft (7.3 m x 14.6 m) and represents a typical Florida house construction technique through the completion of the slab, with no additional building shell. The measurements reported here are obtained from Test Slab #2 which is constructed with 24 in (0.6 m) of sand fill material above the natural soil, which is also sandy in nature (Figure 1). This test slab utilizes a polyethylene curtain placed along the stem wall for half the perimeter of the slab. This effectively seals the block walls from air infiltration for that portion of the slab.

The site provides an excellent facility for mapping the pressure field created by a variety of different suction point configurations and comparing them with the pressure fields generated from the computer simulation for those experimental conditions.

The Test Slab has a series of 22 3/4-in. (0.02 m) holes drilled through the concrete slab in a regular pattern across the slab (Figure 1). These holes serve as the measurement points for pressure field mapping and velocity measurements. A suction pit in the form of a 12 in. (0.3 m) radius hemisphere was created below the suction point penetration and was not backfilled with any material in this series of experiments.

The experimental procedure for pressure field mapping consisted of applying a suction pressure of 500 Pa to a central suction point while all other penetrations remained sealed. Suction pressure was created by an industrial vacuum cleaner fitted to a regulating valve. Pressure at the suction point was monitored throughout the experiment using a Neotronics micromanometer, Model MP20SR. Airflow out of the suction point was calculated from a measurement of

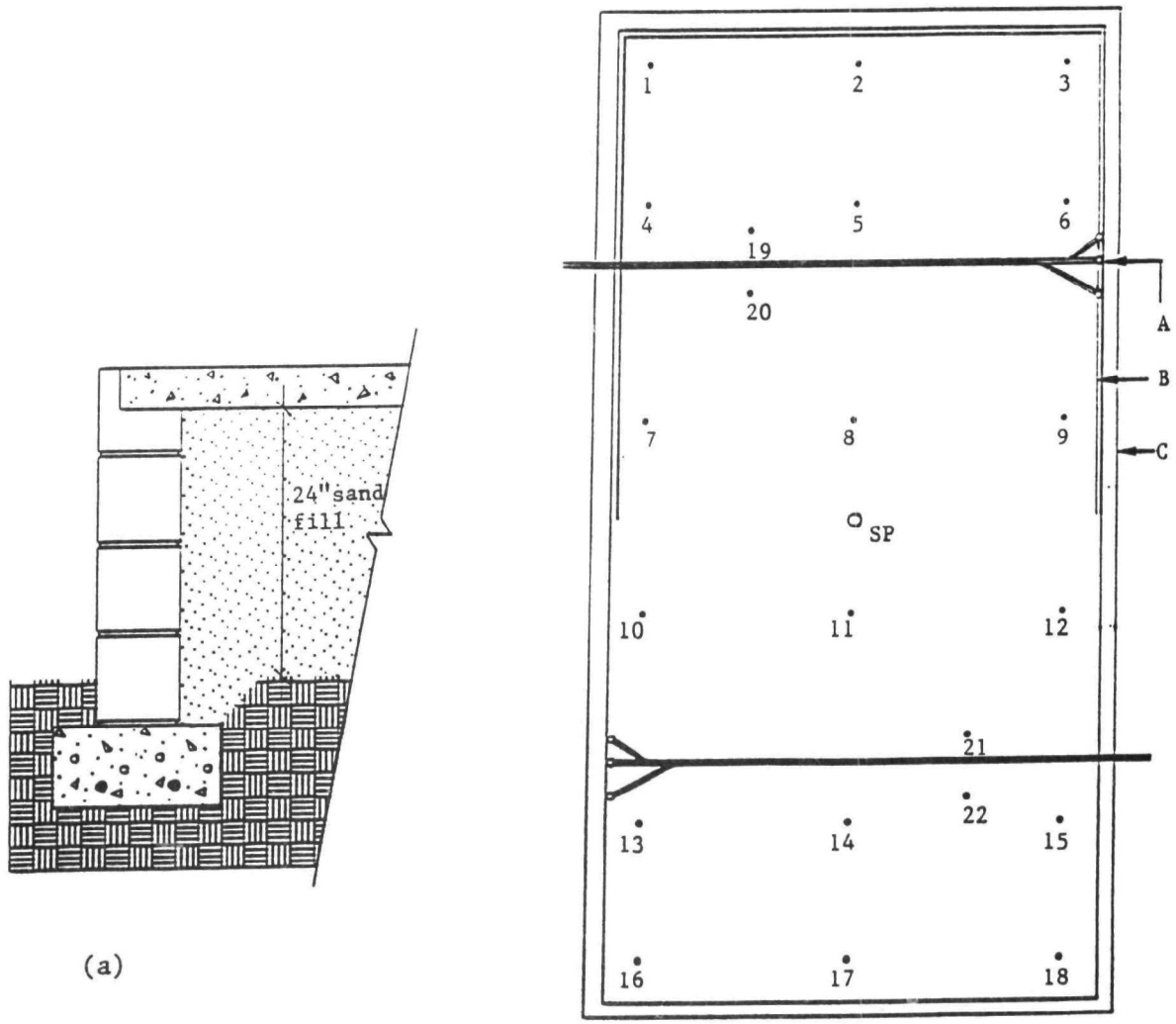

Figure 1. University of Florida Test Slab Configuration. (a) A horizontal cut-away of the footing, stemwall, slab, and fill construction. (b) A vertical view of the test slab illustrating the plumbing rough-in (A), stemwall curtain (B) stemwall (c), suction point (SP), and test points.

the velocity of the air flowing through a pipe from the suction point. Air velocity was measured with a Kurz Model 440 air velocity meter. The induced pressure was sequentially measured at each of the test points by inserting the measurement hose of a micromanometer (Neotronics, Model MP20SR) through the test hole and sealing it from the above slab atmosphere. All pressures were measured and reported relative to atmospheric pressure. A commercial software package (Surfer, Golden Software) was used to interpolate between data points, using a Kriging algorithm, and to develop contour lines of constant pressure. The empirical pressure fields developed for the central suction point configuration are illustrated in Figure 2a.

Pressure field extension measurements, total system airflow, and indoor radon measurements were also made on four research houses. These houses were initially evaluated using EPA Diagnostic Protocols(3). Based upon the information obtained during these visits, sub-slab depressurization systems were designed for each of these houses utilizing the computer simulation. The parameters describing the operation and performance for each of these systems are measured and compared to the predictions. The airflows are predicted from measurements of the soil permeability and applied suction pressure, along with the geometric dimensions of the specific house slab and compared to the measurements made at each suction point which are shown in Table 1. All but one of these sub-slab depressurization systems consist of two suction points connected to a single fan.

The system is also configured so that the suction points may be individually valved off. By valving one suction point off and measuring the pressure induced at that point by the other suction point, it is possible to obtain a measure of the pressure field that may be compared with the predicted pressure field. The pressure field due to single suction point operation as predicted by the computer model for House 789 is illustrated in Figure 3 with the measurement of the pressure induced at the opposite suction point posted at that location. The reduction of indoor radon concentration by the designed pressure fields is listed in Table 1.

RESULTS AND DISCUSSION

The pressure fields generated under the test slabs are simulated by utilizing the computer model configured to the same boundary conditions as the test slab. This configuration permits the comparison of the model results with experimental results for two different sets of boundary conditions: sealed and unsealed stemwalls. The boundary conditions utilized for the model that correlate with the test slab are: 1) no interaction of the sub-slab environment with the outdoor atmosphere along the outer perimeter of the slab to a depth of 1 m, corresponding to the case of the polyethylene-curtained stemwalls, and 2) differential pressure equal to atmospheric pressure at the outer perimeter of the slab, corresponding to unsealed stemwalls. The test slab pressure-field contours developed from the computer simulation, Figure 2b, may be directly compared with the contours developed from the experimental test points, Figure 2a. The simulated contours coincide with the experimental data over the entire

Table 1. COMPARISON OF EXPERIMENTAL MEASUREMENTS AND MODEL PREDICTIONS FOR RESEARCH HOUSES

House Suction Point	R_0(cm)	P_o(Pa)	Q_{exp}(cfm)	Q_{pred}(cfm)	k_d(m^2)	k_c(m^2)	$[Rn]_{Before}$	$[Rn]_{After}$
789-1	46	385	3.6	4.3	6.0×10^{-11}	5.0×10^{-11}	12	1.9
789-2	40.7	388	2.2	3.9	6.0×10^{-11}	3.5×10^{-11}		
797-1	46	387	3.0	4.4	6.0×10^{-11}	4.2×10^{-11}	17.5	1.4
797-2	46	388	3.2	4.4	6.0×10^{-11}	4.2×10^{-11}		
892-1	46	378	2.0	4.5	6.5×10^{-11}	3.0×10^{-11}	18.9	7.1
892-2	42	325	20.4	4.9	6.5×10^{-11}	----		
062-1	46	241	2.6	2.7	6.0×10^{-11}	6.0×10^{-11}	8.9	2.0

R_o - The hemispherical suction pit radius.

P_o - The empirically measured pressure at the suction point. Values are ± 3 Pa.

Q_{exp} - The empirically measured flow rate from the suction point. Values are ± 0.3 cfm (1.4×10^{-4} m^3/s).

Q_{pred} - The flow rate predicted by the computer model calculations.

k_d - The air permeability of the sub-slab soils determined by diagnostic communication tests. Values are ± 20%.

k_c - The corrected air permeability that permits the computer model calculations to reproduce Q_{exp}.

$[Rn]_{Before/After}$ - Indoor radon concentrations averaged over several weeks of lived-in conditions, before and after the installation of sub-slab depressurization systems.

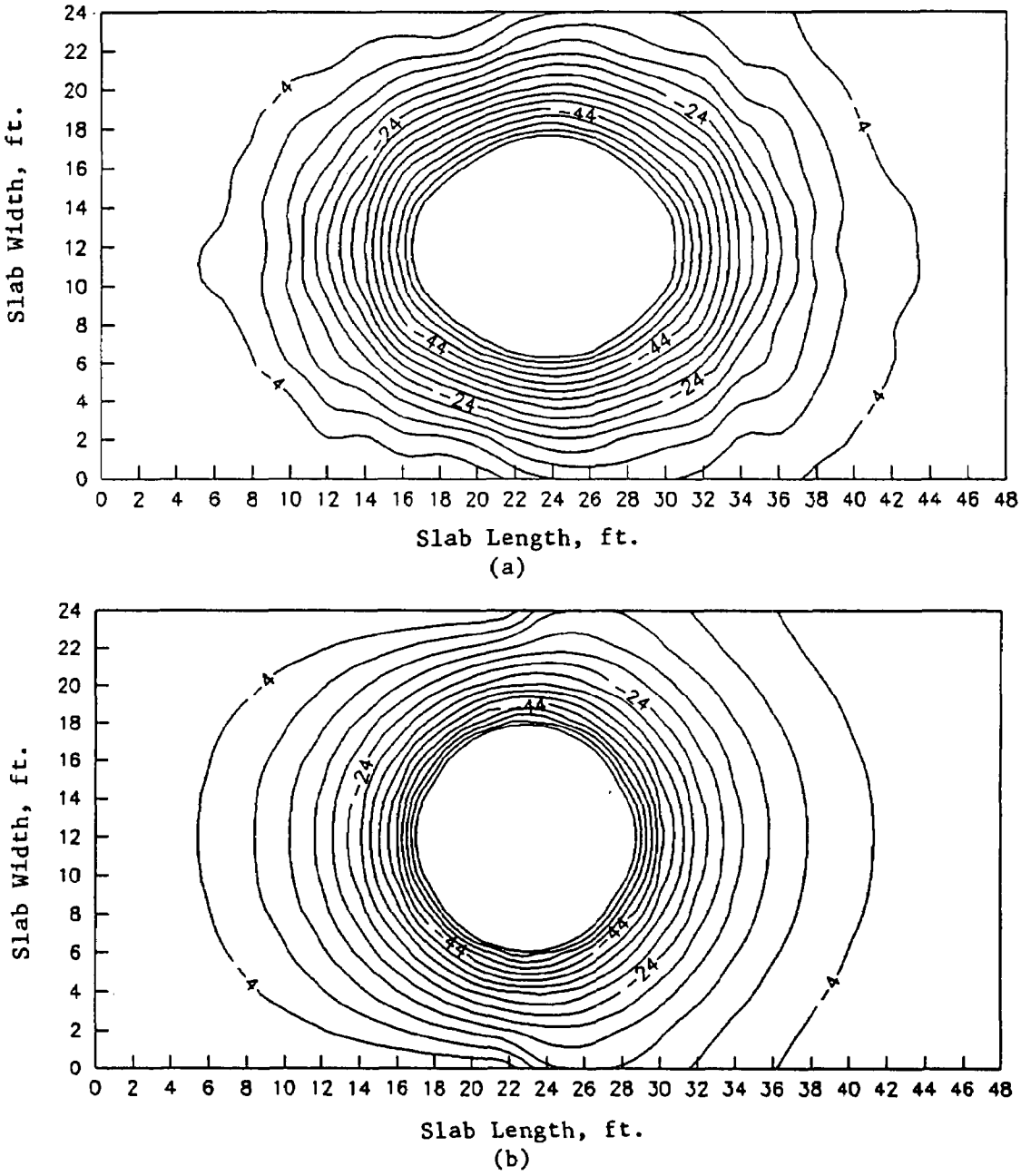

Figure 2. Test Slab Pressure Fields. The vertical and horizontal axes are the slab dimensions in feet, and the right half of the slab incorporates the stemwall curtain. (a) Measured pressure field contours (Pa) from an applied suction pressure of -500 Pa, plotted for pressures greater than -60 Pa. (b) Pressure field predicted by the computer simulation of the experimental conditions.

slab, indicating that the model accurately predicts the pressure fields for both sealed and unsealed stemwall conditions.

Both the experimental results and those from the computer model demonstrate how polyethylene-curtained stemwalls extend the pressure field immediately under the slab. Figure 2 demonstrates that, although sealing the stemwall does not dramatically change the pressure-field extension along the long axis of the slab, it does permit the pressure field to reach the edges of the slab across the short axis. In this example, if a pressure differential of 4 Pa were required to neutralize the natural depressurization of a house, the sealed stemwall could account for an additional 4% of the slab area being maintained below this differential pressure. These results demonstrate how sealing stemwalls from airflow extends the pressure field and that the effect of stemwall sealing will be most evident for small pressures, on the order of a few Pascals. These pressure field extensions can dramatically reduce radon entry by encompassing major entry routes such as the slab/footing joint.

The test slab experiments provide verification of the operation of the sub-slab computer model under well-characterized conditions. Additional experiments and tests were performed using houses participating in a U.S. EPA mitigation research project. Unlike the test slabs, the sub-slab nature of these houses could only be inferred from the results of diagnostic tests performed at each of the houses. These houses, located in Alachua and Marion Counties, Florida, provide data on the range of applicability for the sub-slab computer model in Florida houses, provide the opportunity for whole house verification, and demonstrate the facility of using the computer simulations as an aid in the design of sub-slab depressurization systems. The initial data for these simulations were obtained from diagnostic visits in the fall of 1988. Once a particular design was chosen and installed, experimental measurements were made for comparison with the simulation predictions.

The pressure at the suction point may be predicted by developing a sub-slab system performance curve, applied pressure vs. airflow, and matching it against the fan performance curve. The sub-slab system performance curve is developed by running computer simulations of the sub-slab environment for several applied pressures. The fan performance curve is obtained from the fan manufacturer and verified empirically. The intersection of these two curves describes the pressure and airflow where the entire sub-slab depressurization system will operate, assuming that the system is designed such that there are negligible pressure drops from other sources. Since each of the installations examined here utilizes a single fan, when two suction points are utilized, slightly different pressures may be measured at each of the suction points due to several variables such as differences in suction pit size, length of pipe run, number of elbows, and airflow rates.

While the predicted pressure may be corrected to account for these variables, for the purpose of evaluating the sub-slab computer model and the predicted flowrate, it is most straightforward to perform a simulation utilizing the empirically determined applied pressure. Predicted airflow rates are listed in Table 1 along with the measured flow rates. There is agreement between all

of these measurements except for suction point 892-2. The extraordinarily high flow rate here may be attributed to a crack in the cement floor that runs directly into the suction point.

All of these flow rates were predicted utilizing effective permeability values obtained from the diagnostic sub-slab communication testing. From measurements of the applied pressure and airflow rates, we can use the computer model to calculate an updated value of the permeability. It is therefore likely that some of the variations between the predicted and experimentally measured permeabilities may be attributed to some variation in the sub-slab soil permeability from the fall of 1988 to the installation time.

Since these houses are occupied, it is not possible to obtain a high resolution map of the pressure fields created underneath the slab. As previously discussed, it is, however, possible to obtain a simple measure of the pressure field extension in the houses that utilize multiple suction points. The pressure field induced under such a configuration for one house is demonstrated in Figure 3, along with the predicted pressure field contours from the single suction point operation. These figures indicate that the predicted pressure fields are in agreement with the measured pressure point along the axis connecting the suction points. The pressure fields predicted by simultaneous operation of both suction points are also illustrated in Figure 3. Since the magnitude of the pressure fields from single-point operation and test slab data is correctly predicted, it is reasonable that the pressure fields created from the simultaneous operation of two suction points are also correctly predicted.

The effectiveness of the designed pressure fields in overcoming the pressure-driven flow of radon-222 into these houses is demonstrated by the reduction of the indoor radon concentrations shown in Table 1. One house, House 892, continues to have elevated radon concentrations, although they are reduced from the original concentrations. It is most likely that this is caused by a significant reduction in the pressure field produced at suction point #2 by the crack adjacent to the suction point as previously discussed. It is expected that, when this crack is sealed, the pressure fields will extend to the designed contours and the indoor radon concentrations will be reduced to levels comparable to that achieved through the use of sub-slab depressurization in the other research houses.

The preceding results indicate that the computer model that has been developed accurately matches experimental conditions. The usefulness of such a model lies in its ability to make useful predictions. These may include the use of the computer model as a design tool to increase the efficiency of sub-slab depressurization systems, or as a means of predicting the behavior of sub-slab depressurization systems under conditions that are time-consuming, expensive, or otherwise difficult to measure experimentally.

The ability of this computer model to simulate the operation of a sub-slab depressurization system prior to installation makes it a valuable design tool. For sub-slab depressurization systems to be acceptable to homeowners, it is necessary to install the suction points in inconspicuous locations. These are not usually the optimum locations for the suction points. By performing computer

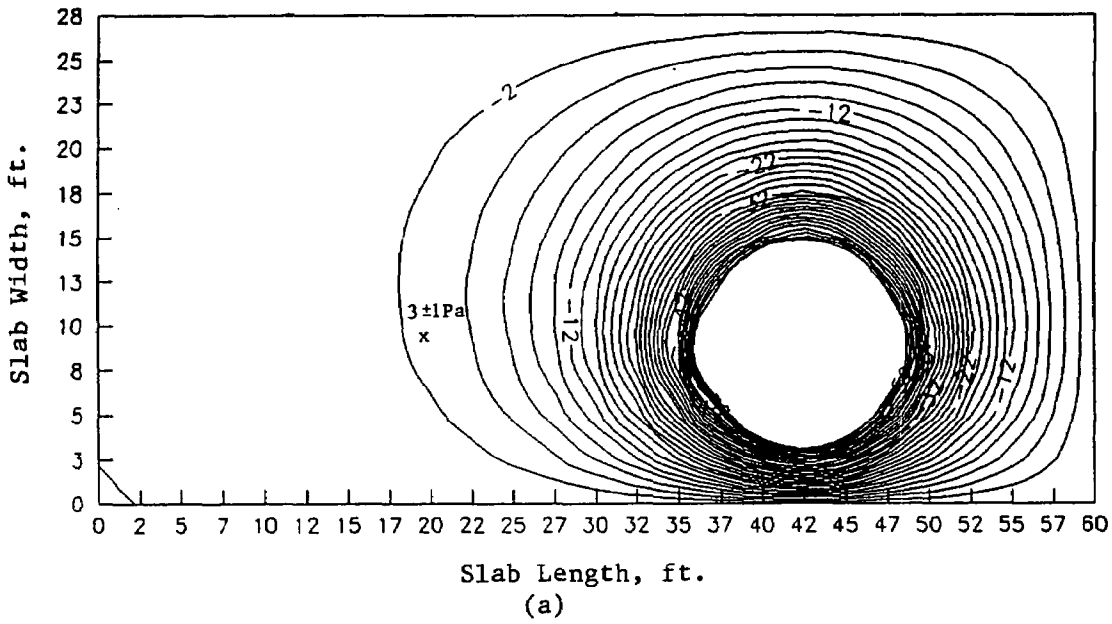

Figure 3. Research House 789 Pressure Fields (a) Predicted contours for pressures greater than -60 Pa from a single suction point. (b) Predicted contours for pressures greater than -60 Pa for the simultaneous operation of both suction points.

simulations, it is possible to evaluate the performance of a sub-slab system utilizing the discrete locations that are available for use. Utilizing this methodology, it is possible to design a sub-slab depressurization system that provides for the optimum number and location of suction points, that maximizes system efficiency, and that minimizes the visual impact to the homeowner.

Predictions of the physical processes that occur during sub-slab depressurization are also possible through these modeling techniques. One of the most important aspects of these modeling techniques concerns the development of pressure fields under conditions of homogeneous permeability. Under these conditions the magnitude of the pressure fields established by the sub-slab depressurization system is independent of the permeability. For a given set of boundary conditions, the pressure fields will always be the same, regardless of the soil permeability. In the case of non-homogeneous soil permeability, the pressure fields created will be modified by the inhomogeneities, but these changes will be a function of the ratios of the different permeabilities, and are still independent of the permeability magnitude.

Permeability does, however, affect soil gas velocity and flow. From Darcy's Law, for a given pressure field gradient, the greater the permeability, the greater the flow rate. Since the pressure field gradients are determined solely by the boundary conditions and are the same regardless of permeability, it follows that changes in the soil permeability must affect the flow rate accordingly. Both of these effects are predicted by the computer model and may also be derived analytically for simple geometries.

An interesting application of the computer model is the simulation of the effects of cracks and other openings in a concrete slab on a sub-slab depressurization system. In order to model this case we have assumed that the crack, or opening, is large enough and that the air velocity moving through it is small enough (small soil permeability) so that the pressure drop across the opening can be neglected. The opening, therefore, permits atmospheric pressure to be maintained under the slab immediately below the opening. This becomes an additional boundary condition for this problem.

The incorporation of this boundary condition leads to two effects on the physical conditions present beneath the slab. The induced pressure in the sub-slab volume surrounding the penetration will be reduced and the flow through the sub-slab volume, and out of the suction point, will be increased. The increased flow, predicted by the computer model, will provide an indirect reduction in the applied pressure by changing the sub-slab performance curve in such a manner that it intersects the fan performance curve at a higher flow rate, and therefore a smaller applied pressure. In most practical cases the increase in flow rate is small enough that these effects are negligible.

The computer model predicts that the area under the slab affected by the penetration will be determined by its proximity to the suction point. Figure 4 illustrates the pressure fields produced in two situations for a constant applied pressure and where only the position of the penetration has been changed. This demonstrates that a penetration closer to the suction point affects a smaller slab area than one farther away. The penetration near a suction point

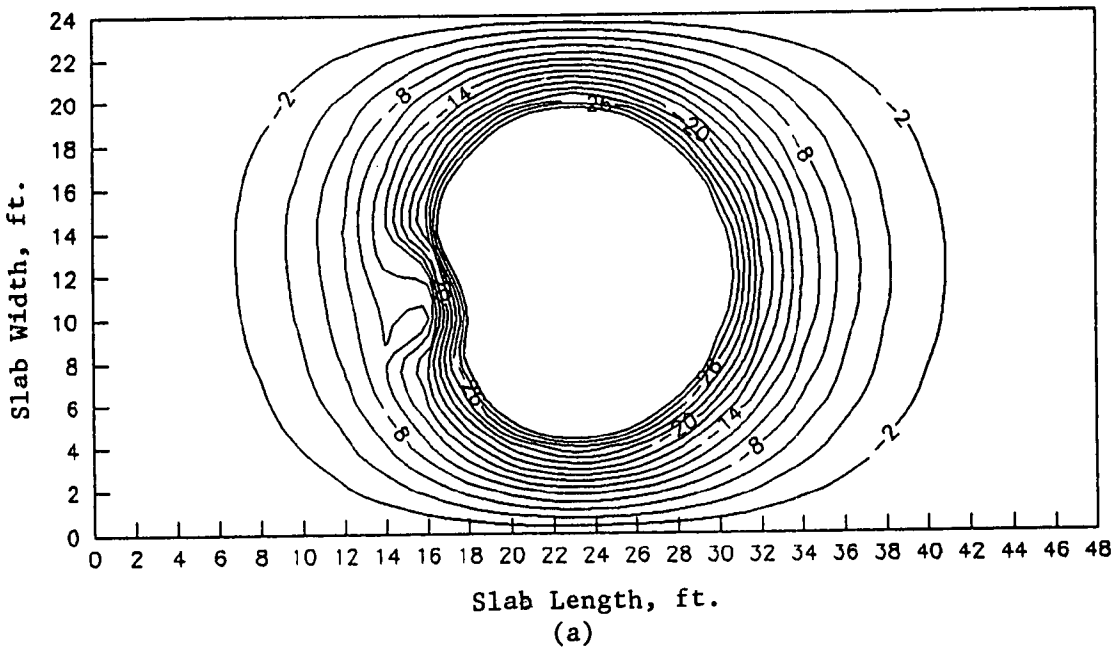

Figure 4. Effects of slab penetrations on the pressure field: (a) A 12 x 36 in. (0.3 x 0.9 m) penetration close to the suction point. (b) A 12 x 36 in. (0.3 x 0.9 m) penetration far from the suction point.

may decrease the pressure field below that required to overcome the negative house pressure only in the immediate vicinity of the penetration. The pressure field quickly recovers in this case and develops nearly unperturbed except for that small area. When the penetration is farther from the suction point, where the pressure gradients are smaller, a much larger slab area is affected. Under these conditions, the lower limit of the pressure fields are greatly perturbed, and can greatly affect the area under the slab where sub-slab depressurization is effective.

These results indicate that, unless cracks near a suction point are so extensive that the applied pressure cannot be maintained, it is not worth a large expenditure of effort to seal them. Conversely, cracks near the perimeter of the pressure field should be sealed if the sub-slab depressurization system is required to maintain its effectiveness at distances beyond that from the suction point.

CONCLUSIONS

A computer simulation that describes the operation of sub-slab depressurization systems has been developed by modeling the physical processes that occur when this mitigation technique is applied to slab-on-grade construction. The model has been verified by extensive pressure field mapping at the University of Florida Test Slab Site and has demonstrated its effectiveness in the design of sub-slab depressurization systems for several radon mitigation research/demonstration houses. The physical processes predicted by the model make it a useful tool for the design of these systems, and permit it to make valuable predictions concerning the performance of these systems for a variety of physical conditions. These simulations permit accurate evaluations of various sub-slab depressurization configurations that can be performed without the time and expense associated with the construction of elaborate test facilities and extensive instrumentation.

REFERENCES

1. Bear, J. The Fundamental Fluid Transport Equations in Porous Media. In: Dynamics of Fluids in Porous Media. Dover Publications, New York, 1988.

2. Furman, R.A. and Hintenlang, D.E. Sub-Slab Pressure Field Extension Studies on Four Test Slabs Typical of Florida Construction. In: Proceedings of the 1990 International Symposium on Radon and Radon Reduction Technology, Atlanta, Georgia, to be published.

3. Harris, D.B., Henschel, D.B., Sanchez, D.C. and Witter, K.W. Field Measurements in the EPA/AEERL Radon R&D Program. In: Proceedings: The 1988 Symposium on Radon and Radon Reduction Technology, Volume 2, EPA-600/9-89-0066 (NTIS PB86-167498), March 1989.

INTERPRETING THE VACUUM SUCTION TEST

by: Terry Brennan
Camroden Associates
Oriskany, NY 13440

ABSTRACT

Some investigators use a vacuum cleaner to temporarily induce a low air pressure field beneath concrete slabs. This test is performed to gain insight into the prospects for soil depressurization as a radon control method. A protocol is suggested that can provide a basis for deciding whether sub-slab depressurization or pressurization is likely to succeed or fail. Enough data can be collected to select a fan with appropriate performance characteristics. Examples are drawn from field work to illustrate the collection and interpretation of the data.

Lacking X-ray vision, a vacuum suction test can be done to explore strength and size that a low air pressure field can be extended beneath a floor slab. How far the pressure field is extended and at what strength depends two things :

- how resistant to airflow is the material immediately beneath the slab
- how tight the surrounding soil and covering foundation are

The results of this test can yield insight into both of these important variables. First a vacuum cleaner is used to apply suction to a hole through the slab, called FA by convention. The amount of suction created by the vacuum pulling on the "system " beneath the slab is measured in the vacuum nozzle (FA), at a hole 10 inchs away (FB, again by convention) and at other test holes (FC, FD etc.) several feet away (usually 10 to 30 feet). If the material beneath the slab is loose (say stone pebbles) and foundation and surrounding soil are fairly resistant to airflow, then a low pressure can be induced a great distance from the suction point. If there is loose material beneath the slab and there are large airleaks through the foundation or the surrounding soil or bedrock, then a weak pressure field will be induced and will extend only as far as the leaks (eg. French drain or shattered bedrock). If there is fine but porous material beneath the slab then a strong vacuum will be induced at the suction point (FA) but it will be defeated by the resistance to airflow of the fine material and not extend very far from the suction point. See Figure 7 for a conceptual model and illustration of these ideas.

Figure 1 - The Vacuum Suction Test

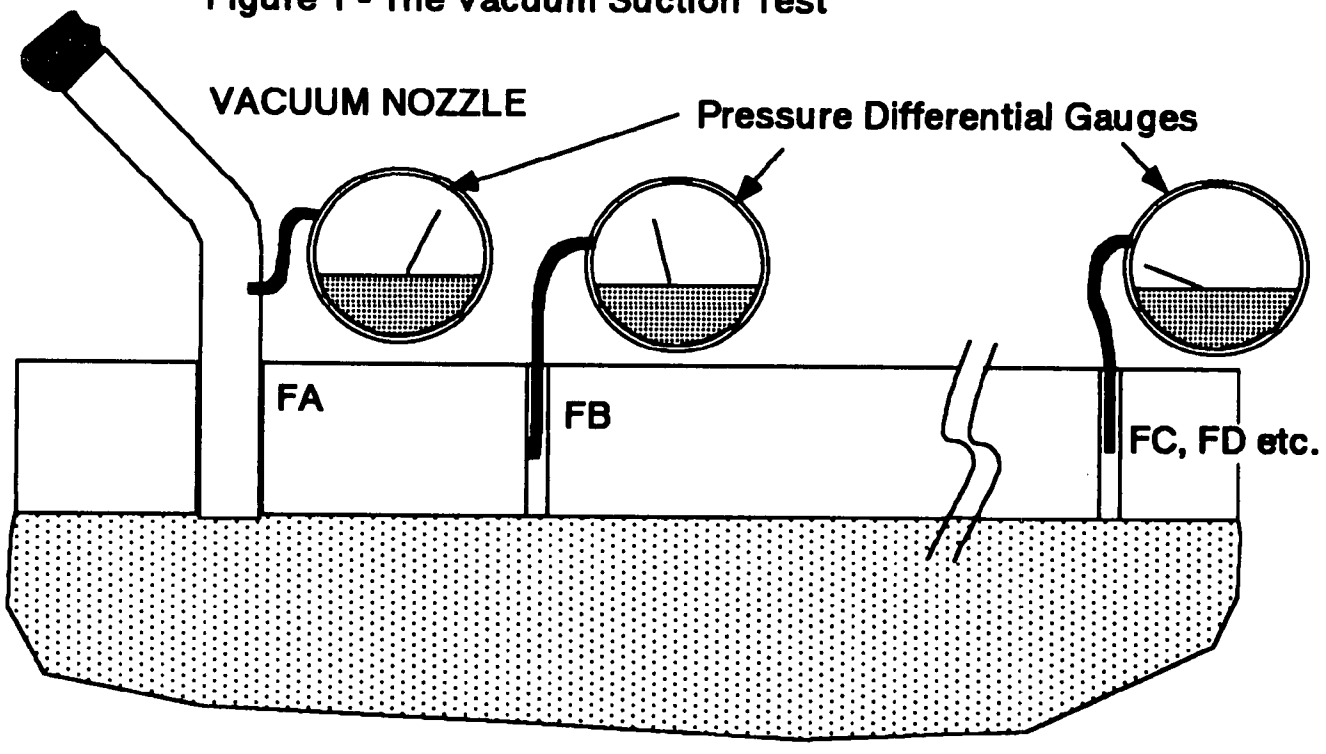

Figure 2 - Measure the vacuum in the closed nozzle (zero airflow) and open nozzle (maximum airflow). This establishes a rough guide to the amount of air the vacuum can pull from under the slab, which can be used with Figure 3 to select the fan type. Alternately the airflow could actually be measured.

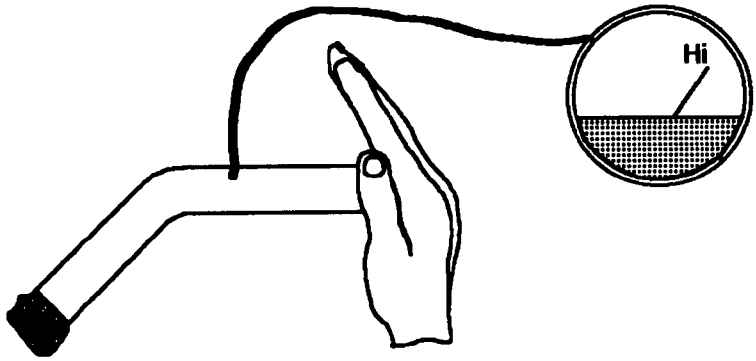

Cover the vacuum nozzle with your hand. The airflow thru the vac is zero. The amount of suction measured in the nozzle is the most the vacuum can pull. For a Eureka Mighty Mite with a clean bag this is about 40 inchs WC.

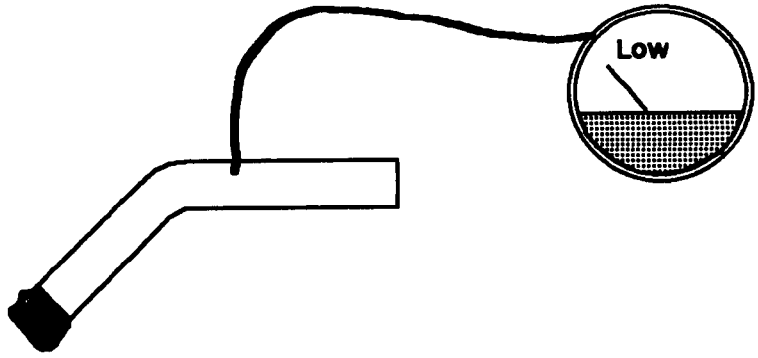

Measure the suction in the nozzle with the vacuum nozzle in open air. This is the lowest amount of suction the vacuum will pull because it is the minimum resistance to airflow it can have. For a Eureka Mighty Mite with a clean bag this is about 5 inchs WC.

Figure 3 - Select Fan Type

Suction at FA	FB	Fan Type
Low-Medium	<1.5 inchs WC	In Line Centrifugal
High	<1.5 inchs WC	Vortex
Medium-High	>1.5 Inchs WC	Radial

Figure 4 - Fan and "System " Curves

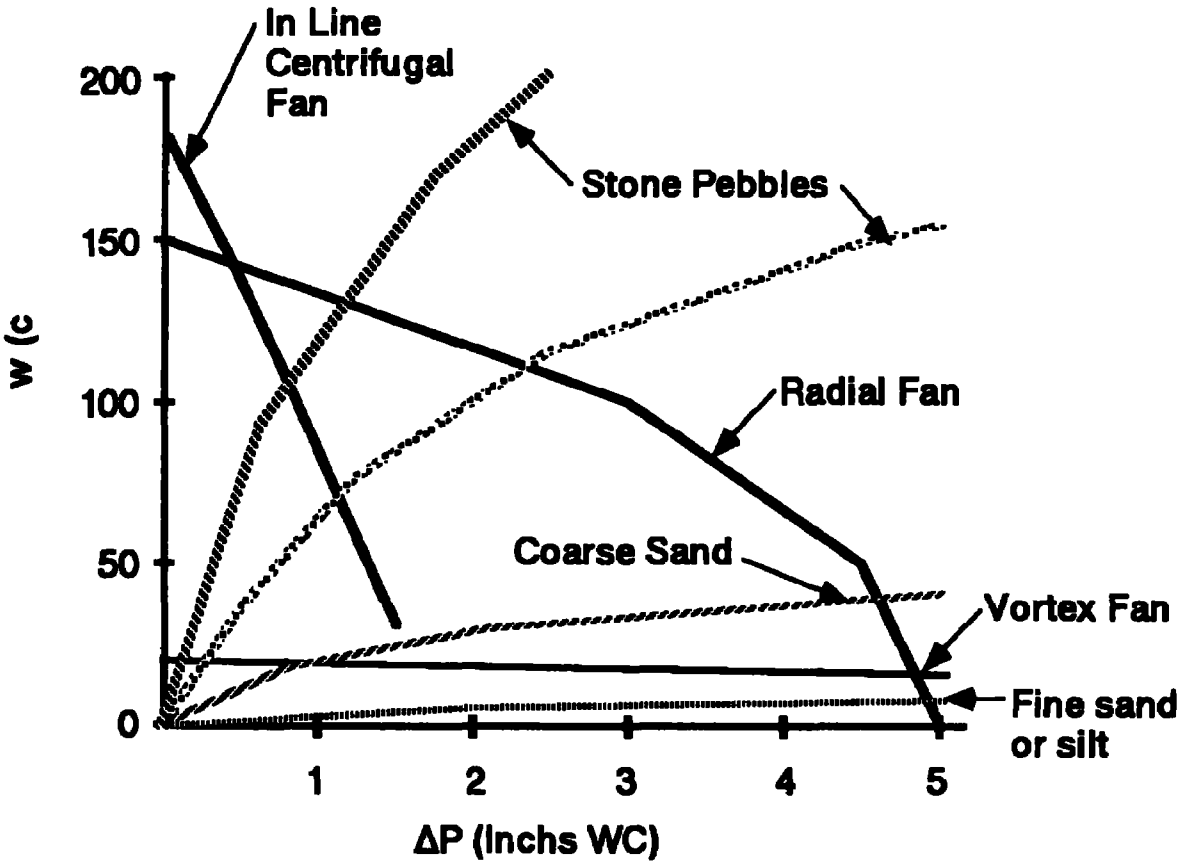

The four "system " curves are measured field data that appear "typical " for the conditions listed. As with all things radon it is likely that there are many exceptions to these "typical " curves.

Notice that for different sub-slab conditions the in line centrifugal fans normally used for soil depressurization systems is probably not appropriate. Both the coarse sand and fine sand and silt curvesintersect the in line centrifugal fan curve below the manufacturers suggested minimum airflow.

The power consumed by an air handler depends on how much air it is moving. This table shows the measured Wattage range of the fans whose curves are shown in the graph.

In Line Centrifugal 63-83 Watts
Radial 87 - 245 Watts
Vortex 67-132 Watts

Figure 5 - Select Number of Suction Points

Suction at		Probable Sub Slab Condition	Number of Suction Points
FA	FC, F D etc.		
Low-Medium	Good everywhere	(stone pebbles)	1 anywhere
	Good around slab edge	(sand with perimeter drain tile)	1 anywhere at slab edge
High	Drops off quickly (6 to 10 feet)	(clay or silt)	1/300 square feet
Medium-High	Drops off quickly (10 to 15 feet)	(coarse sand)	1/600 square feet
Low	Drops off quickly (8 to 15 feet) or marginal everywhere	large leaks under the slab through the foundation or underlying soil or bedrock. (Shattered shale or limestone, glacial outwash or riverbed gravels)	pressurize beneath the slab or more suction points or seal foundation leaks if they are large (french drain, sump hole)

Figure 6 - Select Pipe Diameter

Suction at FA	Pipe Diameter
High	Four inch
Medium	Three inch
Low	Two inch legs, three inch headers

Figure 7 - A Conceptual Model for Soil Depressurization

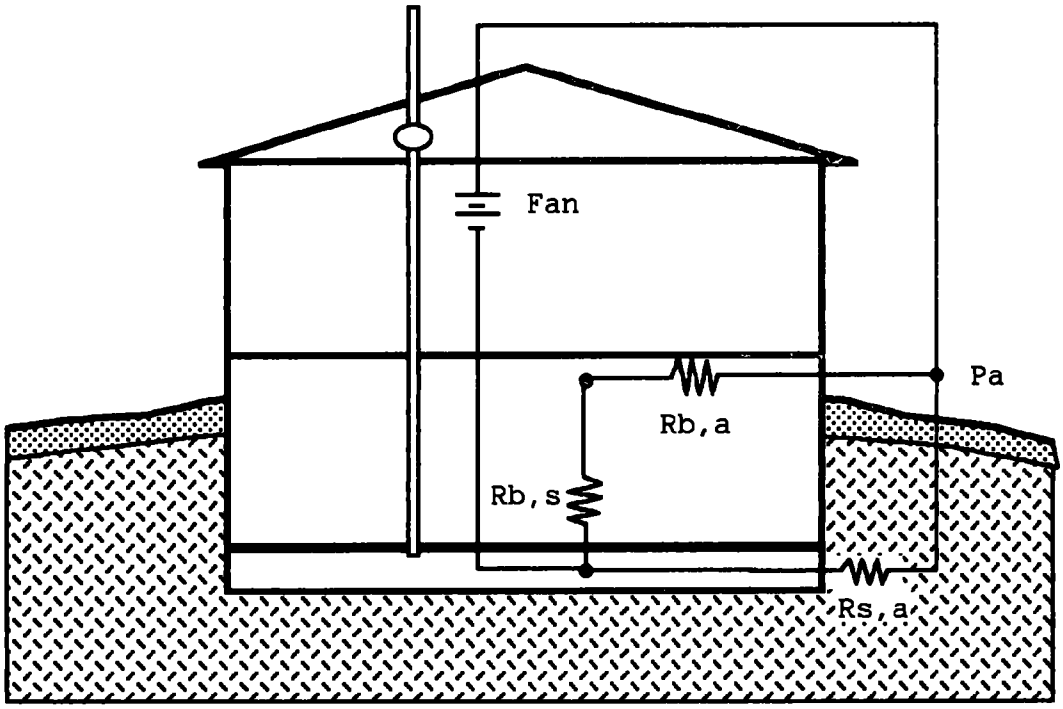

If the material beneath the slab has very little resistance to airflow compared to that of the surrounding soil or bedrock (Rs,a) and that of the leaks through the foundation to the sub slab air (Rb,a), then the amount of air and vacuum induced by the sub slab fan is a function of these two variables and the fan performance curve.If the material beneath the slab is fine enough so that the resistance to airflow through a few feet of it is comparable to the other two (Rb,s and Rs,a) then this model is too simple. The material beneath the slab would have to be divided up into numerous "bits" and the resistance between each bit the and the surrounding "bits", outside air and basement air would need to be accounted for.This is the case when fine sands, silts and clays are found directly beneath the slab and it has important implications for both radon entry and the prevention of radon entry by soil depressurization.

SEASONAL VARIATIONS OF INDOOR RADON CONCENTRATIONS

by: Benny Majborn
Risø National Laboratory
DK-4000 Roskilde, Denmark

ABSTRACT

Seasonal variations of indoor radon concentrations have been studied in a cluster of 10 single-family houses. Eight of the houses are of a similar construction with slab-on-grade foundations. The remaining two houses have different substructures, one of them having a crawl space, and the other having partly a basement and partly a crawl space. A "normal" seasonal variation of the radon concentration with a maximum in winter and a minimum in summer was observed in most of the houses. In these houses the variation showed a strong correlation with the indoor-outdoor temperature difference on a 2-month basis. However, deviating seasonal variations were observed in some of the houses, notably in the two houses having different substructures.

A re-examination of the data obtained in a previous study indicates that winter/summer ratios of indoor radon concentrations in Danish houses depend on the house substructure. The mean winter/summer ratios were about 2.1 for houses with slab-on-grade foundations, 1.5 for houses having a basement, and 1.0 for houses with a crawl space (geometric mean values). However, a study with more houses in each substructure category will be needed to show whether or not the indicated differences are generally valid for Danish houses.

INTRODUCTION

In this paper some results on seasonal variations of indoor radon concentrations in Danish single-family houses are reported and discussed. The results have been obtained in two different studies. One of these is an extension of an investigation of factors influencing indoor radon concentrations carried out in 1986-87 (1). The investigation comprised 16 houses built on the same site, and included integrating radon measurements

in the living-room and in a bedroom of all the houses on a two-month basis throughout the two years. These measurements have been extended through 1988 in ten of the houses. The other study is a pilot investigation of natural radiation in Danish houses carried out in 1983-84 (2). In that work integrating radon measurements were made in 70 single-family houses and 12 apartments during three months in winter and three months in summer. The data on seasonal variations obtained in the pilot study have been re-examined after obtaining additional information on the substructure of the houses.

Knowledge of temporal variations of indoor radon concentrations and the variability of such variations is needed for a proper appraisal of the significance of results obtained from short-term measurements and for estimating the uncertainties involved in attempts to predict annual averages from measurements covering shorter time periods (3,4). Knowledge of temporal variations and the identification of causes of such variations can also contribute to improve our understanding of the mechanisms of radon entry into houses (5,6).

METHODS

Integrating radon measurements were made with passive closed dosemeters equipped with CR-39 track detectors. The dosemeter design and its properties have been described elsewhere (2,7). The performance of the dosemeter was tested in CEC radon dosimetry intercomparisons in 1984 (8), 1987 (9), and 1989, in all cases with good results.

HOUSE TYPES

The 10 houses in which radon was measured on a two-month basis during 1986-88 are situated next to Risø National Laboratory. The site of the houses forms an area of about 150 m by 300 m, and the soil below the houses is mainly moraine clay. The houses are one-storey single-family houses built of bricks. Eight of the houses have slab-on-grade foundations and differ only in length, having one bedroom more or less. The remaining 2 houses have different substructures, one having a crawl space and the other having partly a basement and partly a crawl space. A special feature is a district-heating duct which is extended into each house, where it proceeds circumferentially along the outer walls as an integral part of the foundation.

The 70 single-family houses included in the pilot study in 1983-84 are distributed throughout Denmark. They were not chosen to be representative for the Danish building stock as the purpose of the investigation was primarily to establish and test measurement procedures.[1]

---

[1] A representative survey was conducted in 1985-86 (10), but in that work two six-month integration periods were used, and the seasonal variation was not measured in each single house.

Out of the 70 single-family houses 25 had a basement, but no further differentiation of the houses according to substructure was made at the time when the study was carried out. Recently, additional information on the type of substructure has been acquired for most of the houses, so that these may be grouped into the categories: 1) full basement, 2) basement + crawl space, 3) basement + slab-on-grade, 4) crawl space, and 5) no basement or crawl space, i.e. mostly slab-on-grade houses.

RESULTS

Figure 1 shows the seasonal variations during 1986, 1987 and 1988 of the mean radon concentrations in seven of the Risø houses. The figure shows the geometric mean value of the radon concentrations for each 2-month period for all 14 rooms (7 living-rooms and 7 bedrooms). The geometric standard deviations range from 1.6 to 2.1 for the 18 measurement periods. In the remaining 3 houses, including the two houses having a different substructure, there was not a pronounced seasonal variation

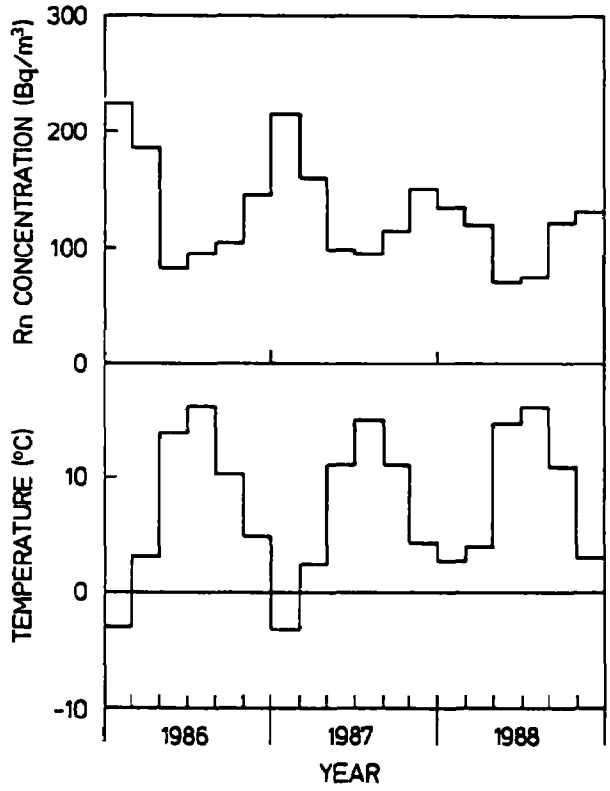

Figure 1. Seasonal variations during 1986, 1987 and 1988 of 1) the geometric mean value of the radon concentrations in 7 houses, and 2) the average outdoor temperature.

of the radon concentration, except that the house with a crawl space appeared to show a summer maximum in 1986. Figure 1 also shows the average outdoor temperature (2-month averages) at the nearby meteorological station at Risø National Laboratory. The correlation coefficients (linear regression) between outdoor temperature and indoor radon (geometric mean value for 14 rooms) were found to be -0.97 for 1986, -0.98 for 1987, and -0.91 for 1988. As the variations of the average indoor temperature are small compared with those of the outdoor temperature, the results indicate a strong correlation on a 2-month basis between the average indoor-outdoor temperature difference and the average indoor radon concentration in this group of houses.

In the pilot study integrating radon measurements were made in a 3-month winter (1 Dec. 1983 to 29 Feb. 1984) and a 3-month summer period (22 May to 13 Aug. 1984). Figure 2 is a plot of the summer results for

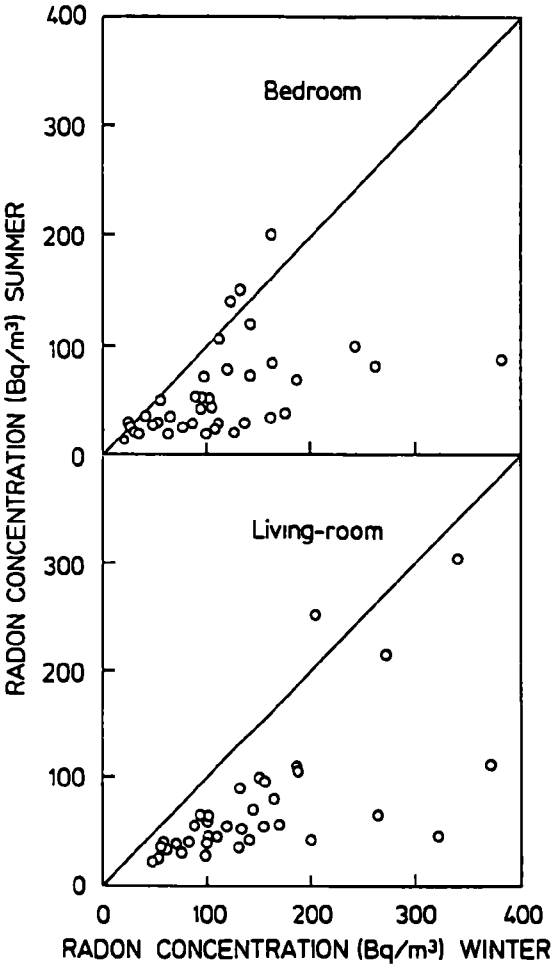

Figure 2. Summer versus winter radon concentrations in 38 houses without basement or crawl space. The straight lines represent a slope = 1.

each of the houses without a basement or crawl space (i.e. mostly slab-on-grade houses) versus the winter results for the same houses. Similarly, figure 3 shows the summer versus winter results for the houses having a basement. In Table 1 the winter and summer radon concentrations and the winter/summer ratios (geometric mean values and geometric standard deviations) are given for 1) houses with a basement, 2) houses with a crawl space, and 3) houses without a basement or crawl space. The houses with a full basement or basement + crawl space have been grouped together, because the mean radon concentrations and winter/summer ratios did not differ significantly between the two groups. Three houses having a basement + slab-on-grade foundation had mean radon concentrations in the

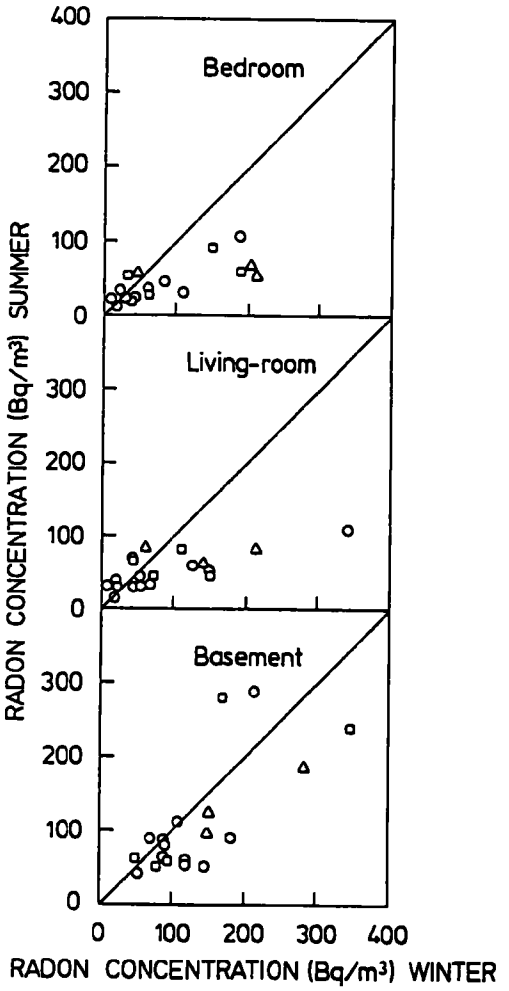

Figure 3. Summer versus winter radon concentrations in houses having a full basement (circles), basement + crawl space (squares), or basement + slab-on-grade foundation (triangles). The straight lines represent a slope = 1.

TABLE 1. WINTER AND SUMMER RADON CONCENTRATIONS AND WINTER/SUMMER RATIOS (GEOMETRIC MEAN VALUES AND GEOMETRIC STANDARD DEVIATIONS) FOR DIFFERENT HOUSE TYPES.

House type Room	Number of houses	Radon concentration Winter GM (Bq/m^3)	GSD	 Summer GM (Bq/m^3)	GSD	Winter/summer ratio GM	GSD
Basement*	16						
Living-room		68	2.2	47	1.6	1.46	1.7
Bedroom		60	2.2	38	1.8	1.57	1.7
Basement		115	1.7	88	1.9	1.32	1.6
Crawl space	3						
Living-room		59	2.6	63	2.5	0.93	1.3
Bedroom		48	2.4	49	2.6	0.97	1.1
No basement or crawl space	38						
Living-room		122	1.7	57	1.9	2.13	1.5
Bedroom		92	2.0	46	2.0	2.02	1.8

* Include 11 houses with full basement and 5 houses with basement + crawl space.

living-rooms and bedrooms that were close to the mean values found for the slab-on-grade houses. The results from these 3 houses have not been included in Table 1. There are only 3 houses with a crawl space in this sample. All 3 houses had winter/summer ratios close to unity in both rooms (range 0.7 - 1.2). The average radon concentrations were about 20, 70, and 120 Bq/m^3 in the 3 houses.

Within each category of houses the mean winter/summer ratios are not different between living-rooms and bedrooms (98% of the living-rooms and 79% of the bedrooms were on the first floor). For the 16 houses having a basement or basement + crawl space the lower mean winter/summer ratio found for basement rooms (1.3) is not significantly different from that found for living-rooms and bedrooms (1.5). The differences between the mean winter/summer ratios found for living-rooms and bedrooms in 1) houses without basement or crawl space (2.1), 2) houses with basement (1.5), and 3) houses with crawl space (1.0) are significant at the 95% level.

DISCUSSION AND CONCLUSIONS

Seasonal variations of indoor radon concentrations may depend on a number of factors, including geological factors, climate, house characteristics and living habits. Figure 1 shows an example of the influence of climate. The figure shows the seasonal variations during 3 years of the mean radon concentrations in a group of houses with slab-on-grade foundations. The variations show a strong correlation with the indoor-outdoor temperature difference on a 2-month basis. A major difference between the 3 years was an unusually cold January-February in 1986 and 1987 and an unusually mild January-February in 1988. This difference is clearly reflected in the observed radon concentrations.

The results reported in this paper on winter/summer ratios indicate that houses with slab-on-grade foundations have higher mean winter/summer ratios than houses with a basement or crawl space. Similar observations have been reported in a Finnish study (11), where measured seasonal variations of indoor radon concentrations were compared with model calculations. Data from the USA suggest that winter/summer ratios tend to be greater for the first floor than for the basement of houses (4). The same tendency was observed in the present work. It should be noted, however, that the results reported in this paper are based on a limited number of houses. A study with more houses in each substructure category will be needed to show whether or not the indicated differences are generally valid for Danish houses.

The work described in this paper was not funded by the U.S. Environmental Protection Agency and therefore the contents do not necessarily reflect the views of the Agency and no official endorsement should be inferred.

ACKNOWLEDGEMENTS

This paper is partly based on two studies that were partly funded by the Commission of the European Communities. The author would like to thank S.P. Nielsen for valuable discussions.

REFERENCES

1. Majborn, B., Sørensen, A., Nielsen, S.P., and Bøtter-Jensen, L. An investigation of factors influencing indoor radon concentrations. Risø-M-2689, Risø National Laboratory, Roskilde, Denmark, 1988. 58 pp.

2. Sørensen, A., Bøtter-Jensen, L., Majborn, B., and Nielsen, S.P. A pilot investigation of natural radiation in Danish houses. Risø -M-2483, Risø National Laboratory, Roskilde, Denmark, 1985. 40 pp.

3. Swedjemark, G.A. Radon and radon daughters indoors, problems in the determination of the annual average. SSI Scientific Report 84-11-12, National Institute of Radiation Protection, Stockholm, Sweden, 1984. 47 pp.

4. Bierma, T.J., Croke, K.G., and Swartzman, D. Accuracy and precision of home radon monitoring and the effectiveness of EPA monitoring guidelines. JAPCA 39: 953, 1989.

5. Nazaroff, W.W., Moed, B.A., and Sextro, R.G. Soil as a source of indoor radon: Generation, migration and entry. In: W.W. Nazaroff and A.V. Nero, Jr. (ed.), Radon and its decay products in indoor air. J. Wiley & Sons, New York, ISBN 0-417-62810-7, 1988, p. 57.

6. Arvela, H., and Winqvist, K. Influence of source type and air exchange on variations of indoor radon concentration. STUK-A51, Finnish Centre for Radiation and Nuclear Safety, Helsinki, Finland, 1986. 32 pp.

7. Majborn, B. Measurements of radon in dwellings with CR-39 track detectors. Nuclear Tracks 12: 763, 1986.

8. Miles, J.C.H., and Sinnaeve, J. Results of the second CEC intercomparison of active and passive dosemeters for the measurement of radon and radon decay products. EUR 10403 EN, Commission of the European Communities, Brussels, Belgium, 1986. 64 pp.

9. Miles, J.C.H., and Sinnaeve, J. Results of the third CEC intercomparison of active and passive detectors for the measurement of radon and radon decay products. EUR 11882 EN, Commission of the European Communities, Brussels, Belgium, 1988. 80 pp.

10. Ulbak, K., Stenum, B., Sørensen, A., Majborn, B., Bøtter-Jensen, L., and Nielsen, S.P. Results from the Danish indoor radiation survey, Radiat. Prot. Dosim. 24: 401, 1988.

11. Arvela, H., Voutilainen, A., Mäkeläinen, I, Castren, O., and Winqvist, K. Comparison of predicted and measured variations of indoor radon concentration. Radiat. Prot. Dosim. 24:231, 1988.

DYNAMIC MULTI-COMPARTMENT MODELLING: THE TRANSPORT OF RADON AND ITS DECAY PRODUCTS INDOORS

by: Craig P. Wray, P.Eng. and
Grenville K. Yuill, Ph.D., P.Eng.
G.K. Yuill and Associates Ltd.
Winnipeg, Manitoba R3T 2C4

ABSTRACT

A microcomputer program has been developed so systematic radon and radon progeny control techniques of optimal effectiveness can be formulated for designing or retrofitting houses. An existing multizone airflow/contaminant dispersal analysis computer program was modified by adding a model of radon progeny plate-out on indoor surfaces.

Three simulation exercises of radon and radon progeny levels in the rooms of a hypothetical house for two different HVAC systems were carried out using the new program. Comparisons of these parameters were made with those for the same house with only natural ventilation. The simulations showed that significant differences in average radon levels and total EEDCs can occur between rooms of a house. These differences demonstrate the need for a multizone model and indicate caution should be used in applying radon and radon progeny level measurements taken in one room to any other room in a house. The simulation exercises also showed that radon and radon progeny levels in a house strongly depend on the type of ventilation system in the house.

INTRODUCTION

In a large fraction of Canadian houses, radon concentrations indoors are significantly higher than those outdoors. These elevated levels can compromise the health of occupants who are exposed to them over long periods of time. Although several mitigation techniques have been used recently to reduce these concentrations to acceptable levels, the reasons for their effectiveness are not well understood, and no systematic approach has been established for implementing an appropriate procedure in each situation.

The behavior of radon and its progeny in houses is too complex to predict without simulation. Although field monitoring could be used to study radon and radon progeny transport, this approach is prohibitively expensive if even a few common combinations of house geometry, ventilation system types, and soil characteristics are to be examined.

As a step towards the improvement of existing mitigation techniques and the formulation of mitigation strategies, it is desirable to synthesize previous research about radon and radon progeny transport with current multizone modelling techniques to produce a model that can predict the accumulation of these pollutants in a house on a time-varying basis. In the work described here, an existing multizone airflow/pollutant analysis microcomputer program was modified. Parametric studies using the modified program (CONAIR 89-2) can be carried out in the future to gain a better understanding of radon transport, so systematic radon and radon progeny control techniques of optimal effectiveness can be developed for new and existing houses.

CONAIR 89-1: AN EXISTING SIMULATION TOOL

CONAIR 89-1 is an existing multizone airflow/contaminant dispersal network analysis microcomputer program that has most, but not all, of the capabilities required for the work described here. It was developed by G.K. Yuill and Associates Ltd. using two computer programs (AIRNET and CONTAM 87) obtained from the U.S. National Bureau of Standards as its core (1). CONAIR 89-1 begins by modelling airflows between zones and between indoors and outdoors in a multizone building. It simulates wind and stack effects on envelope leaks, friction in ducts, fan characteristics and two-way buoyancy-driven flow through large openings such as doors. Calculations are done using hourly mass-balances on a macroscopic basis assuming well-mixed zones. Recirculation within a single room is not simulated. Steady-state calculations are done for each set of hourly operating conditions supplied, such as weather data, fan settings, or damper settings. The program ignores subhourly pressure transients, because their time constants are typically too short to be of significance in this kind of calculation.

CONAIR 89-1 also has the capability to model pollutant concentrations. This part of the program uses the airflows determined in the first part, along with source strengths and reaction and decay rates for the various pollutants present, to predict the pollutant concentrations in each zone. The program does a steady-state analysis, but can also do a dynamic analysis to predict time-varying concentrations.

RADON DAUGHTER PLATE-OUT MODEL

CONAIR 89-1 assumes all pollutants are airborne and thus are subject to transport in ventilation airflows. However, this assumption is inappropriate for some pollutants such as radon progeny (^{218}Po, ^{214}Pb, and ^{214}Bi), which plate-out on surfaces within a house such as walls or furniture. With the exception of ^{218}Po, once these progeny are deposited on these surfaces, they do not produce significant numbers of progeny that return to the air where they can be transported from room to room or from indoors to outdoors. Thus, surface-deposited ^{214}Pb and ^{214}Bi remain trapped in the particular room in which they plated-out. The concentrations of these two surface-deposited radon daughters are of no significance from a health standpoint therefore, because they cannot be inhaled once they plate-out. However, ^{214}Pb formed from decaying surface-deposited ^{218}Po can return to the air through a recoil mechanism, so CONAIR 89-1 needed upgrading to model surface-deposition of ^{218}Po with recoil.

CONAIR 89-1 uses air and pollutant mass-balances to determine the mass transport rate of up to eight different species through simple flow elements with or without filters. The flow through an element is assumed to be instantaneous and well-mixed. Axley (2) defines the transport of a pollutant species α between two nodes by flow element equations from node i to node j due to an air mass flow rate $w^e(t)$ as follows:

$$ {}^{\alpha}w_i^e = w^e(t)\,{}^{\alpha}C_i \qquad (1) $$

$$ {}^{\alpha}w_j^e = w^e(t)({}^{\alpha}\eta - 1)\,{}^{\alpha}C_j \qquad (2) $$

where

- ${}^{\alpha}w_i^e$ = mass transport rate of species α from node i through element e, nuclei/h.
- ${}^{\alpha}w_j^e$ = mass transport rate of species α from node j through element e, nuclei/h.
- $w^e(t)$ = air mass flow rate from node i to node j through element e as a function of time t, g_{air}/h.
- ${}^{\alpha}\eta$ = fraction of species α removed by filter in element e, d'less.
- ${}^{\alpha}C_i$ = concentration of species α at node i, nuclei/g_{air}.
- ${}^{\alpha}C_j$ = concentration of species α at node j, nuclei/g_{air}.

Since CONAIR 89-1 assumes all species are airborne, equations 1 and 2 state that all species are transported into element e where they can be removed to some degree by a filter. Thus, to account for surface-deposition of a particular species at a node, it is necessary to eliminate the mass transport of that species into element e. This blocking of airborne transport in CONAIR 89-2 was achieved by defining a surface-deposition coefficient $\propto s$ that affects the species mass transport rates as follows:

$$\propto w_i^e = w^e(t)(\propto s)\propto C_i \quad (3)$$

$$\propto w_j^e = w^e(t)(\propto \eta - 1)(\propto s)\propto C_j \quad (4)$$

For airborne transport of a particular species, $\propto s$ is set to unity, so it has no effect on the mass transport rate of that species. For a particular species that is surface-deposited, $\propto s$ is set to zero, so the mass transport by ventilation of that species through all flow elements connecting every node is eliminated.

The nature of each pollutant (airborne or surface-deposited) is identified in the CONAIR 89-2 contaminant input file by specifying the pollutant type as either type "A" (airborne, $\propto s = 1.0$) or type "S" (surface-deposited, $\propto s = 0.0$).

INPUT PARAMETERS FOR THE RADON AND RADON PROGENY MODEL

RADON AND RADON PROGENY KINETICS

In the Jacobi model (3), the sources of radon in the indoor air are the entry of radon in soil gas infiltrating into the basement through foundation penetrations and in the outdoor air infiltrating through above-grade leaks in the building envelope. The removal of radon and the removal and production of radon progeny in the Jacobi model by radioactive decay, attachment, deposition, and recoil can be described by a set of linear first-order differential equations for each room. CONAIR 89-1 already has the capability to model these processes (2), with the exception of surface-deposition that involves recoil. Therefore, it was only necessary to define the differential equations and to select a value for each of the rate constants in these equations for each room.

The Jacobi model can be simplified for the purposes of this project. There is no need to determine the concentrations of surface-deposited ^{214}Pb or ^{214}Bi, because these species do not pose a health risk once they are removed from the air by the plate-out process. The probability they will produce recoiling atoms once deposited is negligible. This leaves eight species to consider: airborne-unattached ^{222}Rn (URn2), airborne-unattached ^{218}Po (UPo8), airborne-unattached ^{214}Pb (UPb4), airborne-unattached ^{214}Bi (UBi4), airborne-attached ^{218}Po (APo8), airborne-attached ^{214}Pb (APb4), airborne-attached ^{214}Bi (ABi4), and surface-deposited ^{218}Po (SPo8).

The differential equations describing the radon and radon progeny kinetics indoors (excluding ventilation) for any given room are:

$$\frac{d[URn2]}{dt} = -\lambda_o [URn2] \quad (5)$$

$$\frac{d[UPo8]}{dt} = \lambda_o [URn2] - (\lambda_a + \lambda_d^u + \lambda_1) [UPo8] \quad (6)$$

$$\frac{d[UPb4]}{dt} = \lambda_1 [UPo8] - (\lambda_a + \lambda_d^u + \lambda_2) [UPb4] + P_1 \lambda_1 [APo8] + P_o \lambda_1 [SPo8] \quad (7)$$

$$\frac{d[UBi4]}{dt} = \lambda_2 [UPb4] - (\lambda_a + \lambda_d^u + \lambda_3) [UBi4] \quad (8)$$

$$\frac{d[APo8]}{dt} = \lambda_a [UPo8] - (\lambda_1 + \lambda_d^a) [APo8] \quad (9)$$

$$\frac{d[APb4]}{dt} = (1 - P_1) \lambda_1 [APo8] + \lambda_a [UPb4] - (\lambda_d^a + \lambda_2) [APb4] \quad (10)$$

$$\frac{d[ABi4]}{dt} = \lambda_2 [APb4] + \lambda_a [UBi4] - (\lambda_d^a + \lambda_3) [ABi4] \quad (11)$$

$$\frac{d[SPo8]}{dt} = \lambda_d^u [UPo8] + \lambda_d^a [APo8] - \lambda_1 [SPo8] \quad (12)$$

where

λ_o = radioactive decay constant of ^{222}Rn, h^{-1}.

λ_1 = radioactive decay constant of ^{218}Po, h^{-1}.

λ_2 = radioactive decay constant of ^{214}Pb, h^{-1}.

λ_3 = radioactive decay constant of ^{214}Bi, h^{-1}.

λ_a = attachment rate of free species onto aerosols, h^{-1}.

λ_d^u = surface-deposition rate of unattached species, h^{-1}.

λ_d^a = surface-deposition rate of species attached to aerosols, h^{-1}.

P_1 = recoil probability of ^{214}Pb from aerosols, d'less.

P_o = recoil probability of ^{214}Pb from surfaces in the room, d'less.

[X] = concentration of species X in the room, nuclei/g_{air}.

Based on the eight differential equations listed here, a set of five key parameters that characterizes radon and radon progeny kinetics must be specified in CONAIR 89-2 for each room. These parameters are: the attachment rate, the unattached species deposition rate, the attached species deposition rate, the recoil probability of ^{214}Pb from aerosols, and the recoil probability of ^{214}Pb from room surfaces.

SELECTION OF INPUT PARAMETER VALUES

The radioactive transmutation coefficients (λ_0, λ_1, λ_2, and λ_3) used in the Jacobi model are not unique to each room. Instead, they are physical constants related to the isotope half-lives.

Porstendörfer (4,5), Bruno (6), and Nazaroff and Nero (7) report that the attachment rate of radon progeny onto aerosols can vary widely indoors (4 to 2000 h^{-1}). The attachment rate strongly depends on the aerosol size distribution and aerosol concentration. Maximum attachment rates correspond to particle sizes in the range of 0.1 to 0.2 μm (7) and to high aerosol concentrations. These concentrations vary from 2 to 500,000 particles/cm^3 depending on the amount of cooking and smoking and on the effectiveness of air filtration systems, if any are used. Cooking and smoking can increase aerosol concentrations indoors by two to three orders of magnitude (7), which in some cases can result in significant variations in attachment rates from room to room in a house.

An attachment rate of 50 h^{-1} was used indoors. This rate was selected from values listed in the literature for clean air (approximately 10,000 to 20,000 aerosol particles/cm^3). Unfortunately, reported attachment rates tend to list only the corresponding aerosol concentration, but not the particle size distributions, so it is difficult to determine a typical value for typical conditions. The attachment rate used here was assumed to be constant everywhere in the house for simplicity in demonstrating the new models. An attachment rate of 40 h^{-1} was used outdoors based on Jacobi (3). This lower rate recognizes that although the aerosol concentrations outdoors usually are higher than those indoors when there is no cooking or smoking (7), these activities generally would be expected to result in higher average aerosol concentrations indoors.

CONAIR 89-2, which implements the modified flow element equations described earlier, can model the surface-deposition of radon-daughters by specifying the unattached and attached species deposition rates. The deposition rate of a particular unattached species in a specific room is dependent on the area of exposed surfaces in that room, on the volume of that room, and on the deposition velocity of the particular species as follows:

$$\lambda_d^u = \nu_d^u S F/V \qquad (13)$$

where

λ_d^u = surface deposition rate of unattached species in a given room, h^{-1}.

ν_d^u = average deposition velocity of free (unattached) species in the room, m/h.

S = total area of enclosure surfaces in the room exposed to air (including walls, doors, windows, floors, and ceilings, but excluding other surfaces such as furniture), m^2.

F = correction factor to account for additional exposed area of furniture or other surfaces in the room, d'less.

V = volume of air in the room, m^3.

This rate expression assumes all surfaces exposed to air in a given room are equally effective in removing any radon daughter through the use of an average deposition velocity that is the same for all radon progeny. Although an analogous equation can be applied to attached species, this was not done because the deposition velocities of attached species are usually much smaller than those for unattached species. Nazaroff and Nero (7) report that the ratio of unattached to attached deposition velocities is approximately 100.

Deposition velocities are strongly influenced by air motion. Equation 13 assumes there is sufficient air motion in each room so the radon progeny concentration in the room is uniform. However, most deposition velocities found in the literature are not accompanied by quantitative descriptions of the air movement conditions during the deposition velocity experiments. Bruno (6) reports a deposition velocity for unattached ^{218}Po in still air of 0.54 m/h, which is not typical of real houses. He also reports that the deposition velocity for unattached ^{218}Po in rooms with low ventilation is 7 m/h and with moderate ventilation is 22 m/h. Bigu (8) lists values of 2-19 m/h for a 26 m^3 chamber equipped with a circulating fan. The higher value corresponds to operation of the fan, while the lower value corresponds to periods when the fan was off. The circulation rate of the fan is not provided by Bigu. Scott (9) reports unattached deposition velocities in the range of 3.6 to 18 m/h, with the higher values corresponding to higher ventilation rates.

Unattached deposition velocities of 8 m/h in rooms and 20 m/h in ducts were assumed. The value for rooms was selected as an average value (7). The value for ducting was selected in recognition of their high airflow rates. This value may be an underestimate, since it is based on maximum room deposition velocities, but there does not appear to be any literature available on radon progeny deposition rates in ducting.

Room surface areas and volumes as required for equation 13 were estimated from building plans. A correction factor of 2.5 (10) was applied to increase the surface area exposed to air in each room, except in hallways where furnishings tend to be sparse. A factor of 1.0 was used in hallways. Porstendörfer (10) does not quantify room or furnishing surface areas, so these factors are somewhat arbitrary. The deposition rate for attached progeny in a given room was assumed to be 1/100 of the unattached deposition rate in that room.

The unattached deposition velocity outdoors was assumed to be 17 m/h so the outdoor equilibrium fraction would be 0.56 (7). Therefore, the outdoor value has little direct basis on real conditions. It is assumed all deposition rates described here are constant over time for simplicity in demonstrating the new models.

The literature reviewed here does not differentiate between radon progeny when specifying deposition rates or attachment rates, so the Jacobi model described here assumes the same attachment rate or the same deposition rate can be applied to each of the three radon progeny considered. Research should be carried out in a future project to determine the impact of this assumption on CONAIR's predictions of radon progeny concentrations.

When atoms of attached or surface-deposited ^{218}Po decay, a fraction of the ^{214}Pb atoms produced can become detached and move into the room air. The recoil probability describes the chance this process will occur for any given atom. The maximum probability is 1.0. In this case, all of these ^{214}Pb atoms are released into the room air. The recoil probability depends on whether the ^{218}Po is attached to an aerosol or to a surface in the room.

For ^{218}Po attached to aerosols, a range of ^{214}Pb recoil probabilities from 0.4 to 0.83 has been reported (11, 12). The higher recoil probabilities are expected to correspond with smaller aerosol sizes (12). Field investigations to determine this recoil probability in the real house were beyond the scope of this project, so a typical indoor value of 0.5 (3, 5) was assumed for the case considered here.

A different recoil probability of 0.83 was used outdoors for ^{214}Pb produced by ^{218}Po attached to aerosols. This value was selected so the outdoor equilibrium fraction would be 0.56 (7).

For surface-deposited ^{218}Po, ^{214}Pb recoil probabilities tend to be lower. Due to the presence of a laminar boundary layer on indoor surfaces, it is unlikely all recoiling ^{214}Pb atoms will escape into the room air. Instead, a significant fraction (as much as 50%, (6)) will escape into the boundary layer, from which they will redeposit on the surface they escaped from. Typically, this recoil probability is estimated to be 0.25 (7, 13). For lack of any other evidence, this typical value has been used indoors and outdoors in the case considered here.

EXAMPLE ANALYSES USING CONAIR 89-2

INTRODUCTION

Three simulation exercises were carried out using CONAIR 89-2. The purpose of these exercises was to demonstrate the capabilities of the modified program through analyses of the radon levels and EEDCs in the rooms of a hypothetical house for two different HVAC systems, and through comparisons of these parameters with those for the same house with only natural ventilation. Hypothetical soil properties and radon progeny transport phenomena characteristics used in these simulations were based on ranges of values cited in the literature and not on field trials, because the purpose of these simulations did not justify the expense of an intensive measurement effort to determine these values.

NATURALLY-VENTILATED HOUSE DESCRIPTION

A hypothetical house based on a real single-storey house located in a suburban area of Winnipeg, Manitoba was simulated. The house has an Equivalent Leakage Area (ELA) of 1540 cm^2. The total surface area indoors exposed to air (subject to radon progeny plate-out) is 1769 m^2, including furnishings. The house was divided into the following eight zones: basement; kitchen/dining room/living room; hallway joining living room, bathroom, and bedrooms; bathroom (sink area); bathroom (tub area); master bedroom; bedroom 2; and bedroom 3. The kitchen, living room, and dining room were lumped together as one zone because there are no significant flow resistances between these regions.

Using the total ELA of the house and assumptions of leakage area distributions, inputs were developed for CONAIR 89-2 to characterize the magnitude and location of unintentional leaks in the building envelope. The only leaks considered between zones were interior doorways, which were simulated as if the doors were wide open.

The soil surrounding the hypothetical house was a wet sandy silt, with coarse sand backfill around the walls and beneath the floor slab. The total ELA of the combination of soil leakage and the 5 mm wide crack at the wall-floor interface was 4 cm^2 or 0.26% of the total ELA of the house.

The hypothetical house is heated electrically with baseboard heaters and has no mechanical ventilation system. All windows and exterior doors were simulated in their closed position, so the only source of ventilation in the house was natural infiltration and exfiltration driven by wind and stack effects through leaks in the house envelope.

HRV-VENTILATED HOUSE DESCRIPTION

A second hypothetical house was simulated with characteristics identical to those described for the naturally-ventilated house, but with two changes. The baseboard heating system was replaced with a central electric forced-air furnace, and a balanced heat recovery ventilator (HRV) system was added. The supply airflow rates from the furnace to each zone were sized to meet the same design heating load as the baseboard heaters. Return airflows for each zone were also specified. Indoor air was exhausted continuously through the HRV from the kitchen/dining room/living room area at a rate of 30.6 L/s and from the bathroom tub area at a rate of 14.2 L/s.

An extra zone was simulated in this case to represent the estimated combined volume of the added ducting and furnace (5 m^3). The surface area of these components exposed to the air was estimated to be 60 m^2. The plate-out and attachment rates for the combined ducting and furnace were described earlier, along with appropriate ^{214}Pb recoil probabilities.

LAFSW-VENTILATED HOUSE DESCRIPTION

A third hypothetical house was simulated with characteristics identical to those described for the naturally-ventilated house, but with two changes. An LAFSW system with damper-controlled air inlets on the windows in the living room and in the three bedrooms (14) was added, along with a central exhaust fan in the basement. The central exhaust fan was connected through short pieces of ducting to the kitchen/dining room/living room area and to the bathroom tub area. Exhaust airflow rates identical to those of the HRV were specified.

Each air inlet had an ELA of 23.6 cm^2 with the damper in the fully-open position. These inlets were controlled on a diurnal schedule corresponding to normal residential activity. From 8 a.m. to 11 p.m., the air inlets in the living room were fully open, while those in the bedrooms were fully closed. From 11 p.m. to 8 a.m. when people would occupy the bedrooms, the air inlets in the bedrooms were fully open, while those in the living room were fully closed.

WEATHER DATA AND OUTDOOR CONCENTRATIONS

The three simulations were carried out using hourly Winnipeg weather data from a four-day period in August 1981. In all cases, every indoor zone had a constant temperature of 21° C. The average outdoor dry-bulb temperature during this period was 20.3° C. The average wind speed was 3.3 km/h. Real wind direction data were not available, so the wind was simulated by rotating it around the house on a 59 hour cycle.

The infiltration of radon in outdoor air can be a significant contribution to typical indoor levels, even though it is negligible at higher indoor levels. Radon concentrations in outdoor air are usually in the range of 0.1 to 0.4 pCi/L (7). A typical value of 0.2 pCi/L (15) was assumed for the cases simulated in this project. A constant equilibrium fraction of 0.56 was assumed outdoors (7). The total EEDC outdoors based on this equilibrium fraction was 0.11 pCi/L.

SIMULATION RESULTS AND ANALYSES

Tables 1 through 3 summarize the CONAIR 89-2 predictions of radon and radon progeny concentrations by listing zonal and whole-house average radon levels, unattached EEDCs, attached EEDCs, total EEDCs, and equilibrium fractions for the three cases considered here. Whole-house averages were calculated as the sum of the zonal averages, weighted by the fraction of the total volume of the house in each zone. To understand how the two different ventilation systems affect radon and radon progeny concentrations in different areas of the house, consider the basement, living room and one bedroom

(Bedroom 2) separately. Bedroom 2 was selected for illustration purposes, but either of the other two bedrooms could have been used instead, since all three bedrooms have similar radon and radon progeny levels.

A particularly interesting set of comparisons is that of the living room to basement average radon concentration and total EEDC ratios. These ratios provide an insight into the inaccuracies that can result from measuring the radon level or total EEDC in one region of the house such as the basement and attempting to apply the same results to other regions of the house, such as the living room.

For the naturally-ventilated house the average radon level in the living room was only 50% of that in the basement, while the average total EEDC in the living room was 48% of that in the basement. The average radon level and the average total EEDC in the living room of the HRV-ventilated house were closer to those in the basement (ratios of 68% and 71% respectively) than in the naturally-ventilated house. These reduced differences between the living room and basement averages were due to the effects of air mixing caused by the furnace air-handling system in the house with the HRV. Table 2 shows this mixing effect in particular through the lack of variation in main floor average zonal radon level and total EEDC predictions. For the house equipped with the LAFSW system, the average radon level and the average total EEDC in the living room were further from those in the basement (ratios of 37% and 37% each) than in the naturally-ventilated house. The LAFSW system was intentionally designed to have this effect. By providing outdoor air specifically only to occupied regions that require ventilation, the LAFSW system saves the energy an HRV system wastes by not ventilating the entire house when all of the house is not occupied.

These observations indicate that significant differences in average radon levels and total EEDCs could occur between basements and living rooms, so caution should be exercised in applying measured radon level or total EEDC data from one region to another.

The advantage of the LAFSW system in providing local ventilation is emphasized by the average radon levels and total EEDCs in the bedrooms. In bedroom 2 of the LAFSW-ventilated house, the average radon level was slightly below that outdoors (0.20 pCi/L) because of the combined effects of direct ventilation with only outdoor air and the radioactive decay process. The HRV-ventilated bedroom had a lower average radon level (0.34 pCi/L) than that in the naturally-ventilated bedroom (0.71 pCi/L), but it was higher than that for the LAFSW-ventilated bedroom due to mixing with other regions of the house caused by the furnace air-handling system. Bedroom 2 of the LAFSW-ventilated house had an average total EEDC of 0.08 pCi/L, which was lower than that outdoors (0.11 pCi/L) due to the combined effects of direct ventilation with only outdoor air, radioactive decay, and plate-out in the bedroom. As for the average radon level, the HRV system lowered the average total EEDC in bedroom 2 slightly to 0.14 pCi/L compared with 0.26 pCi/L in the naturally-ventilated house. However, due to the effects of mixing with other regions of the house caused by the furnace air-handling system, the HRV-ventilated house could not achieve a reduction in bedroom average total EEDC to below the outdoor level.

Since people normally spend a large fraction of their time at home sleeping in their bedrooms, these results indicate that local ventilation provided by the LAFSW system in these bedrooms could significantly reduce the total long-term exposure of occupants to radon progeny.

CONCLUSIONS

CONAIR 89-2, which is based on an existing computer program, was developed so it could simulate the accumulation of radon and its progeny within houses. A radon progeny plate-out model was implemented in the program and a set of typical coefficients describing radon progeny kinetics was suggested for a hypothetical house.

Three simulations of different ventilation strategies were carried out using CONAIR 89-2. Average radon levels and total EEDCs in several rooms of the naturally-ventilated hypothetical house with baseboard heat were compared with those of a similar house equipped with a furnace/HRV system and with those in one having a baseboard-heat/LAFSW system. There were significant differences in average radon levels and total EEDCs between rooms of the house, which demonstrated the importance of using a multizone model instead of a single-zone model to predict radon and radon progeny levels indoors. These differences also indicate caution should be exercised in extrapolating radon and radon progeny level measurements taken in one room to any other room in a house.

The simulations predicted that the baseboard-heat/LAFSW system can control radon levels in the bedrooms better than the furnace/HRV system. Since the average radon levels and total EEDCs in the bedrooms ventilated using the LAFSW system were below those outdoors, and since people normally spend a large fraction of their time at home sleeping in these bedrooms, it appears that the LAFSW system could significantly reduce the risk of lung cancer.

ACKNOWLEDGEMENTS

This project was carried out with the support of National Research Council Canada, Energy, Mines and Resources Canada, the Canada Mortgage and Housing Corporation, and Manitoba Hydro. We gratefully acknowledge the contributions of George Walton of the U.S. National Institute of Standards and Technology and Jim Axley of the Massachusetts Institute of Technology. The use of their programs (AIRNET and CONTAM 87) in CONAIR 89-2 greatly facilitated program development. The work described in this paper was not funded by the U.S. Environmental Protection Agency and therefore the contents do not necessarily reflect the views of the agency and no official endorsement should be inferred.

REFERENCES

1. Yuill, G.K. and Wray, C.P. A microcomputer program for evaluating the performance of buildings equipped with ventilator window/baseboard heating systems. In: Proceedings of the 1989 Annual SESCI Conference, Penticton, 1989.

2. Axley, J. Progress toward a general analytical method for predicting indoor air pollution in buildings - Indoor air quality modelling: Phase III report. U.S. National Bureau of Standards to U.S. EPA, NBSIR 88-3814, July 1988.

3. Jacobi, W. Activity and potential α-energy of ^{222}radon- and ^{220}radon-daughters in different air atmospheres. Health Physics. 22(May): 441-450, 1972.

4. Porstendörfer, J., Wicke, A., and Schraub, A. The influence of exhalation, ventilation and deposition processes upon the concentration of radon (^{222}Radon), thoron (^{220}Radon) and their decay products in room air. Health Physics. 34(May): 465-473, 1978.

5. Porstendörfer, J. Indoor radon exposure in the Federal Republic of Germany. In: Proceedings of the Second Air Pollution Control Association Specialty Conference: Indoor Radon II, 1987. pp. 57-67.

6. Bruno, R.C. Sources of indoor radon in houses: A review. Journal of the Air Pollution Control Association. 33:(2, February): 105-109, 1983.

7. Nazaroff, W.W. and Nero, A.V. Jr. Radon and its decay products indoors. New York: John Wiley and Sons, 1988.

8. Bigu, J. Radon daughter and thoron daughter deposition velocity and unattached fractions under laboratory-controlled conditions and in underground uranium mines. Journal of Aerosol Science. 16(2): 157-165, 1985.

9. Scott, A.G. Radon daughter deposition velocities estimated from field measurements. Health Physics. 45(2): 481-485, 1983.

10. Porstendörfer, J. Behavior of radon daughter products in indoor air. Radiation Protection Dosimetry. 7(1-4):107-113, 1984.

11. Kruger, J. and Nöthling, J.F. A comparison of the attachment of the decay products of radon-220 and radon-222 to monodisperse aerosols. Journal of Aerosol Science. 10: 571, 1979.

12. Mercer, T.T. The effect of particle size on the escape of recoiling RaB atoms from particulate surfaces. Health Physics. 31: 173-175, 1976.

13. Shimo, M., Asano, Y., Hayashi, K., and Ikebe, Y. On some properties of ^{222}Rn short-lived decay products in air. Health Physics. 48(1): 75-86, 1985

14. Yuill, G.K. and Comeau, G.M. Demonstration and performance testing of the laminar airflow super window - humidity controlled air inlet - baseboard heating (LAFSW/HCAI/BH) system in a Winnipeg house. In: Proceedings of the 1989 Annual SESCI Conference, Penticton, 1989.

15. Bodansky, D., Robkin, M.A., and Stadler, D.R. Indoor radon and its hazards. Seattle: University of Washington Press, 1989.

TABLE 1
Summary of Average Radon Levels, EEDCs, and Equilibrium Fractions: Natural Ventilation

Volume (m^3)	Zone Name	Rn222 (pCi/L)	EEDCu (pCi/L)	EEDCa (pCi/L)	EEDCt (pCi/L)	Equil Frac
206 83	Basement	1 59	0 03	0 75	0 78	0 49
135 07	Living Room	0 80	0 02	0 36	0 37	0 47
7 80	Hallway	0 81	0 02	0 38	0 40	0 49
19 51	Bedroom 3	0 73	0 01	0 27	0 28	0 38
7 93	Bath (Sink)	0 00	0 00	0 00	0 00	0 29
5 42	Bath (Tub)	0 00	0 00	0 00	0 00	0 29
39 72	Master Bedroom	0 72	0 01	0 29	0 30	0 42
23 20	Bedroom 2	0 71	0 01	0 25	0 26	0 37
	Outdoors	0 20	0 01	0 11	0 11	0 56
	Soil	304 59	0 00	0 00	0 00	0 00
Total	Whole-house					
446 48	Avg Conc	1 13	0 02	0 50	0 52	0 46

TABLE 2
Summary of Average Radon Levels, EEDCs, and Equilibrium Fractions: HRV System

Volume (m^3)	Zone Name	Rn222 (pCi/L)	EEDCu (pCi/L)	EEDCa (pCi/L)	EEDCt (pCi/L)	Equil Frac
206 83	Basement	0 50	0 01	0 21	0 22	0 44
135 07	Living Room	0 35	0 01	0 15	0 16	0 45
7 80	Hallway	0 34	0 01	0 15	0 15	0 47
19 51	Bedroom 3	0 34	0 01	0 13	0 14	0 41
7 93	Bath (Sink)	0 34	0 01	0 13	0 14	0 41
5 42	Bath (Tub)	0 34	0 01	0 13	0 13	0 38
39 72	Master Bedroom	0 34	0 01	0 14	0 15	0 43
23 20	Bedroom 2	0 34	0 01	0 13	0 14	0 40
	Outdoors	0 20	0 01	0 11	0 11	0 56
	Furnace	0 34	0 00	0 15	0 15	0 43
	Soil	304 58	0 00	0 00	0 00	0 00
Total	Whole-house					
446 48	Avg Conc	0 42	0 01	0 17	0 17	0 42

TABLE 3
Summary of Average Radon Levels, EEDCs, and Equilibrium Fractions: LAFSW System

Volume (m^3)	Zone Name	Rn222 (pCi/L)	EEDCu (pCi/L)	EEDCa (pCi/L)	EEDCt (pCi/L)	Equil Frac
206 83	Basement	1 23	0 03	0 56	0 59	0 48
135 07	Living Room	0 45	0 01	0 21	0 22	0 48
7 80	Hallway	0 30	0 01	0 13	0 14	0 47
19 51	Bedroom 3	0 20	0 00	0 08	0 08	0 41
7 93	Bath (Sink)	0 30	0 01	0 12	0 13	0 42
5 42	Bath (Tub)	0 30	0 00	0 11	0 12	0 40
39 72	Master Bedroom	0 20	0 00	0 08	0 09	0 44
23 20	Bedroom 2	0 20	0 00	0 07	0 08	0 40
	Outdoors	0 20	0 01	0 11	0 11	0 56
	Soil	193 72	0 00	0 00	0 00	0 00
Total	Whole-house					
446 48	Avg Conc	0 76	0 02	0 34	0 36	0 47

A DATA ACQUISITION SYSTEM FOR MONITORING RADON ENTRY AND DISTRIBUTION

R.P. Sieber
Graduate student
Department of Mechanical Engineering
University of Saskatchewan
Saskatoon, Sk., Canada, S7N OWO

D.A. Figley
Research officer
Prairie Regional Station
Institute for Research in Construction
National Research Council of Canada
Saskatoon, Sk., Canada, S7N OW9

R.W. Besant
Head
Department of Mechanical Engineering
University of Saskatchewan
Saskatoon, Sk., Canada, S7N OWO

G.J. Schoenau
Professor
Department of Mechanical Engineering
University of Saskatchewan
Saskatoon, Sk., Canada, S7N OWO

ABSTRACT

This paper describes the development of a micro-computer based Radon Data Acquisition System (RDAS) for monitoring the entry and distribution of radon gas in houses. The information obtained will be valuable for the evaluation of control measures used to reduce radon concentrations to acceptable levels.

There are many proposed control measures for reducing radon levels. However, these methods are not always reliable since they do not accurately account for uncontrolled interacting factors. Some of these factors include interzonal and building air leakage, ventilation rate, pressure and temperature gradients, radon concentrations in soil gas, and environmental factors such as wind and relative humidity. The RDAS simultaneously measures pressure, temperature, and radon gas concentration at several points. In addition, the RDAS characterizes the interzonal air exchange rate using tracer gas techniques. Radon is measured with semiconductor sensors capable of measuring concentrations continually over a period of time; the output is transmitted to the data logger. Careful design of an experimental protocol will account for other uncontrolled factors.

INTRODUCTION

The presence of elevated radon gas concentrations in residential housing can lead to serious health problems for the occupants if they are exposed over an extended period of time. Some control measures for minimizing radon concentration levels include increased ventilation, sub slab depressurization using externally vented fans, and sealing potential leakage passages (1-2). Typically, evaluation of these control measures have been limited to a before/after air sample analysis and are unlikely to account for temporal variations in the environment or building factors. Conclusions drawn from studies of this nature can contain substantial errors. The purpose of this paper is to outline briefly the experimental variables that must be measured to conduct detailed building science based studies on radon and to describe a data acquisition system designed to continuously monitor these variables.

The Institute for Research in Construction (IRC) of the National Research Council of Canada (NRC) is developing a data acquisition system, the RDAS, capable of continuous measurement of experimental parameters necessary to evaluate the effectiveness of radon control measures. The parameters include ventilation rate, indoor/outdoor pressure difference at various surfaces above and below grade, indoor and outdoor air temperature, and radon gas and radon daughter concentrations in the air and soil gas. An important component of this research activity is the development of analytical models that describe the functional relationships between the various parameters. These models will provide a broader understanding of the dynamic processes involved, but they must be validated with well characterized experimental data to be reliable.

The RDAS will allow accurate evaluation of radon characterization in case-control (paired) studies and assist in the development of relationships based on building science principles. This will provide valuable information to guide development of design and construction techniques for buildings.

BUILDING SCIENCE PRINCIPLES

There are many potential sources of radon gas in buildings. One of the most important is the soil surrounding the foundation. To accurately assess radon in buildings, various parameters such as the indoor concentration, ventilation rate, and transportation of radon gas into the space need to be quantified. Considering a well mixed, single zone chamber with an outdoor air supply, indoor and outdoor radon sources and internal space conditioning (Figure 1), a simple mass balance model yields the equation:

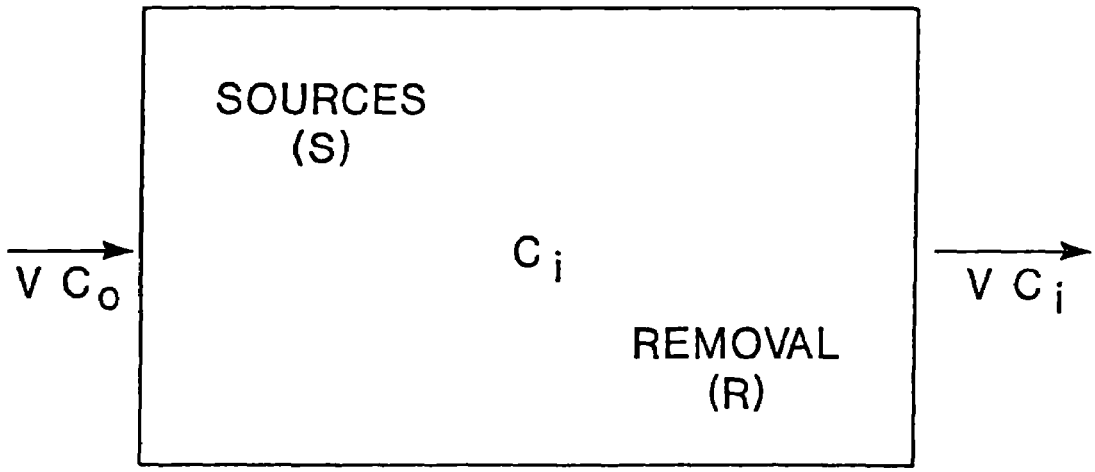

Figure 1. Single zone steady-state mass balance model

$$C_i = C_o + \frac{S - R}{K \cdot V} \qquad (1)$$

where:
- C_i = indoor radon gas concentration (pCi/m^3)
- C_o = outdoor radon gas concentration (pCi/m^3)
- S = indoor radon gas source strength (pCi/s)
- R = radon gas removal rate (pCi/s)
- K = ventilation efficiency
- V = outdoor air exchange rate (m^3/s)

Equation 1 is a simplified expression that can be used to identify the major parameters that must be considered and the impact that changes in the parameters will have on the resulting indoor radon gas concentration. In practice, temporal and spacial variations in these factors must be accurately monitored to avoid errors in analysis. Other potential interacting factors including soil porosity and relative humidity may also effect the radon concentration level. In multi-zoned buildings, data will be required on conditions within individual zones and on communication among zones which add to the complexity of the data acquisition system requirements.

SYSTEM COMPONENTS

A schematic diagram of the RDAS is shown in Figure 2.

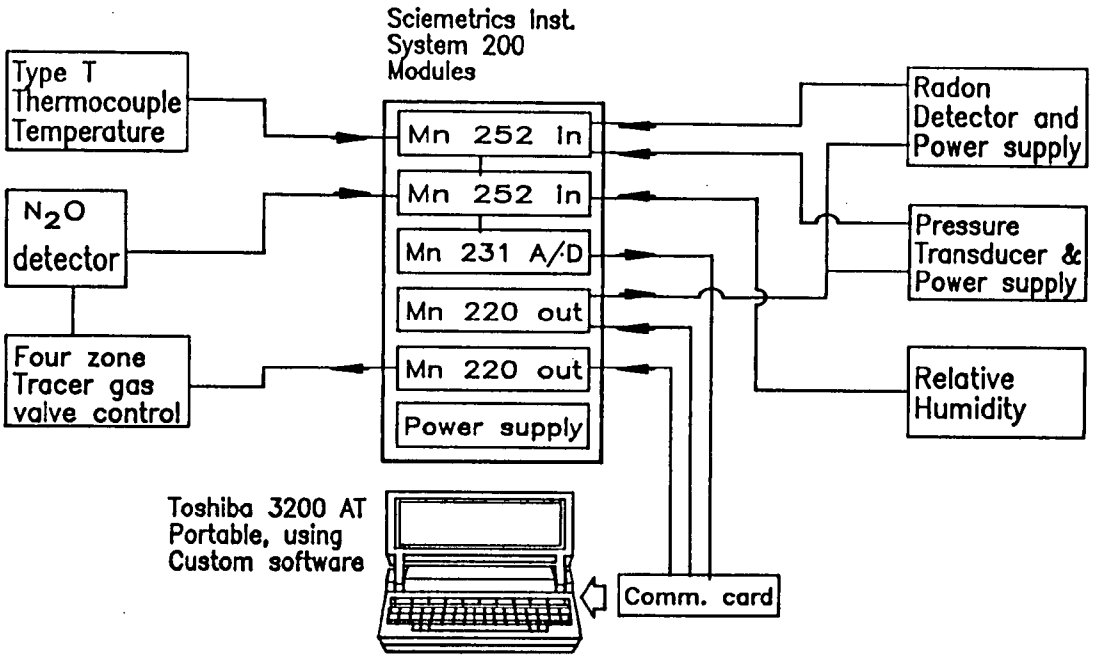

Figure 2. Schematic diagram of RDAS

The system includes a central MS DOS portable computer and a Sciemetrics System 200 data acquisition module. The System 200 is a modular, general purpose, measurement system suited to numerous applications including data acquisition and process control. Included in the RDAS are two model 220 relay cards, a model 231 analog/digital converter, and two model 252 expansion card (32 channels each). Communication between the modules and the personal computer is accomplished with the System 200 I/O module 802 interface card. Customized software is added to set up channel sampling frequency, feedback control and data processing and storage.

The menu driven software allows the RDAS operator flexibility in setting up individual experiments. The number of transducers, gains or calibration coefficients and scan rate can be input from the keyboard to suit the experimental requirements.

The techniques to measure pressure difference across the building envelope surfaces, air ventilation and infiltration in the various internal zones, internal and external temperature distribution, and radon gas concentrations are presented in more detail below.

1) PRESSURE MEASUREMENT

Below grade air infiltration due to lower pressures in basement air compared to surrounding soil gas pressures has been identified as the primary cause of high radon gas levels in houses (1,3). Potential entry points of airborne radon gas include floor and wall cracks, floor drains, and line cracks where the slab and wall intersect (Figure 3). Methods to reduce radon gas infiltration into basements are to eliminate or reduce the flow of soil gas into the basement by sealing entry points or by eliminating the air pressure differences which cause air infiltration into the basement foundation.

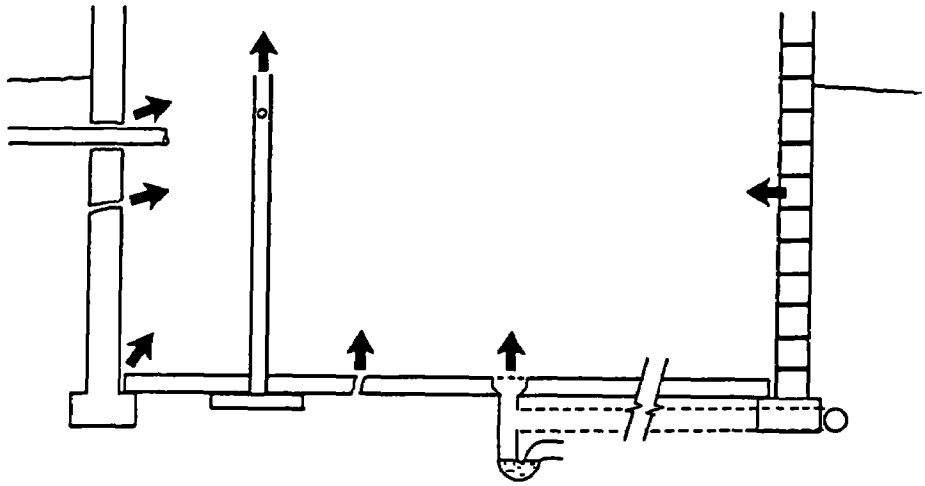

Figure 3. Potential soil gas entry sites

The rate of airflow through an opening such as a crack or a hole is given by:

$$Q = C(\Delta P)^n \qquad (2)$$

where:
- Q = airflow rate (m^3/s)
- C = flow coefficient ($m^3/s \cdot Pa^n$)
- P = pressure difference across opening (Pa)
- n = flow exponent (between 0.5 - 1.0)

The total pressure difference across the opening is the sum of the pressure gradients due to wind, stack, changes in atmospheric pressure, and pressure differences created by the mechanical system. In the case of radon gas in soil, equation 2 can be coupled with the radon concentration in the soil gas to determine the radon source strength due to airflow as:

$$S_p = Q \cdot R \qquad (3)$$

where: S_p = radon source strength due to airflow (pCi/s)
R = radon concentration in the soil gas (pCi/m^3)

For a foundation, the flows and pressure fields are coupled in a complex network as shown in Figure 4. The flow coefficient is more complex than the case of a simple crack or hole. The overall flow resistance is a combination of the flow resistance of the foundation opening, R_f, and the adjacent soil, R_s.

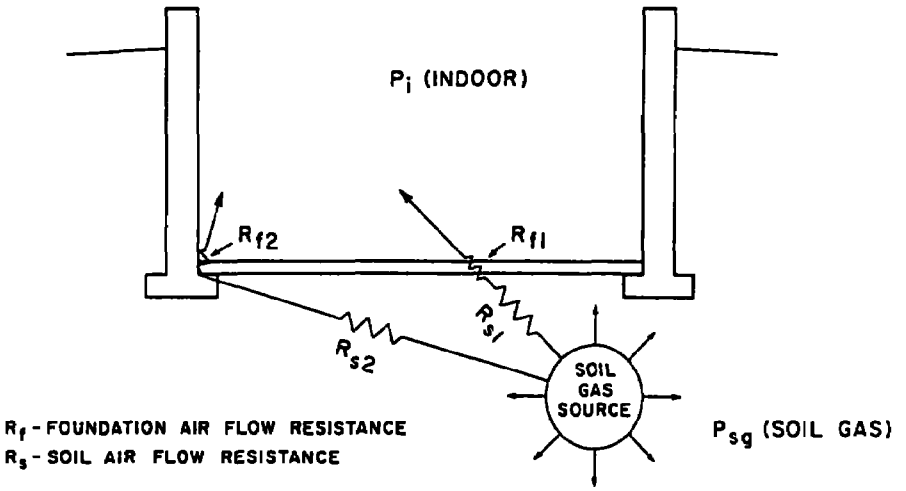

Figure 4. Soil gas and resistor network

For below grade components, the airflow resistance of the soil can cause large time shifts between the atmospheric pressure and the soil gas pressure on the outside of the below grade building envelope. It is necessary to measure the pressure difference across individual building components in order to calculate component specific airflows.

The movement of air and airborne pollutants within a building is driven by pressure gradients. Although the RDAS estimates air movement by tracer gas techniques, the pressure regime inside and outside the building must be measured independently for inputs to the analytical models.

The RDAS can record the output from 10 individual pressure transducers. Modus T10 differential pressure transducers with 0-5 VDC outputs were selected for the system. The range of the transducers is matched to the expected range in pressure to minimize measurement errors. Maximum error is specified as ± 2% of full scale capacity.

2) VENTILATION MEASUREMENT

The total ventilation rate of a building is a combination of infiltration and mechanical ventilation. While techniques exist for estimating or calculating these components, they may not be sufficiently accurate for research purposes. Further, the distribution of the ventilation will directly affect the indoor pollutant concentrations.

Ventilation rates are determined through the use of tracer gas techniques. The tracer gas decay rate is an exponential time function related to ventilation. The tracer decay method consists of an initial injection of tracer into the space followed by recording tracer gas concentrations as a function of time. For a well mixed zone with no sources or sinks, the tracer gas concentration is given by the equation:

$$c(t) = c_o \cdot \exp[-(q/V)t] \qquad (4)$$

where:
- c = tracer concentration
- c_o = initial tracer concentration
- V = space volume (m^3)
- q = outdoor air exchange rate (m^3/hr)
- t = time (hr)

Knowing the effective zone volume and the current and initial tracer concentrations enables the infiltration rate to be determined. The air change rate (air changes/hour) is the ratio of the air exchange rate, q, and space volume, V.

A four zone Air Change per Hour Measuring Apparatus (ACHMA) was designed to evaluate ventilation and air movement within and between zones. N_2O was selected as the tracer gas for estimating ventilation rates. N_2O is easy to measure and suitable for small and medium sized buildings. To estimate air leakage characteristics between zones additional tracer gases (CO_2 and SF_6) can be incorporated into the system.

The requirements for the ACHMA are:

1) Set tracer gas maximum and minimum zone concentrations (0-100 ppm).
2) Discharge N_2O tracer gas into one or a combination of four well mixed zones.
3) Sample in one or a combination of four zones.
4) Return sample to zone or purge outside.

A small amount of N_2O is injected into the zone and the decay in gas concentration is measured as a function of time. Once the tracer concentration has decayed below the minimum allowed concentration, additional tracer can be injected into the zone. This allows for an extended testing period. Proper mixing of air within the zone is essential for unbiased sampling since equation 4 assumes perfect mixing within the zone. The time period selected for the solution of equation 4 must be carefully considered. Initially, following a tracer gas injection, the tracer will not be well mixed. During a test, changes in the air exchange rate can occur which will confuse the analysis if the change

is not recorded within the time step. A shorten time step requires a higher rate of sampling and increases the load on the sampling system. A zone sampling rate of five minutes was selected as the best compromise between system requirements and accuracy of estimation of air exchange rate.

A schematic of the ACHMA is shown in Figure 5. The ACHMA consists of a network of solenoid valves, tubing, an air pump, gas analyzer, and tracer gas source tank equipped with a pressure regulator. The N_2O analyzer is a Beckman Model 865 infrared gas analyzer with a span of 0 to 100 ± 1 ppm (0-100mVDC output). Rotameters are used to monitor and control flow since only approximate flow rates are required.

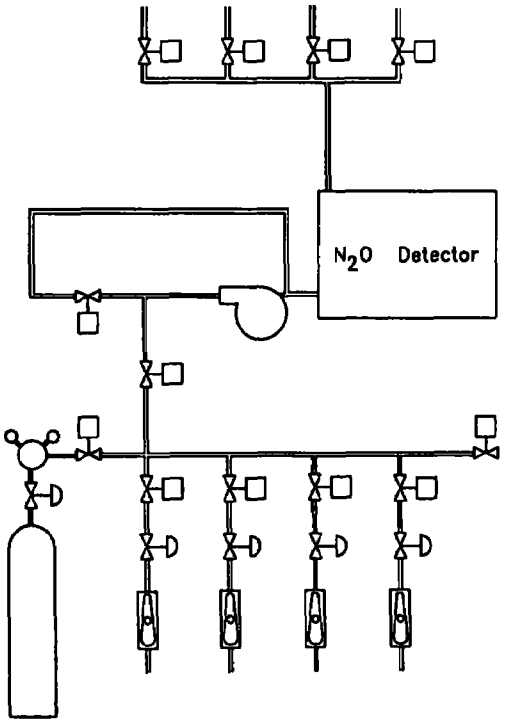

Figure 5. Four zone ACH measuring apparatus

3) TEMPERATURE MEASUREMENT

Temperature differences across the skin of a building often cause air infiltration while internal temperature differences may or may not cause air circulation. Temperatures are measured with Type T (copper-constantan) thermocouples. The original data logger was modified to include an isothermal junction for the thermocouple connections. This improved the original accuracy from ± 2°C to ± 0.1°C. The isothermal junction can accommodate 24 individual thermocouple inputs.

4) RADON MEASUREMENT

In general, radon concentrations can be determined by measuring the time-average value, where the average radon concentration is calculated over a specified period of time, or by instantaneous measurement, otherwise known as grab sampling. Time-averaging does not identify transient variations while manual grab sampling becomes time consuming and laborious when sampling a large population. Due to various interacting factors, radon levels can fluctuate substantially over an extended period of time (Figure 6). The RDAS includes radon meters capable of continuous "real time" measurement. This allows analysis of both the transient and steady state response associated with various control measures or disturbances.

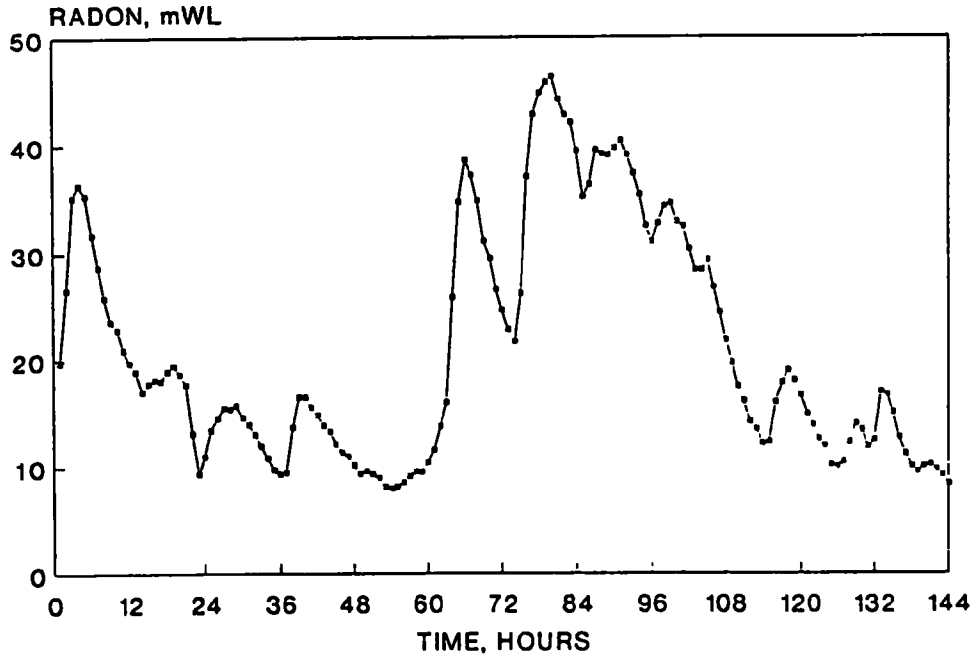

Figure 6. Temporal variations of radon levels

While many previous studies on radon measurement focused on the house as a whole, information is needed at suspected radon gas entry points and to examine the spacial distribution of radon within the building. Spacial variations of radon gas within a zone or between zones are often large enough to warrant the use of several detectors. The RDAS incorporates 10 radon meters into its design.

The radon meters are designed by Thomson & Nielsen Electronics Ltd. They produce a time integrated measurement similar to that of other radon meters, however, the time constant is relatively small (five minutes) compared to other radon detectors. Although the radon data is not actually instantaneous, the integrated values are acceptable since radon levels are not expected to change

significantly over the five minute interval.

Semiconductor sensors are used to produce a voltage signal proportional to the radon concentration, or alpha activity. An integral pump draws air through the an intake filter, into a chamber, then out through an exhaust filter. The intake filter absorbs radon daughters which are present. As the radon gas continues through the chamber, the gas decays and the daughters are deposited on the second filter. With both filters in place, radon gas is detected. With no intake filter, only the daughters are detected. Alpha activity on the filters is counted and processed into a zero to five volt DC output and recorded on the data logger. Each meter has its own power source and pump for air sampling. The accuracy of the radon meters are within ± 10% of the true value.

FUTURE APPLICATIONS

The RDAS is being installed in an experimental house to examine the effect of various ventilation system operating modes on the distribution of pollutants within the house. Initial studies will focus on line source and point source pollutants originating at the foundation. Tracer gas sources will be used to simulate radon entering through cracks and holes in the foundation. Subsequent studies will investigate the effect of building envelope and mechanical system operation modifications on the radon entry and distribution characteristics.

The work described in this paper was not funded by the U.S. Environmental Protection Agency and therefore the contents do not necessarily reflect the views of the Agency and no official endorsement should be inferred.

ACKNOWLEDGMENTS

Special thanks are extended to D.M. Guenter of IRC, Saskatoon for assistance in the design and construction of the RDAS, to M.E. Lux of IRC, Saskatoon for valuable discussion, and to Canada Mortgage and Housing Corp. (CMHC) for their financial assistance in the form of a scholarship.

REFERENCES

1. Radon Reduction Techniques for Detached Houses - Technical Guidance, EPA/625/5-86/019, United States Environmental Protection Agency, Research Triangle Park, NC., June, 1986.

2. Figley, D.A., Dumont, R.S. Techniques For Measuring The Air Leakage Characteristics Of Below Grade Foundation Components. In: Proceedings of the 82nd Annual Meeting of the Air and Waste Management Association, Anaheim, Ca., June, 1989.

3. Indoor Air Quality Environmental Information Handbook: Radon, DOE/PE/72013-2, United States Department of Energy, Washington, D.C. February, 1985. pp. 2-1.

4. Figley, D.A., Dumont, R.S. Radon in Houses - A Building Science Approach, Accepted for presentation at the Proceedings of the 5th Conference on Building Science and Technology, February, 1990.

5. Dumont, R.S., Figley, D.A. Control of Radon in Houses. In: Canadian Building Digest 247, February, 1988.

6. Determining Air Leakage Rate By Tracer Dilution. In: Annual Book of ASTM Standards, Vol 04.07, E741-83, November, 1983.

7. ASHRAE Handbook 1989 Fundamentals, American Society of Heating, Refrigeration and Air Conditioning Engineers, Atlanta, Ga., 1989. pp. 23-1 - 23-10.

8. Discussions with M.E. Lux., Research officer, Prairie Regional Station, Institute for Research in Construction, National Research Council of Canada, Saskatoon, Sk., Canada, S7N OW9

Session C-VI:

Radon in the Natural Environment—POSTERS

PRELIMINARY IDENTIFICATION OF HIGH RADON POTENTIAL AREAS IN TWENTY-FIVE STATES

R. Thomas Peake

U. S. Environmental Protection Agency

ABSTRACT

A preliminary radon potential map of 25 states has been prepared showing areas of high radon potential. The data used to create this map include:

1) National Uranium Resource Evaluation (NURE) aerial radiometric data. NURE data in glaciated and non-glaciated areas have to be interpreted differently because the properties of the surficial material can be as important as the radium concentration.

2) State/EPA Indoor Radon Survey Data. Indoor radon data for 25 states have been analyzed by house construction by county and regionally.

Both sets of data have been compared to geology to produce a county scale map. Areas of high radon potential include, but are not limited to, the Upper Midwest, the Rocky Mountain region and portions of the Applachian Mountains. This map will be used in EPA's efforts to identify and characterize high radon potential areas for school and workplace surveys, and for building code development.

This paper has been reviewed in accordance with the U. S. Environmental Protection Agency's peer and administrative review policies and approved for presentation and publication.

SECULAR VARIATIONS OF RADON IN METROPOLITAN VANCOUVER, BRITISH COLUMBIA, CANADA

By: M.M. Ghomshei[1] and W.F. Slawson[2]

1. Orchard Geothermal Inc. 401-134 Abbott Street, Vancouver, B.C. V6B 2K4 (Canada)

2. Department of Geophysics and Astronomy, University of British Columbia, Vancouver, B.C. V6T 1W5 (Canada)

ABSTRACT

Sampling of radon within the soil from three sites in metropolitan Vancouver is reported. Alpha track bi-weekly measurements during a period of 4 years show secular variations with a period of 8-15 months. There are low-radon and high-radon episodes enduring several months to a year. Average radon level during the high-radon episodes reaches 5-10 times that of the low-radon periods. During high-radon episodes the high-frequency variations show very high amplitudes. After filtering of the high-frequency fluctuations, the data from different sites demonstrate remarkably similar trends. It is suggested that along with hydrogeological events, stress relaxation in rocks, earthquake, and magma emplacement may contribute to the sources of secular variations of radon. Because of long-term variations, radon level in urban areas should be monitored on a continuous basis. Single measurements, even those integrating radiation over a period of few months, may sample a low-radon episode, and provide a false assurance, or occur during a high-radon episode and give a false alarm.

INTRODUCTION

Temporal variation of atmospheric radon is a known fact especially to those involved in uranium, and geothermal exploration, hydrogeology, and environmental science (e.g. 1,2,3,4,5,6). These variations are controlled by: 1- factors which affect the release of radon from the source geological material (e.g. radium-bearing mineral) and 2- factors which affect the radon transport systems. The emanation and diffusion of radon from the radium-bearing mineral to a porous media containing a fluid phase (e.g. water, steam, or other gases) is mainly controlled by the volume, shape and structure of the porosity (e.g. 7). Continuously varying factors such as temperature and the pressure of the fluid secondary phase have some control on the emanation process (e.g. 8). Co-seismic activities in ground may have a major control on the release of radon to atmosphere. This control is mainly through producing microfractures which speed the process of diffusion of radon from the source rock into the highly mobile fluid phase.

Since the discovery of hazardous radon levels in the urban areas (e.g. 9), the prime concern of the environmental researchers have been the spatial variations of radon. Study of temporal variations have comparatively been neglected, resulting in a lack of a long-term data base. It is often wrongly assumed that alpha track "single-shot" surveys with an exposure time of few months would average out the temporal fluctuations. Besides the common high-frequency (diurnal and weekly or monthly) fluctuations, the low-frequency (seasonal or secular) variations demonstrate high amplitudes which should be taken into account in the risk assessment calculations.

The present work introduces data on the significance of short-term and long-term temporal variations. Possible causes of these variations are discussed. The data were collected during the period of 1977 - 1981 and are being reported now in view of the recent wide-spread interests in radiation protection and earthquake prediction.

EXPERIMENT

SITES

A number of sites within the Greater Vancouver (British Columbia, Canada) area were selected for long-term monitoring (Fig. 1). The selection was made to include a variety of geological and hydro-geological environments. Site YVR was located in the Fraser River delta, lying over several hundred meters of Recent Sediments. The UBC site was located above about 90 meters of Glacio-marine

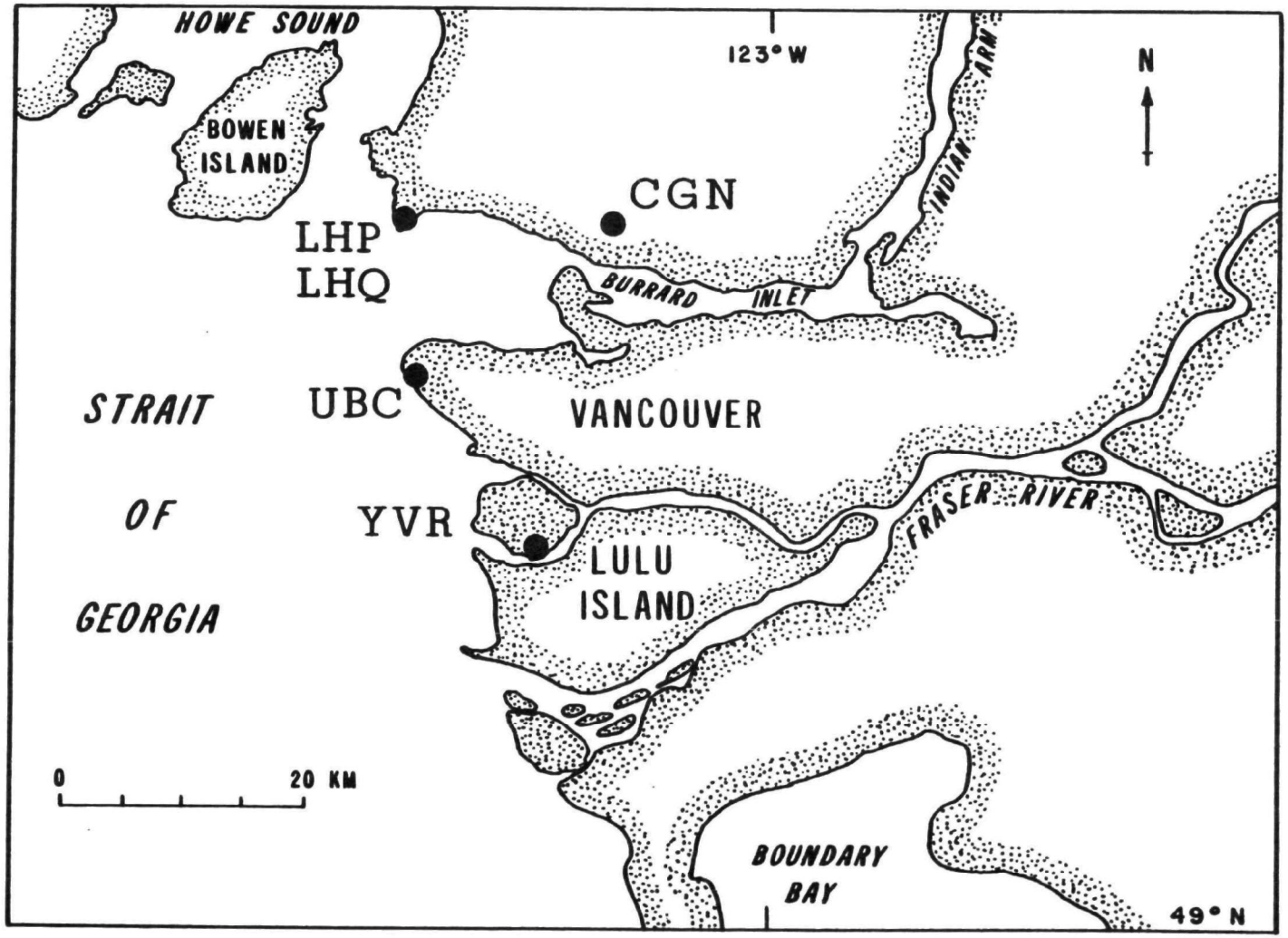

Fig. 1. Location map, Greater Vancouver Area.

deposits. Several meters of glacial outwash overlying the Late Cretaceous Coast Range granodiorite made the host for site CGN. Only UBC and CGN were operated over the more than 4 year period. We report here the sites UBC, CGN and YVR. Data from two other sites were not considered reliable due to frequent flooding.

ANALYTICAL PROCEDURE

Alpha-track measurement system (10,11,9) was employed for all the sites. Detectors were placed in 60 cm deep cased holes and were exposed for approximately two week periods (Fig. 2). The plastic track detector (from Terradex) was placed at the closed end of a cup. The open end was covered with a thoron filter. The filter consisting of a single layer of "Gladwrap" delays the diffusion of gases into the cup by almost a day, eliminating all the thoron and a small fraction of radon. The data is reported as counted alpha particles per square meter of detector per second. Average background (blank) signal was determined by another study and did not exceed 2 ± 1.5 counts m^{-2} s^{-1}. The linear correlation between track density (cm^{-2}) and dose ($pCiL^{-1}Day$) are reported by Fleischer and coworkers (9).

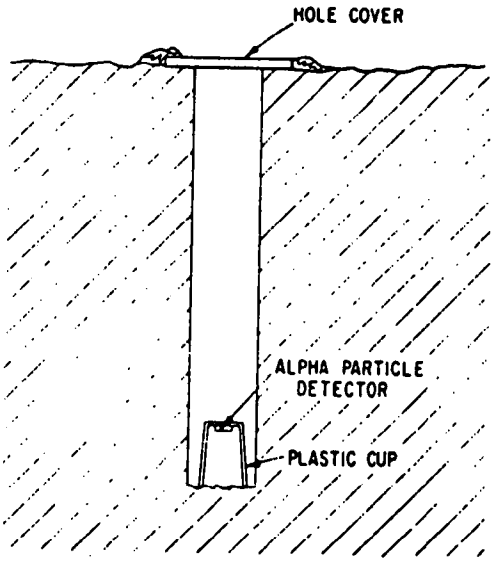

Figure 2. The installation of a TRACK-ETCH detector.

RESULTS AND DISCUSSION

The results are presented in the Figure 3. A low pass filter was applied to smooth the high-frequency fluctuations and better highlight the longer-term effects.

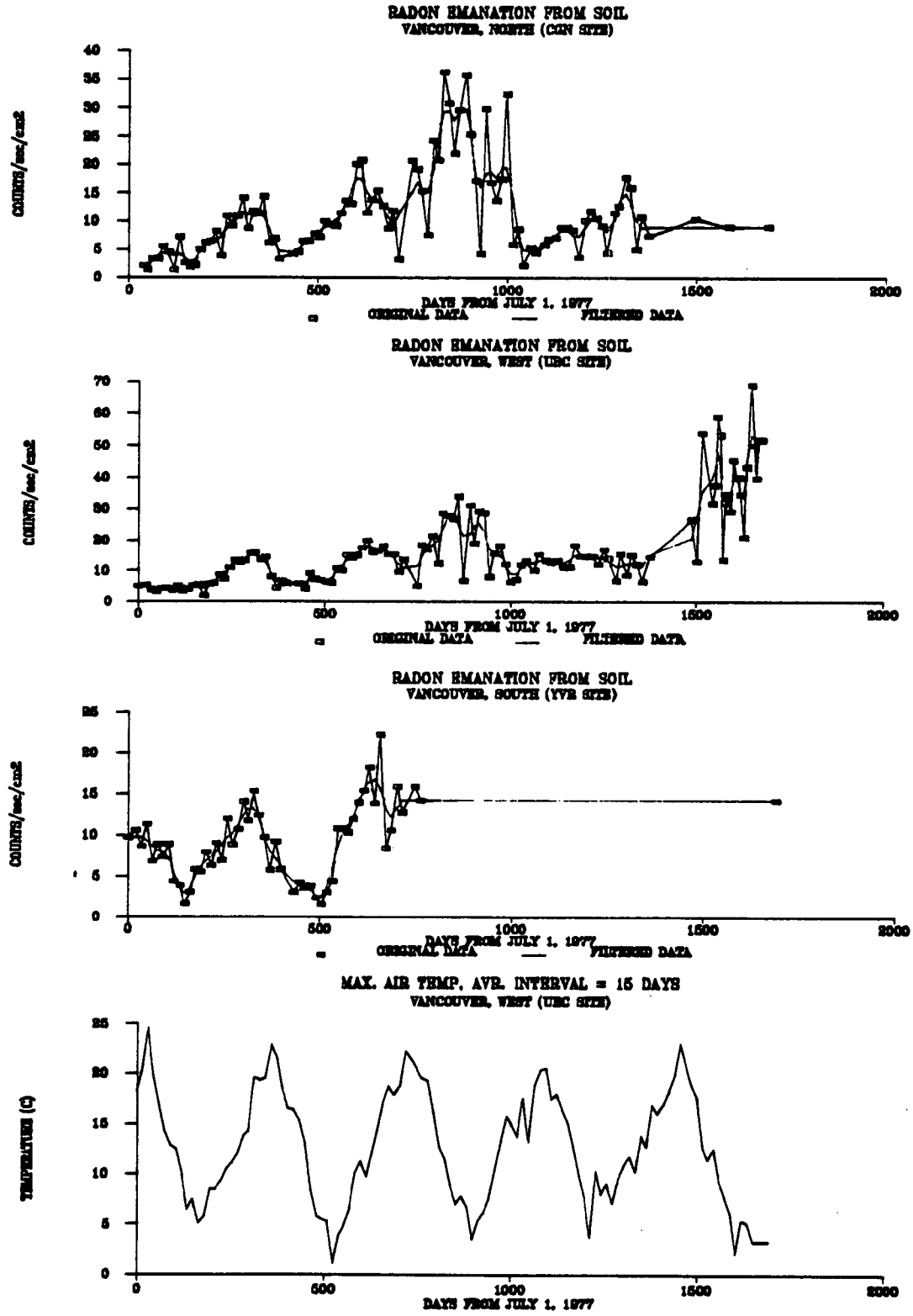
RADON EMANATION FROM SOIL
VANCOUVER, NORTH (CGN SITE)
COUNTS/sec/cm2
DAYS FROM JULY 1, 1977
ORIGINAL DATA
FILTERED DATA
RADON EMANATION FROM SOIL
VANCOUVER, WEST (UBC SITE)
COUNTS/sec/cm2
DAYS FROM JULY 1, 1977
ORIGINAL DATA
FILTERED DATA
RADON EMANATION FROM SOIL
VANCOUVER, SOUTH (YVR SITE)
COUNTS/sec/cm2
DAYS FROM JULY 1, 1977
ORIGINAL DATA
FILTERED DATA
MAX. AIR TEMP. AVR. INTERVAL = 15 DAYS
VANCOUVER, WEST (UBC SITE)
TEMPERATURE (C)
DAYS FROM JULY 1, 1977

Fig. 3

The spectrum of data appears to contain two main frequencies: 1- variations with a period of several weeks (few data points). 2- Variations with a longer period of several months to a year. A third longer-term variation can be depicted from the overall rising trend visible in all the sites. The 4 year data collection period does not seem sufficient to detect any periodicity in this trend. The short-period variations are controlled to some extent by the transient atmospheric perturbations such as precipitation, pressure and temperature (e.g. 6,4,3). Our data did not show any significant correlation with atmospheric parameters. It is possible that the bi-weekly time-averaged measurements have filtered the fluctuations related to relatively rapid atmospheric perturbations. As to the low-frequency variations, most of the data (first 1000 days) demonstrate a periodicity close to 1 year which might be tentatively correlated with seasonal temperature patterns. This correlation is not however consistent over the entire data spectrum (Fig. 3). The variations induced by the atmospheric events may be overshadowed by more vigorous changes induced by non-atmospheric dynamic factors such as stress relaxation in the bedrock, related degassing, and some fluid mobilization. It should also be noted that the combination of the meteorological changes which affect the soil parameters is not necessarily of yearly frequency. Radon episodes, therefore, may not coincide with yearly temperature seasons. To avoid confusion, we suggest the term episode (instead of season) to be employed for these long-term variations of radon. According to our data the frequency of the high- and low-radon episodes is not necessarily associated with the calendar year.

An interesting observation can be made on the amplitude of the short-term and long-term variations. It seems the amplitude of the short-term variations is positively correlated with that of the long-term variations. The short-term fluctuations demonstrate a higher amplitude during the high-radon episodes (crest of the long-term variations). This observation strongly suggests that the long-term background enhancement is the major source of radon fluctuations. The short-term atmospheric factors do not have a causal relation with radon emanation. These factors act only as transient mobilizers. The mobilization is naturally proportional to the existing free radon in the rock-soil system. By free radon we mean the radon which has been released from the rock to a secondary fluid media and consequently more dynamic environment.

The geological factors which may contribute to the background enhancement are either of a pulse nature such as seismic activities, or of events of longer duration such as stress relaxation in the rock formation due to plate adjustment (dilatancy-diffusion). Some relatively fast stress relaxations precede brittle deformations and can be used as an earthquake precursor. Fast relaxation may induce extremely high radon

background in the rock-soil system. The degassing of this radon to the atmosphere can cause "radon storms" or "impulsive radon emanation" (12). On our data the relatively sharp increase in radon in 1981 may be related to this type of phenomenon.

A second observation suggesting a lithospheric origin for the long-term variation is the similarity of data-spectra from different sites. The general rising trend is remarkable on all 3 sites. Other shorter-period variations appear also to reflect regional behaviour. The coincidence of the "episodic" variations from the three sites is obvious. Although these variations may be to some extent related to long-term meteorological cycles, the remarkable similarities of the data spectra are suggestive of a common subsistent lithospheric component.

CONCLUDING REMARKS

The data presented in this work suggest that the temporal variations of radon are composed of high- and low-frequency components. The high-frequency variations may reflect the effect of the transient atmospheric perturbations on the dynamic properties of soil and its contained fluids. These variations demonstrate large amplitude when they are superimposed on the crest of the low-frequency variations. The low-frequency variations are the main source of overall radon enhancement at regional scale. These variations may be related to a combination of long-term meteorological cycles and crustal events. Therefore, only measurement spanning several years constitutes valid base-line data.

ACKNOWLEDGEMENTS

Data collection project was supported by grants to WFS from the Geophysics Division of the DEMR. C.Y. King of USGS (Menlo Park), and J. Gingrich of Terradex Corp. were very helpful and supportive during the period of 1979 - 1981.

The work described in this paper was not funded by the U.S. Environmental Protection Agency and therefore the contents do not necessarily reflect the views of the Agency and no official endorsement should be inferred.

REFERENCES

1. Malmqvist, L., Isaksson, M. and Kristiansson, K. Radon migration through soil and bedrock. Geoexploration, 26: 135, 1989.

2. Kruger, P. and Semprini, L. Radon as in-situ tracer in geothermal reservoirs. Electric Power Research Institute Inc.

(EPRI), Report No. AP-5315, 1987.

3. Ghomshei, M.M. Concentrations des radioelements naturels (l'uranium, le thorium et le potassium) et evolution des magmas (exemple de quatre series volcaniques). Doctoral Thesis, University of Paris - XI, 1983. 201 pp.

4. Fleischer, R.L. and Mogro-Campero, A. Radon enhancements in the Earth: Evidence for intermittent upflows. Geophysical Research Letters, 5: 361, 1979.

5. Pearson, J.E. Natural environmental radioactivity from radon 222. Public Health Service Publications (U.S. Government), 1967.

6. Pearson, J. E. and Moses, H. Atmospheric radon 222 concentration variations with height and time. J. of Applied Meteorology, 5: 175, 1965.

7. Tanner, A.B. Radon migration in the ground: A supplementary review: United States Geological Survey Open-File, Report 78-1050, 1978. 62 pp.

8. Satomi, K. and Kruger, P. Radon emanation mechanism from finely ground rocks. Proceedings of Fourth International Symposium on Water-Rock Interactions, Misasa, Japan, August, 1983.

9. Fleischer, R.L., Girard, W.R., Mogro-Campero, A., Turner, L.G., Alter, H.W. and Gingrich, J.F. Dosimetry of environmental radon: Methods and theory for low-dose integrated measurements. Health Physics, 39: 957, 1980.

10. King, C.Y. Episodic radon changes in subsurface soil gas along active faults and possible relation to earthquakes. J. of Geophysical Research, 85: 3065, 1980.

11. Fleischer, R.L. Price, P.B., and Walker, R.M. Nuclear Tracks in Solids: Principles and Applications: University of California Press, Berkeley, California, 1975. 605 pp.

12. King, C.Y. Impulsive radon emanation on a creeping segment of the San Andreas Fault, California. Pageoph., 122: 1.

RADON IN HOMES, SOILS, AND CAVES OF NORTH CENTRAL TENNESSEE

by: Paul D. Collar
U.S.G.S.
G.P.O. Box 4424
San Juan, PR 00936

and

Albert E. Ogden
Center for the Management, Utilization, and
Protection of Water Resources
Tennessee Technological University
Cookeville, TN 38505

ABSTRACT

Radon concentrations were measured in soils, caves, and homes of north central Tennessee. Soil radon concentration ranged from 72.5 to 349.2 picoCuries/Liter (pCi/L) and had a mean of 130.5 pCi/L; the maximum was measured within a soil developed on the uraniferous Chattanooga Shale. Cave radon ranged from 7.2 pCi/L to 386 pCi/L. Caves within Ordovician limestones had a mean radon concentration of 129.1 pCi/L while caves in Mississippian limestones had a mean radon concentration of 30.1 pCi/L. Home radon concentration ranged from 0.2 pCi/L to 37.6 pCi/L and had a mean of 2.02 pCi/L; twenty-three percent of the home radon concentrations exceeded 4 pCi/L.

Homes built on Fort Payne limestone had the highest geometric mean (2.91 pCi/L) of lithologically classified samples; homes built on the Warsaw limestone had the lowest mean (1.58 pCi/L). A weak inverse correlation between radon concentration and distance above the Chattanooga Shale was indicated by a Pearson correlation coefficient of -0.165. The confidence the relation was not coincidental, however, was only 81.4 percent. Crawl space homes and basement homes were found to have statistically similar mean radon concentrations. The depth of home excavation varied directly with radon concentration at a confidence of 99.9 % using the Pearson product-moment correlation.

INTRODUCTION

Radon concentrations were measured in 9 soils, 22 caves, and 98 homes of north central Tennessee. The radon concentration of soils and caves were analyzed in order to characterize the local geologic environment for its potential to introduce radon to houses located in the field area. Radon levels in homes were correlated with several geological and home construction factors in an attempt to determine if geological and engineering controls on radon's distribution in the indoor environment could be quantified for incorporation into mitigative home construction strategies.

FIELD AREA

Physiographically, the field area encompasses terrain from both the Outer Central Basin and Eastern Highland Rim Provinces of north central Tennessee (Figure 1). A simplified northwest-southeast trending cross-section is provided in Figure 2 and shows that rocks cropping out in the field

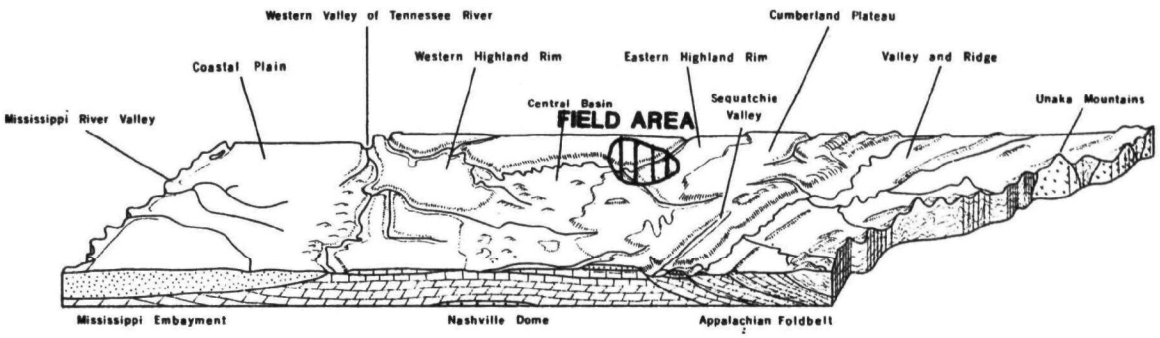

Figure 1. Physiography of central Tennessee showing location of study area (modified after (1)).

area include Ordovician and Mississippian carbonates and the Devonian Chattanooga Shale. Table 1 summarizes the insoluble percentages and the phosphate content associated with each of the major rock units exposed in the field area. The differing solubilities of the various lithologies in the field area strongly govern the physiography of central Tennessee (2). The Central Basin is a rolling lowland which has resulted from the greater solubility of the Ordovician carbonates relative to the siliceous, Mississippian Fort Payne and Warsaw limestones. Soils develop to a maximum thickness of about 20 feet in the Central Basin (3); for the most part, however, soils do not exceed six feet in depth. The Fort Payne and Warsaw Formations contain a high percentage of silica. In the Fort Payne, silica occurs predominantly as thick-bedded cherts; in the Warsaw silica occurs mostly as silt and sand. As a result, these units are erosionally resistant

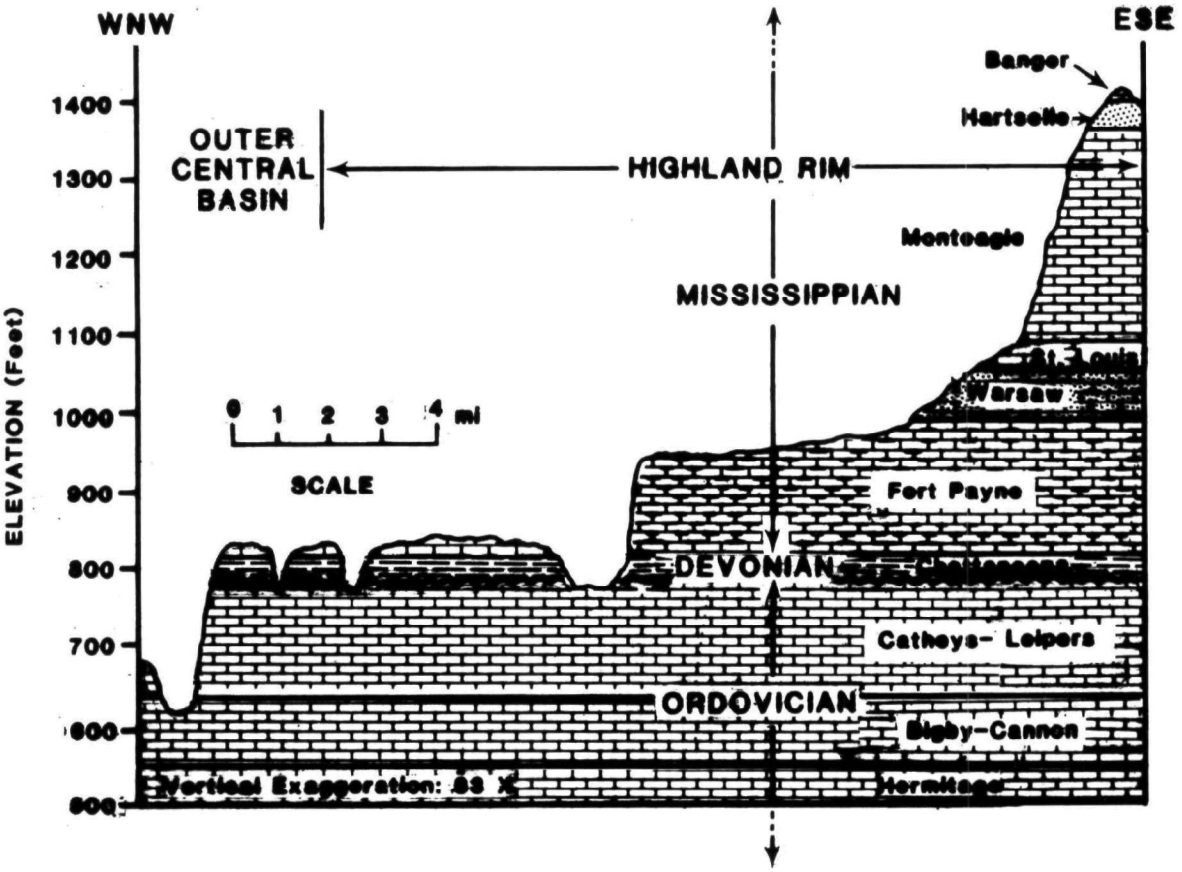

Figure 2. Cross-section within study area showing the principal lithologies.

Table 1. Percentage of insoluble constituents and phosphate in each of the major carbonate lithologies of the field area (modified after (5) and (6).

Rock Unit	Percent Insoluble Constituents	Percent Phosphate (as P205)
Monteagle	3.15	0.030
St. Louis	?	?
Warsaw	1.8 to 7.3	0.033
Fort Payne	4.04	0.017
Leipers	7.48	0.179
Catheys	7.48	0.179

and constitute a plateau surface known as the Highland Rim Province. Soil thicknesses often exceed 50 feet in the Highland Rim and have been reported up to 100 feet (4). The Mississippian lithologies above the Warsaw Formation are for the most part relatively pure and highly subject to dissolution. The St. Louis Limestone forms a sinkhole plain on the easternmost flank of the Highland Rim Plateau surface. A steep escarpment abuts the sinkhole plain and rises to the Cumberland Plateau. This escarpment is underlain by the Monteagle, Hartselle, and Bangor Formations. Despite the fact that the Warsaw Limestone contains abundant silica, several caves are present in this unit as a result of the vertical continuity of cave systems originating in the St. Louis Limestone. The Fort Payne Formation, although abundantly fractured and highly porous relative to adjacent lithologies, is characterized by small pocket caves. The caves analyzed for radon in the present survey were all in either the Ordovician carbonates or the Mississippian Warsaw or Monteagle Limestones.

The Chattanooga Shale has been shown (7 and 8) to contain relatively high quantities of uranium throughout most of its geographic extent. Whole rock uranium analyses of the organic-rich Gassaway Member of the Chattanooga Shale ranged from 13 to 97 microgram per gram (ug/g) and averaged 55 ug/g (8). The uranium content of the Chattanooga Shale is therefore significantly higher than most granites and comparable to highly uraniferous granites. The Chattanooga Shale's potential as a source of environmentally threatening radon is probably minimized, however, by the limited thickness of the rock unit. Throughout central Tennessee, the Chattanooga Shale averages about 30 feet in thickness, and the uranium-rich Gassaway Member averages only 15 feet in thickness (9).

RESULTS AND DISCUSSION

SOIL AND CAVE RADON MEASUREMENTS

Soil Radon Survey

Track-etch radon measurements in nine soil associations yielded a range from 78 to 345 picoCuries per liter (pCi/L), a geometric mean of 130.5 pCi/L, and an arithmetic average of 153.6 pCi/L (Table 2). The limited number of samples prohibitted the clear definition of the type of data distribution, but the data appear to be lognormally distributed. The two lowest soil radon measurements were taken in floodplains of creeks during the wet months of December and January, when the water table was near the land surface. These lower measurements may reflect the inhibitting effect of a nearby water table on radon's diffusive migration through soil. Nevertheless, the geometric mean and average of all soil radon measurements are both higher than the national average soil radon concentration of 100 pCi/L (10), suggesting that north central Tennessee soils may introduce slightly more radon to area homes than do soils on the national average.

Cave Radon Survey

Radon analyses in 22 regional caves were made with carbon canisters over a 4 to 5 day exposure period. Elementary statistics are summarized in Table

Table 2. Summary of elementary statistics of variously classified radon data sets.

Dataset	n	Geometric Mean (pCi/L)	Arithmetic Mean (pCi/L)	Standard Deviation (pCi/L)	Coefficient of Variation (%)	% in excess of 4 pCi/L
HOME RADON						
Overall	98	2.02	3.07	2.54	125.74%	23.47%
LITHOLOGIC POPULATIONS						
Warsaw	42	1.58	2.46	2.8	177.22%	21.43%
Fort Payne	25	2.91	3.53	1.84	63.23%	32.00%
Chattanooga	10	1.7	2.03	1.98	116.47%	10.00%
Ordovician	21	2.31	4.24	2.8	121.21%	19.05%
HOME TYPES						
Crawl space	64	1.87	2.61	2.4	128.34%	20.97%
Concrete slab	34	2.31	3.87	2.78	120.35%	30.56%
DEGREE OF WEATHERIZATION						
Very Low	9	1.62	2.28	2.63	162.35%	16.67%
Below Average	16	1.52	1.75	1.77	116.45%	0.00%
Average	49	2.03	2.85	2.48	122.17%	23.26%
Above Average	17	2.81	5.43	3.63	129.18%	31.58%
Very High	7	2.46	2.93	1.53	62.20%	16.67%
SOIL RADON	9	130.5	153.6	1.78	1.36%	N/A
CAVE RADON						
Overall	22	41.3	84.7	4.26	10.31%	N/A
Mississippian	16	30.13	62.6	4.2	13.94%	N/A
Ordovician	6	129.1	164.1	2.33	1.80%	N/A

2. Caves in Ordovician rocks had a significantly higher geometric mean (129.1 pCi/L) than did caves in Mississippian rocks (30.1 pCi/L). This is thought to reflect mineralogical differences between the two limestones. The Mississippian Monteagle Formation is a relatively pure limestone (Table 1) with an average of 0.03 percent phosphate (as P2O5); similarly, the underlying Warsaw Formation contains an average of 0.033 percent phosphate and the Fort Payne an average of only 0.017 percent phosphate. The Ordovician Leipers and Catheys Formations, on the other hand, have phosphate-rich horizons with up to 20 percent phosphate by weight (5). The average phosphate concentration in the Catheys and Leipers formations is 0.179 percent. Insoluble constituents average 7.48 percent within the Catheys and Leipers (Table 1). Unlike the overlying siliceous Fort Payne and Warsaw limestones, however, the majority of the insoluble portion of the Ordovician strata consists of interbedded shales and disseminated clays.

The lattices of calcium phosphate minerals have been shown to readily accomodate uranium as an isomorphic substituent (11). Uranium is also commonly adsorbed onto the surfaces of clay minerals. The relatively higher proportion of clay minerals and phosphate in the Ordovician rocks is therefore likely to provide a suitable environment for the regional incorporation of uranium into the Ordovician rock matrix. Although some of the uranium may have been introduced into the sedimentary basin by the deposition of clays, it is also possible that ground water mobilization of uranium from the Chattanooga Shale has resulted in the concentration of uranium in phosphatic horizons below the Chattanooga Shale.

GEOLOGICAL CONTROLS ON INDOOR RADON MEASUREMENTS

Basements and crawl spaces were tested for radon with carbon canisters in homes built upon the Catheys, Leipers, Chattanooga, Fort Payne, and Warsaw Formations. Measurements ranged from 0.1 to 37.6 pCi/L. The data were lognormally distributed, with a geometric mean of 2.02 pCi/L (Table 2). Twenty three percent of the measurements were above the U.S. Environmental Protection Agency recommended maximum of 4 pCi/L (12). The mean of 2.02 pCi/L was higher than the national geometric mean of 0.89 pCi/L (13). However, the maximum of 37.6 pCi/L was one or two orders of magnitude below the extremes measured in other parts of the United States. The 37.6 pCi/L maximum of the present study was measured in a home constructed within 100 feet of the cave passage possessing the highest cave radon measurement (386 pCi/L) made in this study. Radon was shown to enter the home via a fracture system connecting the cave and the substructure of the house (14), demonstrating that near surface cave systems can pose a potential avenue of radon entry to nearby houses.

Indoor radon measurements were classified according to underlying bedrock; the data from each lithological class was found to possess a lognormal distribution. The elementary statistics describing these classes are given in Table 2. Homes built on the Fort Payne Formation possessed the highest geometric mean (2.9 pCi/L) while homes built on the Warsaw Formation possessed the lowest geometric mean (1.6 pCi/L). These were the only two populations which proved to be statistically separable at an alpha of 0.05 with the Student's t-test.

Despite the fact that the Chattanooga Shale has a uranium content significantly greater than the overlying and underlying limestone lithologies, homes built on the Shale did not have anomalously high radon concentrations. The low observed measurements (Table 2) may be due to the very limited 2 to 2.5 feet soil thickness developed on the Chattanooga. A thin soil can minimize soil radon concentrations and the radon introduced to overlying homes in several ways. At soil depths less than 3 feet, only a portion of the diffusion length of radon is utilized, thereby limiting radon production. A thin mantle of soil is furthermore subject to atmospheric influences to a greater extent than is a thick soil. Consequently, wind and temperature fluctuations are potentially more effective in removing radon from the soil. Precipitation is more likely to produce a saturated zone near the land surface within a thin soil, thereby decreasing the effective diffusivity of the soil.

Besides the soil thickness, another factor which may explain the low radon content of Chattanooga homes is the location of radium ions within the soil matrix. The emanation coefficient of a given soil is strongly controlled by the location of radium ions in the solid matrix (15). If radium is primarily present as adsorbed ions on the exterior of clay grains, then the emanating fraction of the total volume of radon produced by the decay of radium is likely to be high. If, however, radium is bound in individual grains a distance greater than a few microns from interstitial pore space, then the radon that actually escapes the grains and enters the pore space is likely to be significantly lower and result in a lower overall emanation coefficient. The proportion of clays in Chattanooga-derived soils was found to be noticeably lower than that characterizing soils weathered from carbonate lithologies. Correspondingly, rock fragments were more abundant within Chattanooga soils than within any of the other soils augered. The relative abundance of rock fragments and paucity of clay in the Chattanooga soil, combined with the low radon measurements in homes, may suggest that radium is bound within the interior of rock fragments and not predominantly attached to the exterior of clay surfaces by adsorption.

Based on a radon survey of 1733 homes in Tennessee and the knowledge that the Chattanooga Shale was the most highly uraniferous stratum exposed statewide, Tennessee Department of Health and Environment (16) characterized the surface outcrop of the Chattanooga Shale and downslope areas in Tennessee with its highest "radon occurrence potential" ranking. In order to further assess the effects of the Chattanooga Shale in promoting high radon concentrations in adjacent homes, the stratigraphic distance above and beneath the Chattanooga Shale was calculated for each of the homes tested during the present survey using geologic maps, topographic maps, structure contour maps, and well logs. The distance from the Chattanooga Shale was plotted against the logarithm of the radon concentration for the two sets of homes (those beneath the shale and those above the shale). Logarithmic transformation of the raw data was necessary in order to permit the parametric statistical comparison of the two variables by calculation of Pearson correlation coefficients.

As Figure 3 shows, no relation was manifested between distance beneath the shale and radon concentration, suggesting that downslope drift of weathered Chattanooga Shale residuum does not appear to be a significant

control on radon distribution in Central Basin soils adjacent to the Chattanooga Shale outcrop. The plot of radon concentration versus distance above the Chattanooga Shale is shown in Figure 4 and appears to manifest a weak inverse correlation between the two variables. A mathematical correlation of the two variables yielded a Pearson coefficient of -0.165 at an alpha of 0.186, implying only an 81.4 percent probability that the relation is not coincidental. The weak dependence of radon concentrations on distance above the shale appears to be lost altogether beyond about 180 feet above the Shale. The degree of home weatherization is identified in Figure 4 and shows that highly insulated homes plot generally in the uppermost portion of the field whereas poorly insulated homes plot generally in the lowermost portion of the field. These generalizations are not all-encompassing, however, suggesting that radon distribution is influenced by other factors as well.

The strength of the correlation is insufficient to conclude that the location of the Chattanooga Shale has a predictable effect on the radon concentration within overlying lithologies. Nevertheless, the weak trend cannot be dismissed outright as coincidence either. What the distribution of the data appear to indicate is that radon distribution in the subsurface and indoor environment is an extremely complex function of a large number of variables. As a result, the analysis of one or two factors which may partially control its distribution cannot be expected to yield perfect data fits with low covariance. The apparent relationship between radon concentration of homes and distance above the Chattanooga Shale--if it is in fact real and not coincidental--may be the result of at least three fundamentally separate processes. These are briefly summarized below.

1. The inverse relationship could indicate that radon is produced within the Chattanooga Shale and migrates through the subsurface to overlying homes. Homes more removed from the Shale would therefore be expected to have a lower radon concentration. One problem with this interpretation is that the Chattanooga Shale forms the lower boundary of an aquifer developed within the Fort Payne and Warsaw. Consequently, radon produced in the Chattanooga Shale would have to travel a tortuous subsurface path through ground water and ground air, all within the time constraint imposed by its limited decay period.

2. The upward diffusion of uranium throughout geologic time as a result of ground water reworking could have promoted higher uranium concentrations within overlying rock. In such a case, uranium content would be expected to be progressively reduced with increasing distance above the Shale. Under this circumstance, radon would be derived from the decay of radium grains contained within Fort Payne soils and not the underlying Chattanooga itself.

3. Finally, the apparent reduction in average radon concentration moving away from the Chattanooga Shale could reflect a change in the source or quantity of clays introduced into the sedimentary basin and be completely independent of the uranium content of the underlying shale. This possibility would imply that radon is

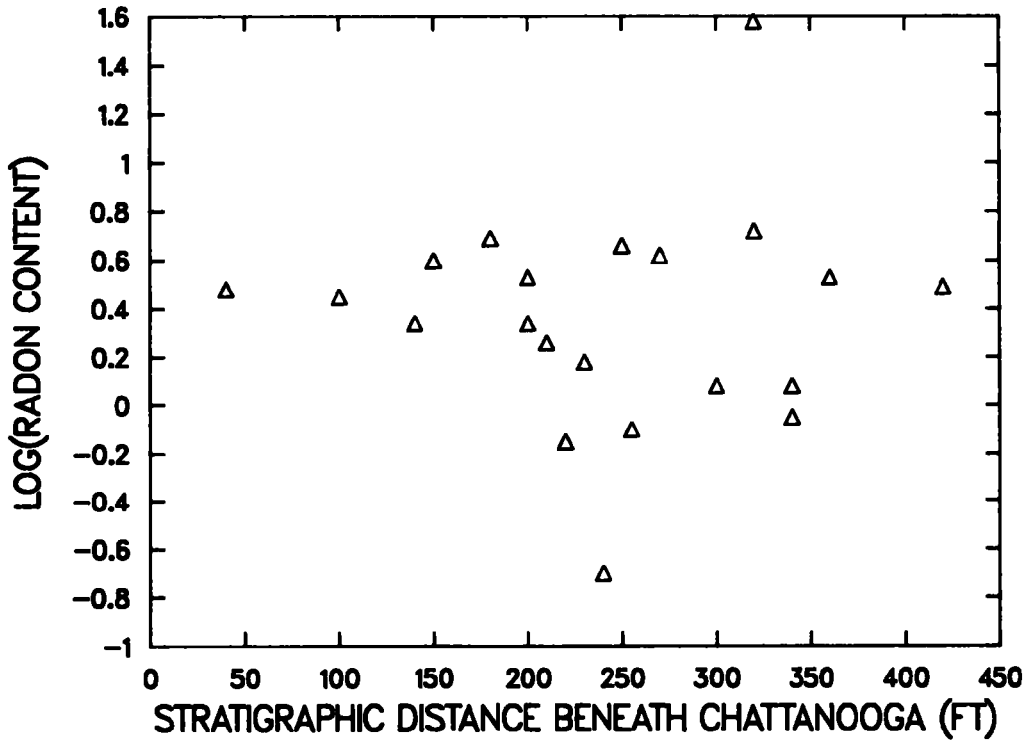

Figure 3. Log(radon content) plotted against stratigraphic distance beneath the Chattanooga Shale.

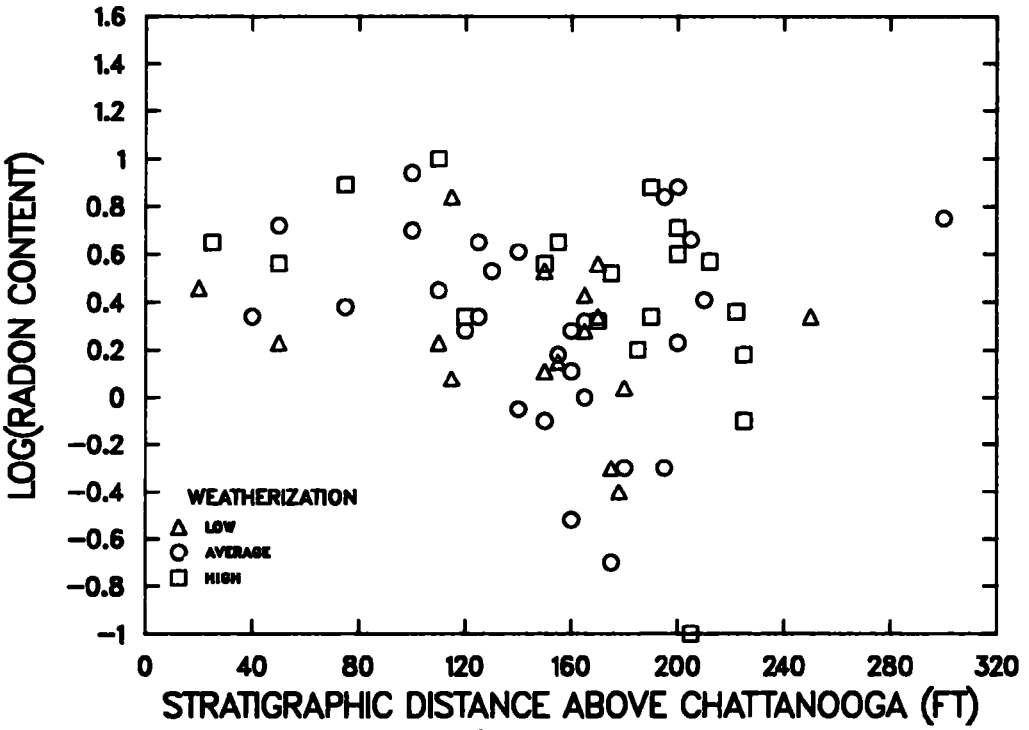

Figure 4. Log(radon content) plotted against stratigraphic distance above the Chattanooga Shale for populations classified according to degree of home weatherization.

derived from clays within the soils underlying homes and not from distant subsurface sources.

HOME CONSTRUCTION CONTROLS ON INDOOR RADON CONCENTRATIONS

Although geological environment is expected to provide an important control on the magnitude of radon's localized availability, home construction characteristics have been shown (17) to play a strong role in determining the extent to which radon is admitted into a structure and concentrated there. The effects of three construction factors were considered in describing the radon distribution in this study. These factors were: 1) home type, 2) degree of home weatherization, and 3) depth of basement excavation.

Home Type

Homes surveyed were of two types: homes with basements and concrete foundations, and homes with crawl spaces and earthen foundations. Both data sets exhibitted lognormal distributions, and Table 2 summarizes simple statistics calculated for the two populations. Homes with basements had a larger geometric mean (2.3 pCi/L) than homes with crawl spaces (1.9 pCi/L), but the difference was not statistically significant with the t-test at an alpha of 0.10 (evaluated with log-transformed data). This implies that the greater air exchange characteristic of the crawl space homes studied is sufficient to overcome their heightened susceptibility to radon entry resulting exclusively from the absence of a concrete foundation radon diffusion barrier. Correspondingly, the data strongly indicate that the presence of a concrete foundation does not ensure that homes with excavated basements are immune from the effects of radon entry.

Degree of Home Weatherization

Figure 5 shows that the degree of home weatherization is a factor which influences the magnitude of indoor radon concentrations. Highly weatherized homes had higher geometric means than homes which were poorly insulated. The coefficients of variation indicate that well insulated homes similarly had the most homogeneous radon concentrations, suggesting that air exchange promoted by "leaky" houses had a diagnostic effect on the variability of measured radon concentrations.

Depth of Home Excavation

Depth of excavation was determined onsite for each of the homes tested. This parameter was correlated with log-transformed radon concentration using the Pearson product-moment correlation, yielding a coefficient of 0.51 at an alpha of 0.001. The relationship is depicted in Figure 6 in which a linear regression is plotted. Excavation depth was similarly correlated with log(radon) for each lithology. None of the lithologically classified data sets provided statistically significant correlations at an alpha level of 0.1 or lower except for the Fort Payne data set, which yielded a Pearson coefficient of 0.47 at an alpha of 0.012. A linear regression of the Fort Payne data is also shown in Figure 6. Comparison of the two trends indicate that the minimum radon concentrations of Fort Payne homes is higher than the

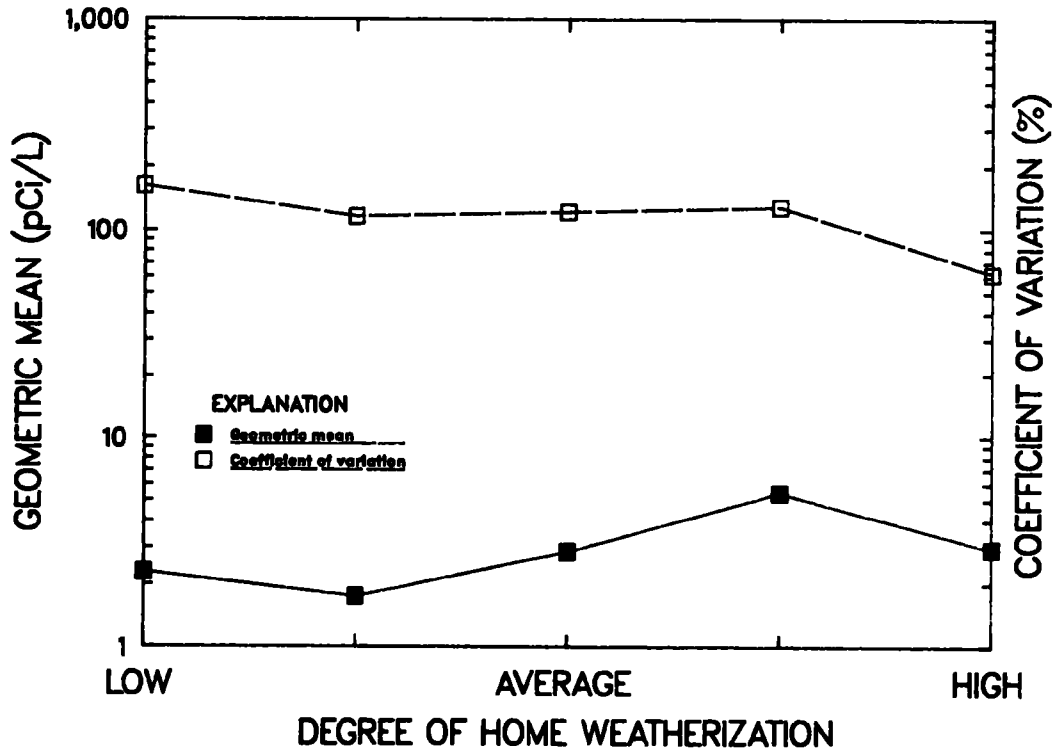

Figure 5. Plot showing the geometric mean and coefficient of variation of populations classified on the basis of degree of home weatherization.

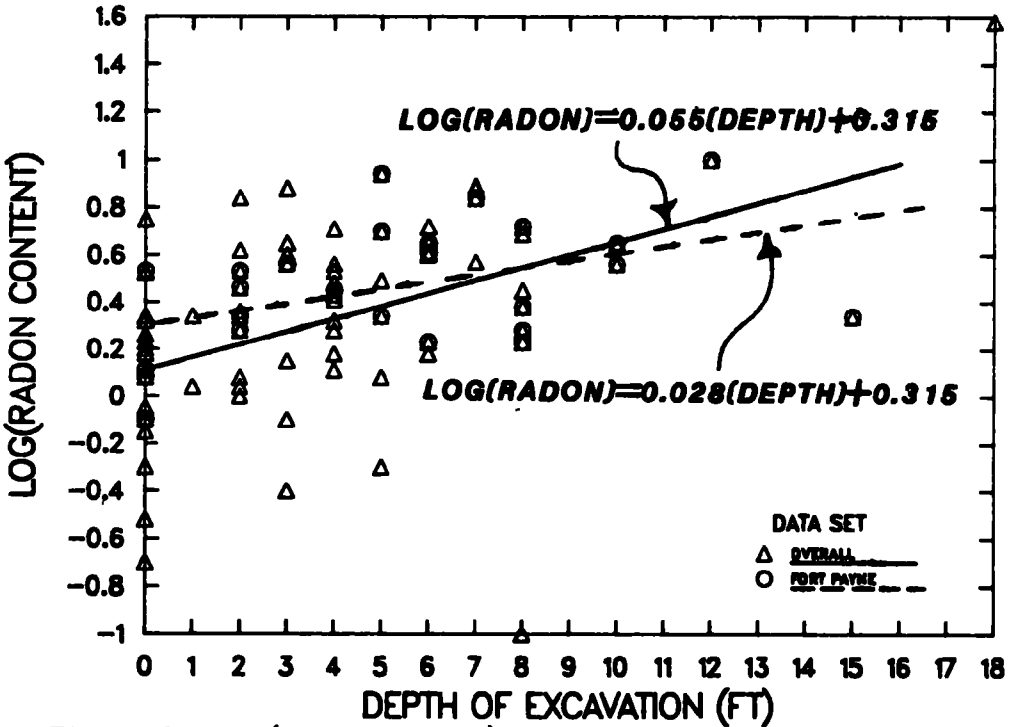

Figure 6. Log(radon content) plotted against depth of home excavation showing overall and Fort Payne populations.

minimum concentrations of homes built within other lithologies, that is, the y-intercept of the Fort Payne regression has a higher magnitude. Conversely, the overall data set manifests the greater slope, indicating that the probability of higher radon concentrations at greater excavation depths is higher among lithologies other than the Fort Payne. The regression equations loosely represent data with high covariance. The error in their prediction of radon concentration based on excavation depth was generally less than 15 percent but as high as 30 percent. The regression functions suggest that on the average, 4 pCi/L radon will be exceeded in the overall data set at excavation depths greater than 8.2 feet and among Fort Payne homes at excavation depths greater than 10.1 feet.

The close correspondence between depth of excavation and radon concentration in homes built on the Fort Payne is thought to reflect the fact that the radon source lies within the soil itself and not in the Chattanooga Shale. An additional indication that the source of radon is within the soil among the Fort Payne homes is the relatively low coefficient of variation for the Fort Payne population (63 percent) compared to the other lithologic populations, which ranged from 116 percent to 177 percent. If radon were derived from the Chattanooga Shale and transported along solutionally enlarged fracture systems within the Fort Payne, radon concentrations in the Fort Payne soil would be expected to be variable with high radon concentrations above fracture zones and low radon concentrations above non-fractured rock. The fact that the coefficient of variation is the lowest among Fort Payne samples argues that radon is not transported along fracture systems but is derived from radium grains within the soil itself.

CONCLUSIONS

Radon concentrations in north central Tennessee homes and soils are slightly higher than indoor radon concentrations on a national average. However, radon is present in quantities much lower than in areas of the United States considered by the Environmental Protection Agency and equivalent state agencies to be radon "hot spots".

In the homes surveyed, radon was shown to vary as a function of many different factors related to both geology and home construction. Homes built upon soil derived from the Fort Payne Formation had the highest mean radon concentration, and homes built upon the overlying Warsaw Formation had the lowest radon concentration. There was an apparent inverse correlation between distance above the Chattanooga Shale and radon concentration; the confidence that this relation was not coincidental, however, was only 81.4 percent. Homes possessing crawl spaces were shown to have a geometric mean statistically similar to homes having basements with concrete foundations. Depth of home excavation and log(radon) manifested a direct correlation with a confidence of 99.9 % that the relation was not coincidental. A linear regression predicted that the U.S. Environmental Protection Agency recommended maximum of 4 pCi/L would be exceeded on the average at excavation depths greater than 8.2 feet for the overall data set and 10.1 feet within Fort Payne homes.

The work described in this paper was not funded by the U.S. Environmental Protection Agency and therefore the contents do not necessarily reflect the views of the Agency and no official endorsement should be inferred.

ACKNOWLEDGEMENTS

The authors wish to acknowledge the Center for Management, Utilization, and Protection of Water Resources at Tennessee Technological University for funding of the research summarized herein. Acknowledgments are due Brad Neff, who collected most of the cave radon measurements. Additionally, we would like to thank Joe Troester and Gregg Hileman of the U.S.G.S. for the technical reviews each provided.

REFERENCES

1. Miller, R.A., 1979, The Geologic History of Tennessee: Dept. of Cons., Div. of Geol., Bulletin 74, 59 p.

2. Reesman, A.L., and Godfrey, A.E., 1972, Chemical Erosion and Denudation Rates in Middle Tennessee: Tenn. Dept. of Cons. Div. Water Resources Series 4, 35 p.

3. Burchett, C.R., and Moore, G.K., 1971, Water Resources in the Upper Stones River Basin, Central Tennessee: Tenn. Dept. Cons. Div. Water Resources series 8, 62 p.

4. Moore, G.K., and Wilson, J.M., 1972, Water Resources of the Center Hill Lake Region, Tennessee: Dept. of Cons. Div. of Water Resources Series 9, 77 p.

5. Hershey, R.E. and Maher, S.W., 1985, Limestone and dolomite resources of Tennessee: Tenn. Div. of Geol. Bull. # 65, 252 p.

6. Milici, R.C., Briggs, G., Knox, L.M., Sitterly, P.D., and Statler, A.T., 1979, The Mississippian and Pennsylvanian Systems in the United States--Tennessee: U.S. Geological Survey Professional Paper 110-G.

7. Glover, L., 1959, Stratigraphy and uranium content of the Chattanooga Shale in northeastern Alabama, northwestern Georgia, and eastern Tennessee: U.S. Geological Survey Bulletin 1087-E, pp. 133-168.

8. Leimer, H.W., and Matthews, R.D., 1981, Chattanooga Shale of the Eastern Highland Rim, Tennessee, and methods of sampling; Synthetic Fuel from Oil Shale II, symposium and field trip, Institute of Gas Technology.

9. Conant, L.C. and Swanson, V.E., 1961, Chattanooga Shale and related rocks of central Tennessee; U.S. Geological Survey Professional Paper 357.

10. Brookins, D.G., 1988, The indoor radon problem: studies in the Albuquerque, New Mexico area: Environ. Geol. Water Sci., v. 12, n. 3, pp. 187-196.

11. Rogers, J.J.W. and Adams, J.A.S., 1969: Uranium; IN: Handbook of Geochemistry, Springer, Berlin, Chapter 92, 1962.

12. U.S. Environmental Protection Agency, 1986-a, A Citizen's Guide to Radon: USEPA/OPA-86-004, 14 p.

13. Nero, A.V., 1988, Radon and its decay products in indoor air: an overview: in: Radon and its Decay Products in Indoor Air, Nazaroff W.W. and Nero, A.V. eds, Wiley-Interscience; 518 p.

14. Collar, P.D. and Ogden, A.E., 1989, Radon in homes, soils, and caves of north central Tennessee and implications for the home construction industry: Third Interdisciplinary Conference on Sinkholes and Environmental Problems in Karst Terranes; St. Petersburg, Florida, Oct. 14, 1989.

15. Nazaroff, W.W., Moed, B.A., and Sextro, R.G., 1988, Soil as a source of indoor radon: generation, migration and entry: in: Radon and its Decay Products in Indoor Air, Nazaroff W.W. and Nero, A.V. eds, Wiley-Interscience; 518 p.

16. Tennessee Department of Health and Environment, 1987 Summary Report of the Tennessee Radon Survey.

17. U.S. Environmental Protection Agency, 1987, Radon Reduction in New Construction: an Interim Guide: EPA/OPA-87-009.

GRAIN SIZE AND EMANATION AS CONTROLLING FACTORS IN SOIL RADON

Linda C. S. Gundersen

U. S. Geological Survey

ABSTRACT

A comparison of two soil radon sampling techniques, the Reimer grab sampling technique (RG) and the EPA flow through grab sample technique (EFT), reveals a strong control of grain size and sorting on the soil radon measured. Moisture produces secondary effects on sampling, sometimes determining whether a sample can be obtained at all. Emanation, however is the ultimate control on the amount of radon sampled and it appears to be influenced most by the abundance of metal-oxides and the siting of uranium and radium in and around grains.

In well sorted, medium to coarse grained sands the two sampling techniques obtain similar radon concentrations, usually within 10% of each other. In poorly sorted sands, especially clayey sands, the RG obtains higher concentrations than the EFT. Under high moisture conditions including saturated conditions, the EFT cannot obtain a radon sample while the RG will obtain a sample approximately 50% of the time. Permeability measured at all of these sites has no apparent correlation with the radon concentration.

Equivalent uranium from gamma spectrometry at the surface and uranium and radium measured chemically in the soil have been compared with the soil radon concentrations. Although a generally positive correlation exists, anomalous amounts of soil radon with respect to its parent radionuclides are found in a variety of geologic settings. The common factor causing these anomalous concentrations is the occurrence of metal oxides, particularly iron, and the sorption or precipitation of uranium and radium in association with the metal oxides, dramatically enhancing the emanation in the rocks and soils.

This paper has been reviewed in accordance with the U. S. Environmental Protection Agency's peer and administrative review policies and approved for presentation and publication.

EFFECTS OF REGIONAL AND SEASONAL VARIATIONS IN SOIL MOISTURE AND TEMPERATURE ON SOIL GAS RADON

Arthur W. Rose, Department of Geosciences
Edward J. Ciolkosz, Department of Agronomy
John W. Washington, Department of Geosciences
Pennsylvania State University
University Park, PA 16802

ABSTRACT

Radon in houses depends partly on Rn concentration in soil gas, which is affected by water in a variety of ways. In this paper, temperature-dependent effects of Rn partitioning between changing proportions of air and water in pore space are shown to be capable of causing variations in Rn concentration up to 5-fold. A map of regional soil moisture and temperature regimes, in combination with the moisture/temperature effects on Rn, suggests that soil gas Rn will be most elevated by moisture effects in eastern U.S. and other regions with the Udic soil moisture regime. Large seasonal differences are also predicted for soils of the Udic moisture regime, with soils of the Frigid temperature regime having higher Rn in summer than winter. Aridic (dry) soils show negligible effects. Clay-rich soils will generally be most strongly affected by moisture variations.

INTRODUCTION

The main source of radon (Rn) in houses is now generally accepted to be soil gas entering through the foundation, driven by small pressure gradients between the outside and inside of the house (1). The total flux of Rn into a house via soil gas is a function of two factors, the flow rate of soil gas into the house, and the concentration of radon in the soil gas. The first factor, the flow rate of soil gas, varies with time owing to changes in the pressure gradient with changing conditions inside and outside the house, and temporal changes in air-filled porosity due to moisture changes. In addition, the flow rate varies from one house to another because of differences in construction details, as well as differences in permeability of soil and backfill along the path of air flow into the house. The second factor, the Rn concentration in the entering soil gas, depends largely on the radium (Ra) content, moisture and physical properties of the soil and backfill around the house. In general, increased Rn in soil gas is expected to lead to increased flux of Rn into the house, given equal influx rate of soil air.

The intent of this paper is to discuss some effects of soil moisture and temperature variations on the Rn content of soil air. The main emphasis is on effects involved in Rn equilibrium between air and water in the soil. This phenomenon has an important influence on absolute soil gas Rn concentrations as well as the nature of changes with time in the Rn concentration available to enter a house. The same phenomena are also important considerations in the interpretation of soil gas Rn surveys to predict Rn hazard.

TYPES OF MOISTURE EFFECTS

A large number of processes involving water have been proposed to affect the Rn content of soil gas. The following processes involving liquid water (but not ice) can be distinguished (2, 3, 4, 5, 6): (1) The sealing effect of a water-saturated zone at the surface or within the soil profile; (2) inhibition of diffusion in water-saturated pores because of much slower diffusion in water than air; (3) the flushing effect of water percolating through the soil and either pushing air ahead of it or transporting dissolved radon; (4) changes in volume of the soil due to changes in moisture, leading to cracking and swelling; (5) for relatively dry soils, an increase in Rn emanation coefficient with increasing moisture; (6) for radon transport into houses, the effect of the water table in limiting the depth of air flow; (7) temperature-dependent partition of Rn between water and air in soil pore space (2). Most of these processes must be considered theoretical, because unambiguous

field evidence demonstrating one cause of Rn variability and eliminating all other causes is scarce.

In most soil profiles, the Rn concentration decreases toward the surface because of diffusion from the relatively high concentrations (200-5000 pCi/l) generated in the soil compared to negligible concentration in open air (0.2 pCi/l). In soils with dominantly air-filled pores, this zone of markedly varying concentrations ranges from a few tens of centimeters to several meters in thickness, depending on the effective diffusion coefficient and air-filled porosity of the soil. However, the Rn diffusion coefficient in water is smaller by a factor of about 10^4 than the diffusion coefficient in air (2). Because the concentration gradient due to diffusion depends on the square root of the diffusion coefficient, the zone of changing concentration in water- saturated soil is condensed to about 1% of its thickness in soil with air-filled pores.

One result of this phenomenon is that a rainfall event intense enough to saturate the surface soil can create a seal for Rn, leading to high Rn levels beneath the water- saturated zone. Several half lives of Rn are required for the full increase to occur. A low permeability zone within the soil can have a similar effect.

As a soil is progressively wetted, the pores fill with water in the order of smallest to largest because of surface tension effects. Because of the low diffusion rate of Rn in water, transport of Rn in water-filled micropores is very slow. Thus, saturated micropores may effectively cause a dual pore system: a small proportion of air-filled pores separated by water-filled micropores and having high Rn concentration, and a separate set of connected macropores in which Rn concentration is controlled by diffusion in air, and flushing effects discussed below. This condition may be further complicated during intense rainfall events when the network of connected macropores may be the preferred pathway for rapid water movement through the soil.

Rainfall or other precipitation leading to percolation of water through the soil can displace Rn-rich air upwards. Some Rn is expected to dissolve from the soil air into the downward percolating water, resulting in additional Rn transport downward with the water. These processes can lead to a temporary depletion of Rn in the zone above the percolating water.

In a soil, Rn atoms are generated by radioactive decay of Ra atoms occurring in soil grains. The proportion of Rn atoms that escape into the pore space is termed the emanation coefficient. Emanation coefficients in very dry soils are markedly lower than in moist soils (7). Typical values in soils with at least 5% of the pore space filled by water are 0.15 to 0.35, with about 0.2 a

common value. Although this effect has been clearly demonstrated in experiments, it appears that few soils are dry enough to have significantly decreased emanation coefficients.

In most soils, the pore space is filled with a mixture of air and water. These phases are expected to be in close enough contact that Rn will redistribute itself between air and water by local diffusion between pores. At depths below the zone of significant diffusive loss to the atmosphere, when the soil air and water have remained long enough for emanated Rn to reach radioactive equilibrium, the concentration of Rn per unit volume of air-filled pore space (C_{Rn}) is given by the following relation (6):

$$C_{Rn} = \frac{C_{Ra} E D}{P(F(K-1)+1)} \qquad (1)$$

where C_{Ra} is the concentration of Ra per unit mass of soil particles, E is the emanation coefficient, D is the dry bulk soil density, P is the volume fraction of total pore space, F is the volume fraction of total pore space occupied by water, and K is the partition coefficient of Rn between unit volumes of water and air ($C_{Rn,water}/C_{Rn,air}$). The value of K depends on temperature (T), and ranges from 0.54 at 0°C to 0.23 at 25°C (6).

The effects of air-water partition may be isolated from equation (1) and expressed as Q, the factor by which variations in moisture and temperature increase Rn concentration in air-filled pore space:

$$Q = \frac{1}{(F(K-1)+1)} \qquad (2)$$

Given this relation, Figure 1 shows the effects of changes in F and T on Rn concentrations of soil air, given fixed values of C_{Ra}, E, D and P. C_{Rn} is seen to vary by a factor of 5 between F=0, T=0°C and F=1.0, T=30°C. Variations of a significant fraction of this range can occur at a single site at different times, and most of the above range occurs within soils of the United States.

REGIONAL AND LOCAL VARIABILITY OF SOIL MOISTURE AND TEMPERATURE

Soil moisture and temperature are very important in the growth of crops, so soils are classified partly in terms of these properties (8). Based on mean annual soil temperature (MAST), soils of temperate regions are classified as Frigid (MAST=0-8°C), Mesic (MAST=8-15°C), Thermic (MAST=15-22°C) or Hyperthermic (MAST>22°C). Soil moisture regimes are basically defined by groundwater level and proportion of the year in which moisture is held at tensions of 1500 kPa or less, the maximum tension at which common crops can grow. Most U. S. soils are classified as

Aridic, Ustic or Udic in order of increasing length of the growing season with moist soil. In addition, the Xeric soil moisture regime occurs in areas of Mediterranean climate, i. e., moist cool winters and hot dry summers, in contrast to moist summers and dry winters of the Ustic regime.

Figure 2 gives a generalized distribution of soil temperature and soil moisture regimes for the U.S., compiled from references 9-12. In the eastern and central U. S., soil temperature regimes follow a simple pattern of Frigid, Mesic, Thermic and Hyperthermic from north to south. East of about 97°W Long., soils are relatively moist (Udic), and westward to the Rocky Mountains they are Ustic. In the western U. S., Frigid regimes extend southward along the Rocky Mountains, and Aridic regimes are common in the southwest. Regions of Xeric soil moisture regime are common in California and nearby areas.

Based on Figures 1 and 2, soils with identical values of C_{Ra}, E, D and P would be expected to increase in C_{Rn} in the sequence Aridic-Ustic-Udic eastward across the U. S, and to increase in the order Frigid-Mesic-Thermic-Hyperthermic southward. Table 1 lists a few sites for which the relevant parameters have been measured or estimated. For most sites in regions of Udic moisture regime, the observed Rn (especially the maximum observed Rn) exceeds the values calculated for dry soil by factors of 1.5 to 5, as expected for soils of Udic moisture regime. For site 14-80, where measurements of moisture and temperature have been made, the values calculated from equation (1) match the measured values within measurement error (6). The sole exception, site 14-82, is strongly affected by water saturation effects for much of the year. In contrast, at the site at Socorro, NM, in an Aridic moisture regime, the calculated and observed Rn agree closely. The moisture content of this soil is reported as 4 wt.%, equivalent to F=0.17, a reasonable value for the aridic regime. For the site at Denver, CO, the observed Rn levels for moist seasons distinctly exceed the values calculated for dry conditions, and during dry seasons the soil cracks to allow air penetration to depth. These data are consistent with a significant moisture effect.

Extension of the relations discussed above leads to the hypothesis that radon in houses should vary according to the moisture and temperature regimes, if not obscured by variations in C_{Ra}, E, D and P, and flux of soil air. This hypothesis was tested using statewide averages of Rn in homes from a compilation of 175,000 measurements by The Radon Project of Pittsburgh, PA, as compiled by Dr. Bernard Cohen of the University of Pittsburgh.

The data on houses do not fit the hypothesis. In eastern and central U. S., the highest values are in IA, SD, and several other northern plains states with an Ustic moisture regime and

Frigid or Mesic thermal regime, rather than in states with a Udic-Thermic regime. Values tend to be low in most states of southeastern U. S. with a Thermic temperature regime. Likely explanations of the failure of the hypothesis are regional differences in Ra and U, lower indoor-outdoor temperature differences in the southeast leading to lower pressure gradients, regional differences in home construction (specifically the use of slab-on-grade construction in the southeast vs. basements in northern states), and error from grouping by state. Also, in areas of high soil moisture, the air permeability may be greatly decreased by blockage of small pores by water.

Local differences in drainage and moisture are probably also of significant importance in soil gas Rn. Many relatively flat valley areas are floored by alluvium or soil that is water saturated at the surface, to form the Aquic moisture regime. Other poorly drained areas may have a thin zone of moist soil above the water table. Radon content of soil gas is expected to be relatively high in such areas, but air permeability may be so low that little Rn transport is possible.

EFFECTS OF SEASONAL VARIATIONS IN SOIL MOISTURE / TEMPERATURE

Soils literature also allows estimates of seasonal change in moisture and temperature, leading to estimates of seasonal changes in Rn concentrations. Tables 2, 3, and 4 give these estimates.

The soil moisture states and soil moisture tension ranges given in Table 2 were developed by the USDA Soil Conservation Service (14). The data given in Table 2 for the sandy loam and silty clay loam was calculated as follows: A bulk density of 1.60 g/cm^3 (sandy loam) and 1.45 g/cm^3 (silty clay loam) was used to calculate (assuming a particle density of 2.65 g/cm^3) a total pore space of 40% for the sandy loam and 45% for the silty clay loam. Soil moisture content based on data from Petersen et al. (15) and Ciolkosz and Dobos (16) for 1500 and 33 KPa tensions was used to interpolate the values given in Table 2 using the soil moisture tension/moisture content relations given by Thorne and Thorne (17). These data were used to compute the percent pore space filled with water (% soil moisture x bulk density/total pore space). Table 3 gives estimated winter and summer soil moisture regimes for the upper 1.5 meters of soils of the United States. These data are based on numerous soil moisture state evaluations (18, 19) for various soils of the United States. The soil temperatures given in Table 4 were calculated from mean monthly air isotherms (20) using the method of van Wambeke (21) for the various soil temperature/moisture regions given in Figure 3. This method may give conservative values for bare soil areas (22), therefore the soil temperatures may have a greater range than given for the arid area.

These data have been used to derive the estimates of Q shown in Table 5. Several conclusions of interest may be drawn from this data:

1. The largest seasonal effects of moisture and temperature are expected in the Udic moisture regime. In the warmer parts of Udic regions, winter Rn values may be more than double the summer values.

2. Summer Rn values higher than winter values are predicted for the Frigid-Udic regime, and are possible in the Mesic-Udic regime. This behavior has been recognized at several sites in central Pennsylvania (14-80, 14-81, 14-82, 14-83), which is on the cold edge of the Mesic thermal regime.

3. Summer Rn exceeding winter Rn is possible in the Ustic regime, but in general, large changes are not expected.

4. In the aridic regime, moisture is low enough that seasonal effects are very small, but typically winter levels will slightly exceed summer values.

5. In the Xeric regime, winter Rn values are expected to markedly exceed summer values.

6. Seasonal effects are expected to be much larger in clay-rich soils than in sandy soils, because of the generally higher moisture saturation of clay-rich soils.

CONCLUSIONS

Although many effects of water on Rn in soil gas are proposed, the effect of varying proportion of pore space occupied by water appears to be among the largest and most universal. Temperature also affects soil gas Rn because of its effect in varying the partition of Rn between water and air. The process affects moist soils at all depths, but can be evaluated best for depths where diffusion toward the surface is negligible.

In the soils literature, major regional differences in soil moisture and temperature are well documented, and have been compiled as a map. The meager data on Rn in soil gas agrees with the proposed moisture temperature effects. However, within houses the effects of soil moisture and temperature are masked by other Rn-determining factors (regional differences in Ra, house construction, house pressurization, etc.) so that a clear regional effect of the soil moisture and temperature is not obvious in a large data set on Rn in houses.

Seasonal variability in soil gas Rn has been predicted from estimated temporal soil moisture and temperature variations. Large seasonal variations are predicted for soils of the Udic moisture regime, characteristic of the eastern U.S. For the northeastern U.S., from New England through Minnesota, summer soil gas radon is predicted to exceed winter values, as found at several sites in Pennsylvania. Contrastingly, in soils of the

Xeric moisture regime, distinctly higher values are predicted in the winter than the summer. Clay-rich soils are more susceptible to moisture-induced elevated Rn than are sandy soils. However, local variations of moisture caused by variability in drainage are undoubtedly also of considerable importance.

The work described in this paper was not funded by the U.S. Environmental Protection Agency and therefore the contents do not necessarily reflect the views of the Agency and no official endorsement should be inferred.

ACKNOWLEDGEMENTS

The authors acknowledge the financial support of the U.S. Department of Energy (Grant DE-FG02-87ER60577).

REFERENCES

1. Environmental Protection Agency. A citizen's guide to radon. USEPA, Doc. OPA-86-004, 1986. 13 pp.
2. Tanner, A.B. Radon migration in the ground: A review. In: J.A.S. Adams and W.M. Lowder (ed.), The Natural Radiation Environment. University of Chicago Press. 1963. p. 161.
3. Tanner, A.B. Radon migration in the ground: A supplementary review. In: T.F. Gesell and W.M. Lowder (ed.), The Natural Radiation Environment III. DOE Symposium Series, CONF-780422. 1980. p. 5.
4. Schery, S.D., Gaeddert, D.H., and Wilkening, M.H. Factors affecting exhalation of radon from a gravelly sandy loam. J. Geophys. Res. 89: 7299, 1984.
5. Schumann, R.R., Owen, D.E., and Asher-Bolinder, S. Weather factors affecting soil-gas radon concentrations at a single site in the semiarid western U.S.. In: Proceedings of the 1988 E.P.A. Symposium on Radon and Radon Reduction Technology. EPA-600/9-89/006B, U.S. Environmental Protection Agency, Cincinnati, Ohio, 1989. p. 3.1.
6. Washington, J.W. and Rose, A.W. Regional and temporal relations of radon in soil gas to soil temperature and moisture. Geophys. Res. Lett. in press: 1990.
7. Nielson, K.K., Rogers, V.C., Mauch, M.L., Hartley, J.N., and Freeman, H.D. Radon emanation characteristics of uranium mill tailings. In: Symposium on Uranium Mill Tailings Management. Colorado State University, Fort Collins, CO, 1982. p. 355.
8. Soil Survey Staff. Soil Taxonomy. Agricultural Handbook No. 436, Soil Conservation Service, U.S. Department of Agriculture, 1975. 754 pp.
9. Soil Survey Staff. Soil areas of the midwest region. Soil Conservation Service, U.S. Department of Agriculture. Midwest Nat. Tech. Center, Lincoln, NE. 1972. 1 page map.
10. Soil Survey Staff. Soil moisture regime and soil temperature map. Soil Conservation Service, U.S. Department of

Agriculture. South Nat. Tech. Center, Fort Worth, TX. 1975. 1 page map.
11. Soil Survey Staff. Composite map of soil moisture and temperature as presented by individual states. Soil Conservation Service, U.S. Department of Agriculture. West Nat. Tech. Center, Portland, OR. Draft of the WRRC-50 committee project. Map and text.
12. Smith, H. Soil temperature regimes of the northeastern United States. Soil Conservation Service, U.S. Department of Agriculture. Northeast Nat. Tech. Center, Chester, PA. 1984. 1 page map.
13. Schumann, R.R., and Owen, D.E. Relationships between geology, equivalent uranium concentration, and radon in soil gas, Fairfax County, Virginia. Open-File Report 88-18, Geological Survey, U.S. Department of the Interior, Denver, Colorado, 1988. 27 pp.
14. Quandt, L.A. and Grossman, R.B. Soil water states for select soils in the northeast region. Soil Conservation Service, U.S. Department of Agriculture. Northeast Nat. Tech. Center, Chester, PA. 1983. 51 pp.
15. Petersen, G.W., Cunningham, R.L., Matelski, R.P. Moisture characteristics of Pennsylvania soils: I. Moisture tension as related to texture. Soil Sci. Soc. Am. Proc. 32: 271, 1968.
16. Ciolkosz, E.J., and Dobos, R.R. Penn State Soil Characterization Laboratory Data Base. Department of Agronomy, Penn State University. University Park, PA.
17. Thorne, D.W. and Thorne, M.D. Soil, water, and crop production. AVI Pub. Co., Westport, CT. 1979. 353 pp.
18. Soil Survey Staff. Proceedings of the 1981 national technical work-planning conference of the cooperative soil survey. Soil Conservation Service, U.S. Department of Agriculture, Washington, D.C., 1982. p. 19.
19. Soil Survey Staff. Proceedings of the 1983 national technical work-planning conference of the cooperative soil survey. Soil Conservation Service, U.S. Department of Agriculture, Washington, D.C., 1983. p. 114.
20. Environmental Data Service. Climatic atlas of the United States. Superintendent of documents, Environmental Science Services Administration, U.S. Department of Commerce, Washington, D.C. 1968.
21. van Wambeke, A. Calculated soil moisture and temperature regimes of South America. SMSS Tech. Monogr. No. 2, Soil Conservation Service, U.S. Department of Agriculture, Washington, D.C. 1981.
22. Murtha, G.G. and Williams, J. Measurement, prediction, and interpretation of soil temperature for use in soil taxonomy: Tropical Australian experience. Geoderma. 37: 189, 1986.

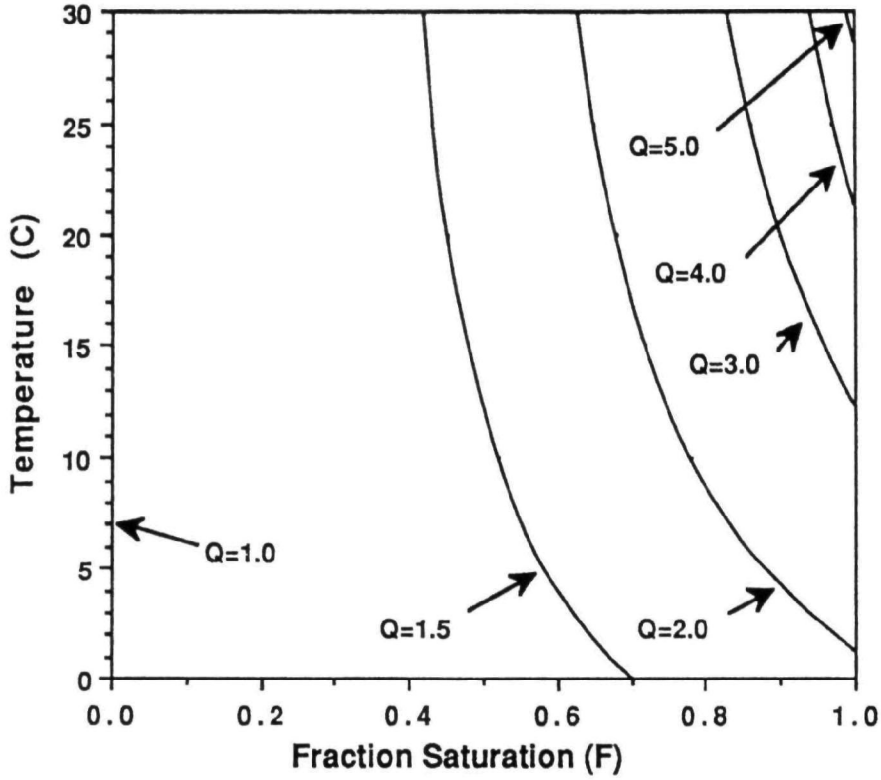

Figure 1: Values of Q (factor by which soil gas Rn is increased) as a function of temperature ($T^{o}C$) and fraction moisture saturation (F)

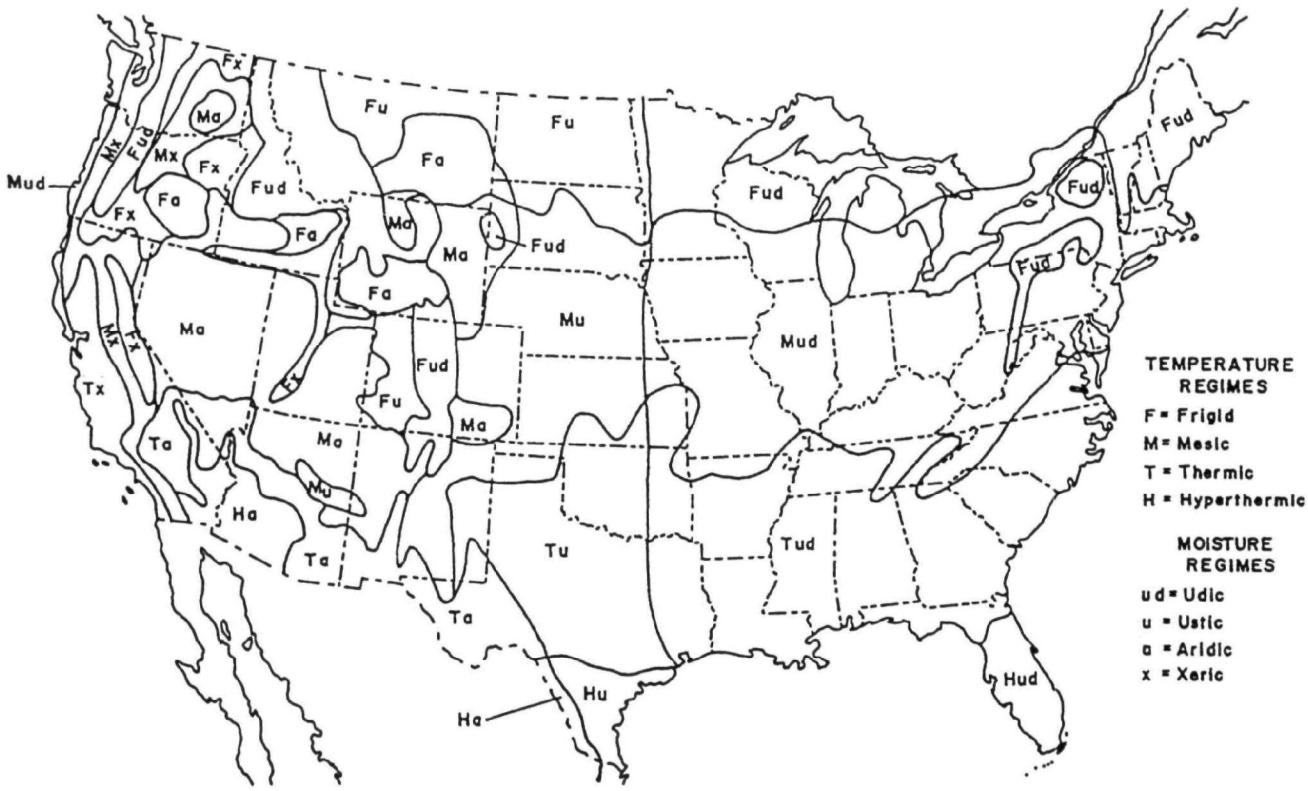

Figure 2: Generalized distribution of soil moisture-temperature regimes in the U.S.

Table 1. Comparison of calculated and observed radon in soil gas.

Site[a]	C_{Ra}[b] (pCi/g)	E[c]	D (g/cm^3)	P	C_{Rn} (pCi/l) Calc (dry)[d]	C_{Rn} (pCi/l) obs, mean[e]	C_{Rn} (pCi/l) obs, max[f]	Moisture[g]	Reference
14-80 (PA)	2.37	0.20	1.46	0.45	1540	2433	4690	ud	This study
14-81 (PA)	1.15	(0.2)	1.65	0.38	997	1584[h]	2560	ud	This study
14-82 (PA)	0.85	(0.2)	1.87	0.29	1096	860[h]	1323	ud	This study
14-83 (PA)	0.54	0.21	1.91	0.28	775	510[h]	1115	ud	This study
6-10 (PA)	1.32	(0.2)	1.15	0.56	542	1300	1556	ud	This study
NC-1 (NC)	2.37	(0.2)	1.30	0.51	1210	5841	8674	ud	This study
Socorro, NM	0.90	0.38	1.5	0.35	1465	1400		a	(4)
Denver, CO	0.8	(0.2)	(1.5)	(0.43)	560		1200	u	(5)
Fairfax Co, VA[i]	0.8±0.12	(0.2)	(1.5)	(0.4)	600	1000	3700	ud	(13)

a. Sites 14-80 through 14-83 are in Centre Co., PA; site 6-10 is in Berks Co., PA; and NC-1 is at Justice, NC.
b. Radium or uranium in soil.
c. Measured value, or assumed as 0.2 if in parentheses.
d. Calculated from equation 1.
e. Mean value for 1-2 years by alpha-track detector at sites of this study.
f. Maximum reported value for alpha track detectors exposed 2-3 months, or single reported value.
g. Moisture regime: ud, udic; u, ustic; a, aridic
h. Alpha track detector submerged part of year.
i. Based on samples with 1.5 to 2.5 ppm eU on plot of soil gas Rn vs eU (Figure 7). The observed "mean" is the approximate median.

Table 2. Soil moisture states, percent moisture, and percent saturated pore space for a typical sandy loam and silty clay loam soil.

Soil Moisture		Sandy Loam percent		Silty Clay Loam percent	
State	Tension (KPa)	Moisture+	Pore space Saturated++	Moisture+	Pore space Saturated++
Dry					
Very Dry (VD)	100,000*-10,000	0-1	0-4	0-2	0-6
Slightly Dry (SD)	10,000-1,500	1-6	4-24	2-12	6-39
Moist					
Slightly Moist (SM)	1,500-200	6-11	24-44	12-18	39-58
Moderately Moist (MM)	200-33	11-14	44-56	18-23	58-74
Very Moist (VM)	33-1	14-24	56-96	23-31	74-99
Wet	< 1		100		100

* Air dry (50% relative humidity); oven dry = 1,000,000 KPa

\+ by weight

++ by volume

Table 3. Estimated average soil moisture states for the soil temperature regimes of the United States. See Table 2 for abbreviations.

Soil Temperature Regime	Soil Moisture States							
	Xeric		Aridic		Ustic		Udic	
	Winter	Summer	Winter	Summer	Winter	Summer	Winter	Summer
Frigid	VM	MM	SM	SD	MM	SM	VM	MM
Mesic	VM	SM	SM	SD	MM	SM	VM	MM
Thermic	MM	SD	SM	SD	MM	SM	VM	SM
Hyperthermic	--	--	SD	SD	SM	SM	VM	SM

Table 4. Approximate mean January and July air and soil temperature (degrees C at 51 cm depth) for the various soil temperature-moisture regime areas of the United States. Mean annual soil temperature: Frigid 0-8°C; Mesic 8-15°C; Thermic 15-22°C; and Hyperthermic > 22°C mean.

Soil Temperature Regime Air and Soil Temperature	Western States				Eastern States
	Xeric	Aridic	Ustic	Udic	Udic
Frigid					
Air					
January	-4	-7	-9	-6	-9
July	16	18	18	16	19
Soil					
January	2	1	-2	1	-2
July	14	16	16	14	16
Mesic					
Air					
January	2	-3	-2	4	-2
July	18	21	24	21	24
Soil					
January	7	4	5	10	5
July	18	19	22	21	22
Thermic					
Air					
January	9	7	7	--	7
July	23	29	28	--	27
Soil					
January	14	14	13	--	13
July	23	28	27	--	26
Hyperthermic					
Air					
January	--	11	13	--	18
July	--	33	29	--	28
Soil					
January	--	18	19	--	22
July	--	32	29	--	28

Table 5. Estimated winter and summer values of Q for soil moisture-temperature regimes.

Regime[a]	Winter (Jan.)				Summer (July)				Higher[b] Season
	T°C	F	Q Range	Q Midpoint	T°C	F	Q Range	Q Midpoint	
A. Silty Clay Loam									
Fud	-5.4	.74-.99	(1.39-1.60)	(1.498)	16.1	.58-.74	1.69-2.08	1.866	S
Mud	5	.74-.99	1.73-2.30	2.011	21.6	.58-.74	1.77-2.25	1.981	O
Tud	13	.74-.99	1.99-2.99	2.448	26.1	.39-.58	1.44-1.83	1.601	W
Hud	22	.74-.99	2.26-3.93	2.967	28	.39-.58	1.45-1.85	1.616	W
Fu	-2.2	.58-.74	(1.35-1.49)	(1.418)	16.1	.39-.58	1.38-1.69	1.510	S
Mu	5	.58-.74	1.50-1.73	1.605	21.6	.39-.58	1.41-1.77	1.563	O
Tu	13	.58-.74	1.64-1.99	1.797	27.4	.39-.58	1.45-1.85	1.611	W
Hu	19	.39-.58	1.64-1.73	1.539	29	.39-.58	1.45-1.87	1.623	S
Fa	0.6	.39-.58	1.24-1.41	1.316	16.1	.06-.39	1.04-1.38	1.183	W
Ma	4	.39-.58	1.28-1.48	1.364	19	.06-.39	1.05-1.40	1.191	W
Ta	14	.39-.58	1.36-1.66	1.487	28	.06-.39	1.05-1.45	1.212	W
Ha	18	.06-.39	1.04-1.39	1.188	32	.06-.39	1.05-1.47	1.219	O
Fx	2.2	.74-.99	1.64-2.09	1.866	14.4	.58-.74	1.66-2.03	1.829	O
Mx	7.2	.74-.99	1.80-2.47	2.128	17.7	.39-.58	1.39-1.71	1.526	W
Tx	13.8	.58-.74	1.65-2.01	1.816	22.7	.06-.39	1.05-1.42	1.200	W
B. Sandy Loam									
Fud	-5.4	.74-.99	(1.06-1.10)		16.1	.58-.74	1.08-1.11		
Mud	5	.74-.99	1.09-1.16		21.6	.58-.74	1.09-1.12		
Tud	13	.74-.99	1.10-1.19		26.1	.39-.58	1.05-1.09		
Hud	22	.74-.99	1.11-1.22		28	.39-.58	1.05-1.09		

a. Moisture-temperature regime. Temperature regimes: F, Frigid; M, Mesic; T, Thermic; H, Hyperthermic; Moisture regimes: ud, udic; u, ustic; a, aridic; x, xeric.
b. Season with highest predicted Rn: S, summer; W, winter; O, subequal.

* U.S. GOVERNMENT PRINTING OFFICE: 1990 748-010/25003